

NORTHWESTERN UNIVERSITY

Energy Deprivation Elevates BACE1 Protein Levels and  
Promotes Amyloidogenesis *via* EIF2alpha Phosphorylation

A DISSERTATION

SUBMITTED TO THE GRADUATE SCHOOL IN PARTIAL  
FULFILLMENT OF THE REQUIREMENTS

for the degree

DOCTOR OF PHILOSOPHY

Field of Cell and Molecular Biology  
Integrated Graduate Program in the Life Sciences

By

Tracy O'Connor

EVANSTON, ILLINOIS

December 2008

## ABSTRACT

### Energy Deprivation Elevates BACE1 Protein Levels and Promotes Amyloidogenesis *via* EIF2alpha Phosphorylation

Tracy O'Connor

The cause(s) of A $\beta$  overproduction and accumulation in sporadic Alzheimer's disease (SAD) are unknown; however, several lines of evidence indicate that impaired energy metabolism in the brain may be involved. Furthermore, the rate-limiting enzyme in A $\beta$  production, BACE1, is elevated in SAD brains around amyloid plaques, indicating that BACE1 may also play a causal role in SAD pathogenesis. Here, we show evidence that BACE1 is directly elevated in response to energy deprivation, both *in vitro* and *in vivo*.

This appears to occur through a translational mechanism, previously unknown to regulate BACE1—stress-induced phosphorylation of the eukaryotic translation initiation factor 2 $\alpha$  (eIF2 $\alpha$ -P). In support of a role for eIF2 $\alpha$  phosphorylation in SAD pathogenesis, pharmacological induction of eIF2 $\alpha$  phosphorylation is directly amyloidogenic *in vitro*. Chronic energy deprivation in APP-overexpressing mice elevates BACE1 protein levels post-transcriptionally, eIF2 $\alpha$ -P levels, total A $\beta$  levels, and accelerates amyloid plaque pathology in the brain. Interestingly, BACE1 and eIF2 $\alpha$ -P are both elevated in APP-overexpressing mice compared to non-transgenic, indicating that BACE1, eIF2 $\alpha$ -P, and A $\beta$  may operate together in a positive feedback loop that may further exacerbate amyloid pathology. Importantly, BACE1 protein levels, eIF2 $\alpha$ -P levels, and amyloid load were all significantly correlated in human AD brains, indicating that these molecular pathways may play an important role in the development of SAD.

## TABLE OF CONTENTS

ABSTRACT .....	2
LIST OF TABLES .....	5
LIST OF FIGURES .....	6
ACKNOWLEDGEMENTS .....	9
Chapter	
1. INTRODUCTION .....	12
Brief history of Alzheimer's disease .....	12
Clinical features of Alzheimer's disease .....	14
The molecular pathology of Alzheimer's disease: plaques and tangles .....	16
Amyloid $\beta$ : The primary component of senile plaques .....	18
BACE1: Identifying the $\beta$ -secretase.....	22
BACE1 as a drug target for AD .....	24
BACE1 and sporadic Alzheimer's disease .....	25
Regulation of BACE1 .....	27
Energy metabolism and Alzheimer's disease .....	33
Physiological function of BACE1 ....	36
Overview of thesis .....	38
2. ACUTE ENERGY INHIBITION ELEVATES BACE1 PROTEIN LEVELS IN THE BRAIN VIA A POST-TRANSCRIPTIONAL MECHANISM <i>IN VIVO</i> .....	41
Introduction .....	41
Materials and methods .....	42
Results .....	48
Discussion .....	58
3. ENERGY INHIBITION ELEVATES BACE1 PROTEIN IN VITRO VIA PHOSPHORYLATION OF THE TRANSLATION INITIATION FACTOR eIF2 $\alpha$ AT SERINE 51 .....	63
Introduction .....	63
Materials and methods .....	65
Results .....	73
Discussion .....	95
4. PHOSPHORYLATION OF eIF2 $\alpha$ AT SERINE 51 ELEVATES ENDOGENOUS BACE1 PROTEIN AND ACCELERATES AMYLOID $\beta$ PRODUCTION IN PRIMARY CULTURED NEURONS.....	103
Introduction .....	103
Materials and methods .....	104
Results .....	109
Discussion .....	113

5.	CHRONIC ENERGY INHIBITION IN VIVO ELEVATES BACE1 PROTEIN, ENHANCES eIF2 $\alpha$ PHOSPHORYLATION, AND ACCELERATES AMYLOID PATHOLOGY IN THE BRAIN .....	119
	Introduction .....	119
	Materials and methods .....	120
	Results .....	126
	Discussion .....	136
6.	BACE1 PROTEIN AND PHOSPHO-eIF2 $\alpha$ LEVELS ARE ELEVATED IN 5XFAD BRAINS AND BACE1, PHOSPHO-eIF2 $\alpha$ , AND AMYLOID LOAD ARE ALL CORRELATED IN HUMAN AD BRAINS .....	145
	Introduction .....	145
	Materials and methods .....	146
	Results .....	150
	Discussion .....	156
7.	DISCUSSION .....	163
	Translational Control of Proteins .....	163
	The Eukaryotic Translation Initiation Factor 2 (eIF2) .....	167
	Role of BACE1 in Neurodegeneration and Energy Metabolism.....	181
8.	REFERENCES .....	195



**LIST OF TABLES**

Table 3.1	List of primary antibodies used to probe BACE1-293 Immunoblots.....	70
Table 4.1	List of primary antibodies used to probe neuron lysates and brain homogenates.....	107

## LIST OF FIGURES

Figure 1.1	The pathological hallmarks of Alzheimer's disease.....	13
Figure 1.2	Amyloid Precursor Protein (APP) Processing.....	20
Figure 1.3	Endogenous BACE1 and APP are elevated in all postnatal brain regions.....	28
Figure 1.4	Endogenous BACE1 and APP are elevated in postnatal brain via a post-transcriptional mechanism.....	31
Figure 1.5	Myelination is reduced in BACE1 $-/-$ mice.....	37
Figure 2.1	Constructs and relevant DNA sequences used in experiments....	43
Figure 2.2	The effect of pharmacological energy inhibitors on neuronal energy metabolism.....	50
Figure 2.3	Acute energy inhibition causes no detectable neurodegeneration or astrogliosis in the brain.....	52
Figure 2.4	Acute energy inhibition elevates endogenous BACE1 protein levels in young Tg2576 mice.....	53
Figure 2.5	Acute energy inhibition in young Tg2576 mice enhances pro-amyloidogenic processing of APP.....	55
Figure 2.6	Acute energy inhibition elevates endogenous BACE1 protein levels <i>via</i> a post-transcriptional mechanism in young C57/BL6 mice.....	57
Figure 3.1	Glucose deprivation increases BACE1 protein levels in BACE1-293 cells.....	74
Figure 3.2	Glucose deprivation elevates BACE1 protein in BACE1-293 cells <i>via</i> a post-transcriptional mechanism.....	76
Figure 3.3	Glucose deprivation in BACE1-293 cells does not alter BACE1 protein stability.....	78
Figure 3.4	The BACE1 5'UTR is required for glucose deprivation-induced BACE1 protein elevation in HEK-293 cells.....	80
Figure 3.5	Convergence of stress signaling pathways on translation initiation. 4E-BP.....	82

Figure 3.6	eIF4E is not involved in glucose deprivation-induced BACE1 protein elevation.....	84
Figure 3.7	Glucose deprivation increases eIF2 $\alpha$ phosphorylation and activates a specific set of stress-response signaling pathways in BACE1-293 cells.....	84
Figure 3.8	Regulation of eIF2 $\alpha$ and translation initiation by phosphorylation at Ser51.....	87
Figure 3.9	Direct phosphorylation of eIF2 $\alpha$ elevates BACE1 protein in BACE1-293 cells.....	88
Figure 3.10	Inhibition of eIF2 $\alpha$ phosphorylation prevents glucose deprivation-induced BACE1 protein elevation.....	90
Figure 3.11	Treatment of cells with a chemical chaperone prevents glucose deprivation-induced BACE1 protein elevation.....	91
Figure 3.12	Inhibition of the amino acid-regulated eIF2 $\alpha$ kinase, GCN2, cannot prevent glucose deprivation-induced BACE1 protein elevation in BACE1-293 cells.....	93
Figure 3.13	The UPR-inducible eIF2 $\alpha$ kinase, PERK, is responsible for glucose deprivation-induced BACE1 protein elevation in BACE1-293 cells .....	94
Figure 4.1	Glucose deprivation in primary cultured neurons induces eIF2 $\alpha$ phosphorylation and elevates BACE1 protein levels post-transcriptionally.....	110
Figure 4.2	Direct phosphorylation of eIF2 $\alpha$ elevates BACE1 protein and promotes A $\beta$ production in cultured Tg2576 neurons.....	112
Figure 4.3	Full-length APP, presenilin 1, and A $\beta$ degrading enzymes are unaffected by salubrinal in neurons.....	114
Figure 5.1	Chronic energy deprivation causes no visible neurodegeneration or astrogliosis in Tg2576 brain.....	128
Figure 5.2	Chronic energy deprivation elevates eIF2 $\alpha$ -P and BACE1 protein in Tg2576 brain.....	130

Figure 5.3	Chronic energy deprivation elevates BACE1 protein post-transcriptionally in C57/BL6 brain.....	132
Figure 5.4	Chronic energy deprivation accelerates A $\beta$ production and exacerbates amyloid plaque pathology in Tg2576 brain.....	135
Figure 5.5	Other components of the amyloidogenic pathway and A $\beta$ degrading enzymes are not affected by chronic energy deprivation.....	137
Figure 6.1	The 5XFAD (Tg6799) mouse model of rapid amyloid pathology.....	151
Figure 6.2	Post-transcriptional elevations of BACE1 protein level in 5XFAD brain are correlated with eIF2 $\alpha$ -P.....	152
Figure 6.3	Phosphorylated eIF2 $\alpha$ , BACE1 protein, and amyloid load are all correlated in human AD brain.....	155
Figure 7.1	eIF2 $\alpha$ -mediated regulation of BACE1 translation.....	182
Figure 7.2	The role of eIF2 $\alpha$ phosphorylation in sporadic Alzheimer's disease pathogenesis.....	194

## Acknowledgements

I would like to acknowledge the contribution of numerous scientists and physicians over the past hundred years that have dedicated their careers to the fight against Alzheimer's disease. Their work has been instrumental to our current understanding of the disease and serves as an essential foundation for all future work, including the results described in this thesis.

This work would not have been possible without generous contributions from the community, our collaborators, and funding from the National Institute of Health (NIH). Thanks to Richard Scarpulla for key intellectual contributions to this work and general expertise in the area of energy metabolism, Adriana Ferreira for expertise in neuronal cultures, and Marina Yasvoina and Peizhen Shao for performing tissue sectioning and immunohistochemistry. The 3D5 antibody, which made much of this work possible, was created by Jie Zhao in collaboration with Skip Binder's lab. Their expertise in antibody production was greatly appreciated. Human AD brain tissue samples were a gift from participants in Rush Hospital Memory and Aging Project (R01AG17917; Bennett, David A; PI). Thanks to Sven Lammich, Stefan Lichtenthaler, and Christian Haass from Ludwig Maximilians University in Munich for providing the -5'UTR and +5'UTR constructs. The GADD34 $\Delta$ N, GADD34CON, PERKDN, and P58 constructs were a generous gift of David Ron (NYU), and the GCN2DN construct was a gift from Ron Wek at Indiana University. Also, thanks to Sebastian Hebert and Bart DeStrooper from the Catholic University in Leuven, Belgium for performing miRNA analysis on our samples. This work was supported by the John Douglas French Foundation (Sarah L. Cole), and

NIH grants 5T32AG020506-04 (John F. Disterhoft), 1F31AG030965-01A1 (Tracy O'Connor), 5T32AG000260 (Linda J. Van Eldik), R01 AG022560 (Robert Vassar), and R01 AG030142 (Robert Vassar).

I would like to thank all of the extraordinary people that I've met in Chicago and have guided me through this project over the years. I would like to thank the members of my committee for their support and guidance during this project: Skip Binder, Richard Miller, Laura Herzing, and Richard Scarpulla. I would also like to thank Jenny Knauss and Don Moyer and Susan and Bob Houston for opening up their homes and their lives to me and Sarah in order to educate the scientific community about the realities of living with Alzheimer's disease. I would especially like to thank Rod Velliquette for his support, guidance, and friendship during my first years at Northwestern. I also want to thank my fellow graduate students, especially Wendy, Diana and Laurie, for being there through good times and bad, and being the only people who really and truly understood. I don't know where I would be without the Vassar lab veterans: Sarah, Jie, and especially Erika. Thanks so much for all you have taught me and for serving as general guardians over my sanity, with appropriate interludes of alcohol and hilarity. I have also very much enjoyed getting to know the new members of the Vassar lab: Katherine, Brian, and Will. Best of luck to you all in the future, and I implore you not to abandon your inherited lab duty of giving Bob a hard time. A very special thanks is owed to my advisor, Bob Vassar, for his good-humored patience, his encouragement, and his amiable leadership. We didn't always understand Bob's master plan, or, in fact, know if he even had one, but we followed him, nonetheless. The road was sometimes alarming

and sometimes comical, but in the end the Vassar lab came out in the lead, and we had a great time along the way, which I suspect is what Bob had in mind all along. I learned a great deal from my advisor, most of which had nothing at all to do with BACE1. Cheers to Bob and the rest of the Vassar lab for all of the friendship, the laughter, and the knowledge. I wouldn't have traded it for anything. I would also like to thank my "rocks" --- the people who were there before, during, and will be there after grad school. Thanks to Jovan, for ultimately being the reason I moved to Chicago, though I didn't know it at the time. Thanks to Caitlyn, my BFF, for loving me even though I abandoned her for Chicago, and then having the patience to sit there and listen to me when I had the audacity to *complain about it*. And thanks to Erin, for making the trek to Chicago with me and seeing me through many a trial and tribulation. The most special thanks goes to my parents, Ken and Linda, who remain my greatest source of knowledge, even after receiving a PhD.

# CHAPTER 1

## INTRODUCTION

### **Brief history of Alzheimer's disease**

Alzheimer's disease (AD) was originally described in 1907 by Alois Alzheimer. Upon examination of a female dementia patient in her fifties, Alzheimer identified a unique type of dementia characterized by severe memory deficits with preserved motor function. Upon post-mortem histological brain examination, the microscopic "fibrils" (neurofibrillary tangles) and "miliary foci" (senile plaques) were described for the first time, which have since become pathological hallmarks of Alzheimer's disease (Alzheimer, 1907) (Fig 1.1). Due to the unusually young age of Alzheimer's initial patient, the link between Alzheimer's findings and the more common senile dementias occurring in much older patients went undetected for nearly seventy years. "Alzheimer's disease," coined by Emil Kraepelin in honor of his student's discovery, would be considered a rare dementia occurring exclusively in middle-aged individuals for the next several decades. It was not until an influential review was published in 1976 that the pervasiveness of Alzheimer's disease in the general population began to be recognized (Katzman, 1976). This review summarized the findings of several physicians who reported that the majority of much older patients being diagnosed with "senile dementia" in the clinic, upon post-mortem examination also exhibited the characteristic neurofibrillary tangles (NFTs) and senile plaques described in Alzheimer's paper.



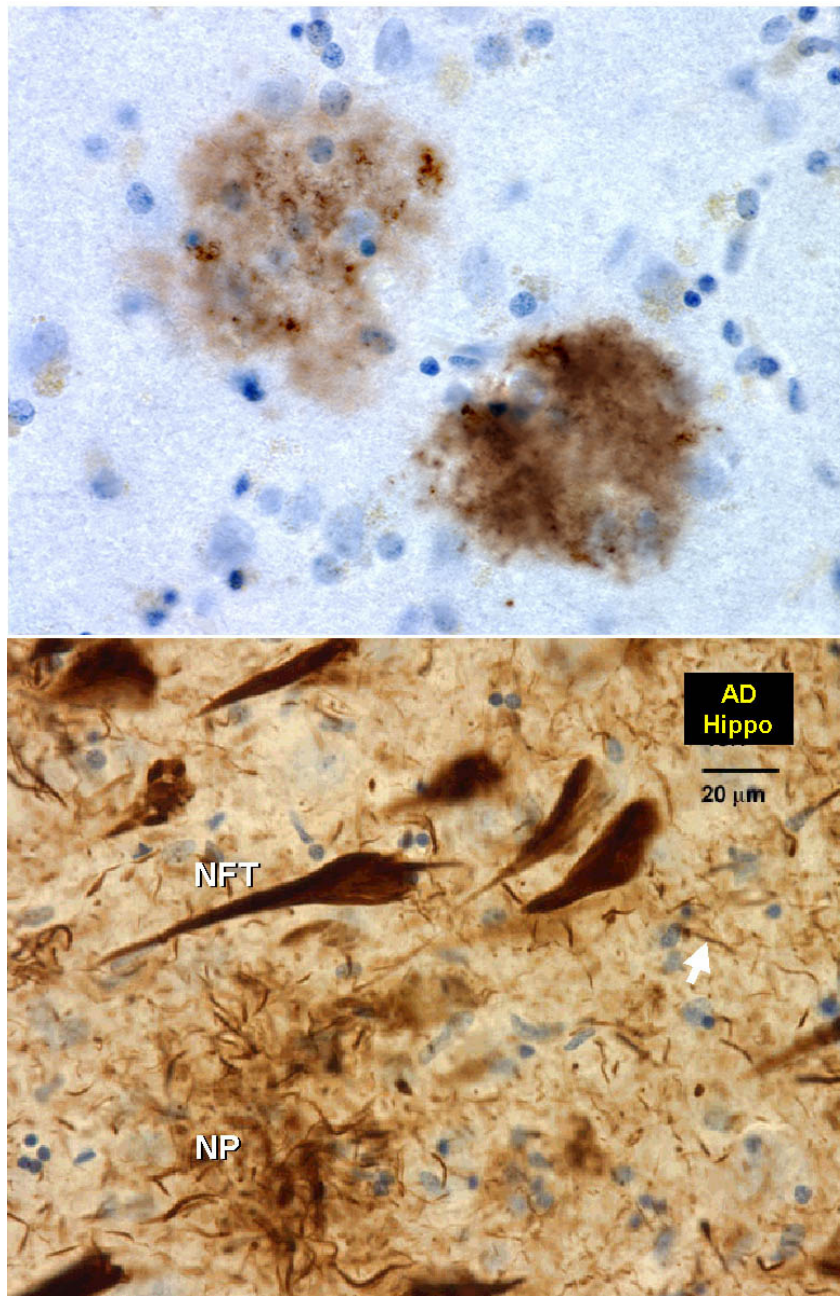


**Figure 1.1: The pathological hallmarks of Alzheimer's disease. (Upper panel)** (courtesy of Jie Zhao) Brightfield image of anti-4G8 stained section from human AD brain. The antibody recognizes dense, extracellular lesions (senile/amyloid plaques), which are composed of  $\beta$ -pleated sheets of amyloid  $\beta$  ( $A\beta$ ) peptide. **(Lower panel)** (courtesy of Skip Binder's lab) Brightfield image of anti-tau 4.6 stained section from human AD brain showing various types of tau pathology in the human AD brain. Notably, intracellular lesions composed of long, hyperphosphorylated and insoluble aggregates of the microtubule-associated protein, tau, which are known as neurofibrillary tangles (NFTs) can be seen, which are characteristic of AD brain.

Today, Alzheimer's disease is the leading cause of dementia in the elderly, affecting 4.5 million people in the United States alone and an estimated 26 million people worldwide. Alzheimer's disease is currently the third most expensive disease in the United States. Ironically, due to medical advances and ever-increasing life-spans in first-world countries, the incidence of Alzheimer's disease is expected to triple within the next fifty years, making this disease a serious socio-economic and medical concern (Alzheimer's Association, 2008).

### **Clinical features of Alzheimer's disease**

Alzheimer's disease is primarily characterized by a progressive loss of memory and impaired cognition. A definitive diagnosis of Alzheimer's disease can only be made post-mortem upon histological identification of both neurofibrillary tangles and senile plaques in the brains of patients suffering from dementia. According to the Diagnostic and Statistical Manual of Mental Illness (DSM-IV), a diagnosis of probable Alzheimer's disease (PRAD) or dementia of the Alzheimer's type (DAT) can be made if a patient fits the criteria for dementia, if the profile of dementia fits the "usual" pattern of AD, and if other identifiable causes of dementia have been ruled out. The criteria for dementia include a history of a persistent and progressive decline of cognition, comportment, personality, or daily living activities, scores that fall beyond two standard deviations from age and education matched ranges in one or more neuropsychological tests, and a change of scores in any cognitive domain (memory, language, orientation, praxis, judgement, personality, or problem solving) that exceeds one standard deviation within a six to twelve-month test-retest period. The "usual" pattern of AD includes progressive

memory impairment over a period of 15-20 years, beginning with mild impairment in the recall of recent events, finally progressing to impairment in other cognitive domains, such as language, reasoning, spatial orientation, and executive function, in addition to more severe impairments in memory. Sensory and motor functions remain preserved until the end stages of the disease, and death usually results from cardiopulmonary arrest or complications of infection. The rare, dominantly-inherited familial form of Alzheimer's disease (FAD) accounts for less than 5% of all Alzheimer's disease cases and results from mutations occurring on chromosomes 1, 14, and 21. Age of onset in these patients most commonly occurs in a patient's 50's, although onset of dementia has been reported as early as 30 years old, in some cases. The more common, sporadic form of Alzheimer's disease (SAD) generally occurs later in life, most commonly after age 80. The pathology and progression of SAD is identical to that of FAD; however, the specific cause(s) of SAD remain unknown (Mesulam, 2000). There are a number of known genetic and environmental risk factors for developing SAD. The primary risk factor for developing SAD is age; indeed, the risk for developing AD becomes exponentially higher with increasing age. The most common genetic risk factor for developing SAD is carrying the ApoE4 allele, which is estimated to account for at least 50% of all SAD cases. Three different isoforms of the ApoE gene exist in the human population ( $\epsilon 2$ ,  $\epsilon 3$ , and  $\epsilon 4$ ). By age 80, 91.3% of  $\epsilon 4/\epsilon 4$  homozygotes have developed SAD and 47.8% of people with the  $\epsilon 3/\epsilon 4$  genotype, whereas only 20% of individuals without an  $\epsilon 4$  allele have developed SAD by this age (Ashford, 2004; Corder et al., 1993). People with high serum cholesterol levels are also at a three times increased risk for developing SAD (Notkola et al., 1998). Conversely, individuals taking

cholesterol-lowering drugs, such as statins, have a 70% reduced risk of developing SAD (Wolozin et al., 2000). Women also appear to be at a greater risk for developing Alzheimer's disease than men, although the relative risk for women versus men varies greatly across studies. This is thought to occur as a result of estrogen loss after menopause; however, a recent study of the effect of hormone replacement therapy on reducing the risk of Alzheimer's disease yielded discouraging results (Baum, 2005). Other factors that appear to be associated with SAD incidence include atherosclerosis, traumatic brain injury, and education level (Casselerly and Topol, 2004; Stern, 2006; Van Den Heuvel et al., 2007).

## **The molecular pathology of Alzheimer's disease: Plaques and tangles**

Once the pervasiveness of Alzheimer's disease in the general population was recognized, scientific interest in the disorder began to grow. Furthermore, advances in molecular biological and biochemical technology made intensive investigation into the molecular pathogenesis underlying the disorder possible. The intraneuronal NFTs were finally shown to be composed of the microtubule-associated protein, tau (Brion, 2006; Kosik et al., 1986; Nukina and Ihara, 1986; Wood et al., 1986). During the course of neurodegeneration, the tau protein dissociates from the microtubule and becomes cleaved and progressively hyperphosphorylated, eventually forming long, insoluble filaments, which are presumably toxic to the neurons in which they reside. Inherited mutations in tau do not cause familial Alzheimer's disease, but another

neurodegenerative disorder known as frontotemporal dementia (FTD) (Binder et al., 2005). The second, extracellular lesion in AD brain, known as senile or amyloid plaques, was shown to be composed of the protein amyloid  $\beta$  ( $A\beta$ ) (Glennner and Wong, 1984a, b; Masters et al., 1985). Dysregulation in  $A\beta$  homeostasis is thought to be upstream of tau dysregulation in the chronology of AD pathology, because all FAD mutations directly affect the production of the  $A\beta$  peptide in the brain, indicating that this is the first pathological event that occurs. This theory is known as the “amyloid cascade hypothesis” (Hardy and Selkoe, 2002). Surprisingly, despite the overwhelming genetic evidence of the involvement of  $A\beta$  in AD pathology, it has been noted that the number of senile plaques in AD brains correlates poorly with the degree of dementia. In fact, it has long been known that the number of NFTs in AD brains is a much better predictor of the degree of dementia (Wilcock and Esiri, 1982). This observation led to the hypothesis that senile plaques themselves are not actually toxic, and there exists some other form of aggregated  $A\beta$  mediating neuronal toxicity and triggering downstream pathology. An emerging theory is that a soluble oligomeric form of  $A\beta$  is actually the toxic intermediary, and the insoluble fibrils that comprise senile plaques are relatively inert (Walsh and Selkoe, 2007). In support of this theory, more recent studies have shown that quantifications of soluble forms of  $A\beta$  in the brain correlate quite well with the degree of dementia in AD patients, in contrast to total plaque number (Lue et al., 1999; McLean et al., 1999; Naslund et al., 2000; Wang et al., 1999). It is thought that  $A\beta$  overproduction or amyloid pathology somehow directly or indirectly triggers tau pathology, because both lesions always occur together in AD, both in the sporadic and the inherited forms of the disease. However, the exact mechanism(s) by which  $A\beta$  triggers tau dysfunction

remains an area of intense investigation (Blurton-Jones and Laferla, 2006). Similarly, the relative contribution of each lesion to neurodegeneration and subsequent memory impairment associated with AD continues to be debated; however, the interdependence of tau and amyloid in the development of AD pathology and neuronal dysfunction is quite clear from both *in vitro* experiments and animal models. Amyloid pathology appears to exacerbate tau pathology *in vivo* (Gotz et al., 2001; Lewis et al., 2001). Conversely, the toxicity of A $\beta$  on cultured neurons appears to be lost in the absence of tau (Rapoport et al., 2002).

### **Amyloid $\beta$ : The primary component of senile plaques**

A $\beta$  is produced *via* the sequential proteolysis of amyloid precursor protein (APP) by  $\beta$ - and  $\gamma$ -secretases. APP is a large, ubiquitously expressed Type I transmembrane protein of unknown function (Panegyres, 2001). During the first step of A $\beta$  production, full-length APP is cleaved at its N-terminus by  $\beta$ -secretase either in the trans-Golgi network or in endosomes.  $\beta$ -secretase cleavage of APP produces a long, secreted fragment, APPs $\beta$ , and a short, membrane-bound fragment, C99. C99 then becomes a cleavage substrate for the  $\gamma$ -secretase complex, which is composed of presenillin 1 and 2 (which comprise the active site of the complex), Aph-1, PEN-2, and nicastrin.  $\gamma$ -secretase activity also appears to occur within the trans-Golgi network (TGN) and endosomes. Intramembraneous cleavage of C99 by  $\gamma$ -secretase liberates the A $\beta$  peptide (De Strooper, 2003; Sisodia and St George-Hyslop, 2002). The vast majority of A $\beta$  produced by  $\gamma$ -secretase cleavage of C99 is 40 amino acids in length (A $\beta$ 40); however, a small fraction of the A $\beta$  produced is 42 amino acids in length (A $\beta$ 42). It is

clear that the A $\beta$ 42 isoform is more fibrillogenic and more readily initiates amyloid plaque formation than the predominant A $\beta$ 40 isoform; however, the reason for this is unknown (Hardy and Selkoe, 2002). In an alternate, competing pathway, APP is cleaved at its N-terminus by  $\alpha$ -secretase, which has been shown to consist of the combined activities of several metalloproteases and the BACE1 homologue, BACE2.  $\alpha$ -secretase cleavage of APP occurs at the plasma membrane through a process known as ectodomain shedding.  $\alpha$ -secretase cleaves APP within the A $\beta$  domain, thus precluding A $\beta$  formation and is therefore considered to be non-amyloidogenic.  $\alpha$ -secretase cleavage of APP produces the long secreted fragment, APPs $\alpha$ , and the short, membrane-bound fragment C83. C83 then becomes a substrate for  $\gamma$ -secretase, which liberates the soluble and presumably non-toxic p3 peptide (Deuss et al., 2008) (Fig 1.2). It is also worth noting that the C-terminal APP fragment produced from  $\gamma$ -secretase cleavage of C83 or C99, the APP intracellular domain (AICD), is being investigated by several groups, due to its postulated role as a transcription factor (Muller et al., 2008). The involvement of the AICD in cellular transcription is hypothesized based on its homology to the Notch intracellular domain (NICD), which is produced from the developmental protein Notch, an alternative  $\gamma$ -secretase substrate (De Strooper et al., 1999). The importance of the NICD in transcription is evidenced by the embryonic lethal phenotype of PS1 knock-out mice, which develop severe developmental abnormalities due to deficiencies in Notch cleavage (De Strooper et al., 1998). An equivalent essential role for the AICD in cellular transcription has never been clearly demonstrated; however, this could be due to compensatory activity of other APP family

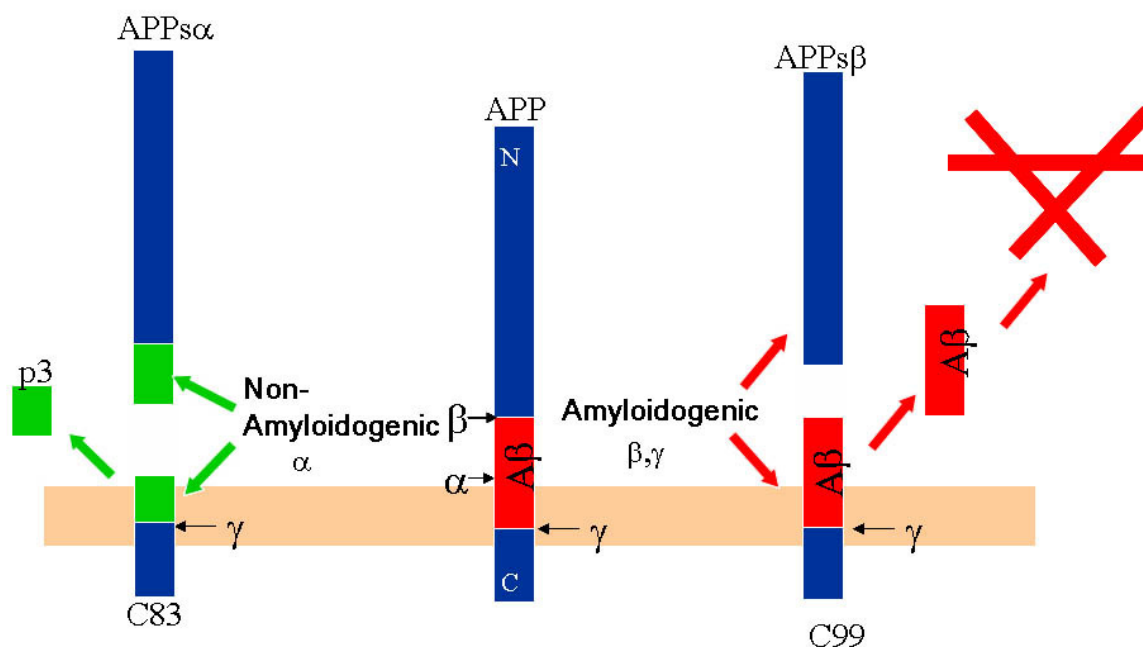


**Figure 1.2: Amyloid Precursor Protein (APP) Processing.** (courtesy of Sarah Cole)

Amyloid precursor protein (APP) is a ubiquitously expressed Type I membrane protein of unknown function that undergoes a series of complex proteolytic cleavages in neurons to form the A $\beta$  peptide associated with senile plaques in Alzheimer's disease. In the pro-amyloidogenic pathway, APP is cleaved at its N-terminus by  $\beta$ -secretase (BACE1) to form APPs $\beta$  and C99. C99 is cleaved intramembranously by the  $\gamma$ -secretase complex (PS1, PS2, Aph-1, PEN2, and nicastrin), liberating A $\beta$ 40 (or A $\beta$ 42 at a low frequency) and the APP intracellular domain (AICD). In the competing, non-amyloidogenic pathway,  $\alpha$ -secretase (TACE, ADAM10, BACE2) cleaves APP at its N-terminus to liberate APPs $\alpha$  and C83. C83 is cleaved by  $\gamma$ -secretase to form the soluble p3 peptide and the AICD.



members (e.g.- the APP-like proteins APLP1 and APLP2). With regard to A $\beta$ , it is important to note that production of this peptide is not a purely pathological event. Both amyloidogenic and non-amyloidogenic processing of APP occur homeostatically in normal neurons, although the normal function of A $\beta$  in the brain remains unknown. Mice that do not produce A $\beta$  (e.g. - APP and BACE1 knock-outs) are viable and exhibit no severe phenotypic abnormalities (Luo et al., 2001; Zheng et al., 1996). The role of A $\beta$  in amyloid pathology, on the other hand, is quite clear. A $\beta$  production may become pathological when APP processing is altered in such a way as to favor the amyloidogenic pathway and/or shift the ratio of A $\beta$ <sub>40</sub>:A $\beta$ <sub>42</sub> production in favor of A $\beta$ <sub>42</sub>. Dominantly-inherited mutations that cause FAD support this hypothesis. Mutations in APP (chromosome 21) occur around the  $\beta$ -secretase cleavage site. These mutations enhance the efficiency of  $\beta$ -secretase cleavage of APP, thereby accelerating A $\beta$  production. Other FAD mutations occur around the  $\gamma$ -secretase cleavage site of APP or in the genes PS1 or PS2, which encode the proteins that comprise the active site of the  $\gamma$ -secretase complex. These mutations alter  $\gamma$ -secretase cleavage of APP to favor A $\beta$ <sub>42</sub> production instead of A $\beta$ <sub>40</sub>, presumably promoting deposition and fibrillogenesis of A $\beta$  into oligomeric entities and senile plaques (Hardy and Selkoe, 2002). Furthermore, overexpression of APP in the absence of aberrant processing also appears to be sufficient to trigger plaque deposition, since Down's syndrome patients form plaques and tangles in the brain and develop memory impairments reminiscent of Alzheimer's disease due to a duplication of the APP gene on chromosome 21 (Beyreuther et al., 1993).

## **BACE1: Identifying the $\beta$ -secretase**

It was evident from a comparison of the protein sequences of APP, A $\beta$ , and other APP fragments that A $\beta$  was formed from APP through a complex series of proteolytic cleavages (Delabar et al., 1987; Glenner and Wong, 1984b; Goldgaber et al., 1987; Kang et al., 1987; Masters et al., 1985; St George-Hyslop et al., 1987). The initial N-terminal APP cleavage confirmed *in vitro* was at the  $\alpha$ -secretase site, which occurs within the A $\beta$  domain (Esch et al., 1990). Initially, non-amyloidogenic processing of APP was considered to be the constitutive cleavage pathway in normal neurons, and it was hypothesized that  $\beta$ -site cleavage of APP only occurred under pathologic conditions. This was later shown not to be true, since normal healthy neurons appeared to be capable of cleaving APP at both the  $\alpha$ - and the  $\beta$ -cleavage sites. (Busciglio et al., 1993; Haass et al., 1992; Seubert et al., 1993; Seubert et al., 1992; Shoji et al., 1992). As the rate-limiting enzyme in the amyloidogenic pathway, it was clear that the  $\beta$ -secretase played a crucial role in Alzheimer's disease pathogenesis. Abolishing  $\beta$ -secretase activity would presumably prevent the production of A $\beta$  and hence render the brain unable to develop amyloid pathology. The therapeutic potential of modulating the enzyme responsible for  $\beta$ -secretase activity was widely recognized, and therefore determining the identity of the enzyme responsible for  $\beta$ -secretase activity became an area of intense investigation. Early reports indicated that the cathepsins might have  $\beta$ -secretase-like activity (Austen and Stephens, 1995; Mackay et al., 1997; Tagawa et al., 1991); however it was later determined that cathepsin more likely exerted its effects on A $\beta$  homeostasis through degradation mechanisms in the lysosomes (Schonlein et al., 1993). Furthermore, amyloidogenic processing of APP remained

intact in mice devoid of cathepsin, effectively ruling these enzymes out as candidate  $\beta$ -secretases (Saftig et al., 1996). A novel, membrane-bound aspartic protease was finally identified as the authentic  $\beta$ -secretase which was named beta-site APP cleaving enzyme 1 (BACE1) (Vassar et al., 1999). BACE1 was identified using an expression cloning screen of a human cDNA library for genes that enhanced A $\beta$  production in APP-overexpressing cells. A good deal of effort had already been devoted to characterizing the  $\beta$ -secretase prior to its identification (Citron et al., 1996; Citron et al., 1995; Gouras et al., 1998; Haass et al., 1995a; Haass et al., 1993; Haass et al., 1995b; Haass et al., 1992; Knops et al., 1995; Koo and Squazzo, 1994; Roher et al., 1993; Seubert et al., 1993; Zhao et al., 1996). It was hypothesized that the  $\beta$ -secretase would have several characteristics, including close membrane association, luminal and endocytic activity, high neuronal expression, and insensitivity to pepstatin. BACE1 exhibited all of these characteristics. Importantly, BACE1 appeared to cleave APP at the predicted  $\beta$ -secretase site, and overexpression or inhibition of BACE1 enhanced or reduced the production of  $\beta$ -site APP cleavage fragments in the expected manner. Unlike  $\alpha$ -secretase,  $\beta$ -secretase activity appeared to result exclusively from BACE1 cleavage of APP, since mice genetically devoid of BACE1 did not produce any detectable endogenous A $\beta$  in the brain (Luo et al., 2001). Further characterization of BACE1 revealed that it is a Type I transmembrane protein 501 amino acids in length with a luminal catalytic domain comprised of two aspartic protease active site motifs. BACE1 is produced as an inactive pro-enzyme, which is cleaved by furin at its N-terminus to produce the mature, active form of BACE1. The mature enzyme contains four N-glycosylation sites and 3 disulfide bridges (Haniu et al., 2000). This same aspartic

protease was independently identified as the  $\beta$ -secretase by several other groups using different methods shortly thereafter (memapsin 2, Asp2), further establishing BACE1 as the authentic  $\beta$ -secretase (Hussain et al., 1999; Lin et al., 2000; Sinha et al., 1999; Yan et al., 1999). Interestingly, subsequent research on BACE1 has revealed that APP is not the only cleavage substrate of this enzyme. BACE1 appears to cleave several other proteins, including neuregulin 1 (NRG1), the APP-like proteins (APLP1 and APLP2), the  $\beta$ 2-subunit of the voltage-gated sodium channel ( $\text{Na}_v1\ \beta$ 2), lipoprotein receptor-related protein (LRP), P-selectin glycoprotein ligand 1 (PSGL1),  $\beta$ -galactoside- $\alpha$ -2,6-sialyltransferase (S6Gal1), and the interleukin-1 receptor II (IL1-R2) (Hu et al., 2006; Kim et al., 2007; Kitazume et al., 2005; Kuhn et al., 2007; Li and Sudhof, 2004; Lichtenthaler et al., 2003; Pastorino et al., 2004; von Arnim et al., 2005; Willem et al., 2004; Wong et al., 2005). These alternative BACE1 substrates may provide further insight into the true physiological function of this enzyme in the future.

## **BACE1 as a drug target for AD**

It became evident shortly after its discovery that BACE1, as suspected, was indeed an ideal AD drug target. BACE1 knock-out mice failed to produce any endogenous  $\text{A}\beta$ , indicating that inhibition of BACE1 would completely eliminate  $\text{A}\beta$  production in the brain. Importantly, BACE1 knock-out mice exhibited no signs of major physiological or behavioral abnormalities, indicating that BACE1 inhibitors, once developed, would lack any serious side effects (Luo et al., 2001). More recent studies using transgenic models of AD have confirmed that complete BACE1 inhibition prevents the development of amyloid pathology in the brain. Tg2576 mice, which overexpress human APP with the

$\beta$ -site mutation (a.k.a. the “Swedish” mutation [APP<sup>sw</sup>]), normally develop modest amyloid plaque pathology in the brain beginning at approximately nine months of age (Hsiao et al., 1996). Tg2576 mice crossed with BACE1 <sup>-/-</sup> mice failed to produce any form of A $\beta$  and failed to develop amyloid plaque pathology at any age. Furthermore, BACE1 deletion appeared to prevent memory impairments normally apparent in this mouse model, indicating that BACE1 inhibition was capable of ameliorating the clinical symptoms of AD (Ohno et al., 2004). Similar results were obtained by crossing a more aggressive model of amyloid pathology, Tg6799 or “5XFAD” mice, with BACE1 <sup>-/-</sup> mice. In addition, BACE1 deletion was able to prevent neuronal loss, which is normally a major phenotype in 5XFAD brains, and is also a hallmark of human AD pathology (Ohno et al., 2006). Preliminary evidence indicates that BACE1 inhibition is also capable of reversing amyloid pathology once it has already started; however, it unclear whether partial inhibition of BACE1 can significantly slow the rate of amyloid plaque development (Laird et al., 2005; McConlogue et al., 2007; Singer et al., 2005). There are no BACE1 inhibitors currently being used to treat AD in humans. However, the development of BACE1 inhibitors suitable for use in humans is a major endeavor being undertaken by several pharmaceutical companies, as well as individual laboratories (Ghosh et al., 2007).

## **BACE1 and sporadic Alzheimer’s disease**

The amyloid cascade hypothesis states that A $\beta$ <sub>42</sub> overproduction is the first in a long series of pathological events that ultimately lead to neurodegeneration associated with AD. This theory relies on evidence from FAD mutations which directly alter A $\beta$

production; however FAD accounts for less than 5% of all AD cases. The vast majority of AD cases are sporadic. Although many risk factors for SAD have been identified, the molecular mechanisms by which these genetic and environmental factors might alter APP processing remain completely unknown. Similarly, much effort has been devoted to validating BACE1 as a drug target for AD; however, the normal function and regulation of this enzyme in the human brain, as well as whether it plays a causal role in SAD pathogenesis are areas of research that have been uninvestigated up until fairly recently. It is clear from studies on the effect of the APP<sup>sw</sup> FAD mutation on APP processing that enhanced BACE1 activity is sufficient to cause FAD (Citron et al., 1992). Whether BACE1 may also play a role in SAD is unclear; however, considering the crucial role this enzyme plays in the amyloidogenic process, it is logical to suspect that factors that are responsible for influencing BACE1 levels and activity normally in the brain could also be involved in the onset of SAD pathogenesis. In support of this hypothesis, several recent studies have reported that BACE1 protein is often elevated in the brains of AD patients compared to age-matched, non-demented controls (Fukumoto et al., 2002; Holsinger et al., 2002; Li et al., 2004; Tyler et al., 2002; Yang et al., 2003; Zhao et al., 2007). Strikingly, immunohistochemical analysis showed that the BACE1 increase in AD brains occurs primarily around the senile plaques, implying a causal role for this enzyme in sporadic amyloid pathology (Zhao et al., 2007). The specific cause and functional significance of BACE1 elevations in AD brain, however, remain unknown.

## Regulation of BACE1

BACE1 mRNA is expressed at low levels in most tissues, with higher expression in the brain and pancreas (Vassar et al., 1999). In the brain, BACE1 mRNA is predominantly neuronal, with low astrocytic expression (Zhao et al., 1996). BACE1 protein exhibits a pan-neuronal expression pattern in the brain, with highest expression in the cortex and hippocampus. Interestingly, immunohistochemical analysis reveals particularly intense BACE1 staining in the mossy fiber pathway of the dentate gyrus (Zhao et al., 2007) (Fig 1.3C). Upon closer microscopic examination, the BACE1 neuronal localization appears to be pre-synaptic (Zhao et al., 2007). Computer analysis of the BACE1 promoter region predicts binding sites for numerous transcription factors (TFs), indicating that BACE1 gene expression is regulatable in response to cell signals that alter gene transcription (Sambamurti et al., 2004). However, very few of these TF interactions with the BACE1 promoter have actually been confirmed. BACE1 mRNA has been reported to be increased in response to oxidative damage, TBI, and hypoxia (Blasko et al., 2004; Sun et al., 2006; Tamagno et al., 2005; Xue et al., 2006; Zhang et al., 2007). Recently, a mechanism was described by which the cyclin-dependent kinase cdk5 becomes aberrantly activated due to cleavage of p35  $\rightarrow$  p25 (a neurodegenerative event) and elevates BACE1 mRNA levels, possibly through the activation of the transcription factor STAT1 (Wen et al., 2008). Full-length BACE1 mRNA contains 9 exons and gives rise to a full-length transcript ~6kb in length (Vassar et al., 1999). There are three BACE1 splice variants that lack parts of exons 3 and 4 (BACE-I-476, BACE-I-457, and BACE-I-432), as well as BACE1 transcripts that differ in length at the 3'UTR. The three isoforms

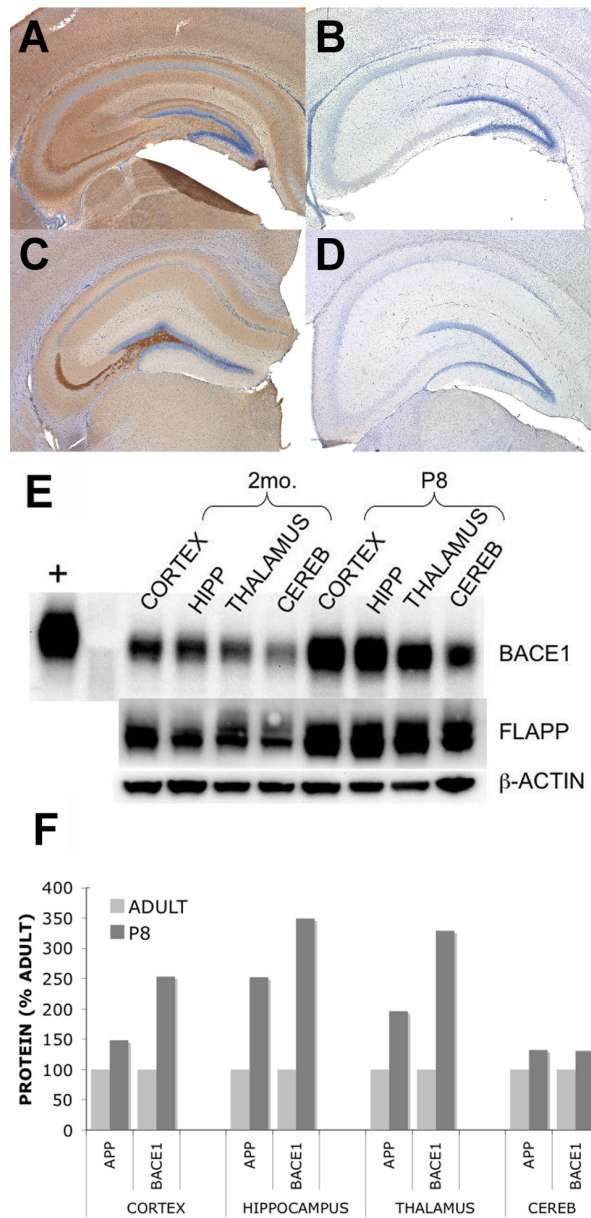


**Figure 1.3: Endogenous BACE1 and APP are elevated in all postnatal brain regions.** Different brain regions from wild-type C57/BL6 postnatal day 8 (P8) and 2 month-old adult mice were analyzed for BACE1 and APP protein expression. **(A-D)** Coronal brain sections from C57/BL6 mice were immunostained with anti-BACE1 antibody (3D5). **(A)** P8 BACE1 +/+ **(B)** P8 BACE1 -/- **(C)** Adult BACE1 +/+ **(D)** Adult BACE1 -/-. **(E)** 10µg protein from different brain regions from C57/BL6 mice were separated *via* SDS-PAGE and analyzed for BACE1 (3D5) and full-length APP (22C11; FLAPP) protein expression *via* immunoblot. **(F)** BACE1 and FLAPP immunosignals were normalized to β-actin and expressed as % Adult brain. BACE1 and FLAPP protein expression were higher in P8 brains compared to adult in all brain regions analyzed. (n=1)



of BACE1 mRNA that differ from full-length BACE1 within the coding region give rise to BACE1 protein variants with reduced or absent enzymatic activity, altered glycosylation, and inhibited transport along the secretory pathway (Bodendorf et al., 2001; Ehehalt et al., 2002; Tanahashi and Tabira, 2001; Zohar et al., 2003). Notably, BACE-I-457, which has no detectable  $\beta$ -secretase activity, is the major transcript expressed in the pancreas, which explains why the pancreas exhibits low  $\beta$ -secretase activity despite robust BACE1 mRNA expression (Bodendorf et al., 2001). The functional significance of these BACE1 splice variants is unknown. The possible role of BACE1 transcription in AD has also been largely unaddressed; however, there is one report of increased BACE1 mRNA levels in AD brains as well as a report that the full-length active BACE1 transcript is preferentially transcribed in Tg2576 brains (Li et al., 2004; Zohar et al., 2005). Post-transcriptional regulation of BACE1 has recently emerged as a topic of intense study due to the observation that BACE1 protein is consistently elevated in AD brains without an apparent corresponding increase in BACE1 mRNA levels (Fukumoto et al., 2002; Holsinger et al., 2002; Tyler et al., 2002; Yang et al., 2003; Zhao et al., 2007). Several groups are investigating the potential role of translational regulation in modulating BACE1 protein levels due to the long, unstructured, G-C-rich 5'UTR of the BACE1 transcript, which is a likely target for translational regulation. The BACE1 5'UTR is inhibitory to BACE1 translation, resulting in very low BACE1 protein expression under normal conditions (De Pietri Tonelli et al., 2004; Lammich et al., 2004; Mihailovich et al., 2007; Rogers et al., 2004; Zhou and Song, 2006). This can occur through several different mechanisms (Schroder and Kaufman, 2006). The specific mechanism that controls BACE1 translation continues to

be debated; however, it appears likely that the formation of secondary structure or the presence of inhibitory uORFs or a combination of both keep BACE1 protein levels at a minimum under normal conditions. This type of translational inhibition by the 5'UTR is characteristic of proteins involved in growth, differentiation, and stress response, which is interesting, because BACE1 has a proposed function in all of these processes. For example, BACE1 protein is dramatically up-regulated in early postnatal brains compared to adult (Fig 1.4A & B) (Chiocco et al., 2004; Chiocco et al., 2007; Willem et al., 2006). This appears to occur through an unidentified post-transcriptional mechanism (Fig 1.3C). Similarly, BACE1 protein is post-transcriptionally elevated in mouse models of amyloid pathology (Zhao et al., 2007). These two lines of evidence indicate that BACE1 could be translationally controlled during development and also in response to stress stimuli. Translational de-repression of BACE1 has been demonstrated in activated astrocytes, indicating that stress-induced alterations in the translational machinery and enhanced BACE1 translation could be involved in the development of AD pathogenesis (De Pietri Tonelli et al., 2004). Another type of post-transcriptional regulation that has gained recent attention is the control of mRNA stability or translation through the binding of microRNAs to the 3'UTRs of transcripts. The full-length BACE1 transcript has a long 3'UTR (~4kb), which is a prime target for microRNA-mediated regulation. Four microRNAs (miR-107, miR-9, miR-29a, and miR-29b) have already been reported to bind to the BACE1 transcript. Furthermore, three of these microRNAs were reported to be downregulated and inversely correlated with BACE1 mRNA levels in AD brains (Hebert et al., 2008; Wang et al., 2008b). However,

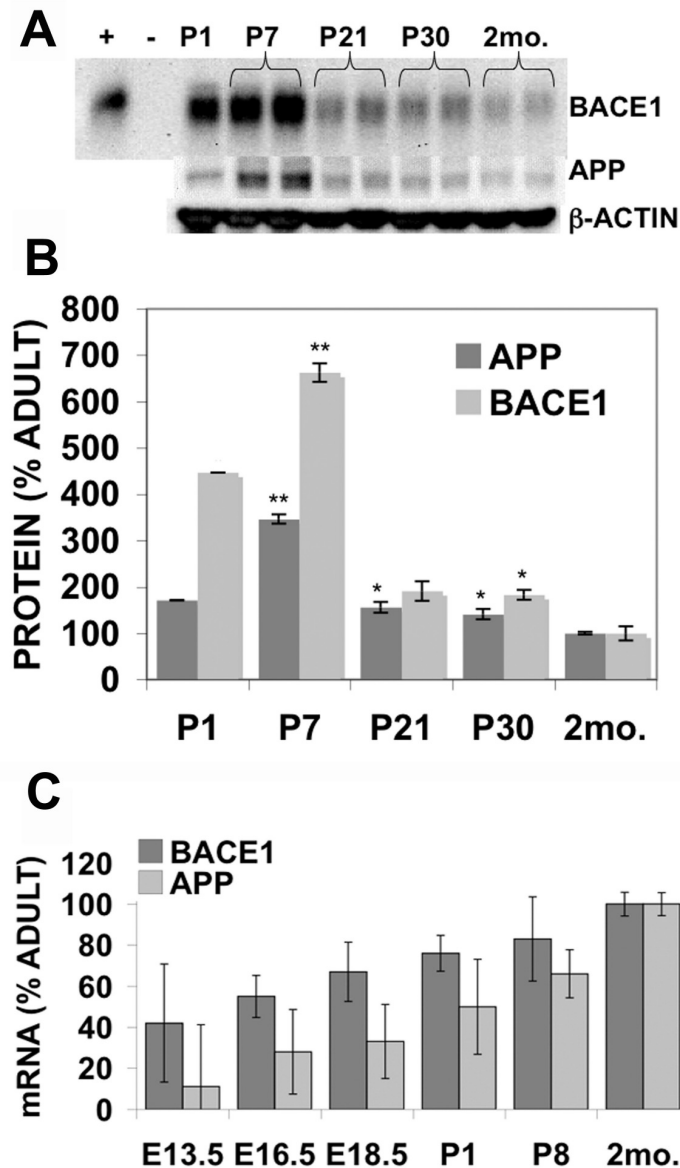


**Figure 1.4: Endogenous BACE1 and APP are elevated in postnatal brain *via* a post-transcriptional mechanism.** (A) 15µg protein from C57/BL6 pups (P1, P7, P21, and P30) and adult (2 mo.) brains were resolved by SDS-PAGE and immunoblotted for BACE1 (3D5) or full-length APP (22C11; FLAPP). (B) BACE1 and FLAPP immunosignals were normalized to β-actin and expressed as % Adult. (n=1-2) (C) Endogenous BACE1 and APP mRNA from embryonic (E13.5, E16.5, E18.5), postnatal (P1 and P8), or adult (2 mo.) C57/BL6 brain were amplified *via* Real Time PCR, normalized to 18s rRNA, and expressed as % Adult. (n=2-5) \*p < 0.05, \*\*p < 0.01. BACE1 and APP protein was elevated in the brains of postnatal mice, but not BACE1 or APP mRNA.

the proposed mechanisms by which microRNAs regulate BACE1 protein levels in each of these studies were quite different. The Hebert et al. study hypothesized that microRNAs regulated the rate of BACE1 translation, since expression of miR-29a, miR-29b, or miR-9 had no effect on BACE1 transcript levels. In contrast, the Wang et al. study concluded that microRNAs could influence both BACE1 mRNA and BACE1 protein levels by regulating BACE1 mRNA stability. Another related mechanism that has recently been reported is the expression of non-coding BACE1 antisense mRNAs which bind to the BACE1 transcript and enhance its stability (Faghihi et al., 2008). Although miRNAs and antisense mRNAs are potentially important in regulating BACE1 protein levels, it is important to note that increased mRNA stability cannot explain the apparent absence of BACE1 mRNA up-regulation in AD brain. Regulation of BACE1 at the level of protein stability has also been investigated. There is one report that inhibition of the proteasome causes BACE1 protein to accumulate, suggesting that BACE1 protein stability may be dependent on the ubiquitin-proteasome pathway (Qing et al., 2004). Other reports indicate that BACE1 may be degraded *via* the lysosomal pathway. Apparently, BACE1 protein is normally shuttled to the lysosome for degradation *via* binding to the adaptor protein GGA3. During apoptosis, pro-caspase 3 becomes activated and cleaves GGA3, reducing the rate of BACE1 trafficking to lysosomes and leading to extended BACE1 protein half-life (Koh et al., 2005; Tesco et al., 2007; Vassar, 2007). Other studies have stressed the importance of BACE1 binding partners, BACE1 post-translational modification, and BACE1/APP cellular localization as major regulators of  $\beta$ -secretase-dependent cleavage of APP (Cole et al., 2005; He et al., 2004; Miller et al., 2006; Rogaeva et al., 2007; Walter et al., 2001). Since  $\alpha$  and  $\beta$ -

secretase cleavage of APP are competing pathways that occur in separate cellular compartments, factors that affect cellular trafficking of BACE1 can dramatically alter the balance between amyloidogenic and non-amyloidogenic processing of APP.

## **Energy metabolism and Alzheimer's disease**

One factor that appears to be closely associated with AD is impaired cerebral energy metabolism. Positron emission tomography (PET) imaging studies have consistently shown that glucose utilization is dramatically lower in AD brain than in age-matched, non-demented brain (de Leon et al., 2007; Mosconi et al., 2007). Moreover, post-mortem analysis of AD brain shows down-regulated expression of mitochondrial enzymes (de Leon et al., 1983; Rapoport, 1999a, b), further indicating that energy metabolism may be deficient in AD. Importantly, young and middle-aged non-demented carriers of the ApoE4 allele (a major genetic risk factor for SAD), and patients with mild cognitive impairment (MCI), a condition that precedes clinical AD, also exhibit reduced brain glucose utilization by PET imaging (Reiman et al., 2004; Wolf et al., 2003), suggesting that impaired cerebral energy metabolism may be an early event in AD pathogenesis rather than a downstream consequence of neuronal loss in the brain. All of the major risk factors for developing SAD appear to be linked by their potential to reduce blood flow and hence energy supplies to the brain or their association with developing a condition with this capability. Common cardiovascular risk factors for SAD, such as high serum cholesterol levels and atherosclerosis, reduce blood flow to major organ systems due to progressive build-up of fatty materials in blood vessels, as evidenced by the propensity of individuals with these conditions to experience strokes

and heart attacks (American Heart Association, 2008). However, even in the absence of major infarcts or cell death, it is likely that individuals with these conditions have chronically reduced blood flow and oxygen delivery to key organ systems, and this may trigger a cellular stress response in organs with high metabolic demand, such as the brain. Traumatic brain injury is another risk factor for SAD that can directly disrupt the vasculature and metabolic state of the brain (Xiong et al., 2001). Other risk factors for SAD may not directly cause impaired energy metabolism in the brain; however, they are all closely associated with cardiovascular diseases. For example the primary risk factor for SAD, aging, is also a major risk factor for developing cardio- and cerebrovascular disease (Decarli, 2004). Intriguingly, the most common genetic risk factor for developing SAD, the apolipoprotein E4 allele (ApoE4), encodes a specific isoform of a lipid transport protein that is strongly associated with both atherosclerosis and high serum cholesterol levels, leading many to postulate that this may be the mechanism by which ApoE4 contributes to increased risk of developing SAD (Mahley and Rall, 2000; Notkola et al., 1998). Indeed, the dramatically lowered risk of developing SAD due to statin treatment, regardless of ApoE genotype, indicates that high serum cholesterol plays a causal role in SAD pathogenesis, rather than merely being associated with the ApoE4 allele (Wolozin et al., 2006). This combined data implies that chronically reduced glucose and oxygen delivery to the brain may be the commonality underlying these heterogeneous risk factors, which may all trigger amyloidogenesis through the same unknown molecular mechanism. In support of this theory, it has been reported that energy inhibition can directly influence APP processing at the molecular level *in vitro* (Busciglio et al., 2002; Gasparini et al., 1997; Hoyer et al.,

2005; Webster et al., 1998). Surprisingly, diabetes, a disease that clearly disrupts energy metabolism in the body, is not considered a classic risk factor for developing SAD. However, several studies have shown that diabetes appears to be associated with an increased risk for Alzheimer's disease and other types of cognitive impairment (Luchsinger, 2008). In comparison to other risk factors for SAD, the potential association of diabetes with SAD has not been widely investigated; therefore, the epidemiological evidence to assess this association is lacking. This may explain, in part, why the topic continues to be debated. Moreover, diabetes is associated with a much higher rate of mortality, and SAD most commonly manifests after age 80, which could also lead to difficulty in assessing co-morbidity. Another problem facing epidemiological studies of Alzheimer's disease is the clinical overlap between Alzheimer's disease and other types of dementia. For instance, diabetes appears to be more closely associated with vascular dementia than Alzheimer's disease. Vascular dementia is defined as cognitive dysfunction with clear evidence of cerebrovascular disease that is judged to be etiologically related to the dementia, such as evidence of a stroke (American Psychiatric Association; DSM-IV). However, vascular dementia and Alzheimer's disease share many of the same risk factors and symptoms, making the two disorders difficult to distinguish. Although Alzheimer's disease and vascular dementias are currently considered separate disorders, increasing evidence suggests that the two diseases are closely related (Cole and Vassar, 2008). Clearly, the theory that SAD pathology may actually result from chronic, cumulative metabolic insults to the brain below the threshold which causes immediate neuronal death, is a viable hypothesis that warrants further investigation.

## **The Physiological Function of BACE1**

Despite its well-defined role in AD pathogenesis, the normal physiological function of the BACE1 protein remains enigmatic. One proposed function for BACE1 is in peripheral (and possibly CNS) myelin maintenance, which is thought to occur due to BACE1 cleavage of NRG1. Consistent with this theory, BACE1 knock-out mice exhibit reduced myelin thickness in peripheral nerves and marginally decreased myelin basic protein in the brain, compared to wild-type mice (Hu et al., 2006; Willem et al., 2006)(Fig1.5). NRG1 has other functions in the brain besides myelination, including synapse formation, astrocyte differentiation, neuronal activity, and neuronal migration (Mei and Xiong, 2008). Therefore, it is possible that BACE1 plays a role in these brain functions, as well. BACE1 protein expression is also elevated in early postnatal brain compared to embryo or adult, indicating that BACE1 plays a role during early postnatal brain development, as well (Willem et al., 2006)(Fig 1.4). Interestingly, the peak of BACE1 protein expression in the postnatal brain coincides with the development of the dentate gyrus in rodent brain, suggesting that BACE1 could play a specific role in the development of this particular brain region (Ribak et al., 1985), although the increase appears to occur over the entire brain, indicating a pan-neuronal developmental function of BACE1 (Fig1.3). Another emerging theory is that BACE1 may act as a stress response protein in the brain. Indeed, the predicted transcription factor binding sequences in the BACE1 promoter indicate that its expression is capable of being modulated by a variety of stress stimuli (Sambamurti et al., 2004). Consistent with this finding, fluctuations in BACE1 expression have been reported in response to oxidative



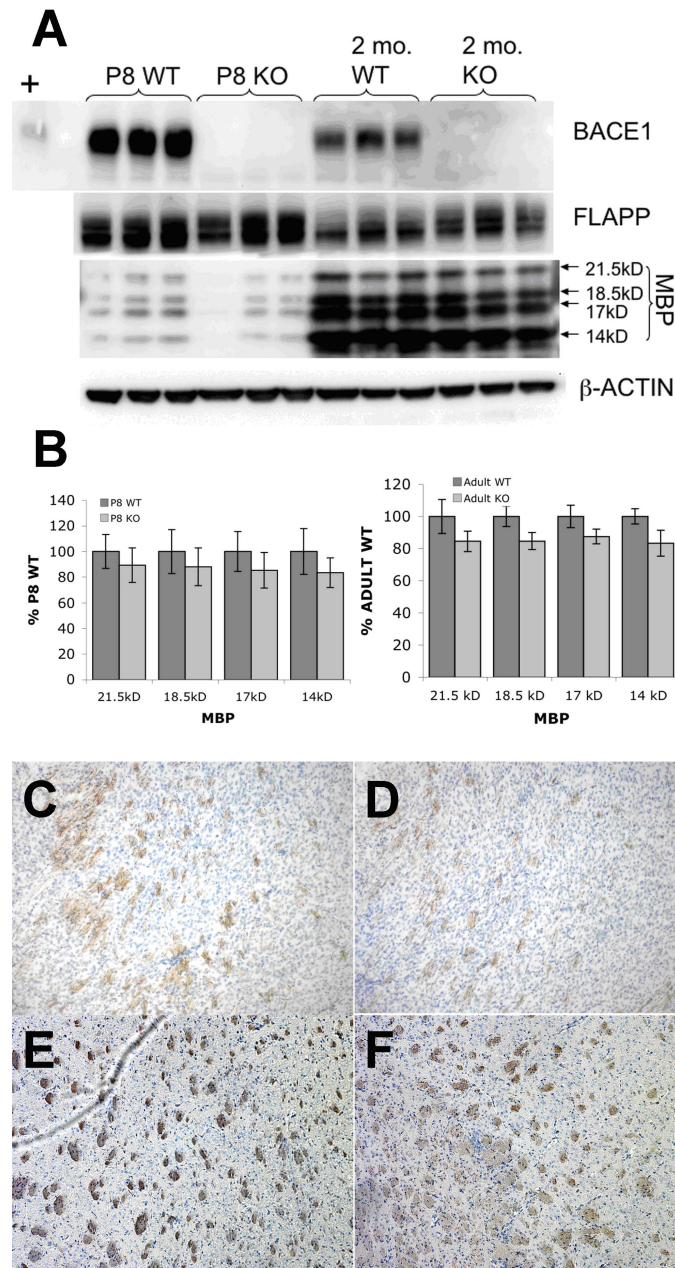


**Figure 1.5: Myelination is reduced in BACE1  $-/-$  mice.** (A) 10 $\mu$ g protein from P8 or 2 mo. C57/BL6 wild-type or BACE1  $-/-$  brain homogenates were separated by SDS-PAGE and immunoblotted with BACE1 (3D5), full-length APP (22C11; FLAPP), or myelin basic protein (MBP; Chemicon) antibodies. (B) BACE1, FLAPP, and MBP immunosignals were normalized to  $\beta$ -actin and expressed as % wild-type (P8 or 2 mo.)  $n=3$  (C-F) Serial sections from P8 or 2 mo. C57/BL6 wild-type or BACE1  $-/-$  brains were immunostained with anti-MBP. (C) P8 wild-type (D) P8 BACE1  $-/-$  (E) 2 mo. wild-type (F) 2 mo. BACE1  $-/-$ . All four isoforms of MBP showed a slight, non-significant decrease in the CNS of both P8 and 2 mo. BACE1  $-/-$  mice compared to wild-type.

stress, ischemia, and traumatic brain injury. (Blasko et al., 2004; Tamagno et al., 2005; Tanahashi and Tabira, 2001; Tesco et al., 2007; Tong et al., 2005; Wen et al., 2004). Interestingly, A $\beta$  itself also appears to be capable of elevating BACE1 protein levels, which may also occur through stress response pathways (Zhao et al., 2007). BACE1 cleavage of APP has been reported to be protective against excitotoxicity *in vitro* (Kamenetz et al., 2003). BACE1's apparent ability to cleave VGSCs may be related to this proposed function. BACE1 is also elevated as a result of cdk5 dysregulation, which is an established marker of cellular distress and neurodegeneration (Wen et al., 2008). The idea that BACE1 may function as a stress response protein in the brain is a particularly attractive one, because it can easily explain how and why BACE1 becomes elevated in SAD. It is logical to hypothesize that upregulated BACE1 in response to acute stress in the brain serves some type of neuroprotective function, either through the production of A $\beta$  itself or through cleavage of one of its other substrates. However, if the stress continually re-occurs, BACE1 and A $\beta$  levels might become chronically elevated, and in the aging brain where clearance and maintenance mechanisms are compromised, A $\beta$  might begin to maladaptively accumulate, eventually leading to the decline of the neuron. The specific type of stress(es) in the brain that might be elevating BACE1 and the mechanism by which this might occur, however, remain unknown.

## Overview of thesis

In order to establish a mechanistic link between energy impairment in the brain, BACE1 levels, and amyloid pathology, we perform a series of energy deprivation experiments

using *in vitro* and *in vivo* models. These experiments uncover a novel stress-induced translational regulatory mechanism controlling BACE1 levels, with important implications for SAD pathogenesis.

- **Chapter 2:** Using an *in vivo* model of acute pharmacological energy deprivation in young mice, we establish post-transcriptional elevations of BACE1 protein and enhanced A $\beta$  production as a biochemical consequence of impaired energy metabolism in the brain.
- **Chapter 3:** Using an *in vitro* model of glucose deprivation in BACE1-overexpressing 293 cells, we identify phosphorylation of the eukaryotic translation initiation factor 2 $\alpha$  (eIF2 $\alpha$ ) *via* the PKR-like endoplasmic reticulum kinase (PERK) as the post-transcriptional mechanism underlying energy deprivation-induced BACE1 protein elevations.
- **Chapter 4:** Using primary cultured neurons, we show that glucose deprivation also elevates endogenous BACE1 protein post-transcriptionally, and we demonstrate that eIF2 $\alpha$  phosphorylation is directly amyloidogenic *in vitro*.
- **Chapter 5:** Using repeated pharmacological administration of metabolic inhibitors in aged transgenic mice, we showed that chronic energy deprivation can accelerate amyloid plaque pathology in the brain.
- **Chapter 6:** We demonstrate that A $\beta$  overproduction can also trigger eIF2 $\alpha$  phosphorylation, which implies the existence of a positive feedback loop in the development of amyloid pathology. Furthermore, we demonstrate that BACE1, eIF2 $\alpha$  phosphorylation, and amyloid pathology are all correlated in human AD brains, indicating that the novel eIF2 $\alpha$  mechanism is relevant to human disease.

- **Chapter 7:** We provide background information on the translational control of proteins with a focus on eIF2 $\alpha$  phosphorylation. We also discuss the role of eIF2 $\alpha$  phosphorylation in the brain, the possible physiological function of energy deprivation-induced BACE1 up-regulation, and how the dysregulation of this physiological function might result in SAD.

## CHAPTER 2

# ACUTE ENERGY INHIBITION ELEVATES BACE1 PROTEIN LEVELS IN THE BRAIN VIA A POST-TRANSCRIPTIONAL MECHANISM *IN VIVO*

### Introduction

Amyloid  $\beta$  ( $A\beta$ ) overproduction and deposition are known to be key initiating events in the plaque pathology of the rare, inherited form of Alzheimer's disease (FAD) (Hardy and Selkoe, 2002); however, the source of  $A\beta$  accumulation in the predominant, sporadic form of AD (SAD) remains unknown. Levels of BACE1, the rate-limiting enzyme in the production of the  $A\beta$  peptide, are increased in SAD brains around amyloid plaques, implicating enhanced cleavage of APP by BACE1 as the source of  $A\beta$  overproduction in SAD (Fukumoto et al., 2002; Holsinger et al., 2002; Li et al., 2004; Tyler et al., 2002; Yang et al., 2003; Zhao et al., 2007). However, it is not known how or why BACE1 levels are elevated in SAD brains. Interestingly, cerebral glucose metabolism and blood flow are both reduced in preclinical AD, suggesting that impaired energy production may be an early pathological event in the disease (de Leon et al., 2007; Mosconi et al., 2007). Additionally, one of the proposed physiological functions of BACE1 is as a stress response protein (Rossner et al., 2006). To determine whether reduced energy metabolism was a stress capable of elevating BACE1 and promoting  $A\beta$  generation in the brain, we developed an *in vivo* pharmacological model of acute energy deprivation in young, pre-plaque APP transgenic (Tg2576) and wild-type

(C57/BL6) mice. To achieve acute energy inhibition *in vivo*, we treated mice with single i.p. injections of pharmacological agents that inhibit energy metabolism by different mechanisms (insulin, 2-deoxyglucose, 3-nitropropionic acid, and kainic acid). BACE1 protein levels were analyzed *via* immunoblot and soluble A $\beta$  levels were measured *via* ELISA in the brains of mice at 4 hrs, 2 days, and 7 days post-injection to determine the effect of acute energy deprivation on BACE1 protein levels and A $\beta$  production in the brain. We then analyzed endogenous BACE1 and APP mRNA levels in the brains of C57/BL6 mice to determine the effect of acute energy deprivation on BACE1 and APP gene expression.

## **Materials and Methods**

### **Animals and Drug Treatments**

C57/BL6 and Tg2576 mice were purchased from Taconic. The Tg2576 (APP<sup>sw</sup>) mouse model (Hsiao et al., 1996) carries a transgene encoding the 695-amino acid isoform of human APP with the Swedish mutation--- K670N, M671L; 770 amino acid isoform numbering (Fig 2.1A)(Mullan et al., 1992). All animals were 2-3 months of age at the time of treatments, and were randomized by age, weight and gender into five experimental groups (n=4-9 animals/group/time) with three recovery times (4 hrs, 2 days, and 7 days): vehicle (0.9% isotonic saline), insulin (18U/kg), 2-deoxyglucose (2DG; 1g/kg), 3-nitropropionic acid (3NP; 100mg/kg), and kainic acid (KA; 30mg/kg). All agents were administered by a single intraperitoneal (i.p.) injection. Insulin was purchased from Henry Schein, and 2-deoxyglucose, 3-nitropropionic acid, and kainic

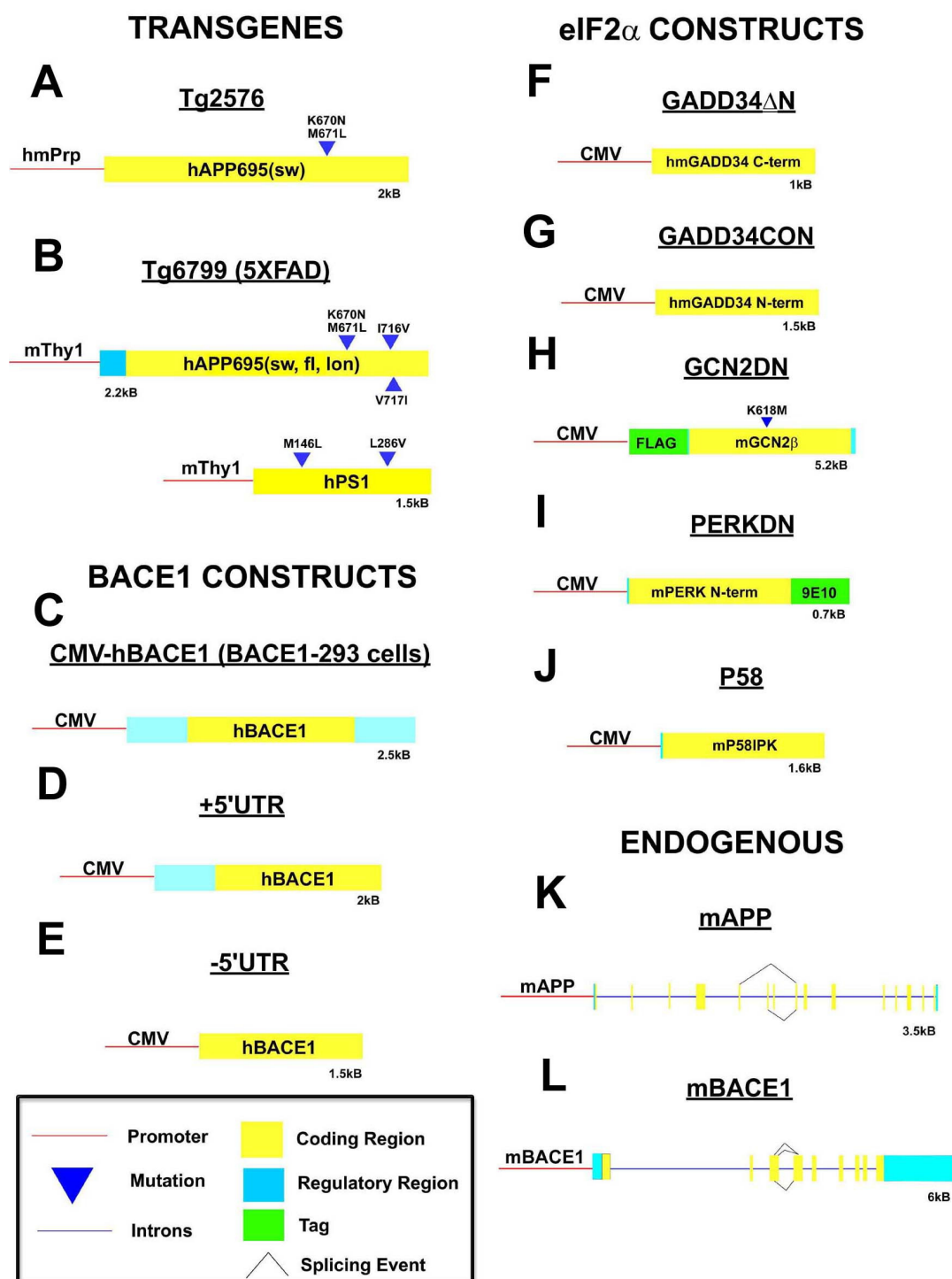


**Figure 2.1: Constructs and relevant DNA sequences used in experiments.** (A-B) Transgene design for murine models of amyloid pathology (C-E) BACE1 constructs used for stable cell lines and transient transfections in HEK-293 cells (F-J) Constructs used to modulate eIF2 $\alpha$  phosphorylation in HEK-293 cells (K-L) Endogenous APP and BACE1 genes in wild-type C57/BL6 mice.

acid were obtained from Sigma. These procedures were carried out with approval from Northwestern University Animal Use and Care Committee.

### **Tissue Preparation**

Following 4 hrs, 2 days or 7 days post-injection, animals were anesthetized with an i.p. injection of pentobarbital (100 mg/kg). Once respiration was stable and the mouse no longer responded to foot pinch, skin was rinsed with 70% ethanol and an incision was made exposing the heart for transcardial perfusion with 20ml of cold perfusion buffer (10 mM HEPES, 137 mM NaCl, 4.6 mM KCl, 1.1 mM  $\text{KH}_2\text{PO}_4$ , 0.6 mM  $\text{MgSO}_4$  and 1.1 mM EDTA) containing protease inhibitors (20  $\mu\text{g/ml}$  PMSF, 5  $\mu\text{g/ml}$  leupeptin, 20  $\mu\text{M}$  sodium orthovanadate and 100  $\mu\text{M}$  DTT). Following perfusion, brains were harvested and divided down the midline. Left hemibrains were placed in 4% paraformaldehyde overnight at 4°C for histology and right hemibrains were snap frozen in liquid nitrogen for biochemical analysis. Left hemibrains were stored in cryopreserve (20% sucrose (w/v), 0.01% Na-azide (w/v), in phosphate buffered saline [PBS]) at 4°C and right hemibrains stored at -80° C. Hemi-brains were homogenized in cold 1x PBS containing protease inhibitors, centrifuged at 2000 x g for 10 min at 4°C to remove insoluble material, and total protein concentration was determined by the BCA method (Pierce).

### **Immunoblot Analysis**

Hemi-brain homogenates (3mg/ml) were prepared in sample boiling buffer (60 mM Tris, 10% glycerol, 5% SDS, pH 6.8), 3.5% loading dye, and boiled for 5 min. 15  $\mu\text{g}$  of protein was run on 10% SDS-PAGE (BioRad Criterion Gel System) and transferred onto PDVF



membranes (0.45  $\mu$ m pore). Blots were blocked at room temperature for 1 hr in 5% non-fat dry milk in Tris-buffer saline containing 0.1% Tween 20 (TBST), then incubated with primary antibody against BACE1 (PA1-757, Affinity Bioreagents; 1:1000 dilution in 5% milk in TBST), APP (22C11, Chemicon; 1:5000), APPs $\beta$ (sw) neoepitope (Cole et al., 2005; Seubert et al., 1993; Vassar et al., 1999) (1:5000) at 4 $^{\circ}$  C overnight or  $\beta$ -actin (Sigma; 1:15000) at room temperature for 1 hr. Blots were then washed in TBST and incubated at room temperature for 1 hr with horseradish peroxidase-conjugated goat anti-mouse or goat anti-rabbit secondary antibodies diluted 1:10,000 in 5% milk in TBST. Immunosignals were detected using enhanced chemiluminescence (Amersham ECL+). Immunosignals were then quantified using a Kodak CF440 imager and normalized against the  $\beta$ -actin signal in the same sample for relative quantification. When necessary, blots were stripped in 100 mM 2-mercaptoethanol, 2% SDS, and 62.5 mM Tris-HCl, pH 7.6 for 30 min at 65 $^{\circ}$  C and washed in TBST before re-incubation with fresh primary antibody.

### **Human A $\beta$ 40 ELISA**

A $\beta$ 40 levels in hemi-brain homogenates were determined using a human-specific A $\beta$ 40 sandwich ELISA (BioSource) according to the manufacturer's recommendations. Briefly, hemi-brains were homogenized in 800  $\mu$ L of 1x PBS with 1% Triton-X-100 and 1x protease inhibitors (AEBSF; Calbiochem), and total protein concentrations were determined using the BCA assay (Pierce). Samples were then sonicated for ~20 seconds and adjusted to the same protein concentration with homogenization buffer. Because two month-old Tg2576 mice are pre-plaque mice, the guanidine extraction

step designed to solubilize amyloid plaques was eliminated. Samples were then further diluted 4.3x with ELISA kit diluent buffer with 1x AEBSF. Equal protein amounts of each sample (35 µg protein/well) and Aβ40 standards were added to the ELISA plate wells in duplicate and processed for colorimetric development according to the manufacturer's protocol. Optical densities at 450 nm of each well were read on a Victor 1420 plate reader (Wallac) and Aβ40 concentrations were determined using a standard curve of purified recombinant Aβ40 protein. All readings were in the linear range of the assay. Aβ40 concentration values for each sample were expressed as pg of Aβ40 (as determined by ELISA) per mg of total protein in the brain (as determined by the BCA assay). The average of the duplicates was determined and then the mean and standard error for a given treatment was calculated.

## **Histology**

Hemi-brains were sectioned parasagittally on a freezing microtome at 30 µm. Alternate serial sections were floated in 0.1 M phosphate buffer, pH 7.6, blocked for 2 hrs in 5% horse serum, and then stained with rabbit anti-GFAP primary antibody (1:10,000; Sigma) in 1% non-fat dry milk and 0.25% Triton-X-100 in 1x Tris-buffered saline (TBS; 0.05 M Tris, 0.15 M NaCl, pH 7.6) overnight at room temperature. Sections were washed in 0.25% Triton, 1x TBS and incubated with secondary biotinylated goat anti-rabbit diluted 1:2000 in 0.25% Triton-X-100 in 1x TBS for 2 hrs at room temperature. The Vectorlabs ABC kit was used with DAB as chromagen to visualize the reaction product. Sections were then mounted on charged slides, dehydrated in a series of alcohols, cleared in xylene and coverslipped. Hematoxylin was used as a counterstain

for GFAP immunohistochemistry. Differential interference contrast (DIC) microscopy was performed using a Nikon E800 microscope with a Spot Advanced digital camera for capturing images.

### **RNA Isolation and Real Time PCR**

Frozen C57/BL6 hemibrains were homogenized in 2.5 mL Qiazol reagent. Total RNA from 0.5 mL of C57/BL6 brain homogenate was isolated using Qiagen's RNeasy Lipid Mini kit according to the manufacturer's specifications. Total mRNA concentrations were measured using  $ABS_{260nm}$  ( $[RNA] \mu g/\mu L = 0.04 \times ABS_{260nm}$ ) on a Beckman spectrophotometer. In general, only mRNA samples with low protein contamination ( $ABS_{260nm}/ABS_{280nm} > 1.8$ ) were used for analysis. mRNA integrity of each sample was confirmed using an Agilent Technologies 2100 Bioanalyzer. mRNA samples were used for analysis if the 28S ribosomal RNA peak was at least two times the area of the 18S ribosomal RNA peak. 1  $\mu g$  of total RNA from each sample was used for first-strand cDNA synthesis using Invitrogen's SuperScript III according to the manufacturer's recommendations (Random hexamers were used as opposed to oligo dTs). Exact cDNA concentrations were determined using a Beckman spectrophotometer, and 112.5 ng cDNA from each sample was amplified *via* Real-Time PCR in triplicate using Applied Biosystems' Assays-on-Demand pre-mixed Taqman primer/probe set for mouse BACE1 and APP mRNA (catalog # Mm00431827\_m1, Mm00478664\_m1) and normalized against 18s rRNA (#4333760F) using an Applied Biosystems 7900HT sequence analyzer. The BACE1 primer/probe set spans exons 1-2 of the murine BACE1 transcript, which are present in all known splice variants of BACE1, and the APP

primer/probe set spans exons 9-11, which are present in all known splice variants of APP. Applied Biosystem's universal cycling parameters were used. Samples were only used for final analysis if the standard deviation between triplicate samples was  $< 0.1$  cycles. Percent of control values were determined using the comparative CT method.

## Statistical Methods

Immunoblot and ELISA quantifications are presented as the mean  $\pm$  standard error of the mean (SEM). Comparisons between groups were made using one-way analysis of variance (ANOVA) using Prism (Graph Pad Software) with post-hoc analysis by Neuman-Keuls test. For Real Time PCR, triplicates were averaged for each sample and the SEM was determined from the variability between different samples in the same group (VEH, 2DG, 3NP, INS, or KA) using a two-way t-test. An effect of treatment was defined as significant if  $p < 0.05$  by the F-test in the analysis of variance. \* $p < 0.05$ , \*\* $p < 0.01$ , and \*\*\* $p < 0.001$

## Results

### Physiological Effect of Acute Energy Deprivation in Mice

To determine the effects of acute energy inhibition on cerebral BACE1 levels and pro-amyloidogenic APP processing *in vivo*, we treated 2 month-old wild-type C57/BL6 and pre-plaque APP-transgenic Tg2576 mice with single doses of vehicle (VEH), insulin (INS; 18 U/kg), 2-deoxyglucose (2DG; 1 g/kg), 3-nitropropionic acid (3NP; 100 mg/kg), or kainic acid. Sub-lethal doses of insulin induce rapid, severe hypoglycemia by stimulating cells to metabolize and deplete glucose stores. 2DG is a competitive

inhibitor of glucose that binds and reversibly inactivates hexokinase, thus reducing glucose flux through glycolysis. 3NP is an irreversible inhibitor of succinate dehydrogenase, which inhibits carbon flux through the Krebs cycle, and disrupts the electron transport chain. Finally, KA is a glutamate analogue that induces seizure and evokes a large energy demand on glutamatergic neurons in the brain (Fig 2.2). Mice were allowed to recover for 4 hrs, 2 days, or 7 days post-injection. All treated mice displayed typical behaviors associated with inhibition of energy metabolism, including low or no motor activity, lethargy, and lack of response to touch. For insulin-induced hypoglycemia, these behaviors correlated with extremely low blood glucose levels (20-30 mg/dL in insulin-injected mice as compared to ~130 mg/dL in vehicle-injected mice). For KA-treated animals, reduced motor activity preceded the onset of mild to moderate seizures (stages 2-4) (McKhann et al., 2003). Behavioral onset was rapid following injections with 2DG, 3NP and KA (~5-10min) and more delayed for insulin treatment (~45-60min). All mice generally recovered within 4 hrs, and no further abnormal behaviors were observed for up to 7 days (the last time point analyzed).

### **Acute Energy Deprivation Causes no Neurodegeneration or Astrogliosis**

These agents and doses have been shown in previous studies to induce acute reduction in brain energy production without causing significant neurodegeneration (Auer et al., 1984; Brownell et al., 2004; McKhann et al., 2003). To confirm that no neurodegeneration or gliosis occurred as a result of treatments, following 7 days of recovery, brains from representative treated mice were harvested and alternate brain sections stained with anti-glial fibrillary acidic protein (GFAP) antibody counterstained

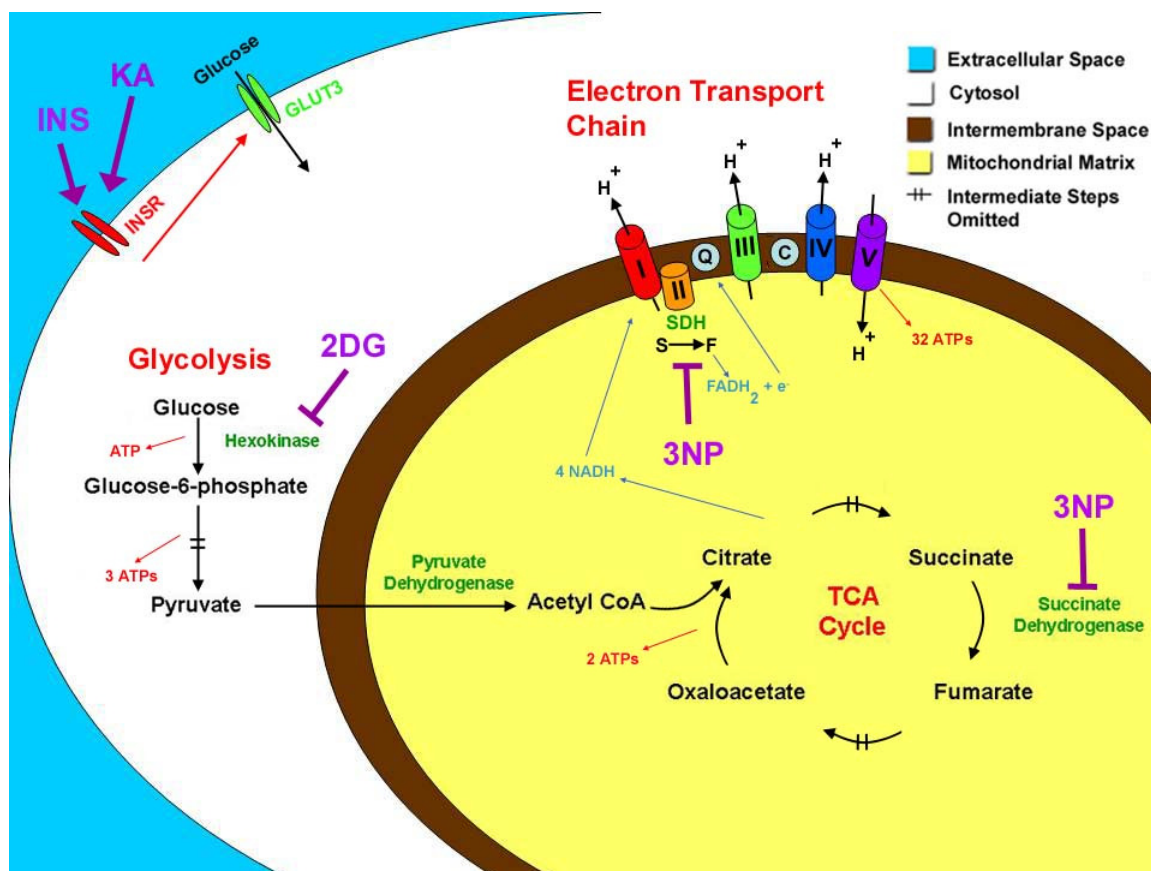


**Figure 2.2: The effect of pharmacological energy inhibitors on energy metabolism.** Insulin (**INS**) stimulates the peripheral cells *via* signal transduction to increase uptake of glucose from the extracellular space, causing glucose stores to be rapidly depleted. Kainic acid (**KA**) induces rapid firing of glutamate-sensitive neurons, which also causes depletion of glucose stores. 2-deoxyglucose (**2DG**) is a glucose analog that competes with glucose for access to the enzyme hexokinase, thereby inhibiting the flux of glucose through glycolysis. 3-nitropropionic acid (**3NP**) is an irreversible inhibitor of the enzyme succinate dehydrogenase (SDH). Inactivation of SDH inhibits the tricarboxylic acid (TCA) cycle, as well as the electron transport chain.

with hematoxylin. GFAP immunoreactivity was not elevated in brains from treated mice as compared to vehicle controls (Fig 2.3), indicating that the energy inhibitors did not induce significant astrogliosis. Importantly, the treatments did not appear to cause obvious signs of neurodegeneration upon examination of hematoxylin-stained (Fig 2.3) brain sections.

### **Cerebral BACE1 Levels Are Elevated Following Energy Inhibition**

Next, we then investigated the effects of acute energy inhibition on cerebral BACE1 levels in Tg2576 mice *via* immunoblot. At 4 hrs post-injection, all treatments resulted in increases of brain BACE1 protein levels in young Tg2576 mice ~150% of vehicle control (Fig 2.4;  $p < 0.01$ ). When Tg2576 mice were allowed to recovery for 2 days or 7 days, BACE1 levels continued to be elevated to ~130-145% and ~127-140% of vehicle control values, respectively (Figure 2.4; 2d  $p < 0.05$ , 7d  $p < 0.01$ ). These results demonstrate that the BACE1 protein increase is an early and long-lasting response to acute energy inhibition Tg2576 brain.

### **Cerebral Amyloidogenesis is Increased Following Energy Inhibition**

Since BACE1 is the key rate-limiting enzyme in the production of A $\beta$ , we next determined whether acute cerebral energy inhibition would also increase pro-amyloidogenic processing of APP in Tg2576 mice. The Tg2576 mouse line is a well-established transgenic model of amyloid pathology that overexpresses human APP with the Swedish mutation (APP<sup>sw</sup>; Fig 2.1A) (Mullan et al., 1992) and develops amyloid plaques at ~9-12 months of age (Hsiao et al., 1996). The level of APPs $\beta$ (sw), the

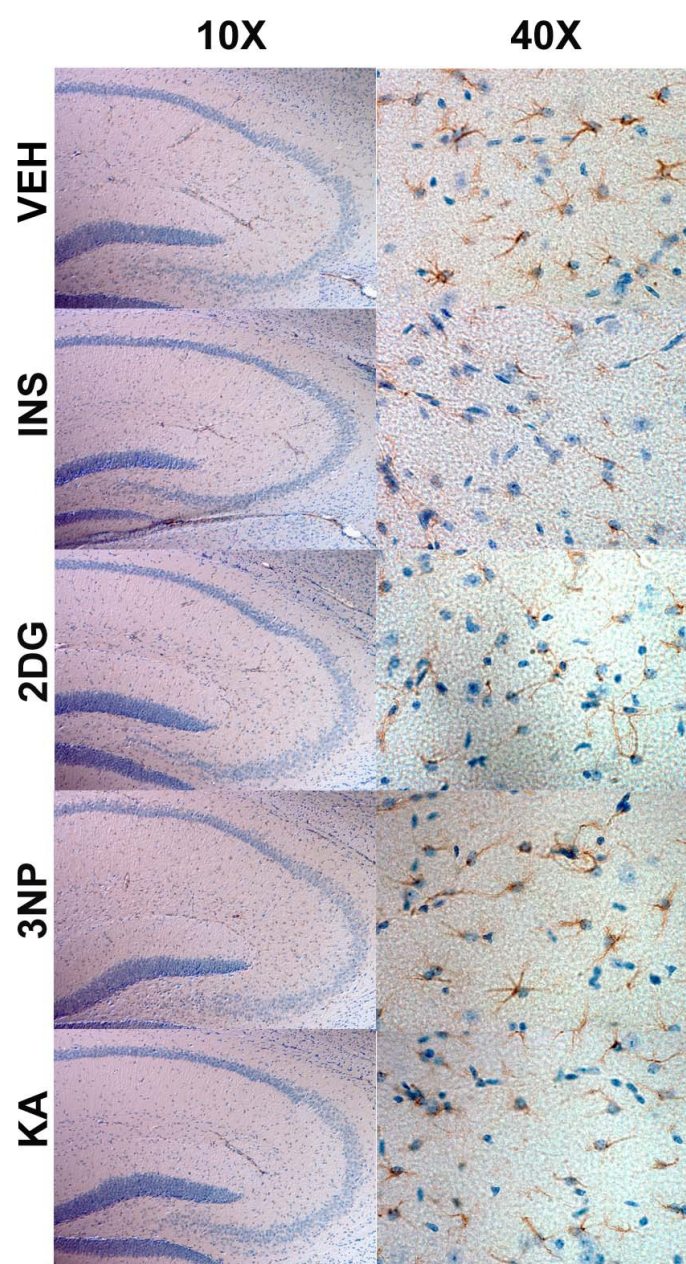


**Figure 2.3: Acute energy inhibition causes no detectable neurodegeneration or astrogliosis in the brain.** 2-3 month-old Tg2576 mice were administered single i.p. injections of vehicle (VEH), insulin (INS), 2-deoxyglucose (2DG), 3-nitropropionic acid (3NP), or kainic acid (KA). 7 days post-injection, brains from VEH, INS, 2DG, 3NP, or KA-treated animals were fixed for immunohistochemistry. Serial parasagittal sections from Tg2576 mice were stained with anti-GFAP and counterstained with hematoxylin. The CA1, CA3, and dentate gyrus regions of the hippocampus were imaged at low magnification (10X) to test for neuronal loss in the cell layers of the hippocampus. The hippocampus was imaged at high magnification (10X) to determine the activation status of individual astrocytes in treated versus control mice.



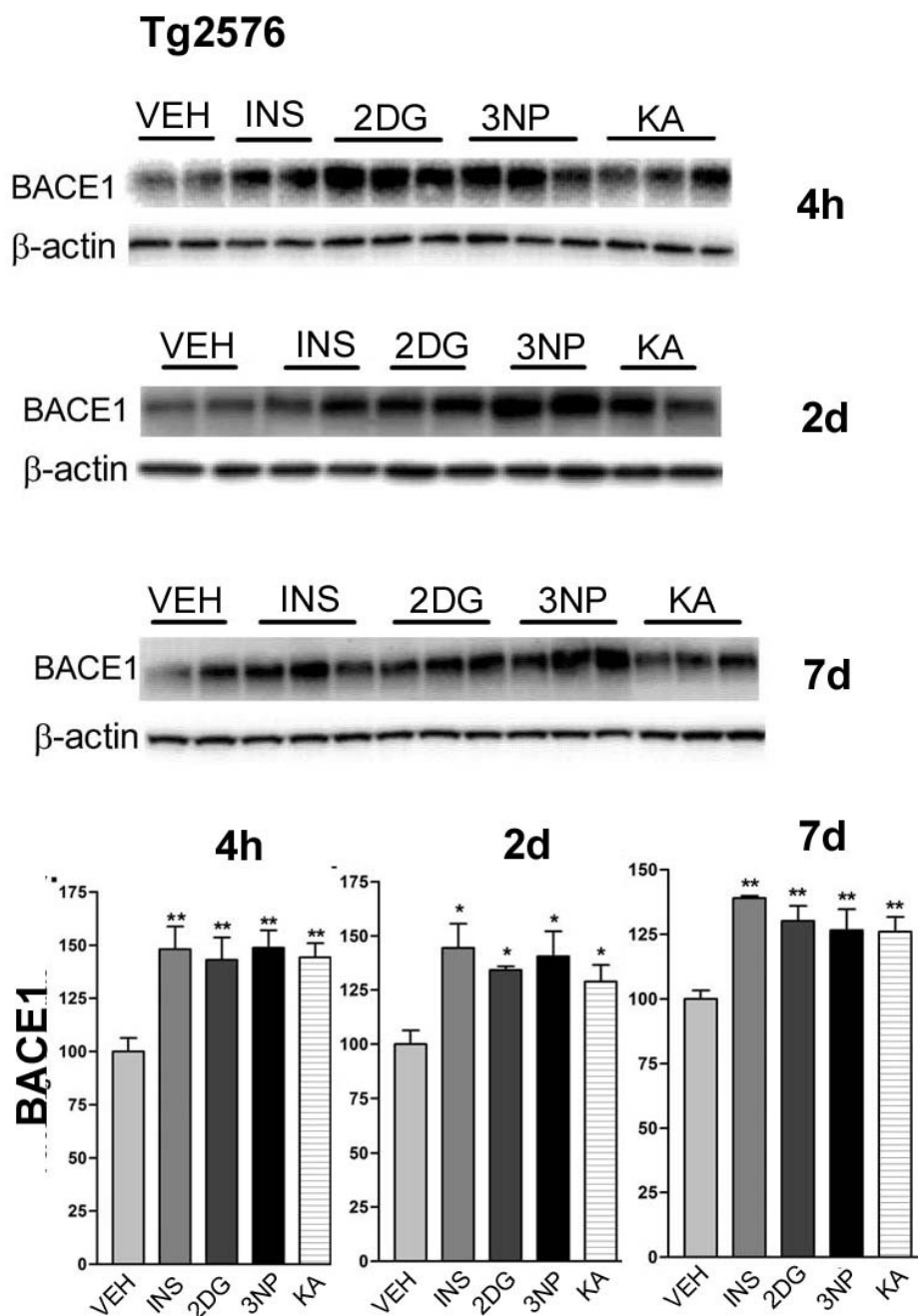


**Figure 2.4: Acute energy inhibition elevates endogenous BACE1 protein levels in young Tg2576 mice.** (from Velliquette et al., 2005) 2-3 month old Tg2576 mice were administered single i.p. injections of VEH, INS, 2DG, 3NP, and KA. 4 hrs, 2 days, or 7 days-post-injection, brains from VEH, INS, 2DG, 3NP, and KA-treated Tg2576 mice were analyzed *via* immunoblot for expression of endogenous BACE1 protein. BACE1 immunosignals were normalized to  $\beta$ -actin and expressed as % VEH. BACE1 protein levels were elevated above VEH in all treatment groups at all timepoints tested. (n = 4-6). \*p < 0.05, \*\*p < 0.01

ectodomain produced after initial  $\beta$ -secretase cleavage of APP<sup>sw</sup>, reflects the amount of BACE1-induced processing of APP and parallels the level of A $\beta$  (Vassar et al., 1999; Sinha et al., 1999; Yan et al., 1999; Hussain et al., 1999; Lin et al., 2000). Therefore, we measured APPs $\beta$ (sw) levels in the brains of treated mice by immunoblot analysis using a neoepitope antibody that recognizes the cleaved C-terminus of APPs $\beta$  ending in the Swedish mutation (APPs $\beta$ (sw)), but reacts only weakly with full-length APP (Seubert et al., 1993; Vassar et al., 1999; Cole et al., 2005). We found that energy inhibition caused APPs $\beta$ (sw) levels to increase by as much as ~175% as compared to vehicle controls after 4h of recovery (Fig 2.5A), indicating that treatment-induced BACE1 elevation led to a rise in  $\beta$ -secretase cleavage of APP *in vivo*. APPs $\beta$ (sw) levels continued to be elevated for 2 days and 7 days following treatments (Fig 2.5A), again demonstrating a long-lasting effect. Immunoblot analysis with anti-APP antibodies did not reveal a significant increase of full-length APP levels following energy inhibition, excluding the possibility that an increase in APP<sup>sw</sup> transgene expression was responsible for the elevated APPs $\beta$ (sw) levels. To determine whether the apparent increase in  $\beta$ -secretase cleavage of APP resulted in elevated A $\beta$  levels, we measured cerebral A $\beta$ <sub>40</sub>, the predominant form of A $\beta$  produced in the Tg2576 model, in treated Tg2576 mice using a human A $\beta$ <sub>40</sub>-specific sandwich ELISA. At 2 months of age, Tg2576 mice have not yet begun to form plaques in the brain, so all of the A $\beta$  in the brain is soluble. After 4 hrs and 2 days of recovery, A $\beta$ <sub>40</sub> levels showed a trend toward elevation for several of the treatments, although significant differences were not found by ANOVA (Fig 2.5B). However, by 7 days of recovery, treated Tg2576 mice had dramatically elevated cerebral A $\beta$ <sub>40</sub> levels, rising to ~200% of vehicle control values (Fig 2.5B). Taken

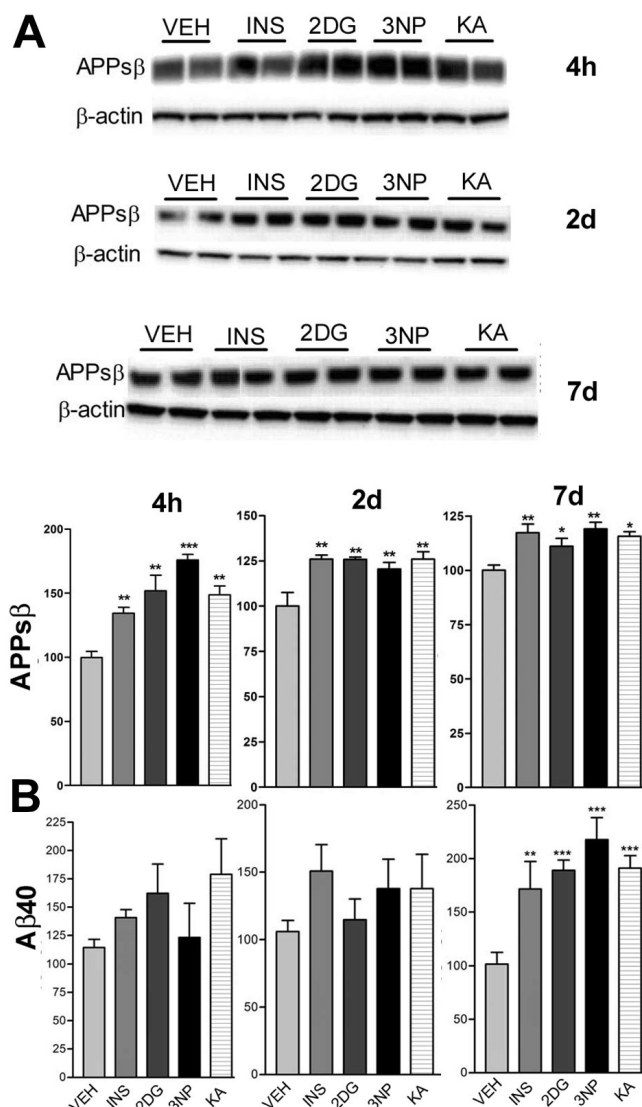


**Figure 2.5: Acute energy inhibition in young Tg2576 mice enhances pro-amyloidogenic processing of APP.** 2-3 month old Tg2576 mice were administered single i.p. injections of VEH, INS, 2DG, 3NP, and KA. **(A)** (from Velliquette et al., 2005) At 4 hrs, 2 days, or 7 days-post-injection, brains from treated Tg2576 mice were analyzed *via* immunoblot for expression of APPsβ(sw); the N-terminal protein fragment produced from BACE1-mediated cleavage of APPsw. APPsβ(sw) immunosignals were normalized to β-actin and expressed as % VEH. APPsβ(sw) was significantly elevated in response to all treatments at all timepoints tested (n = 4-6). **(B)** At 4 hrs, 2 days, or 7 days post-injection, brains from VEH, INS, 2DG, 3NP, and KA-treated Tg2576 brains were analyzed *via* ELISA for total human Aβ40 levels. Aβ40 values were normalized to total protein and expressed as pg Aβ40 per mg of total protein. Aβ40 levels were significantly elevated in Tg2576 brains in response to all treatments 7 days post-injection. (n = 4) \*p < 0.05, \*\*p < 0.01, \*\*\*p < 0.001

together, these results demonstrated that reduction of cerebral energy metabolism, although acute, produced a long-lasting elevation of both BACE1 and A $\beta$  levels in the brain.

### **Endogenous BACE1 protein levels are elevated in response to acute energy deprivation in the brains of C57/BL6 mice**

We showed that acute injection of insulin, 2DG, 3NP, or KA caused a significant increase in cerebral BACE1 protein levels in two month-old Tg2576 mice on a B6/SJL strain background. To determine the effect of acute energy inhibition on endogenous BACE1 and APP proteins in the brains of wild-type C57/BL6 mice (Fig 2.1K,L), we administered acute injections of insulin, 2DG, 3NP, or KA to two month-old C57/BL6 mice and analyzed half of the brain via immunoblot for BACE1 and APP proteins. Consistent to what was observed in the brains of Tg2576 mice, acute *in vivo* inhibition of energy production induced by each of the four pharmacological agents resulted in significant increases in BACE1 protein levels in C57/BL6 brains (~150% of vehicle control values) within 4hrs (Fig 2.6A;  $p < 0.001$ ). Moreover, BACE1 levels continued to be significantly elevated in C57/BL6 brains (~125-150% of vehicle control) after 2 days and 7 days of recovery (Fig 2.6A). In contrast, no difference between endogenous levels of APP, the BACE1 substrate, was observed between vehicle and 2DG, 3NP, or KA-treated animals. These results show that BACE1 protein is regulated similarly in response to acute energy inhibition *in vivo*, regardless of strain background or genotype.

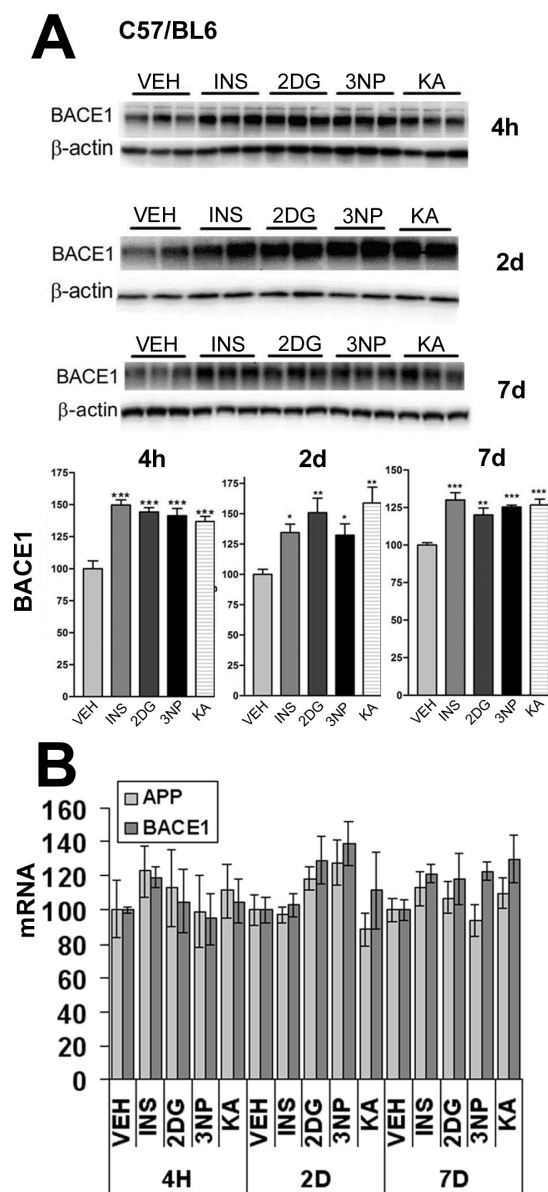


**Figure 2.6: Acute energy inhibition elevates endogenous BACE1 protein levels via a post-transcriptional mechanism in young C57/BL6 mice.** 2-3 month old wild-type C57/BL6 mice were administered single i.p. injections of VEH, INS, 2DG, 3NP, or KA. **(A)** (from Velliquette et al., 2005) Brains from treated C57/BL6 mice were analyzed *via* immunoblot for endogenous BACE1 protein expression. BACE1 immunosignals were normalized to  $\beta$ -actin and expressed as % VEH. (n = 4-9) BACE1 protein levels were elevated in all treatment groups at all timepoints tested. **(B)** mRNA was isolated from brains of treated C57/BL6 and analyzed for endogenous BACE1 and APP mRNA levels *via* Real Time PCR. BACE1 and APP mRNA signals were normalized to 18s rRNA and expressed as % VEH. (n = 2-5) There was no significant difference between BACE1 or APP mRNA levels in any treatment group at any timepoint. \*p < 0.05, \*\*p < 0.01, \*\*\*p < 0.001

## **BACE1 and APP mRNA levels are not elevated in response to acute energy deprivation *in vivo***

In order to gather mechanistic information about the acute energy deprivation-induced BACE1 elevation *in vivo*, we extracted total mRNA from the corresponding hemi-brains of two month-old C57/BL6 mice that had received acute injections of vehicle, insulin, 2DG, 3NP, or KA and had previously exhibited elevated BACE1 protein levels *via* immunoblot. Using Real Time PCR, we measured levels of total endogenous BACE1 and APP mRNA transcripts in the brains of treated mice compared to vehicle. In contrast to the increase in BACE1 protein observed in response to acute energy deprivation, BACE1 mRNA levels were the same in insulin, 2DG, 3NP, and KA-treated mice compared to vehicle. Endogenous APP mRNA levels were not elevated either, consistent with unchanged APP protein levels in the brain (Fig 2.6B).

## **Discussion**

We showed that single pharmacological treatments of a variety of energy inhibitors cause prolonged elevations in cerebral levels of BACE1 in both wild-type and Tg2576 mice, which appear to enhance amyloidogenic processing in young Tg2576 mice. Although the energy inhibitors used in this study all inhibit energy production through different mechanisms, they all showed similar effects on BACE1 protein and amyloidogenic processing, indicating that they may all be promoting amyloidogenesis through the same molecular mechanism.

### **The Effects of Acute Energy Inhibition on Amyloidogenic APP Processing**

Interestingly, a relatively long period of time elapsed between BACE1 and APPs $\beta$  elevations and detectable A $\beta$ 40 increases. It is possible that either the additional step of  $\gamma$ -secretase cleavage of C99 to generate A $\beta$ , or mechanisms of A $\beta$  clearance, may be responsible for this lag period. The temporal relationship between  $\beta$ - and  $\gamma$ -secretase cleavage in neurons is not well understood *in vivo*, and the time for C99 intracellular trafficking to  $\gamma$ -secretase, or the accessibility and/or activity of  $\gamma$ -secretase, may be limiting *in vivo*. Interestingly, a recent study indicates that  $\gamma$ -secretase generation of A $\beta$  is ATP-dependent in a cell-free system (Netzer et al., 2003). If so, the lower ATP levels caused by our energy inhibitor treatments may simultaneously enhance  $\beta$ -secretase cleavage of APP and reduce  $\gamma$ -secretase cleavage of C99, thereby temporarily inhibiting A $\beta$  production. Once a normal metabolic state is restored and  $\gamma$ -secretase is reactivated, accumulated C99 is then cleaved by  $\gamma$ -secretase, leading to a delayed rise in A $\beta$  levels. Elevations of BACE1, the rate-limiting enzyme in A $\beta$  production and its direct cleavage product, APPs $\beta$ , indicate that enhanced production of A $\beta$  is responsible for accumulating A $\beta$  in the brain following acute energy inhibition *in vivo*. However, it is important to note that A $\beta$  homeostasis in the brain is dependent upon both production and clearance pathways. It is possible that impaired energy metabolism affects both the production of A $\beta$  as well as A $\beta$  clearance and degradation pathways in the brain.

## **Mechanisms of BACE1 protein elevation**

We repeated our acute energy inhibition experiments in two-month old wild-type C57/BL6 mice, and all four pharmacological agents (insulin, 2DG, 3NP, and KA) all caused cerebral elevations of BACE1 protein similar in magnitude to the BACE1 protein elevations observed in young Tg2576 mice. This data indicates that the energy inhibition-induced BACE1 protein elevation is robust and is reproducible in different strains and genotypes of mice. (Acute energy deprivation-induced BACE1 protein elevations also occurred in non-transgenic littermates of Tg2576 mice, which are B6/SJL hybrid mice.) Interestingly, BACE1 mRNA levels from these same C57/BL6 brains were not elevated in treatment groups compared to controls, which indicates that increased BACE1 transcription or increased BACE1 mRNA stability cannot explain the energy deprivation-induced BACE1 protein elevation. This is surprising, because altered metabolic states are expected to change the transcriptional profile of the cell dramatically. Nevertheless, the relatively short time period in which BACE1 protein becomes elevated (by 4 hrs) further supports the hypothesis that the energy deprivation-induced BACE1 elevation is post-transcriptional. As previously discussed, BACE1 can be controlled by a variety of post-transcriptional mechanisms, including altered protein stability (through either the ubiquitin-proteasome pathway or the lysosomal degradation pathway), microRNA regulation, or translational control. A cell culture model of energy deprivation will need to be developed in order to determine which of these mechanisms, if any, are operating in response to energy deprivation. Another notable finding of our acute energy deprivation study is that neither APP mRNA nor APP protein appeared to be altered in response to acute energy deprivation in wild-



type C57/BL6 mice. This indicates that increased A $\beta$  levels observed in Tg2576 mice in response to acute energy deprivation are not attributable to effects of acute energy deprivation on endogenous APP. Elevated A $\beta$  levels appear to occur solely through enhanced  $\beta$ -secretase cleavage of APP. The agents used to induce acute energy inhibition did not induce visible signs of neurodegeneration as determined by hematoxylin staining, indicating that the BACE1 protein increase occurs pre-apoptotically. Similarly, GFAP immunoreactivity indicated that acute energy inhibition caused no astrogliosis at the doses used, indicating that the BACE1 increase is non-inflammation-mediated. The specific cell type in the brain that up-regulates BACE1 in response to acute energy deprivation is another important unanswered question. We suspect that the BACE1 increase is neuronal in origin, since BACE1 is predominantly expressed in neurons and expressed at very low levels in glia (Zhao et al., 1996). However, it is still possible that glia are responsible for upregulating BACE1, because even though BACE1 is expressed at very low levels in glia, glia are the predominant cell type in the brain. The specific brain region that up-regulates BACE1 protein is also unknown. We suspect that the BACE1 protein increase occurs over the entire brain, because BACE1 is expressed pan-neuronally in the brain (Zhao et al., 2007). Additionally, our immunoblots of whole brain homogenates readily detected elevated BACE1 protein in response to acute energy deprivation, and if the BACE1 increase had only occurred in a single brain region, it is unlikely that it would have been detected by our assay. However, it is possible that BACE1 protein elevation in response to acute energy deprivation is particularly high only in a specific region of the brain, for example, the hippocampus. BACE1 protein exhibits particularly dense staining in the mossy fiber

pathway of the dentate gyrus under normal conditions, indicating that BACE1 might play a particularly important role there. It has been hypothesized that the hippocampus is particularly sensitive to stress stimuli and neurodegenerative changes. It is also one of the first sites of amyloid plaque formation in Alzheimer's disease (Esch et al., 2002; Mesulam, 2000).

### **Implications for Amyloid Pathology and SAD**

Although the BACE1 elevations were modest (~150% of control), they were long-lasting (at least 7 days). As expected, increases in the levels of the product, A $\beta$ 40, temporally followed those of the enzyme, BACE1. Notably, at 7 days post-treatment, A $\beta$ 40 levels reached ~200% of control, thus exceeding the maximum percent increase for BACE1. Given the catalytic activity of BACE1, prolonged elevation of BACE1 levels could lead to large, cumulative increases of A $\beta$  over time. This is exemplified by our observation that BACE1 and A $\beta$  levels remain elevated for at least one week following a single episode of energy inhibition. The main implication of our acute energy inhibition study is that repeated metabolic insults may maintain elevated BACE1 protein levels in the brain, which may eventually have harmful effects due to cerebral A $\beta$  overproduction. If cerebral A $\beta$  production overwhelms clearance and/or degradation mechanisms in the brain, then A $\beta$  levels will increase and likely trigger SAD, just as it does in FAD.

## CHAPTER 3

# ENERGY INHIBITION ELEVATES BACE1 PROTEIN *IN VITRO* VIA PHOSPHORYLATION OF THE TRANSLATION INITIATION FACTOR eIF2 $\alpha$ AT SERINE 51

### Introduction

BACE1 protein levels are elevated and pro-amyloidogenic processing of APP is enhanced in the brain as a result of acute energy deprivation *in vivo*, which may be an amyloidogenic mechanism in SAD. However, neither BACE1 nor APP mRNA levels were elevated in the brains of wild-type C57/BL6 mice in response to acute energy deprivation, indicating that increased BACE1 protein levels were the result of a post-transcriptional mechanism. In order to identify the specific post-transcriptional mechanism(s) involved in energy deprivation-induced elevations of BACE1 protein, we developed an *in vitro* model of energy deprivation. HEK-293 cells stably overexpressing human BACE1 under the control of the CMV promoter (BACE1-293 cells) were cultured for varying lengths of time in glucose-deficient media (NG). We compared BACE1 protein and mRNA levels in NG-treated versus control-treated BACE1-293 cells to determine whether BACE1 protein was post-transcriptionally elevated in response to impaired energy metabolism *in vitro*. Using this *in vitro* model of energy deprivation, we investigated the specific roles of BACE1 transcription, protein stability, and translation in energy deprivation-induced BACE1 elevation. We tested BACE1 mRNA levels in glucose-deprived BACE1-293 cells and used a transcriptional inhibitor, actinomycin D, in combination with no glucose treatment to determine if transcription was involved in

BACE1 protein elevations. BACE1 protein stability is controlled by the ubiquitin-proteasome pathway and/or the lysosomal degradation pathway, both of which could be altered in response to cellular energy deprivation. In order to determine whether BACE1 protein stability was enhanced under glucose-deficient conditions, we performed a pulse-chase experiment using BACE1-293 cells incubated in glucose-deficient (NG) or media containing 50 mM 2-deoxyglucose (2DG). Another post-transcriptional mechanism that could cause energy deprivation-induced BACE1 elevations is altered translational control of BACE1 mRNA. BACE1 mRNA contains a long (~0.5 kb), G-C-rich (76%) 5'untranslated region (5'UTR) with three uAUGs, which is characteristic of translationally regulated proteins. It has been demonstrated that the BACE1 5'UTR is inhibitory to BACE1 translation under normal conditions (De Pietri Tonelli et al., 2004; Lammich et al., 2004; Mihailovich et al., 2007; Rogers et al., 2004; Zhou and Song, 2006). In order to determine whether there was evidence for altered translational control in BACE1-293 cells as a result of impaired energy metabolism, we compared levels of activation of various signaling pathways known to converge upon components of the cellular translational machinery in NG-treated cells compared to control *via* immunoblot. Using this screen, we observed increased phosphorylation of the alpha subunit of the eukaryotic translation initiation factor 2, a highly conserved eukaryotic cellular stress response mechanism designed to reduce global translation and specifically enhance translation of stress response proteins with long 5'UTRS containing uORFs, similar to BACE1. To determine whether eIF2 $\alpha$  phosphorylation was a valid mechanism controlling BACE1 protein levels we attempted to elevate BACE1 protein levels *in vitro* by direct pharmacological induction of eIF2 $\alpha$  phosphorylation. To

do this, we treated BACE1-293 cells with a drug that selectively enhances basal eIF2 $\alpha$ -P levels (salubrinal), and compared BACE1 protein levels in salubrinal versus control-treated BACE1-293 cells *via* immunoblot. In order to determine whether eIF2 $\alpha$  phosphorylation in response to glucose deprivation was directly causing elevated BACE1 protein levels, we cultured BACE1-293 cells in glucose-deficient media while genetically preventing eIF2 $\alpha$  phosphorylation. We then measured BACE1 and eIF2 $\alpha$ -P levels *via* immunoblot to determine whether inhibition of eIF2 $\alpha$  phosphorylation could prevent NG-induced BACE1 protein elevations. In addition, we overexpressed dominant negative forms of eIF2 $\alpha$  kinases in combination with no glucose in BACE1-293 cells to determine which specific eIF2 $\alpha$  kinase was phosphorylating eIF2 $\alpha$  in response to glucose deprivation.

## **Materials and Methods**

### **Cell Line Cultures**

The 2.5kb full-length human BACE1 coding region containing the BACE1 mRNA 5' (453 nts) and 3' (567 nts) untranslated regions (UTRs; Accession no. AF190725) was cloned into the expression vector pCMVi (pCMV-hBACE1; Cellular & Molecular Technologies, Inc.)(Fig 2.1C). The stably transfected BACE1-293 cell line was created by co-transfecting HEK-293 cells with pCMV-hBACE1 and pRSV-Puro and selecting with 5  $\mu$ g/mL puromycin (Sigma). BACE1-293 cells were maintained in selective Dulbecco's Modified Eagle Medium (DMEM; 10% fetal bovine serum, 1% pen-strep, 400  $\mu$ g/mL G418, and 5  $\mu$ g/mL puromycin; Invitrogen). For energy deprivation experiments, cells were plated on poly-D-lysine-coated (100  $\mu$ g/mL) plates, allowed to grow to ~80%

confluency, and then incubated in selective DMEM without glucose (Invitrogen; Cat #11966). For transient transfections, cells were allowed to grow to ~50% confluency in DMEM containing only 10% FBS and transfected with 1.6 µg/mL DNA complexed with Lipofectamine 2000 according to the manufacturer's recommendations for 4 hrs (Invitrogen). After 4 hrs, transfection media was removed, replaced with selective DMEM, and cells were allowed to recover overnight before onset of treatment. The -5'UTR and +5'UTR vectors were a gift from Sven Lammich, Stefan Lichtenthaler, and Christian Haass at Ludwigs-Maximilians University in Munich. -5'UTR (Fig 2.1E): The entire BACE1 coding region (1503 bps) was PCR amplified from human cDNA and cloned into the pcDNA3.1Zeo(+) CMV expression vector using EcoRI and XhoI restriction sites. +5'UTR (Fig 2.1D): The BACE1 5'UTR sequence was PCR-amplified from human cDNA and cloned into the -5'UTR vector using HindIII and EcoRI restriction sites (Lammich et al., 2004). The GADD34ΔN, GADD34CON, PERKDN, and P58 vectors were a gift from David Ron's lab at NYU:

([www.saturn.med.nyu.edu/research/mp/ronlab/SharedReagents.html](http://www.saturn.med.nyu.edu/research/mp/ronlab/SharedReagents.html)). The GCN2DN vector was a gift from Ron Wek at the University of Indiana in Indianapolis. GADD34ΔN (Fig 2.1F): The C-terminal activation domain of hamster GADD34 (MyD116; aa 292–590) cDNA was subcloned into the BamHI and Sall sites of pBABEpu CMV expression vector (Novoa et al., 2001). GADD34CON (Fig 2.1G): The C-terminal portion of mouse GADD34 cDNA with the PP1c interacting domain deleted was created by isolating the SmaI fragment of mouse GADD34 and subcloning into the SnaBI site of the pBABEpu CMV expression vector. GADD34CON serves as a negative control for GADD34ΔN (Novoa et al., 2001). PERKDN (Fig 2.1H): N-terminal FLAG-tagged full-

length mouse PERK cDNA with the C-terminus containing the kinase domain deleted (by *Sna*BI/*Sma*I cleavage of mPERK cDNA, which eliminates residues 582-1081 of the protein) was cloned into the *Eco*RI and *Xho*I sites of pcDNA3 CMV expression vector. This vector serves as a dominant negative form of the PERK kinase (Harding et al., 1999). GCN2DN (Fig 2.1I): The  $\beta$  variant of full-length mouse GCN2 cDNA with a Lys  $\rightarrow$  Met substitution (K618M) in the kinase domain and a C-terminal 9E10 tag was cloned into the *Kpn*I and *Xba*I sites of the pcDNA3 CMV expression vector. This construct serves as a dominant negative form of the GCN2 kinase (Sood et al., 2000). P58 (Fig 2.1J): Full-length mouse P58 cDNA was subcloned into the pcDNA3 CMV expression vector (Oyadomari et al., 2006). P58 is an inhibitor of the PERK and PKR kinases (van Huizen et al., 2003; Yan et al., 2002). Empty pcDNA3 vector was used as negative control for the PERKDN, GCN2DN, and P58 vectors. For salubrinal experiments, 5 mg of salubrinal was dissolved in DMSO to 10 mM and added to the cell media at 100  $\mu$ M for 24 hrs (Calbiochem # 324895). For actinomycin D experiments, actinomycin D (Sigma # A9415) was dissolved in DMSO to 1 mg/mL and added to the cell media at a concentration of 1.6  $\mu$ g/mL for 12 hrs. For tauroursodeoxycholate (TUDCA; Sigma) experiments, cells were pre-treated with 1  $\mu$ M TUDCA (dissolved in sterile water and adjusted to pH 7.0) for 30 min., then treated for 12 hrs with glucose-deficient media containing 1  $\mu$ M TUDCA. For Mnk kinase inhibitor experiments (N3-(4-fluorophenyl)-1h-pyrazolo[3,4-d]pyrimidine-3,4-diamine; Sigma # CGP 57380) Mnk inhibitor was dissolved in DMSO to 20 mM. BACE1-293 cells were pre-treated with 1  $\mu$ M Mnk inhibitor for 30 min., then incubated in glucose-deficient DMEM containing 1  $\mu$ M Mnk inhibitor for 12 hrs. For biochemical analyses, cells were washed with 1x PBS,

lysed in 1x RIPA buffer (150 mM NaCl, 1% IGEPAL CA-630, 0.5% sodium deoxycholate (DOC), 0.1% SDS, 50 mM Tris, pH 8.0, 1 mM PMSF) supplemented with 1x AEBSF and 1x Halt phosphatase inhibitors (Pierce) and homogenized. Insoluble material was pelleted out by centrifugation, and supernatants were analyzed for total protein content using the BCA assay. For mRNA analysis, culture medium was aspirated, and cells were immediately lysed in 350  $\mu$ L RLT buffer with 1%  $\beta$ -mercaptoethanol (Qiagen). Cell lysates were homogenized and used for mRNA extraction.

### **Neuronal Cultures**

Timed pregnant C57/BL6 females mated were sacrificed *via* carbon dioxide inhalation, and E15.5-E16.5 C57/BL6 embryos were excised, rinsed in 1x BSS (1x Hank's Balanced Salt Solution, 1% pen-strep, 10 mM HEPES), and decapitated. Embryonic cortical tissue was isolated with the aid of a dissecting microscope, dissociated for 15 min. at 37°C in 5 mL of 0.25% trypsin (Invitrogen), washed 3x with 5 mL 1x BSS, and triturated in succession with a regular, sterile Pasteur pipet and a fire-polished Pasteur pipet in 5mL 1x BSS. Triturate volumes were adjusted to 0.25 mL/well with 1x BSS. Neurons were plated in 1 mg/mL poly-L-lysine-coated plates (1 brain per 12-well plate) for 2 hrs in neurobasal media supplemented with 1x B-27, 10% horse serum, 1% pen-strep, 2.5 $\mu$  M glutamate, and 500  $\mu$ M glutamine (Invitrogen). Neurons were maintained for 2 DIV in neurobasal media containing only B-27, 2.5  $\mu$ M glutamate, and 500  $\mu$ M glutamine. At 2 DIV, neurons were switched to media containing only B-27 and 500  $\mu$ M glutamine, after which half of the maintenance media was changed every 2-3 days.



Rapamycin (Cell Signaling # 9904) was dissolved in DMSO to 10  $\mu$ M. At 7 DIV, rapamycin was added to the maintenance media at 10 nM for 12 hrs. For biochemical analyses, neurons were washed with 1x PBS, lysed in 1x RIPA buffer supplemented with 1x AEBSF and 1x Halt phosphatase inhibitors and homogenized. Insoluble material was pelleted out by centrifugation, and supernatants were analyzed for total protein content using the BCA assay.

### **Immunoblotting**

5  $\mu$ g (BACE1,  $\beta$ -actin) or 10 $\mu$ g (all others) protein was boiled for 5 min in sample boiling buffer (60 mM Tris, 10% glycerol, 5% SDS, pH 6.8, 10%  $\beta$ -mercaptoethanol +loading dye) prior to being separated on 4-12% NuPAGE Bis-Tris gels in 1x MOPS running buffer (Invitrogen) and transferred to Millipore Immobilon-P polyvinylidene difluoride (PVDF) membrane. Blots were blocked overnight in 5% bovine serum albumin (BSA) in Tris-buffered saline, 0.1% Tween 20 (TBST; Sigma, T9039; modified form), pH 8.0. Blots were then incubated in primary antibody (Table 3.1). Blots were then washed in TBST followed by 1hr incubation in horseradish peroxidase-conjugated goat anti-mouse (G $\alpha$ M) diluted 1:10,000 in 5% milk in TBST (Jackson Immunological Research). Immunosignals were detected using enhanced chemiluminescence (ECL+, Amersham Biosciences) or SuperSignal West Femto (Pierce) and imaged and quantified using a Kodak CF440 imager.

Antibody	Clone	Dilution	5% Milk/BSA	Time	Source	Catalog No.	MW	Substrate
BACE1	3D5	1:10,000	Milk	1hr	Zhao, 2007		Immature: 50kD Mature: 70kD	ECL+
Actin	AC-15	1:15,000	Milk	1hr	Sigma	A1978	40kD	ECL+
eIF2a-P (Ser51)	119A11	1:2,000	BSA	O.N.	Cell Signaling	3597	38kD	WF
eIF2a		1:2,000	BSA	O.N.	Cell Signaling	9722	38kD	ECL+
c-Jun-P (Ser63)		1:2,000	BSA	O.N.	Cell Signaling	9261	48kD	WF
c-Jun		1:2,000	BSA	O.N.	Cell Signaling	9162	48kD	ECL+
JNK-P (Thr183/185)	G9	1:2,000	BSA	O.N.	Cell Signaling	9255	54/46kD	WF
JNK		1:2,000	BSA	O.N.	Cell Signaling	9252	54/46kD	ECL+
eIF4E-P (Ser209)		1:2,000	BSA	O.N.	Cell Signaling	9741	35kD	WF
Caspase 3		1:5,000	Milk	O.N.	Cell Signaling	9662	Pro: 35kD Cleaved: 19kD	WF

**Table 3.1:** List of primary antibodies used to probe BACE1-293 immunoblots.

## mRNA Isolation and Real Time PCR

All 350  $\mu\text{L}$  of cell lysate from each sample was used for mRNA extraction using Qiagen's RNeasy Mini kit according to the manufacturer's specifications. Total mRNA concentrations were measured using  $\text{ABS}_{260\text{nm}}$  ( $[\text{RNA}] \mu\text{g}/\mu\text{L} = 0.04 \times (\text{ABS}_{260\text{nm}})$ ) on a Beckman spectrophotometer. In general, only mRNA samples with low protein contamination ( $\text{ABS}_{260\text{nm}}/\text{ABS}_{280\text{nm}} > 1.8$ ) were used for analysis. mRNA integrity of each sample was confirmed using an Agilent Technologies 2100 Bioanalyzer. mRNA samples were used for analysis if the 28S ribosomal RNA peak was at least two times the area of the 18S ribosomal RNA peak. 1  $\mu\text{g}$  of total RNA from each sample was used for first-strand cDNA synthesis using Invitrogen's SuperScript III according to the manufacturer's recommendations. (Random hexamers were used as opposed to oligo dTs). Exact cDNA concentrations were determined using a Beckman spectrophotometer, and 112.5 ng cDNA from each sample was amplified *via* Real-Time PCR in triplicate using Applied Biosystems' Assays-on-Demand pre-mixed Taqman primer/probe set for human BACE1 mRNA (catalog # Hs00201573\_m1), which span exons 8-9 of the human BACE1 transcript, which recognizes all known splice variants of BACE1. Signals were normalized against an endogenous internal control signal obtained by co-amplifying mRNA with primers for 18s rRNA (#4333760F), which are not species-specific. Real Time reactions were run using an Applied Biosystems 7900HT sequence analyzer. Applied Biosystem's universal cycling parameters were used. Samples were only used for final analysis if the standard deviation between triplicate samples was  $< 0.1$  cycles. Percent of control values were determined using the comparative CT method.

## **Pulse-Chase**

BACE1-293 cells were plated in poly-D-lysine coated (100 µg/mL) 10-cm plates and allowed to grow to ~80% confluency in selective DMEM. Prior to pulse-labeling, cells were incubated in selective methionine-deficient DMEM (Cat #1642454; MP Biochemicals, Solon, OH) for 1 hr. Cells were pulse-labeled with 2 mL of selective methionine-deficient DMEM supplemented with 0.2 mCi <sup>35</sup>S trans-labeled methionine and cysteine (Cat #5100607; MP Biochemicals) for 20 min. Cells were then “chased” with regular selective DMEM or glucose-deficient selective DMEM containing unlabeled methionine (Invitrogen). At 0 hrs, 3 hrs, 6 hrs, 12 hrs, and 24 hrs post-label, lysates were washed 2x in 1x PBS and collected in 1mL 1x RIPA buffer, homogenized, and 500µL lysate was immunoprecipitated with Sepharose G beads (Amersham) and 3 µg anti-BACE1 (PA1-757; Affinity Bioreagents) according to the manufacturer’s recommendations (Amersham immunoprecipitation protocol). Immunoprecipitates were separated *via* SDS-PAGE using 10% Criterion Tris-acetate gels (BioRad; Hercules, CA). Gels were fixed for 30 min (10% methanol, 3% glycerol, 1% glacial acetic acid), dried for 20 min at 80 °C to filter paper using a heated gel dryer (Hoefer Scientific Instruments, San Francisco, CA), and exposed to a phosphor screen overnight (Amersham). Autoradiographic signals were imaged using a Cyclone Plus Phosphor Imager (Perkin-Elmer).

## **Statistical analysis**

Sample averages were determined and then means and standard error of the means (SEMs; represented by error bars in histograms) were calculated based on the sample

averages (n-values are stated in figure legends). Statistical differences between experimental groups and their respective controls were determined using a two-tailed t-test. Data are presented as the mean  $\pm$  SEM. \* $p < 0.05$ , \*\* $p < 0.01$ , \*\*\* $p < 0.001$ .

## Results

### **Energy deprivation elevates BACE1 protein levels via a post-transcriptional mechanism *in vitro***

Previously, we showed that BACE1 protein is elevated in the brains of two month-old mice following acute energy inhibitor treatments. This elevation in protein was not accompanied by a corresponding increase in BACE1 mRNA, indicating that a post-transcriptional mechanism was involved (Velliquette et al., 2005). To further investigate the molecular mechanism responsible for BACE1 elevation in response to energy impairment, we developed an *in vitro* model of energy deprivation by incubating HEK-293 cells stably expressing human BACE1 cDNA under the control of the CMV promoter (BACE1-293) in glucose-deficient (NG) media. BACE1-293 cells were treated up to 48 hrs in either normal, high glucose-containing (25 mM) media (CON), or in media lacking glucose (NG). Cell lysates were collected and analyzed by immunoblot for BACE1 levels, using a highly specific BACE1 monoclonal antibody (3D5) (Zhao et al., 2007). Glucose deprivation slowed cell growth but otherwise appeared to be non-toxic and caused no change in cell morphology. BACE1 protein levels were already elevated in NG-treated cells after only 2 hrs of glucose deprivation, as compared to cells grown in normal control media, and remained high over a period of at least 48 hrs reaching ~150% of control levels (Fig. 3.1A,B). The BACE1 increase in BACE1-293

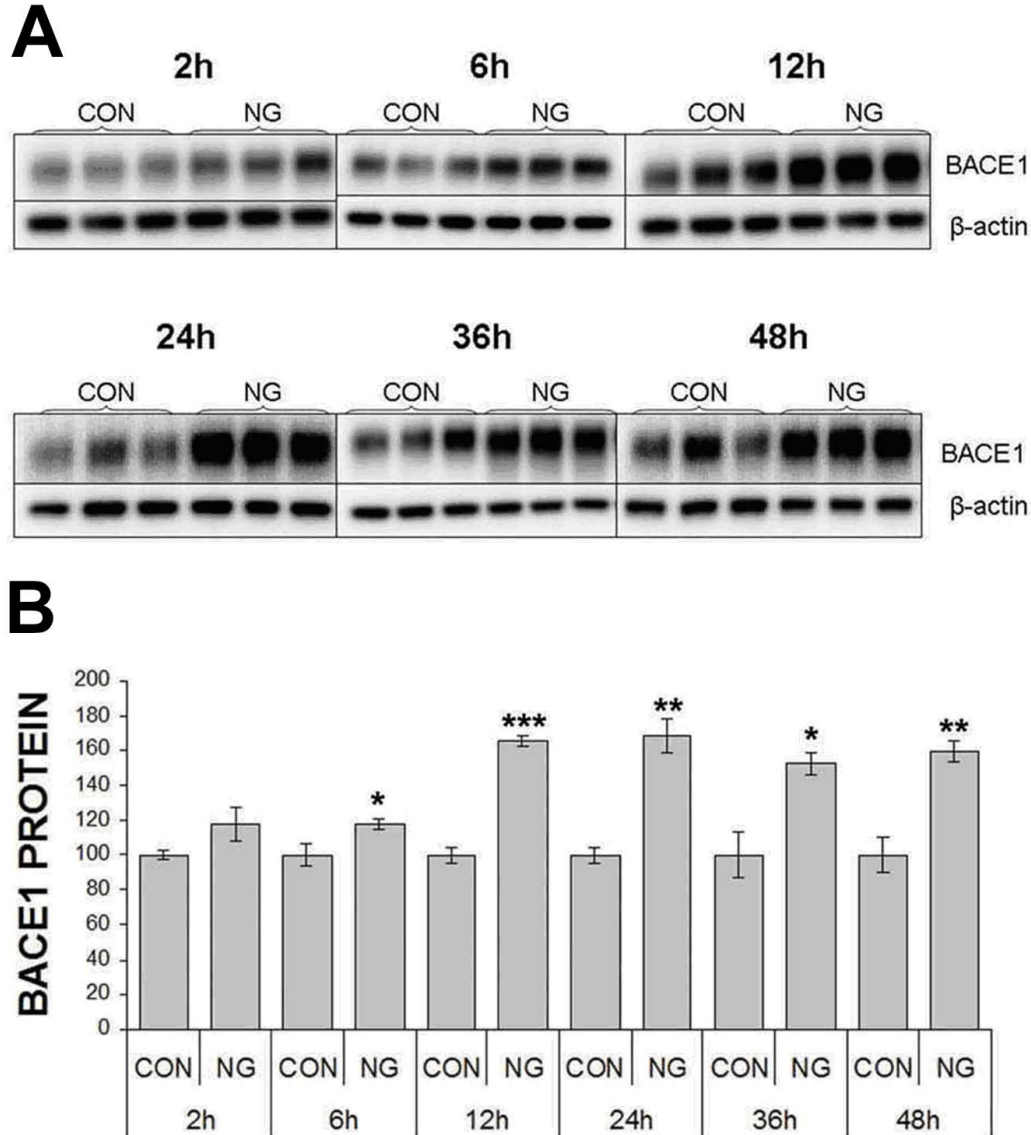


**Figure 3.1: Glucose deprivation increases BACE1 protein levels in BACE1-293 cells.** (A) BACE1-293 cells were incubated for 2, 6, 12, 24, 36, and 48 hrs in either normal DMEM with glucose (25mM; CON) or DMEM without glucose (NG). Cells were lysed at the end of the treatment periods and 5µg of total protein per lane was used for immunoblot analysis of BACE1. β-actin was used as a loading control. (B) BACE1 immunosignals in (A) were quantified by phosphorimager, normalized to β-actin, and expressed as percentage of control (CON) for each time-point. BACE1 protein levels were significantly elevated compared to CON in response to glucose deprivation from 6 through 48 hrs (mean ± SEM; \*,  $p<0.05$ ; \*\*,  $p<0.01$ ; \*\*\*,  $p<0.001$ ). An upward trend for a BACE1 increase was present at 2 hrs of NG treatment (n=3 per group).

cells was similar in magnitude to that observed after acute energy inhibition *in vivo* (Velliquette et al., 2005). We performed TaqMan quantitative real-time PCR analysis of BACE1 mRNA isolated from 12 hr CON and NG-treated BACE1-293 cells using a human BACE1-specific FAM fluorescent reporter-tagged primer/probe set spanning exons 8-9 of the BACE1 coding region, which are present in all known BACE1 transcripts. mRNA analysis revealed similar steady-state levels of BACE1 transcript in both groups (Fig. 3.2C), demonstrating that the BACE1 elevation induced by energy deficiency in BACE1-293 cells was the result of a post-transcriptional mechanism and was not due to either elevated expression of the CMV promoter or increased BACE1 mRNA stability mediated by the BACE1 3'UTR. Additionally, we performed glucose-deprivation experiments in the presence of a transcriptional inhibitor (1.7  $\mu$ g/mL actinomycin D). By 12 hrs of treatment with ActD, BACE1 mRNA levels were reduced to ~25% of control (Fig 3.2A,B); however, corresponding BACE1 protein levels in NG+ActD-treated BACE1-293 cells were still elevated compared to BACE1-293 cells treated with ActD alone, further eliminating transcription as the mechanism elevating BACE1 protein in response to energy deprivation (Fig 3.2A,B;  $p < 0.05$ ).

### **Energy deprivation does not alter BACE1 protein stability *in vitro***

Having eliminated transcription as a probable mechanism regulating BACE1 levels in response to impaired energy metabolism, we next investigated the possible involvement of altered BACE1 protein stability. Recent studies have shown that BACE1 protein stability can be modulated by the lysosomal and ubiquitin-proteasomal degradation pathways (Koh et al., 2005; Qing et al., 2004; Tesco et al., 2007; Vassar, 2007). To test

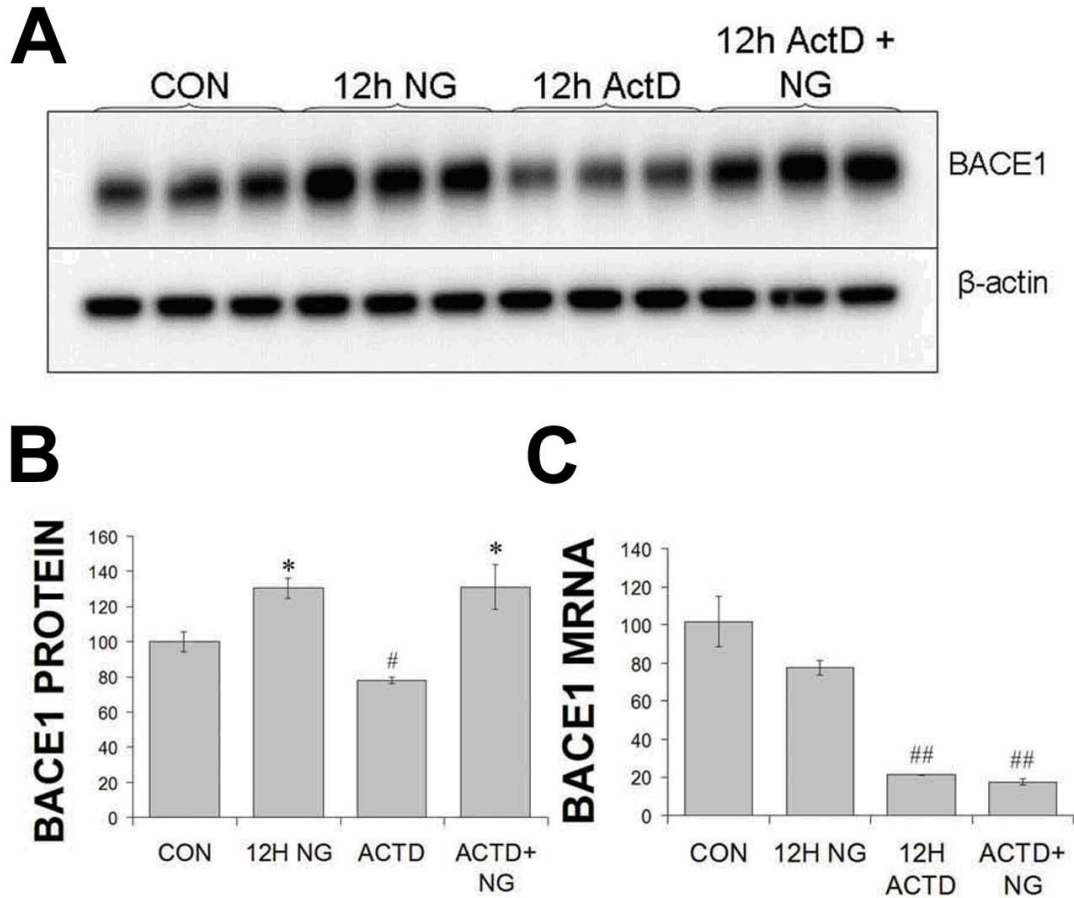


**Figure 3.2: Glucose deprivation elevates BACE1 protein in BACE1-293 cells *via* a post-transcriptional mechanism.** BACE1-293 cells were incubated for 12 hrs in regular DMEM with glucose (CON), DMEM without glucose (NG), DMEM with glucose containing 1.7 $\mu$ g/mL actinomycin D (ActD), or DMEM without glucose containing ActD (ActD + NG). **(A)** 5  $\mu$ g of cell lysate was analyzed *via* immunoblot BACE1 protein expression. **(B)** BACE1 immunosignals were normalized to  $\beta$ -actin, and expressed as % CON. BACE1 protein levels were significantly elevated in response to 12 hrs of NG treatment either in the presence or absence of ActD, and were significantly decreased with 12 hrs of ActD treatment alone. (n = 3) **(C)** Total mRNA was isolated from BACE1-293 cells, and BACE1 mRNA was measured *via* Real-time PCR. BACE1 mRNA levels were normalized to 18S rRNA and expressed as % CON (n=6). 12 hrs ActD treatment alone significantly decreased BACE1 mRNA levels; however, there were no differences in BACE1 mRNA levels between cells treated in media with or without glucose. \*, p<0.05 (increase) #p<0.05, ##, p<0.01 (decrease)



BACE1 protein stability in response to energy deprivation, we used pulse-chase  $^{35}\text{S}$ -metabolic radiolabeling to measure the half-life ( $t_{1/2}$ ) of BACE1 protein in BACE1-293 cells incubated under normal conditions versus conditions of energy inhibition. BACE1-293 cells were grown in normal media, pulse-labeled in media containing  $^{35}\text{S}$ -radiolabeled methionine, and then chased for up to 24 hrs in normal, NG, or media containing 50 mM 2DG.  $^{35}\text{S}$ -labeled BACE1 protein was immunoprecipitated from BACE1-293, separated by SDS-PAGE, and imaged using autoradiography. BACE1  $t_{1/2}$  was determined *via* densitometric analysis of the autoradiographic image. We observed that the  $t_{1/2}$  of BACE1 in BACE1-293 cells was ~12 hours in normal control media, similar to previous reports (Haniu et al., 2000; Huse and Doms, 2000). However, under NG or 2DG chase conditions, the  $t_{1/2}$  of BACE1 protein appeared to be unchanged, indicating that increased BACE1 protein stability is not the post-transcriptional mechanism responsible for increased BACE1 levels in response to energy deficiency (Fig. 3.3A). Furthermore, 24 hrs of glucose deprivation failed to induce activation of caspase 3, which has been shown to enhance BACE1 protein stability after the onset of apoptosis (Fig 3.3B). Taken together, our results eliminated increases of transcription, mRNA stability, and protein stability as possible mechanisms, leaving increased BACE1 translation as the likely cause of the BACE1 elevation following energy deprivation.

### **The BACE1 5'UTR is required for glucose deprivation-induced BACE1 protein elevation**

Translational regulation of proteins is most commonly mediated through the 5'UTR of mRNA transcripts, either through formation of secondary structure that

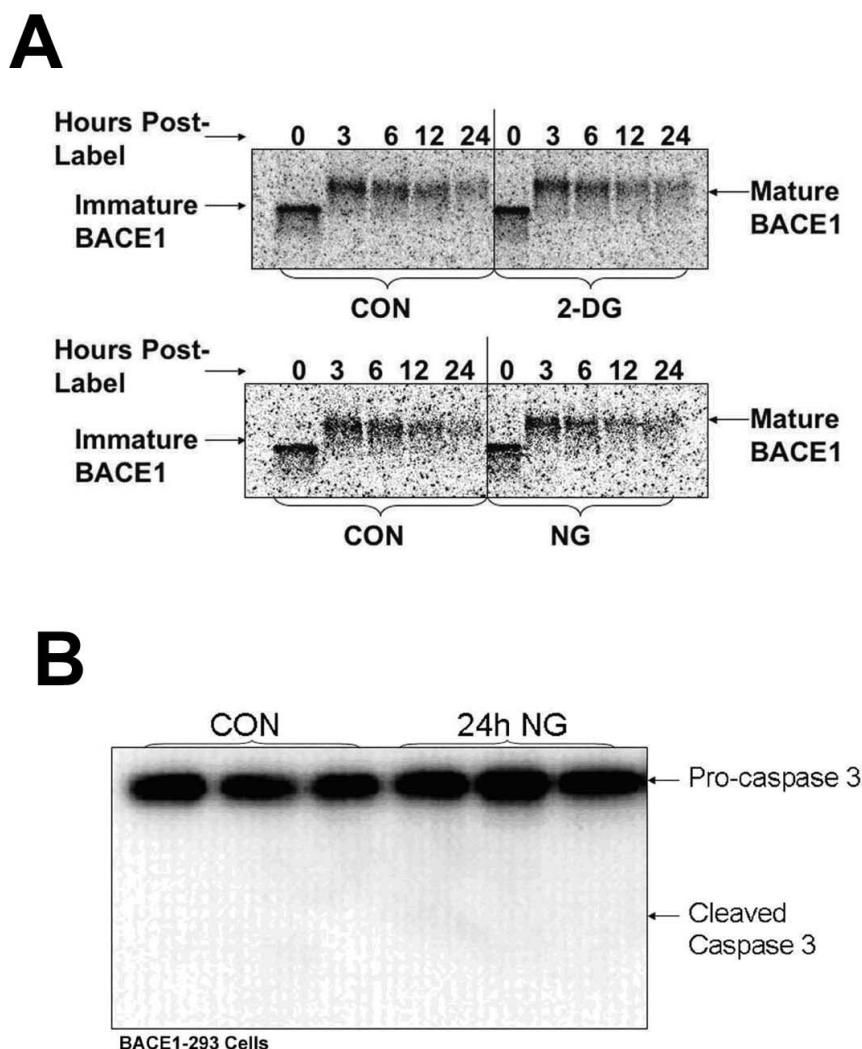


**Figure 3.3: Glucose deprivation in BACE1-293 cells does not alter BACE1 protein stability.** (A) BACE1-293 cells were pulse-labeled in media containing  $^{35}\text{S}$ -methionine/cysteine and chased for up to 24 hrs in normal DMEM with glucose (CON), DMEM without glucose (NG), or DMEM containing 50mM 2-deoxyglucose (2-DG). Radiolabeled BACE1 was immunoprecipitated from cell lysates at 0, 3, 6, 12, and 24 hrs post-label, separated via SDS-PAGE, and visualized by autoradiography. Note that immaturely glycosylated BACE1 is ~50kDa, while maturely glycosylated BACE1 is ~70 kDa. There were no apparent differences between the half-lives of BACE1 protein under CON, NG, and 2DG conditions, indicating that BACE1 increases are not due to BACE1 protein stabilization. In histograms, error bars represent S.E.M. (B) BACE1-293 cells were incubated for 24 hrs in either regular DMEM (CON) or DMEM without glucose (24h NG). 10  $\mu\text{g}$  cell lysate was used for immunoblot analysis of caspase 3 (Cell Signaling # 9662). There was no evidence of activated (cleaved) caspase 3 in control or 24 hr NG-treated BACE1-293 cells

inhibits ribosome binding, differential utilization of upstream open reading frames (uORFs) of the authentic start codon, or internal ribosomal entry sites (IRES) (Schroder and Kaufman, 2006). Protein translation can also be regulated in some cases by the binding of microRNAs to the 3'UTR sequence of transcripts (Jackson and Standart, 2007). Since the hBACE1 construct expressed in BACE1-293 cells contains a truncated 3'UTR (500bp of 4kB), we initially investigated the involvement of the BACE1 5'UTR in regulating glucose deprivation-induced BACE1 protein elevations *in vitro*. Wild-type HEK-293 cells were transiently transfected with a construct expressing the entire human BACE1 coding region under the control of the CMV promoter and lacking both the BACE1 5'UTR and 3'UTR regulatory sequences (-5'UTR). As a control, HEK-293 cells were also transiently transfected with a similar construct containing the entire BACE1 5'UTR (+5'UTR). -5'UTR or +5'UTR-transfected HEK-293 cells were incubated for 24 hrs in either normal or glucose-deficient media and analyzed *via* immunoblot for BACE1 protein expression. As previously reported, deletion of the BACE1 5'UTR, leads to a massive up-regulation of BACE1 protein expression *in vitro* (~200% above -5'UTR;  $p < 0.001$ ; Fig 3.4). The lower migrating band in -5'UTR-transfected cells is most likely intermediately glycosylated forms of BACE1 accumulating in the ER due to overexpression, rather than a C-terminally truncated form of BACE1 previously described (Hussain et al., 2003), since re-probing with a C-terminal BACE1 antibody (Affinity Bioreagents PA1-757) yielded the same results. 24 hr NG treatment elevated BACE1 protein levels over control-treated, as expected, in +5'UTR-transfected cells (~150%,  $p < 0.01$ ; Fig 3.4). In contrast, 24 hr NG treatment failed to increase BACE1 protein levels above control in -5'UTR-transfected cells, demonstrating that the BACE1

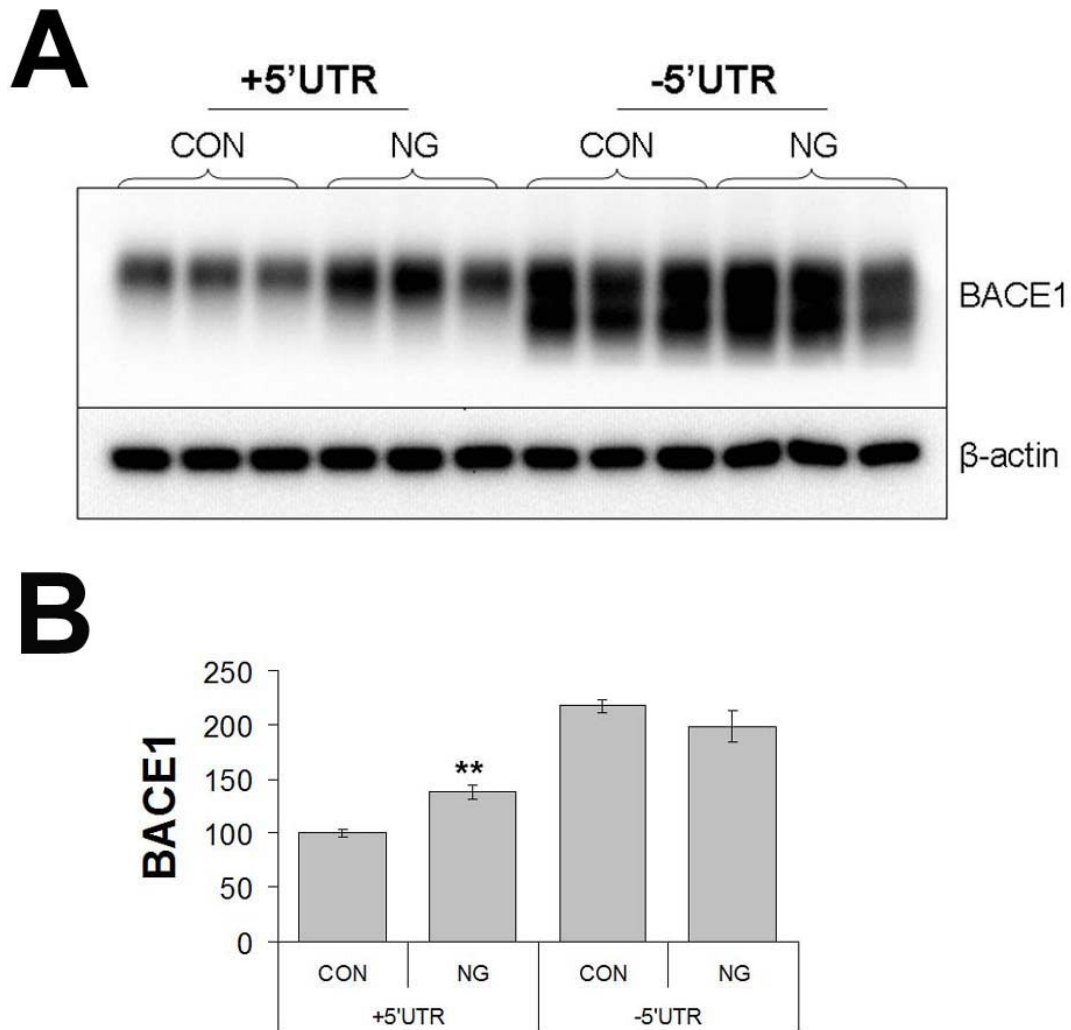


**Figure 3.4: The BACE1 5'UTR is required for glucose deprivation-induced BACE1 protein elevation in HEK-293 cells.** (A) HEK-293 cells were transiently transfected with pcDNA3.1Zeo(+) vector containing the entire human BACE1 coding region (~1.5kb) plus the BACE1 5'UTR (+5'UTR) or pcDNA3.1Zeo(+) vector containing only the human BACE1 coding region (-5'UTR) (Lammich et al., 2004). +5'UTR or -5'UTR cells were incubated for 24 hrs in normal DMEM with glucose (CON) or DMEM without glucose (NG). 5µg of protein was used for immunoblot analysis of BACE1. (B) BACE1 immunosignals were normalized to β-actin and expressed as percentage of +5'UTR control (CON, +5'UTR). The glucose deprivation-induced BACE1 increase did not occur in the absence of the BACE1 5'UTR, implicating a BACE1 5'UTR-dependent translational control mechanism. (n=3 per group; \*\*, comparison between CON and NG, +5'UTR;  $p < 0.01$ ; mean  $\pm$  SEM). Error bars = S.E.M. in all histograms.

5'UTR sequence is required for glucose deprivation-induced BACE1 protein elevations (Fig 3.4). This data further supports the hypothesis that energy deprivation-mediated BACE1 elevation occurs through a translational mechanism.

### **eIF2 $\alpha$ phosphorylation is increased by energy deprivation *in vitro***

It is well established that diverse physiological stresses affect translation at the level of initiation. The two main targets of this type of translational regulation are the eukaryotic translation initiation factors 4E and 2 (eIF4E and eIF2). eIF4E is part of the eIF4F mRNA cap binding complex, which can be regulated by stress stimuli either through phosphorylation at Ser209 (eIF4E-P) or increased association with its inhibitory binding partner, 4E-BP. The other translation initiation factor, eIF2, is part of the translational ternary complex (eIF2, GTP, met:tRNA). eIF2 is phosphorylated on its  $\alpha$  subunit (eIF2 $\alpha$ ) in response to stress stimuli, which inhibits the formation of the ternary complex. Reduced availability of the cap-binding complex or the ternary complex simultaneously reduces the rate of global translation while enhancing the translation rate of specific stress-response mRNA transcripts with regulatory elements in the 5'UTR (Fig 3.5) (Clemens, 2001a). In order to determine whether stress activated alterations in the translation initiation machinery was involved in glucose deprivation-induced BACE1 protein elevations, we screened cell lysates from 24 hr NG-treated BACE1-293 cells *via* immunoblot for translation factors and other stress signaling pathways involved in cellular stress response. Most signaling pathways tested were not activated. This included phosphorylation of eIF4E (eIF4E-P(Ser209)), phosphorylation of p38 (p38-P(Thr180/Tyr182)), which is known to converge upon eIF4E-P, and phosphorylation of

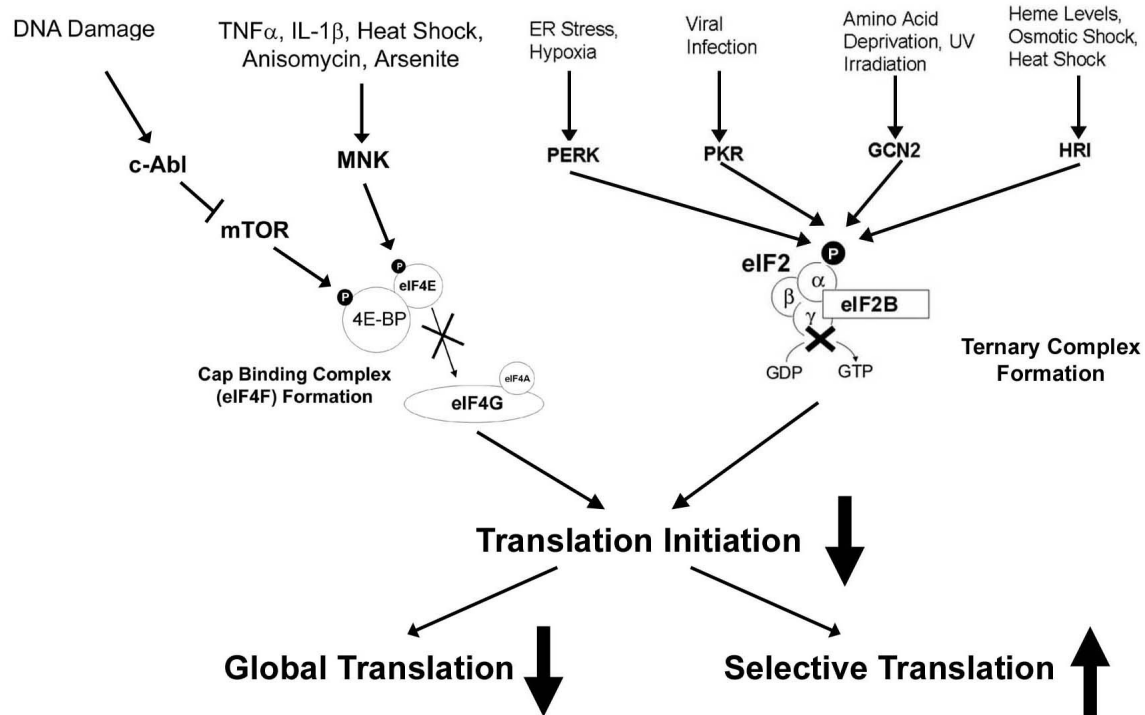


**Figure 3.5: Convergence of stress signaling pathways on translation initiation.** **4E-BP** phosphorylation by mTOR is inhibited by DNA damage-mediated activation of c-abl. Dephosphorylated 4E-BP binds to eIF4E, preventing its association with the cap binding complex (eIF4F). **eIF4E** is phosphorylated by the Mnk kinases, which are activated by the p38 stress pathway. Phosphorylation of eIF4E also prevents the formation of eIF4F. **eIF2 $\alpha$**  is phosphorylated by four different kinases in response to stress, which reduces the availability of the ternary complex. Reduced eIF4F or ternary complex formation reduces the rate of translation initiation, which reduces global translation rates while simultaneously enhancing the translation of certain stress response proteins

translation initiation factor 4G (eIF4G-P(Ser1108)), the scaffolding component of the eIF4F complex (Fig 3.5; Fig 3.7). Furthermore, an eIF4E-P inhibitor could not prevent the NG-induced BACE1 protein elevation in BACE1-293 cells (Fig 3.6C,D), Endogenous BACE1 protein levels were unresponsive to the 4E-BP inhibitor, rapamycin, in cultured C57/BL6 neurons (Fig 3.6A,B), as well as overexpressed human BACE1 in BACE1-293 cells (not shown). There was also no evidence for phosphorylation of the alpha subunit of AMP-activated kinase (AMPK-P $\alpha$ (Thr172)) in response to glucose deprivation in BACE1-293 cells, which also converges upon 4E-BP. We did observe increased phosphorylation of the stress-activated proteins c-Jun and c-Jun N-terminal kinase (JNK) in response to glucose deprivation, which may lead to transcriptional activation of other stress response proteins (Fig 3.7). Notably, using this screen we found that the ratio of phosphorylated eukaryotic translation initiation factor 2 at serine 51 of the  $\alpha$  subunit (eIF2 $\alpha$ -P(Ser51)) to total eIF2 $\alpha$  (eIF2 $\alpha$ -T) was increased to ~200% of control by 2 hrs in NG media ( $p < 0.01$ ) and ~250% of control by 24 hrs in NG media ( $p < 0.01$ ), implicating the involvement of this component of the translation initiation complex in glucose deprivation-induced BACE1 protein elevations (Fig. 3.7). Interestingly, we also observed increased levels of total c-Jun protein, the structural and functional homolog of the yeast protein GCN4, which is a well-established translational target of the eIF2 $\alpha$ -P pathway (Fig 3.7; ~200% of control by 24 hrs in NG media ( $p < 0.001$ )) (Cigan et al., 1993; Struhl, 1987; Vazquez de Aldana et al., 1993; Vogt et al., 1987).

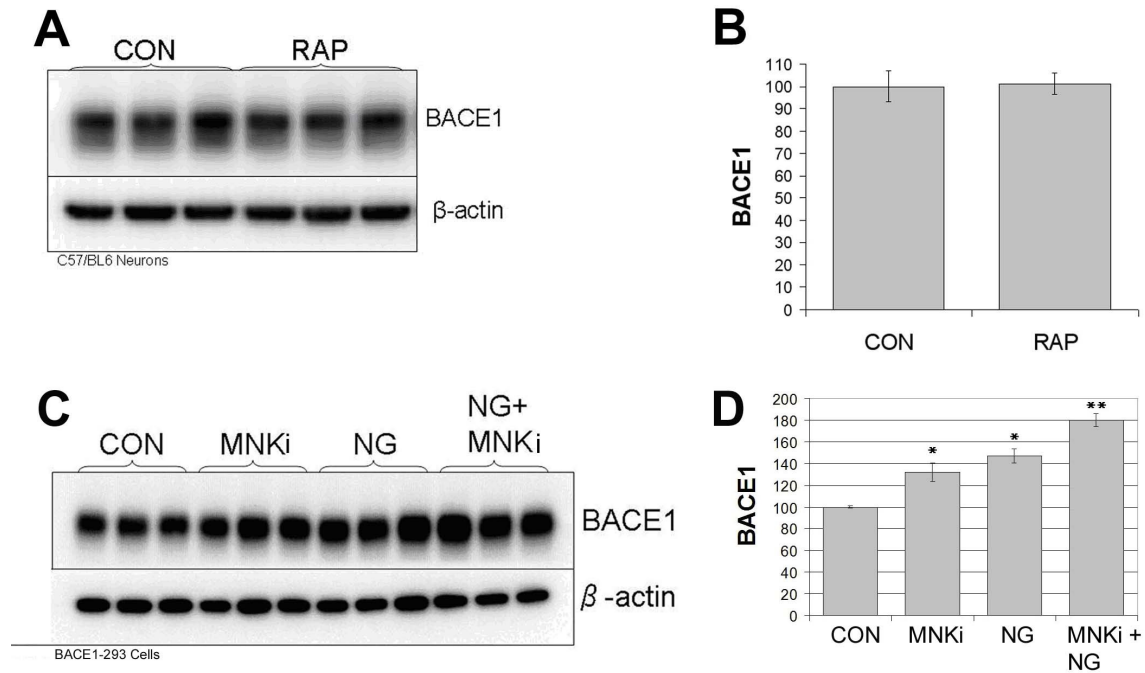


**Figure 3.6: eIF4E is not involved in glucose deprivation-induced BACE1 protein elevation.** (A) Primary cortical C57/BL6 neurons were cultured for 7DIV and then incubated in either normal neurobasal media (CON) or media containing 10 nM of the mTOR inhibitor, rapamycin (RAP), for 12 hrs. 10  $\mu$ g protein was used for immunoblot analysis of BACE1. (B) BACE1 immunosignals were normalized to  $\beta$ -actin. Values were expressed as percentage of control  $\pm$  SEM. There was no significant difference between BACE1 protein levels in CON and RAP-treated neurons, indicating that BACE1 is not regulated by eIF4E availability. (C) BACE1-293 cells were incubated for 12 hrs in normal media (CON), media containing 1  $\mu$ M Mnk inhibitor (MNKi), media without glucose (NG), or media without glucose containing 1  $\mu$ M Mnk inhibitor (NG + MNKi). 5  $\mu$ g protein was used for immunoblot analysis of BACE1 protein. (D) BACE1 immunosignals were normalized to  $\beta$ -actin and expressed as % CON. A Mnk inhibitor could not prevent glucose deprivation-induced BACE1 protein elevation, indicating that eIF4E is not involved. (n = 3). \*,  $p < 0.05$ ; \*\*,  $p < 0.01$ ; \*\*\* $p < 0.001$



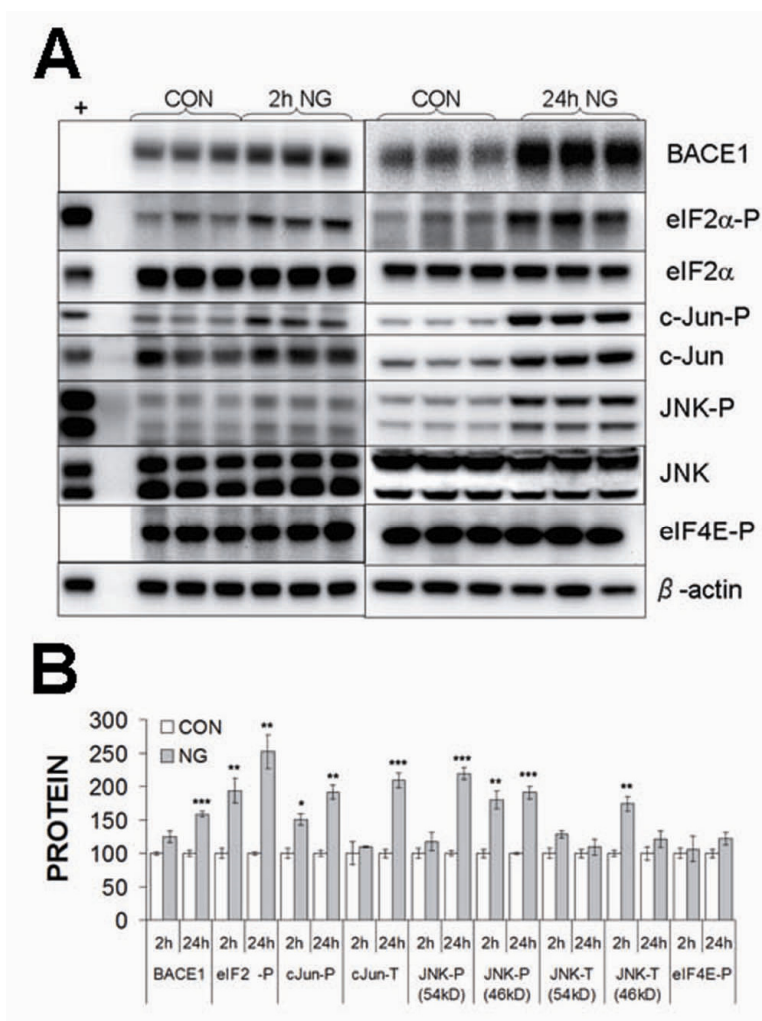


**Figure 3.7: Glucose deprivation increases eIF2α phosphorylation and activates a specific set of stress-response signaling pathways in BACE1-293 cells.** (A) BACE1-293 cells were incubated for 2 or 24 hrs in either normal DMEM with glucose (4.5 g/L; CON) or DMEM without glucose (NG). 5 μg (BACE1) or 10 μg (others) protein was used for immunoblot analysis of BACE1, phospho-eIF2α(Ser51), total eIF2α, phospho-c-Jun(Ser63), total c-Jun, phospho-JNK(Thr183/Thr185), total JNK (54kD and 46kD isoforms), and phospho-eIF4E(Ser209). ~10μg of lysate from UV-treated 293 cells was used as a positive control (+). (B) BACE1, eIF2α, JNK, and eIF4E-P were normalized to β-actin, eIF2α-P was normalized to total eIF2α; c-Jun-P was normalized to c-Jun, and JNK-P was normalized to JNK. Values are expressed as % CON for 2 hrs or 24 hrs. After 2 hrs of NG treatment, eIF2α-P, c-Jun-P, JNK-P(46kD), and JNK(46kD) were all significantly elevated. At 24 hrs NG, eIF2α-P, c-Jun-P, and JNK-P(46kD) remained elevated, and BACE1, c-Jun, and JNK-P(54kD) became significantly increased as well. eIF4E phosphorylation was unaffected by NG treatments at either time-point. These results show that eIF2α-P is temporally increased before BACE1, as expected if eIF2α-P regulates BACE1 translation. (n = 3; mean ± SEM; \*, p<0.05; \*\*, p<0.01; \*\*\*, p<0.001).

### **Direct phosphorylation of eIF2 $\alpha$ elevates BACE1 protein levels**

In a screen of stress-activated signaling pathways activated in response to glucose deprivation *in vitro*, we identified phosphorylation of eIF2 $\alpha$  as a likely pathway through which BACE1 protein might be translationally elevated in response to glucose deprivation. In order to determine whether direct elevation of eIF2 $\alpha$ -P(Ser51) levels could elevate BACE1 levels in the absence of glucose deprivation, we treated BACE1-293 cells for 24 hrs with salubrinal (100  $\mu$ M), a drug that selectively inhibits growth arrest and DNA damage protein 34 (GADD34) (Boyce et al., 2005). GADD34 is a regulatory subunit of protein phosphatase-1c (PP1c), which is the phosphatase responsible for dephosphorylating eIF2 $\alpha$  at Ser51 after the onset of stress conditions (Fig 3.8) (He et al., 1996). Inhibition of GADD34 by salubrinal prevents PP1c dephosphorylation of eIF2 $\alpha$ , thereby elevating basal eIF2 $\alpha$ -P levels. Treatment of BACE1-293 cells with salubrinal caused both eIF2 $\alpha$ -P(Ser51) and BACE1 levels to increase to ~150% of control values (Fig. 3.9A;  $p < 0.05$ ), indicating that BACE1 mRNA is a novel translational target of the stress-activated eIF2 $\alpha$ -P(Ser51) pathway.

### **Inhibition of eIF2 $\alpha$ phosphorylation prevents energy deprivation-induced BACE1 protein elevations**

Glucose deprivation elevates BACE1 and eIF2 $\alpha$ -P levels (Fig 3.7), and direct elevation of eIF2 $\alpha$ -P can elevate BACE1 levels *in vitro* (Fig 3.9), indicating that activation of the eIF2 $\alpha$ -P pathway may be responsible for glucose deprivation-induced BACE1 protein elevations. In order to determine whether glucose deprivation-induced BACE1 protein elevations could be prevented by inhibiting eIF2 $\alpha$  phosphorylation, we transiently

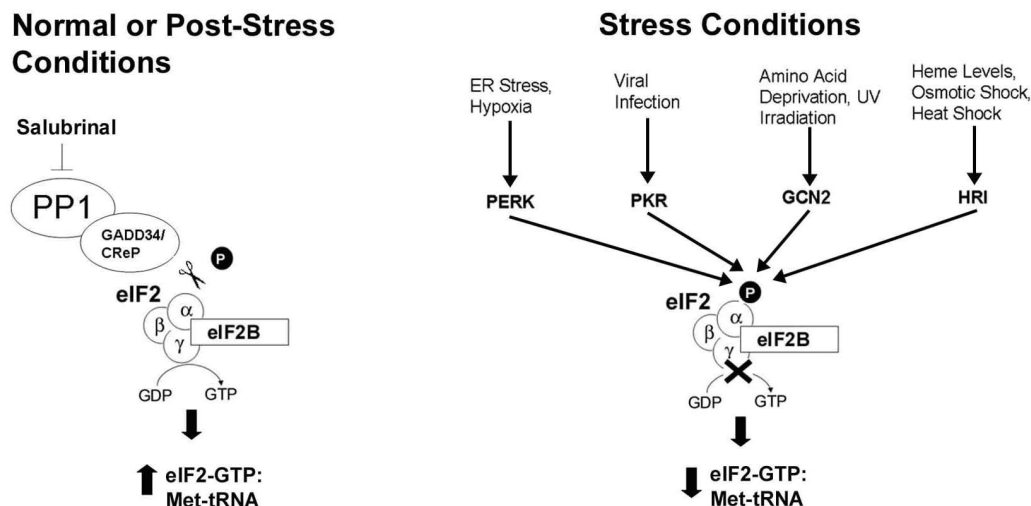


**Figure 3.8: Regulation of eIF2α and translation initiation by phosphorylation at Ser51.** Under normal or post-stress conditions (**left**), eIF2α-P levels are low, due to expression of regulatory subunits of protein phosphatase PP1 (GADD34 and CReP), which direct PP1 phosphatase activity to eIF2α. Salubrinal elevates basal eIF2α-P levels by inhibiting PP1 and preventing eIF2α dephosphorylation. eIF2B catalyzes the exchange of GDP for GTP on the γ subunit of eIF2. In its GTP form, eIF2 assembles into a ternary complex with methionine-charged tRNA (eIF2·GTP·Met-tRNA<sub>i</sub>). The ternary complex binds to the 40S ribosomal subunit and allows the initiation complex to scan the 5'UTR of mRNAs for AUG start codons. Initiation at a start codon leads to the hydrolysis of eIF2-GTP and the release of eIF2 from the ribosome. When eIF2α-P levels are low, ternary complex is readily available, and global translation rates are high. Under stress conditions (**right**), eIF2α is phosphorylated by one of four different kinases. Phosphorylation of eIF2α prevents the dissociation of eIF2B from eIF2, slowing the exchange rate of GDP for GTP on eIF2γ and reducing the availability of ternary complex. Reduced ternary complex availability slows the translation rate of most mRNA transcripts, with the exception of specific stress-response mRNAs that are preferentially translated under conditions of low ternary complex availability.

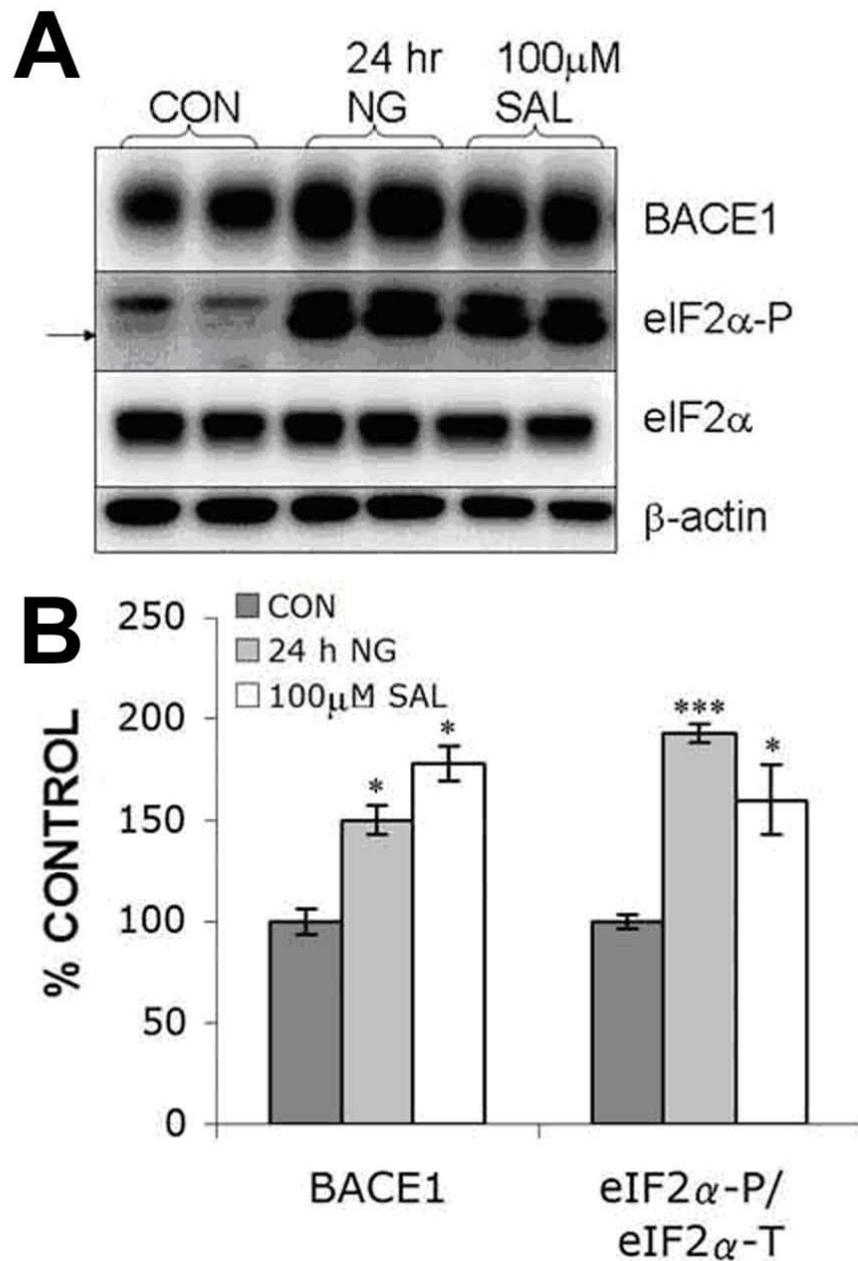


**Figure 3.9: Direct phosphorylation of eIF2α elevates BACE1 protein in BACE1-293 cells.** (A) BACE1-293 cells were incubated for 24 hrs in normal DMEM with glucose (25mM; CON), DMEM without glucose (NG), or DMEM containing 100 μM salubrinal (SAL). 5 μg (BACE1) or 10μg (others) of protein was used for immunoblot analysis of phosphorylated eIF2α, total eIF2α, and BACE1. (B) BACE1 immunosignals were normalized to β-actin, eIF2α-P was normalized to total eIF2α, and values were expressed as % CON. Levels of BACE1 and eIF2α-P/eIF2α-T were significantly elevated in response to both glucose deprivation and salubrinal treatment, compared to control (mean ± SEM; \*, p<0.05; \*\*\*, p<0.001; n = 2 per group).

transfected BACE1-293 cells with an expression construct encoding the C-terminal activation domain of GADD34 (GADD34 $\Delta$ N). Transfection of cells with this construct constitutively activates PP1c-mediated dephosphorylation of eIF2 $\alpha$ . In the presence of continuous phosphatase activity, eIF2 $\alpha$  phosphorylation is effectively prevented (Fig 3.8) (Novoa et al., 2001). Transfection of cells with an inactive GADD34 construct lacking the C-terminal PP1c activation domain (GADD34CON), which has no effect on PP1c activity, served as a transfection control. GADD34 $\Delta$ N and GADD34CON-transfected cells were treated for 12 hrs in NG or normal media, and cell lysates were analyzed by immunoblot for BACE1 and eIF2 $\alpha$ -P. GADD34CON-transfected BACE1-293 cells exhibited the expected increase in levels of BACE1 and eIF2 $\alpha$ -P(Ser51) levels in response to NG treatment (Fig. 3.10). GADD34 $\Delta$ N-transfected cells incubated in NG media, however, showed no increase in eIF2 $\alpha$ -P(Ser51) or BACE1 levels in response to NG treatment compared to control, demonstrating that inhibition of eIF2 $\alpha$ -P can completely block NG-induced BACE1 protein elevations (Fig. 3.10). Interestingly, BACE1 protein elevations induced by 12 hr NG treatment were also prevented by co-treatment of BACE1-293 cells with 1  $\mu$ M tauroursodeoxycholic acid (TUDCA) (Fig 3.11), which has previously been shown to alleviate endoplasmic reticulum (ER) stress by acting as a “chemical chaperone” (Ozcan et al., 2006). Together with our salubrial experiments, these results clearly demonstrate that the increase in BACE1 protein in response to energy deprivation *in vitro* is the result of elevated phosphorylation of eIF2 $\alpha$  at Ser51.

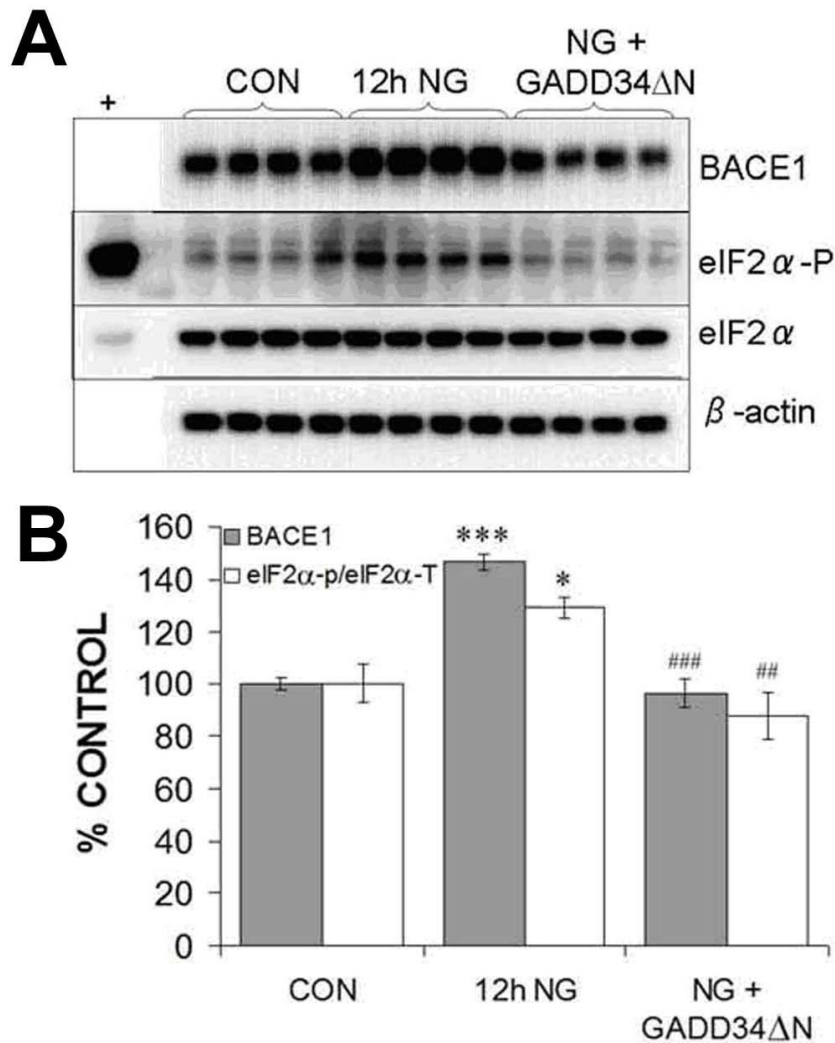


**Figure 3.10: Inhibition of eIF2α phosphorylation prevents glucose deprivation-induced BACE1 protein elevation** (A) BACE1-293 cells were transiently transfected with GADD34 control vector (CON, 12h NG) or GADD34ΔN (NG + GADD34ΔN), the constitutively active PP1 regulatory subunit. Cells were incubated for 12 hrs in normal DMEM with glucose (CON) or DMEM without glucose (12h NG, NG + GADD34ΔN). 5 μg (BACE1, β-actin) or 10 μg (eIF2α-P, eIF2α-T) of protein was used for immunoblot analysis of BACE1, P-eIF2α(Ser51), total eIF2α, and β-actin. "+" lane: 10μg of lysate from UV-treated 293 cells was used as a positive control for eIF2α-P. (B) BACE1 immunosignals were normalized to β-actin, eIF2α-P was normalized to total eIF2α, and values were expressed as % CON. Glucose deprivation-induced increases in levels of BACE1 and eIF2α-P/eIF2α-T were completely prevented by overexpression of GADD34ΔN, demonstrating that eIF2α phosphorylation was responsible for the BACE1 increase. (n=4; comparison between CON and 12h NG: \*, p < 0.05; \*\*\*, p < 0.001; comparison between 12h NG and NG + GADD34ΔN: ##, p < 0.01; ###, p < 0.001; mean ± SEM).

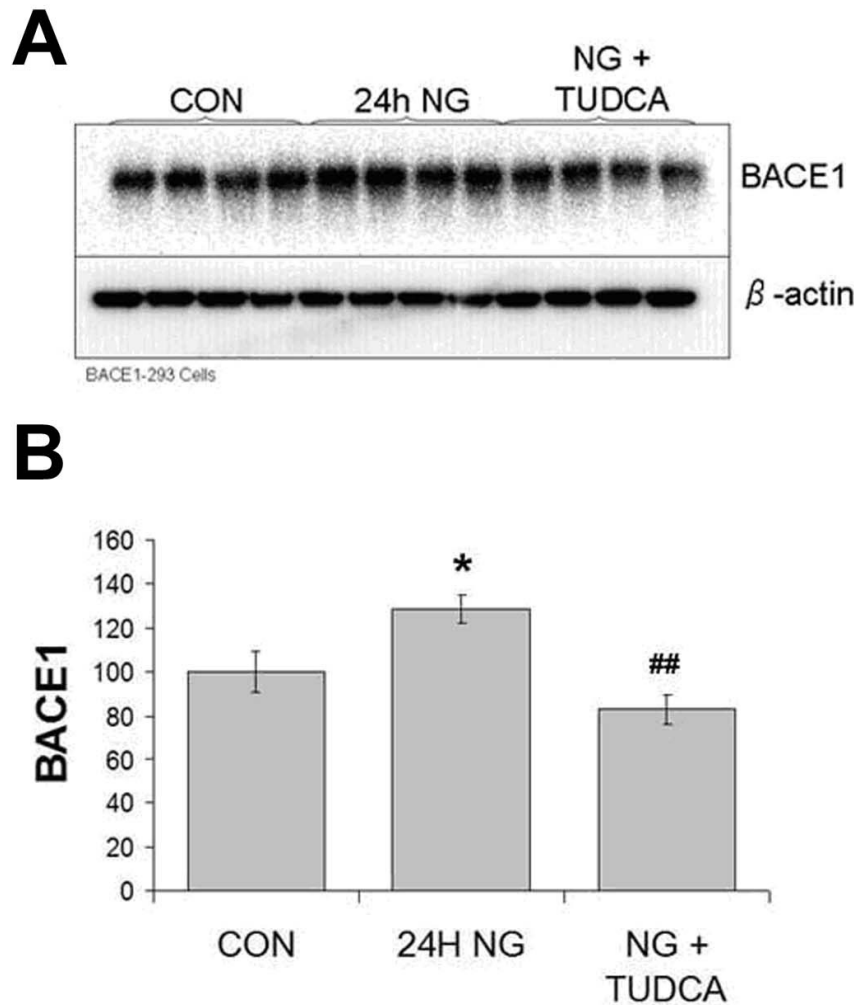


**Figure 3.11: Treatment of cells with a chemical chaperone prevents glucose deprivation-induced BACE1 protein elevation** **(A)** BACE1-293 cells were incubated for 24 hrs in regular DMEM containing glucose (CON), DMEM without glucose (24H NG), or DMEM without glucose supplemented with 1  $\mu$ M tauroursodeoxycholate (NG + TUDCA). Cell lysates were harvested and 5  $\mu$ g protein was used for immunoblot analysis of BACE1 and  $\beta$ -actin. **(B)** BACE1 immunosignals were normalized to  $\beta$ -actin. Values were expressed as % CON. As expected, 24 hrs of glucose deprivation significantly elevated BACE1 levels (24H NG), as compared to control (CON). Treatment with 1  $\mu$ M TUDCA prevented the glucose deprivation-induced BACE1 protein increase (NG + TUDCA). Since TUDCA blocks the ER stress/unfolded protein response (Ozcan et al., 2006), these results provide additional evidence that phosphorylation of eIF2 $\alpha$  serves to regulate BACE1 mRNA translation in response to energy deprivation. (\*,  $p < 0.05$ , comparison of 24H NG and CON; ##,  $p < 0.001$ , comparison of NG + TUDCA and 24H NG).

## **The eIF2 $\alpha$ Kinase PERK is responsible for energy deprivation-induced BACE1 protein elevations *in vitro***

eIF2 $\alpha$  is phosphorylated by at least four known kinases, two of which are likely to be involved in cellular energy metabolism: PKR-like endoplasmic reticulum kinase (PERK), which is activated during the unfolded protein response, and general control non-derepression 2 (GCN2) kinase, which is activated in response to amino acid deprivation (Fig 3.8). To determine if either of these eIF2 $\alpha$  kinases was responsible for glucose deprivation-induced BACE1 elevations in BACE1-293 cells, we transiently transfected BACE1-293 cells with constructs overexpressing kinase-dead forms of PERK (PERKDN), GCN2 (GCN2DN), or a known inhibitor of PERK (P58<sup>IPK</sup>) (van Huizen et al., 2003; Yan et al., 2002). Since these kinases function *via* dimerization and autophosphorylation (Malhotra and Kaufman, 2007), overexpression of kinase-dead forms of these kinases act as dominant negatives that prevent efficient phosphorylation and activation of the endogenous kinases (Harding et al., 1999). BACE1-293 cells were transfected with empty vector as a negative transfection control. PERKDN-, GCN2DN-, P58-, or control-transfected BACE1-293 cells were treated for 24 hrs in either normal or NG media. As expected, both BACE1 and eIF2 $\alpha$ -P were elevated in control-transfected cells incubated in NG media, compared to control-transfected cells grown in normal media (Fig 3.12; Fig 3.13). However, unlike GADD34 $\Delta$ N, overexpression of GCN2DN in combination with no glucose treatment failed to prevent eIF2 $\alpha$  phosphorylation or BACE1 protein elevation in BACE1-293 cells, indicating that GCN2 is not the kinase that phosphorylates eIF2 $\alpha$  under glucose-deficient conditions (Fig 3.12). In contrast, overexpression of PERKDN in combination with NG treatment completely prevented



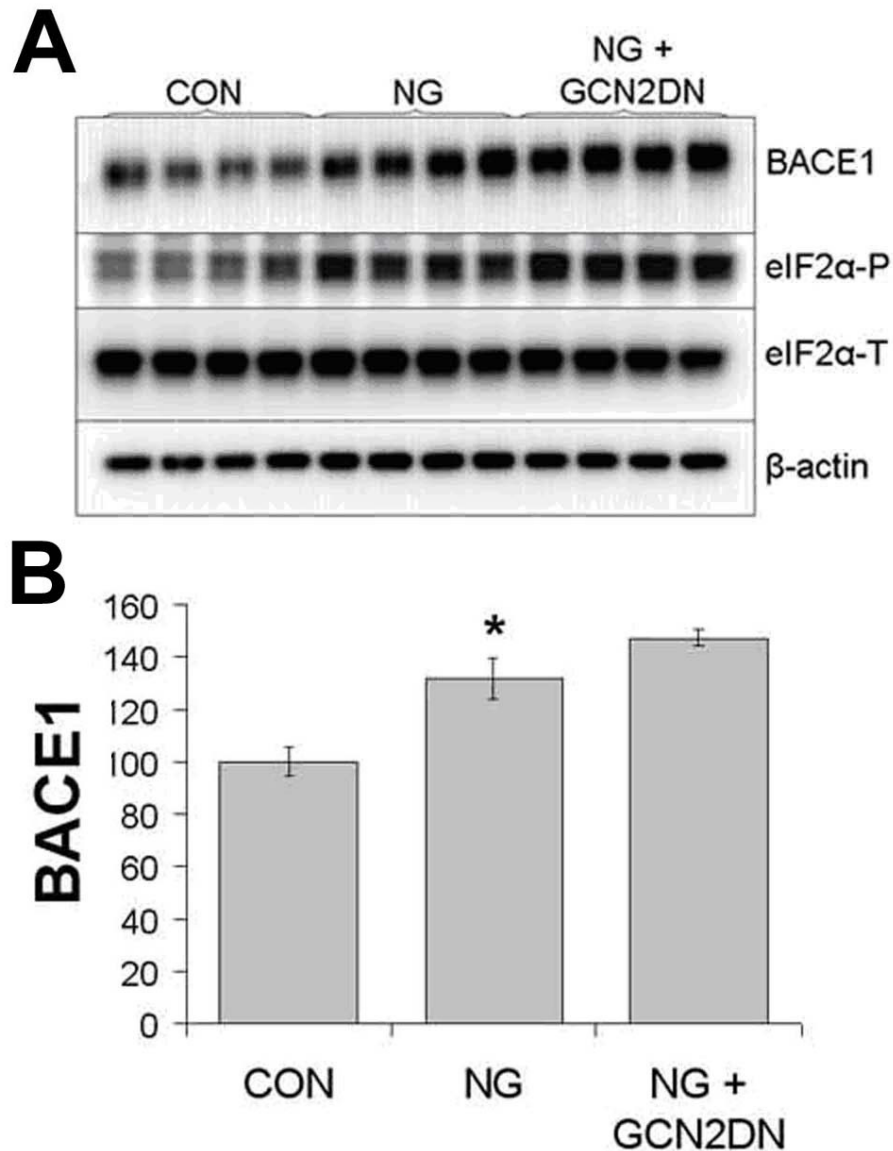


**Figure 3.12: Inhibition of the amino acid-regulated eIF2 $\alpha$  kinase, GCN2, cannot prevent glucose deprivation-induced BACE1 protein elevation in BACE1-293 cells.** (A) BACE1-293 cells were transiently transfected with pcDNA3 empty vector (CON, NG) or dominant negative GCN2 (GCN2DN). Cells were incubated for 24 hrs in normal DMEM with glucose (CON) or DMEM without glucose (NG, NG + GCN2DN). 5  $\mu$ g (BACE1,  $\beta$ -actin) or 10  $\mu$ g (eIF2 $\alpha$ -P, eIF2 $\alpha$ ) of protein was used for immunoblot analysis. (B) BACE1 immunosignals were normalized to  $\beta$ -actin and expressed as % CON. Neither the glucose deprivation-induced BACE1 increase nor the eIF2 $\alpha$ -P increase were prevented by overexpression of GCN2DN, demonstrating that GCN2 was not the eIF2 $\alpha$  kinase responsible for eIF2 $\alpha$  phosphorylation and the BACE1 increase in response to glucose deprivation. (n = 4 per group; \*, comparison between CON and NG, p < 0.05; mean  $\pm$  SEM). Error bars = S.E.M. in all histograms.

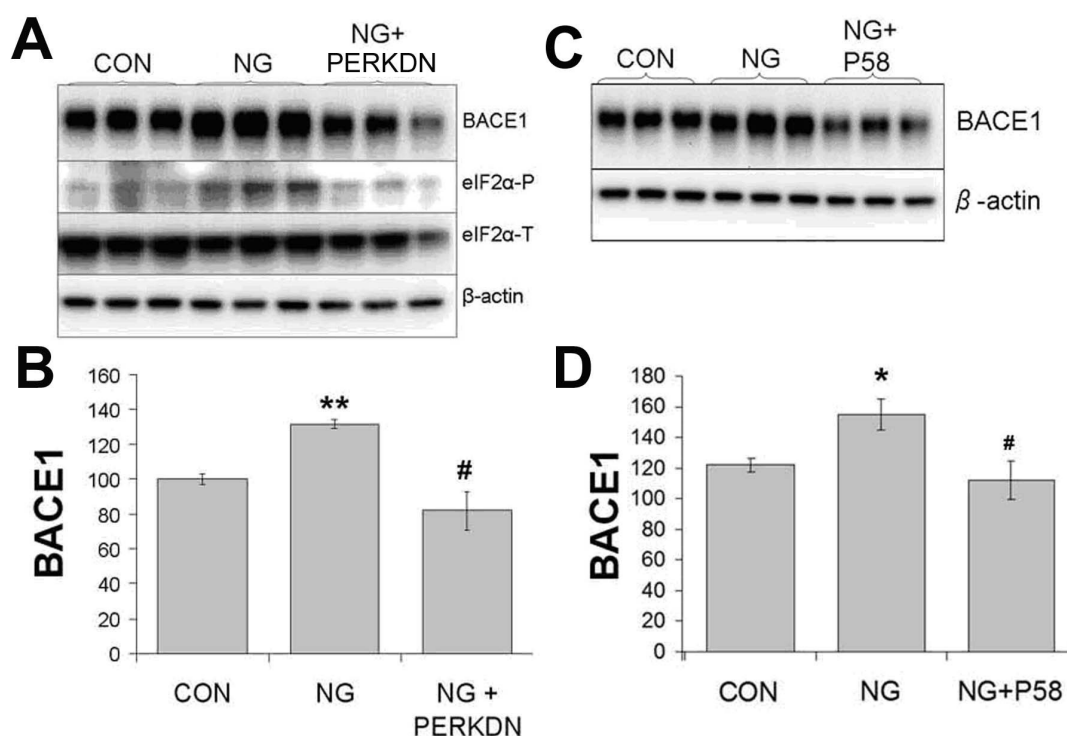


**Fig 3.13: The UPR-inducible eIF2α kinase, PERK, is responsible for glucose deprivation-induced BACE1 protein elevation in BACE1-293 cells.** (A) BACE1-293 cells were transiently transfected with pcDNA3 empty vector (CON, NG) or dominant negative PERK (PERKDN). Cells were incubated for 24 hrs in normal DMEM (CON) or DMEM without glucose (NG, NG + PERKDN). 5 μg (BACE1, β-actin) or 10 μg (eIF2α-P, eIF2α) of protein was used for immunoblot analysis. (B) BACE1 immunosignals were expressed as % CON. Glucose deprivation-induced increases in BACE1 levels were completely prevented by overexpression of PERKDN, demonstrating that PERK was the eIF2α kinase responsible for eIF2α phosphorylation and the BACE1 increase. (C) BACE1-293 cells were transiently transfected with empty pcDNA3 vector (CON, NG) or a construct encoding P58<sup>IPK</sup>, a cellular inhibitor of the eIF2α kinases PERK and PKR (Yan et al., 2002). Cells were incubated for 24 hrs in regular DMEM (CON), or DMEM without glucose (NG, NG + P58). 5 μg protein per lane was used for immunoblot analysis of BACE1 and β-actin. (D) BACE1 immunosignals were normalized to β-actin, and values were expressed as % CON ± SEM. Transfection with P58<sup>IPK</sup> prevented glucose deprivation-induced increase of BACE1 and eIF2α-P in NG-treated cells (NG + P58), providing further support that PERK and eIF2α phosphorylation are responsible for energy deprivation-induced BACE1 elevation. (n = 3; \* p < 0.05, \*\*p < 0.01: comparison of NG and CON; #, p < 0.05, comparison of NG + P58 and NG or NG + PERKDN and NG.)

BACE1 protein elevations, similar to GADD34, indicating that PERK is the specific kinase controlling energy deprivation-induced BACE1 protein elevation, at least *in vitro* (Fig 3.13A,B). Furthermore, overexpression of an inhibitor of PERK (P58) also prevented NG-induced BACE1 protein elevations, lending additional support to the theory that glucose deprivation activates PERK (Fig 3.13C,D). Taken together, these results all indicate that cellular glucose deprivation activates the UPR, which activates the ER stress kinase PERK, which phosphorylates the translation initiation factor eIF2 $\alpha$ , leading to down-regulated global translation and up-regulated translation of certain translationally regulated mRNA transcripts involved in the cellular stress response. Our results show that a novel translational target of this stress-activated pathway appears to be BACE1 mRNA.

## Discussion

In order to identify the molecular mechanism responsible for acute pharmacological energy deprivation-induced BACE1 protein elevations *in vivo*, we designed an *in vitro* model of energy deprivation using glucose deprivation in HEK-293 cells overexpressing human BACE1. Using this model, we identified stress-induced phosphorylation of the translation initiation factor eIF2 $\alpha$  *via* the UPR activated kinase PERK as the mechanism responsible for glucose deprivation-induced BACE protein elevations. Phosphorylation of eIF2 $\alpha$  is a novel mechanism previously unknown to regulate BACE1 levels. This data supports previous studies claiming that BACE is translationally regulated, as well as accumulating evidence that BACE1 plays a normal physiological role in neuronal stress responses.

### **Glucose deprivation in BACE1-293 cells as a model of energy deprivation**

We chose to incubate cells in glucose-deficient media as a method of inducing energy deprivation *in vitro*, as opposed to using pharmacological energy inhibitors. Glucose-deficient media proved to be an excellent model of energy deprivation for two reasons:

- 1) It specifically modeled low energy availability, which we suspected was the common underlying mechanism of BACE1 elevation in response to the pharmacological agents used in our acute study (insulin, 2DG, 3NP, and KA). Indeed, glucose deprivation appeared to have the same post-transcriptional effect on BACE1 protein *in vitro* as insulin, 2DG, 3NP, and KA had on endogenous BACE1 protein in the brain, indicating that glucose deprivation accurately modeled this effect. Incubating cells in glucose-deficient media modeled a more physiologically relevant condition than treating cells with pharmacological agents, which often have off-target effects unrelated to the pathway under investigation.
- 2) Glucose-deficient media eliminated the need to titrate doses of pharmacological agents to a range that inhibited energy production without causing toxicity. Importantly, HEK-293 cells tolerated glucose deprivation extremely well. Glucose deprivation caused no morphological changes or toxicity to BACE1-293 cells at any of the time-points tested. This is an important point when modeling energy deprivation *in vitro*, because BACE1 is also elevated during the onset of apoptosis, a potential confounding factor in our experiments (Koh et al., 2005; Tesco et al., 2007; Vassar, 2007). We used HEK-293 cells stably expressing human BACE1 under the control of the CMV promoter as preliminary cellular model for energy deprivation. HEK-293 cells have the advantage of being highly amenable to experimental manipulations. They can survive a wide range of pharmacological treatments and are readily and

efficiently transfected with plasmid DNA, which they express at high levels.

Furthermore, endogenous BACE1 levels in HEK-293 cells are extremely low. BACE1-293 cells express ~30-fold more BACE1 mRNA than HEK-293 cells, and endogenous BACE1 protein in HEK-293 cells is virtually undetectable *via* immunoblot. This allowed us to study the post-transcriptional effect of energy deprivation on BACE in the absence of its endogenous promoter. Real Time PCR experiments confirmed that energy deprivation had no effect on the CMV promoter, which essentially eliminated transcription as a mechanism operating in our experiments. Despite the clear advantages of using HEK-293 cells as a cellular model of energy deprivation and the indication that our *in vitro* experiments accurately modeled BACE1 protein regulation in the brain, HEK-293 cells and neurons have important fundamental differences, and it will be important to confirm these results in cultured neurons.

### **Transcriptional control of BACE1 in response to glucose deprivation *in vitro***

The absence of the endogenous BACE1 promoter in BACE1-293 cells made transcriptional regulation of BACE1 in this *in vitro* model unlikely. Real Time PCR analysis of control and glucose-deprived BACE1-293 cells confirmed that BACE1 mRNA levels were unaltered and demonstrated that glucose deprivation had no effect on CMV promoter activity or BACE1 mRNA stability. Furthermore, glucose deprivation also elevated BACE1 protein levels in the presence of the transcriptional inhibitor, actinomycin D, despite the fact that BACE1 mRNA levels were reduced to ~25% of control levels, leading us to conclude that the mechanism responsible for energy deprivation-induced BACE1 protein elevations was post-transcriptional. However, it is

important to note that JNK and c-Jun phosphorylation were also elevated in response to glucose deprivation *in vitro*. JNK is a well-established stress-activated kinase that phosphorylates the transcription factor, c-Jun (Johnson and Nakamura, 2007).

Activation of c-Jun and JNK has been previously noted in response to metabolic disturbances (Eizirik et al., 2008). Activation of c-Jun indicates that the transcriptional profile of the cell may be altered in response to glucose deprivation. Although our results clearly demonstrate that transcription is not required for glucose deprivation-induced BACE1 protein elevation *in vitro*, it will be important to test the effect of energy deprivation on BACE1 levels *in vitro* in the context of the endogenous BACE1 promoter, to rule out the possibility that BACE1 mRNA is regulated by energy deprivation-induced c-Jun activation.

### **The effect of glucose deprivation on BACE1 protein stability**

Increased BACE1 protein stability has been reported to occur under stress conditions. Apparently, BACE1 protein is normally shuttled to the lysosome for degradation through its association with the adaptor protein, GGA3. GGA3 is a cleavage target for caspase 3, one of the downstream effectors of apoptosis. Cleavage of GGA3 prevents its association with BACE1, reduces the amount of BACE1 entering the lysosome, and therefore extends the half-life of BACE1 protein (Koh et al., 2005; Tesco et al., 2007; Vassar, 2007). We considered altered BACE1 protein stability an unlikely mechanism controlling BACE1 protein levels in response to energy deprivation for the following reasons: 1) Energy deprivation-induced BACE1 protein elevations occurred rapidly (within 4 hrs *in vivo* and 2 hrs *in vitro*), whereas the turnover of BACE1 protein in the cell

is relatively slow, in comparison ( $t_{1/2} = \sim 12$  hrs). Therefore, our results argue in favor of a rapid production of, rather than a slow accumulation of BACE1 protein in the cell. 2) BACE1 protein elevations occurred pre-apoptotically in response to energy deprivation with no evidence of caspase 3 activation or cellular toxicity (*in vitro*) and no evidence of neurodegeneration (*in vivo*), effectively eliminating the GGA3-mediated mechanism previously described. Consistent with this hypothesis, our pulse-labeling experiment showed that BACE1 protein stability was identical under control versus glucose-deprived conditions *in vitro*. This data combined with our previous finding that BACE1 transcription was not altered, led to the conclusion that altered BACE1 protein translation was the most likely mechanism underlying energy deprivation-induced BACE1 protein elevations.

### **Translational control of BACE1 protein in response to energy deprivation *in vitro***

Deletion of the BACE1 5'UTR completely abolished the glucose deprivation-induced BACE1 protein elevation *in vitro*, implicating translational regulation of BACE1 as the mechanism underlying energy deprivation-mediated control of BACE1 levels.

Importantly, the DNA constructs used in this experiment did not contain the BACE1 3'UTR sequence, and BACE1 elevations were similar to those observed in BACE1-293 cells, eliminating a possible role for microRNA regulation or 3'UTR-mediated BACE1 regulation in response to glucose deprivation (Hebert et al., 2008; Wang et al., 2008b). *In vitro* studies indicate that BACE1 protein is normally translated at very low levels due to the presence of its long, G-C-rich 5'UTR. This is inferred from the observation that BACE1 protein levels can be dramatically increased by deleting the

BACE1 5'UTR, without a corresponding increase in BACE1 mRNA (Fig 3.4) (Lammich et al., 2004). The specific mechanism by which the BACE1 5'UTR inhibits BACE1 protein translation continues to be debated; however available data indicates that BACE1 translational inhibition occurs either through the formation of secondary structure in the 5'UTR that limits ribosomal access to the transcript, translation of inhibitory uORFs, or both. The BACE1 transcript contains four AUGs (three of which form uORFs) upstream of the true BACE1 start codon in the 5'UTR sequence (Lammich et al., 2004). The involvement of these uAUGs in BACE1 translation inhibition has been confirmed by several other groups (De Pietri Tonelli et al., 2004; Mihailovich et al., 2007; Rogers et al., 2004; Zhou and Song, 2006). Therefore, we hypothesize that BACE1 protein elevation in response to glucose deprivation occurs due to differential utilization of uAUGs in the BACE1 5'UTR. Consistent with this hypothesis, uORF utilization can be modulated physiologically *via* growth-stimulated or stress-activated alterations in the translation initiation complex. Phosphorylation of the eukaryotic translation initiation factor eIF2 alpha subunit (eIF2 $\alpha$ -P) is one of the best characterized examples of stress-induced translational alteration. eIF2 $\alpha$ -P is a highly conserved cellular stress response mechanism originally identified in reticulocytes. Consistent with previous reports that eIF2 $\alpha$ -P plays a role in energy metabolism, we found elevated eIF2 $\alpha$ -P levels in glucose-deprived BACE1-293 cells compared to control. Furthermore, salubrinal experiments demonstrated that BACE1 is directly elevated in response to eIF2 $\alpha$  phosphorylation, and inhibition of eIF2 $\alpha$ -P by overexpressing GADD34 in combination with no glucose treatment completely blocked BACE1 protein elevations, indicating that eIF2 $\alpha$ -P was the specific signaling pathway responsible for translational



up-regulation of BACE1. eIF2 $\alpha$  is phosphorylated by four known kinases in response to a wide variety of stress stimuli. PKR is activated in response to viral infection, HRI is activated in response to heme deficiency, GCN2 is activated in response to UV irradiation or amino acid deprivation, and PERK is activated during the unfolded protein response (UPR) (Holcik and Sonenberg, 2005). Overexpression of dominant negative PERK also completely blocked glucose deprivation-induced BACE1 protein elevations in BACE1-293 cells, indicating that PERK is the specific kinase responsible for phosphorylating eIF2 $\alpha$  in response to no glucose treatment. PERK is an ER resident kinase, which is normally contained in an inactive monomeric form through its association with binding immunoglobulin protein (BiP). When unfolded proteins begin to accumulate in the ER, BiP dissociates from PERK and binds to the misfolded proteins, allowing PERK to dimerize and autophosphorylate. Activated PERK then phosphorylates eIF2 $\alpha$ , which down-regulates global protein synthesis to reduce the volume of proteins entering the ER (Schroder and Kaufman, 2006). The UPR is tightly linked to glucose homeostasis; in fact, the UPR was originally discovered through glucose deprivation experiments in fibroblasts (Zhang and Kaufman, 2006). Proper protein folding is an energetically demanding process. ATP is required for protein chaperone function, ER-associated protein degradation (ERAD) of misfolded proteins, and intralumenal Ca<sup>2+</sup> homeostasis essential for protein folding reactions. Our data clearly shows that BACE1 is a direct translational target of altered glucose homeostasis and UPR dysregulation at the biochemical level. Although the physiological importance of BACE1 up-regulation during the UPR is unclear, this data provides a potential mechanistic link between reduced energy metabolism in the brain and the development

of amyloid pathology. Although our *in vitro* data clearly shows that PERK is the kinase mediating eIF2 $\alpha$  phosphorylation in response to glucose deprivation in HEK-293 cells and not GCN2, it is interesting to note that the major eIF2 $\alpha$  kinase expressed in brain tissue is GCN2. The role of GCN2 in the brain remains cryptic. GCN2 deletion does not appear to have any effect on brain development or morphology; however, closer electrophysiological examination shows some disturbances in synaptic transmission, indicating that GCN2 could play a role in this process (Costa-Mattioli et al., 2005). The normal role of PERK in the brain has been uninvestigated; however, its involvement in pathological process, such as AD, Parkinson's disease, and cerebral ischemia has been documented (Schroder and Kaufman, 2006). Further experimentation will be required to investigate the capacity of these two kinases to regulate BACE1 protein in neuronal systems.

## CHAPTER 4

# PHOSPHORYLATION OF eIF2 $\alpha$ AT SERINE 51 ELEVATES ENDOGENOUS BACE1 PROTEIN AND ACCELERATES AMYLOID $\beta$ PRODUCTION IN PRIMARY CULTURED NEURONS

### Introduction

We showed using an acute model of energy deprivation *in vivo* that BACE1 protein levels are elevated post-transcriptionally and pro-amyloidogenic processing of APP is enhanced in the brain, indicating that impaired energy metabolism in the brain may be an early event in SAD pathogenesis. In order to identify the post-transcriptional mechanism underlying energy deprivation-induced BACE1 protein elevations, we developed an *in vitro* model of energy deprivation in BACE1-293 cells deprived of glucose. Using this *in vitro* model of energy deprivation, we identified stress-induced eIF2 $\alpha$  phosphorylation as the post-transcriptional mechanism through which BACE1 protein is elevated *in vitro*. In order to determine whether BACE1 protein was regulated by this same mechanism under conditions of energy deprivation in a cell type relevant to Alzheimer's disease, we repeated our glucose deprivation experiments on cultured primary cortical neurons from wild-type C57/BL6 mouse embryos. We analyzed glucose-deprived wild-type neuron lysates for BACE1 mRNA, BACE1 protein, and eIF2 $\alpha$ -P levels in order to determine whether glucose deprivation would post-transcriptionally elevate endogenous BACE1 in parallel with eIF2 $\alpha$ -P in neurons. Additionally, we treated human APP-overexpressing (Tg2576) neurons with the eIF2 $\alpha$ -P

activating drug, salubrinol, and measured BACE1 protein, eIF2 $\alpha$ -P levels, and secreted A $\beta$ 40 levels in order to determine whether direct activation of eIF2 $\alpha$ -P would elevate endogenous BACE1 protein and promote amyloidogenesis *in vitro*.

## Materials and methods

### Neuronal Cultures

Timed pregnant C57/BL6 females mated to either C57/BL6 or Tg2576 males were sacrificed *via* carbon dioxide inhalation, and E15.5-E16.5 C57/BL6 embryos were excised, rinsed in 1x BSS (1x Hank's Balanced Salt Solution, 1% pen-strep, 10 mM HEPES), and decapitated. Embryonic cortical tissue was isolated with the aid of a dissecting microscope, dissociated for 15 min. at 37°C in 5 mL of 0.25% trypsin (Invitrogen), washed 3x with 5 mL 1x BSS, and triturated in succession with a regular, sterile Pasteur pipet and a fire-polished Pasteur pipet in 5mL 1x BSS. (C57/BL6 embryos were pooled for trituration, while C57/BL6 X Tg2576 embryos were triturated and plated separately.) Triturate volumes were adjusted to 0.25 mL/well with 1x BSS. Neurons were plated in 1 mg/mL poly-L-lysine-coated plates (1 brain per 12-well plate) for 2 hrs in neurobasal media supplemented with 1x B-27, 10% horse serum, 1% pen-strep, 2.5 $\mu$  M glutamate, and 500  $\mu$ M glutamine (Invitrogen). Leftover tissue from each C57/BL6 X Tg2576 embryo was incubated at 55°C overnight in 500  $\mu$ g/mL Proteinase K in "Tail buffer" (1 M Tris-HCl, 0.5 M EDTA, 20% SDS; pH=8.0), diluted 1:10 in sterile, autoclaved water, and used for hAPP<sub>sw</sub> genotyping:

F: 5'-GTGGATAACCCCTCCCCCAGCCTAGACCA-3'

R: 5'-CTGACCACTCGACCAGGTTCTGGGT-3'

Transgene-negative cultures were discarded. Neurons were maintained for 2 DIV in neurobasal media containing only B-27, 2.5  $\mu$ M glutamate, and 500  $\mu$ M glutamine. At 2 DIV, neurons were switched to media containing only B-27 and 500  $\mu$ M glutamine, after which half of the maintenance media was changed every 2-3 days. (For A $\beta$ 40 conditioned media, 24 hrs prior to beginning of salubrial treatment). Treatments began at 7 DIV. For energy deprivation experiments in wild-type C57/BL6 neurons, cells were treated for 36 hrs in Locke's solution (154 mM NaCl, 5.6 mM KCl, 2.3 mM CaCl, 1.0 mM MgCl, 3.6 mM NaHCO<sub>3</sub>, 5 mM HEPES) with or without 20 mM glucose (Cheng and Mattson, 1995). For salubrial treatments in Tg2576 neurons, a 10 mM stock solution of salubrial dissolved in DMSO was added to the maintenance media at 50  $\mu$ M or 80  $\mu$ M for 48 hrs. For biochemical analyses, Tg2576 media was collected and residual cell debris was removed by centrifugation. Neurons were washed with 1x PBS, lysed in 1x RIPA buffer supplemented with 1x AEBSF and 1x Halt phosphatase inhibitors and homogenized. Insoluble material was pelleted out by centrifugation, and supernatants were analyzed for total protein content using the BCA assay. For mRNA analysis, neurons were lysed in 350 $\mu$ L RLT buffer supplemented with 1% BME (Qiagen's RNeasy Mini kit).

### **Immunoblotting**

10  $\mu$ g protein was boiled for 5 min in sample boiling buffer (60 mM Tris, 10% glycerol, 5% SDS, pH 6.8, 10%  $\beta$ -mercaptoethanol +loading dye) prior to being separated on 4-12% NuPAGE Bis-Tris gels in 1x MOPS running buffer (Invitrogen) and transferred to Millipore Immobilon-P polyvinylidene difluoride (PVDF) membrane. Blots were blocked

overnight in 5% bovine serum albumin (BSA) in Tris-buffered saline, Tween 20 0.1% (TBST; Sigma, T9039; modified form), pH 8.0. Blots were blocked overnight in 5% BSA in TBST. Blots were then cut into strips and incubated overnight in primary antibody (Table 4.1). Blots were then washed in TBST and incubated for 1 hr in horseradish peroxidase-conjugated goat anti-mouse or goat anti-rabbit secondary antibody diluted 1:10,000 in 5% milk (Jackson Immunological Research). Immunosignals were detected using enhanced chemiluminescence (SuperSignal West Femto, Pierce) and quantified using a Kodak CF440 imager. Blots were stripped for 5 min in Pierce Restore stripping buffer, washed with distilled water, and re-probed when necessary.

### **RNA isolation and real-time PCR**

All 350  $\mu$ L of cell lysate from each sample was used for mRNA extraction using Qiagen's RNeasy Mini kit according to the manufacturer's specifications. Total mRNA concentrations were measured using  $ABS_{260nm}$  ( $[RNA] \mu g/\mu L = 0.04 \times ABS_{260nm}$ ) on a Beckman spectrophotometer. In general, only mRNA samples with low protein contamination ( $ABS_{260nm}/ABS_{280nm} > 1.8$ ) were used for analysis. mRNA integrity of each sample was confirmed using an Agilent Technologies 2100 Bioanalyzer. mRNA samples were used for analysis if the 28S ribosomal RNA peak was at least two times the area of the 18S ribosomal RNA peak. 1  $\mu$ g of total RNA from each sample was used for first-strand cDNA synthesis using Invitrogen's SuperScript III according to the manufacturer's recommendations (Random hexamers were used as opposed to oligo dTs). Exact cDNA concentrations were determined using a Beckman

Antibody	Clone	Dilution	5% Milk/BSA	Time	Source	Catalog No.	MW	Substrate
BACE1	3D5	1:2,000	Milk	1hr	Zhao, 2007		70kD	ECL+
FLAPP	22C11	1:10,000	Milk	1hr	Chemicon	MAB348	100kD	ECL+
Actin	AC-15	1:15,000	Milk	1hr	Sigma	A1978	40kD	ECL+
eIF2a-P (Ser51)	119A11	1:2,000	BSA	O.N.	Cell Signaling	3597	38kD	WF
eIF2a		1:2,000	BSA	O.N.	Cell Signaling	9722	38kD	ECL+
Caspase 3		1:5,000	Milk	O.N.	Cell Signaling	9662	Pro: 35kD Cleaved: 19kD	WF
Neprilysin		1:1,000	Milk	O.N.	Chemicon	AF1126	100kD	WF
IDE		1:1000	Milk	O.N.	Abcam	ab32216	100kD	ECL+
PS1-NT		1:20,000	Milk	O.N.	Thinakaran, 1998		50kD	ECL+

**Table 4.1:** List of primary antibodies used to probe neurons and brain homogenates.

spectrophotometer, and 112.5 ng cDNA from each sample was amplified *via* Real-Time PCR in triplicate using Applied Biosystems' Assays-on-Demand pre-mixed Taqman primer/probe set for mouse BACE1 mRNA (catalog #Mm00478664\_m1) and normalized against 18s rRNA (#4333760F). The BACE1 primer/probe set spans exons 1-2 of the murine BACE1 transcript, which are present in all known splice variants of BACE1. BACE1 and 18s cDNA were amplified using an Applied Biosystems 7900HT sequence analyzer using Applied Biosystem's universal cycling parameters. Samples were only used for final analysis if the standard deviation between triplicate samples was < 0.1 cycles. Percent of control values were determined using the comparative CT method.

### **Human A $\beta$ 40 ELISA**

Conditioned media from Tg2576 neurons was diluted with A $\beta$  diluent (Biosource) supplemented with 1x AEBSF. Exact dilutions varied across experiments. Total A $\beta$ 40 levels in diluted media were determined using a human A $\beta$ 40-specific sandwich ELISA (BioSource) according to manufacturer's recommendations. Values were expressed as ng A $\beta$ 40 in the conditioned media (as determined by ELISA) per mg of protein in the corresponding cell lysate (as determined by the BCA assay).

### **Statistical analysis**

Sample averages were determined and then means and standard error of the means (SEMs; represented by error bars in histograms) were calculated based on the sample averages (n-values are stated in figure legends). Statistical differences between



experimental groups and their respective controls were determined using a two-tailed t-test. Data are presented as the mean  $\pm$  SEM. \* $p < 0.05$ , \*\* $p < 0.01$ , \*\*\* $p < 0.001$ .

## Results

### **Glucose deprivation enhances eIF2 $\alpha$ phosphorylation and elevates BACE1 protein post-transcriptionally in primary cultured neurons**

To determine whether post-transcriptional increases in BACE1 protein occurred in neuronal cell types *in vitro* following energy deprivation, we performed NG treatments of cultured C57/BL6 mouse primary cortical neurons. After 7 days *in vitro* (DIV), neurons were incubated for up to 48 hrs in Locke's solution containing 20 mM glucose (CON) or Locke's solution without glucose (NG) (Cheng and Mattson, 1995). After 48 hrs, minimal cell death occurred in NG-treated neurons compared to control, with no evidence of caspase 3 activation (Fig 4.1B). Lysates from these cells were analyzed for endogenous BACE1 levels by immunoblot. Increased BACE1 levels were apparent in primary neuron cultures by 24 hrs in NG media, and this elevation peaked at ~36hrs (Fig. 4.1A,C; ~150% of control,  $p < 0.05$ ). TaqMan quantitative PCR analysis of mRNA isolated from NG-treated cultured neurons showed a decrease in BACE1 transcript levels compared to control (Fig. 4.1C;  $p < 0.05$ ), clearly demonstrating that a post-transcriptional mechanism was responsible for the BACE1 increase following NG treatment. In order to determine whether phosphorylation of eIF2 $\alpha$  was involved in energy deprivation-induced BACE1 protein elevations in cultured neurons, we measured eIF2 $\alpha$ -P levels *via* immunoblot. Similar to BACE1-293 cells, the eIF2 $\alpha$ -

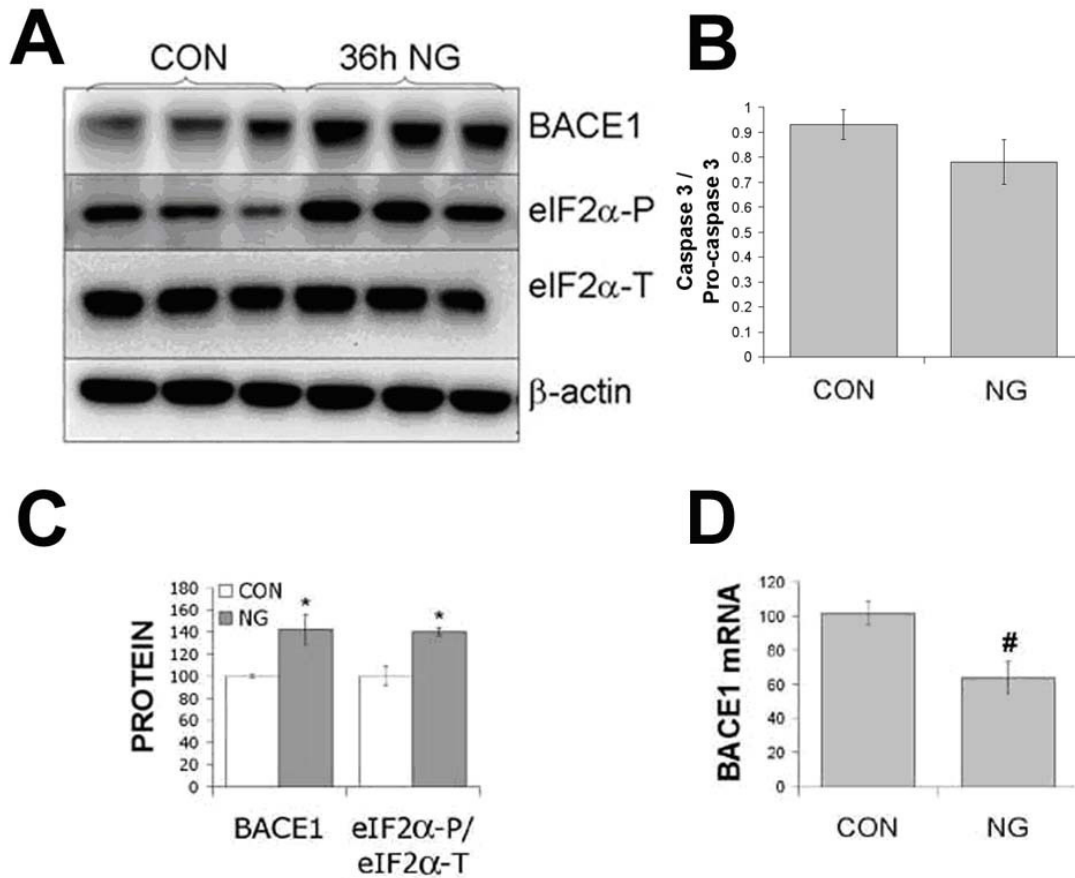


**Figure 4.1: Glucose deprivation in primary cultured neurons induces eIF2α phosphorylation and elevates BACE1 protein levels post-transcriptionally.**

Primary cortical C57/BL6 neurons were cultured for 7 DIV and then incubated for 36 hrs in media containing 20mM glucose (CON) or no glucose (NG). 10μg of protein was used for immunoblot analysis of BACE1, P-eIF2α(Ser51), total eIF2α (eIF2α-T), and β-actin (**A**) or caspase 3. Caspase 3 immunosignals were expressed as the ratio of cleaved caspase 3 to pro-caspase 3 (**B**). (**C**) BACE1 immunosignals were normalized to β-actin, eIF2α-P was normalized to eIF2α-T, and values were expressed as % CON. Levels of endogenous neuronal BACE1 and eIF2α-P/eIF2α-T were significantly elevated in response to glucose deprivation (mean ± SEM; \*,  $p < 0.05$ ;  $n=3$ ). (**D**) C57/BL6 primary neuron cultures were treated as in (A), except that total mRNA was isolated and levels of endogenous BACE1 mRNA measured via the TaqMan real-time PCR relative quantification method and expressed as % CON ( $n=3$ ). Unexpectedly, neuronal BACE1 mRNA levels were significantly reduced in cultures treated with NG-media compared to glucose-containing media (CON) (#;  $p < 0.05$ ; mean ± SEM), clearly demonstrating a post-transcriptional mechanism for the BACE1 protein increase.

P(Ser51):eIF2 $\alpha$  total ratio in 36 hr NG-treated primary neurons was elevated to ~150% of control values (Fig. 4.1A,B;  $p < 0.05$ ) indicating that eIF2 $\alpha$  phosphorylation may be the mechanism of BACE1 protein elevation in neurons, as well.

### **Direct phosphorylation of eIF2 $\alpha$ elevates BACE1 protein and accelerates A $\beta$ production in Tg2576 cultured neurons**

Our immunoblot results from no glucose treatments in wild-type C57/BL6 neurons suggested that BACE1 protein was also elevated *via* eIF2 $\alpha$  phosphorylation in response energy deprivation in neuronal cell types. Furthermore, the effect of glucose deprivation on BACE1 protein levels suggested that stress-induced activation of the eIF2 $\alpha$ -P(Ser51) stress response pathway might be amyloidogenic. To confirm that eIF2 $\alpha$  phosphorylation could directly elevate endogenous BACE1 protein in neurons and to determine whether direct activation of eIF2 $\alpha$ -P could accelerate A $\beta$  production *in vitro*, we treated Tg2576 primary neurons, which readily produce and secrete A $\beta$ 40 into the media in cell culture, with the eIF2 $\alpha$ -P activating drug, salubrinal. Tg2576 primary cortical neurons from E15.5 embryos were cultured for 7 DIV and then treated with 50  $\mu$ M or 80  $\mu$ M salubrinal for 48 hrs. As we observed in BACE1-293 cells, salubrinal treatment significantly increased levels of both eIF2 $\alpha$ -P(Ser51) and endogenous BACE1 protein in Tg2576 neurons, compared to control (Fig. 4.2A,B). In addition, levels of A $\beta$ 40 were elevated in conditioned media from salubrinal-treated neurons, as compared to control (Fig 4.2C; CON =  $13.25 \pm 0.33$  ng A $\beta$ 40/mg protein; 50  $\mu$ M Sal =  $15.88 \pm 0.63$ ,  $p < 0.05$ ; 80  $\mu$ M Sal =  $27.19 \pm 1.61$ ,  $p < 0.01$ ). We also measured levels of full-length

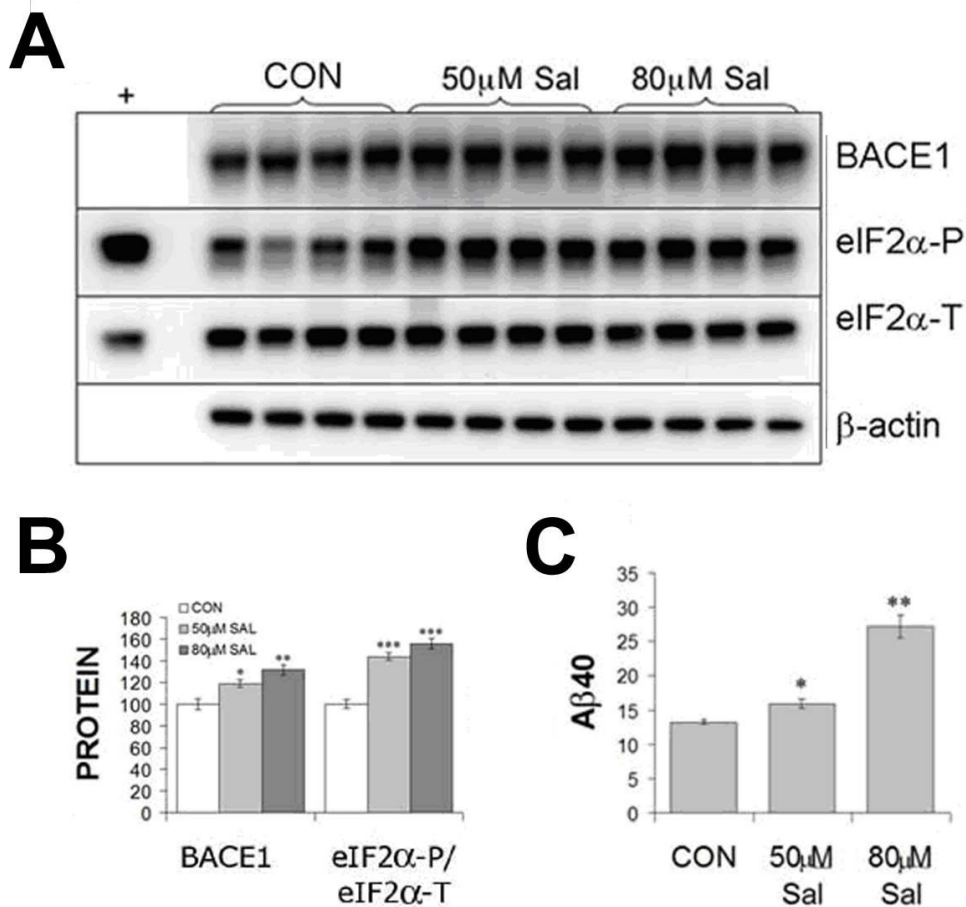


**Figure 4.2: Direct phosphorylation of eIF2 $\alpha$  elevates BACE1 protein and promotes A $\beta$  production in cultured Tg2576 neurons.** (A) Primary cortical Tg2576 neurons were cultured for 7 DIV and then incubated for 48 hrs in normal media (CON), media containing 50  $\mu$ M salubrinal (50  $\mu$ M Sal), or media containing 80 $\mu$ M Sal. 10 $\mu$ g of protein was used for immunoblot analysis of BACE1, phosphorylated eIF2 $\alpha$ , total eIF2 $\alpha$ , and  $\beta$ -actin. 10 $\mu$ g of lysate from UV-treated 293 cells was used as a positive control (+) for eIF2 $\alpha$ -P. (B) BACE1 immunosignals were normalized to  $\beta$ -actin, eIF2 $\alpha$ -P was normalized to eIF2 $\alpha$ -T, and values were expressed as % CON. BACE1 levels and eIF2 $\alpha$ -P/eIF2 $\alpha$ -T ratios were significantly increased in Tg2576 neurons treated with both concentrations of Sal compared to control (n = 4), demonstrating that direct induction of eIF2 $\alpha$  phosphorylation causes BACE1 levels to rise. (C) Conditioned media collected from 48hr salubrinal-treated Tg2576 neurons in (A) were analyzed using a human A $\beta$ <sub>40</sub> ELISA. Values are expressed as ng of A $\beta$ <sub>40</sub> in the media per mg of total protein in the corresponding cell lysate. A $\beta$ <sub>40</sub> levels were significantly elevated in Tg2576 neurons treated with both 50 $\mu$ M and 80 $\mu$ M salubrinal compared to control (CON; n=4; \*, p<0.05; \*\*, p<0.01; \*\*\*, p<0.001; mean  $\pm$  SEM), demonstrating that direct induction of eIF2 $\alpha$  phosphorylation led to an increase in A $\beta$  production.

APP, presenilin 1 (PS1), insulin degrading enzyme (IDE), and neprilysin (NEP) *via* immunoblot in order to determine whether the effect of salubrinal was specific to BACE1 and did not affect other proteins in the amyloidogenic pathway (APP, PS1) or A $\beta$  clearance and degradation mechanisms (IDE, NEP). Immunoblot analysis showed that APP, PS1, IDE, and NEP levels were unchanged in Tg2576 neurons treated with 50  $\mu$ M or 80  $\mu$ M salubrinal (Fig 4.3), indicating that accelerated A $\beta$  production in salubrinal-treated Tg2576 neurons is the direct result of enhanced BACE1 cleavage of APP. Taken together, our results with salubrinal-treated Tg2576 neuron cultures confirm that BACE1 is a direct translational target of eIF2 $\alpha$ -P(Ser51) in neurons and demonstrate that direct induction of eIF2 $\alpha$ -P is amyloidogenic *in vitro*.

## Discussion

We showed previously that endogenous BACE1 protein levels and amyloidogenic processing of APP were elevated upon acute pharmacological energy inhibition *in vivo*, which could be a mechanism contributing to early amyloidogenesis in Alzheimer's disease. In order to identify the post-transcriptional mechanism of energy deprivation-induced BACE1, we used glucose deprivation in BACE1-293 cells as an *in vitro* model of energy inhibition. These experiments clearly showed that glucose deprivation-induced BACE1 elevations were the result of altered translational control of BACE1 mRNA in response to eIF2 $\alpha$  phosphorylation. Although BACE1-293 cells are a useful model in which to investigate BACE1 protein regulation, proteins may be regulated differently in various cell types. Therefore, we repeated as many of our *in vitro*

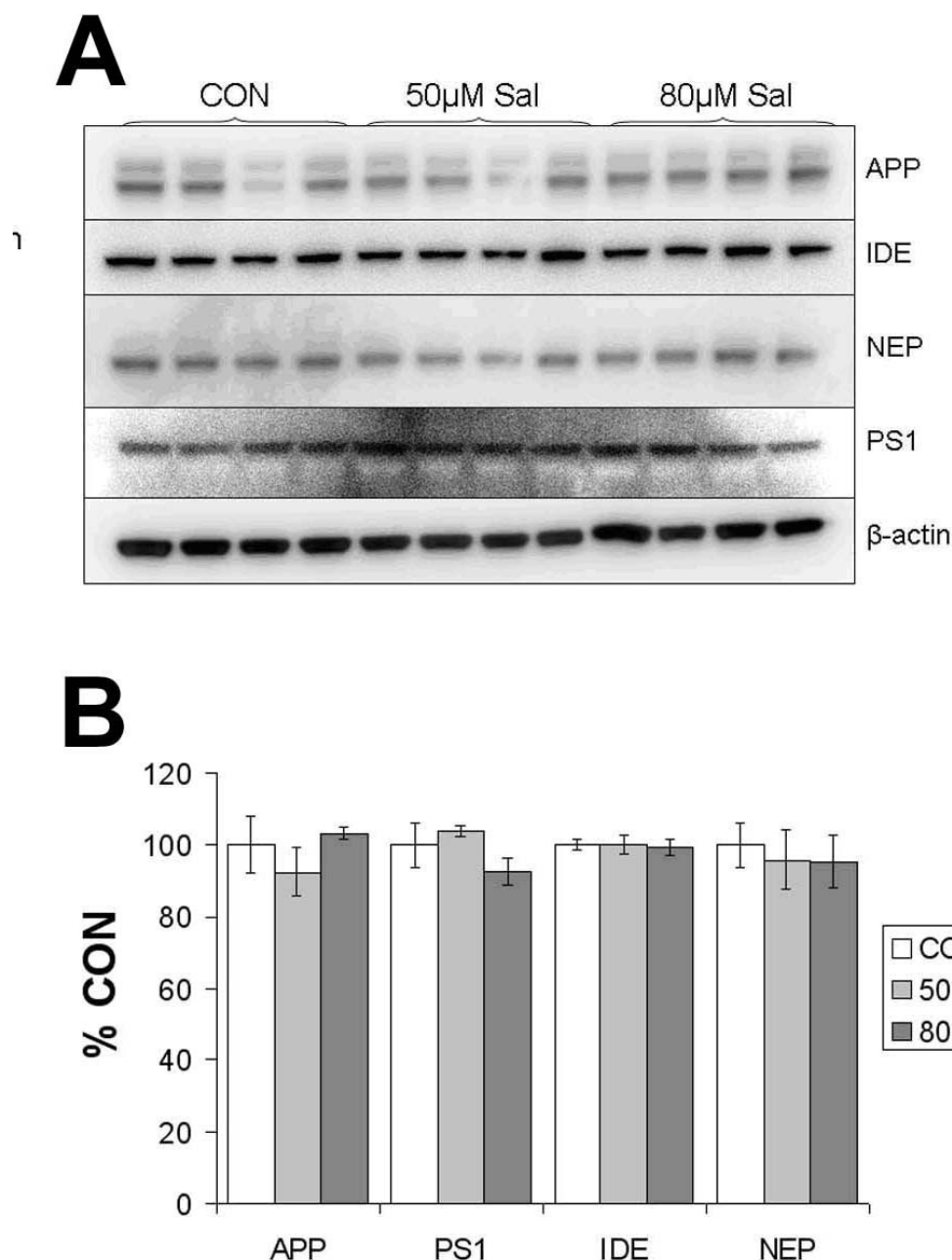


**Figure 4.3: Full-length APP, presenilin 1, and A $\beta$  degrading enzymes are unaffected by salubrin in neurons.** Primary cortical Tg2576 neurons were cultured for 7 DIV and then incubated for 48 hrs in normal media (CON), media containing 50  $\mu$ M salubrin, or media containing 80  $\mu$ M Sal. 10  $\mu$ g of protein was used for immunoblot analysis of full-length APP, presenilin 1 (PS1), insulin degrading enzyme (IDE), and neprilysin (NEP). Levels of APP, PS1, IDE, and NEP were unaltered by salubrin treatment, indicating that accelerated A $\beta$  production was due to elevated BACE1 protein.

experiments as possible in primary cultured neurons, to verify that eIF2 $\alpha$ -mediated regulation of BACE1 was physiologically relevant in the brain.

### **Energy deprivation in BACE1-293 cells versus cultured neurons**

Unlike BACE1-293 cells, BACE1 is under the control of its endogenous promoter and its full-length 3'UTR sequence in neurons (Fig 2.1L), allowing the contribution of these two regulatory elements in controlling energy deprivation-induced BACE1 protein elevations to be assessed. The human and murine BACE1 transcripts are highly homologous (~87%). The murine BACE1 5'UTR sequence is the same length and contains the same uORFs as the human BACE1 5'UTR, and it also has a relatively high G-C content (67%, as opposed to 76% in humans), and is therefore likely to be regulated similarly in mice and humans. Additionally, by culturing neurons from Tg2576 mice, which overexpress human APP<sup>sw</sup>, we can assess the effect of eIF2 $\alpha$  phosphorylation on amyloidogenic processing of APP *in vitro*. All of the experiments that were performed on primary cultured neurons confirmed the results from the BACE1-293 cells, indicating that HEK-293 cells are a good model for studying energy deprivation and regulation of BACE1. Similar to BACE1-293 cells, neurons up-regulated total BACE1 protein to levels comparable to those observed in BACE1-293 cells (~150%). However, BACE1 protein elevations were not apparent in NG-treated neurons compared to control until after ~24 hrs of treatment, reaching a peak around 36 hrs, whereas BACE1 protein levels were significantly elevated in BACE1-293 cells by 6 hrs in culture and peaked around 12-24 hrs in response to acute energy deprivation. One explanation for this discrepancy is that neurons in culture are metabolically inactive, in comparison to

BACE1-293 cells, which are rapidly dividing and therefore metabolically demanding. Neurons in culture therefore metabolize their energy stores more slowly than BACE1-293 cells and take longer to respond to a deficiency of exogenous glucose and initiate a stress response. Furthermore, the variability of BACE1 protein expression in cultured neurons is higher than in BACE1-293 cells, making subtle changes in protein expression more difficult to detect. Similar to BACE1-293 cells, the glucose deprivation-induced BACE1 protein elevation occurred in the absence of any BACE1 mRNA elevation, again implicating a post-transcriptional mechanism. This data rules out the possibility that the BACE1 promoter contributes to glucose deprivation-induced BACE1 protein elevations in neurons. In fact, endogenous BACE1 mRNA appeared to be down-regulated in response to energy deprivation. This may represent general down-regulation of cellular mRNA synthesis in response to glucose deprivation, which may be a method of energy conservation in the neuron. Furthermore, down-regulated BACE1 mRNA may also explain the delayed BACE1 protein increase in glucose deprived neurons, since decreased BACE1 mRNA and enhanced BACE1 translation have opposing effects on steady state BACE1 protein levels. Consistent with data from BACE1-293 cell experiments, eIF2 $\alpha$ -P levels were also elevated in cultured neurons deprived of glucose, compared to control. Based on our biochemical data showing that BACE1 protein is translationally regulated by eIF2 $\alpha$ -P, it is likely that the BACE1 protein elevations observed in response to glucose deprivation in cultured neurons is also the result of increased eIF2 $\alpha$ -P levels.



### **Cultured neurons as an experimental model**

Neurons are the most physiologically relevant cell type for investigating the biochemical mechanisms of brain disorders; however, they have clear experimental limitations. Our data from cultured neurons incubated in glucose-deficient media suggested that BACE1 protein was elevated *via* eIF2 $\alpha$  phosphorylation, as was the case in BACE1-293 cells; however, we could not test this directly. There is no available method of transfecting neurons with DNA at high enough efficiency to be useful for biochemical analysis. Therefore, we couldn't use our GADD34 constructs to verify that elevated eIF2 $\alpha$ -P levels were required for glucose deprivation-induced BACE1 protein elevations. Furthermore, we could not use our PERKDN and GCN2DN constructs to identify the specific kinase responsible for glucose deprivation-induced eIF2 $\alpha$ -P elevations in neurons. We are currently optimizing a method of infecting cultured neurons with high efficiency using adeno-associated viral vectors. These experiments should yield interesting results; however, viral infection itself is a potent activator of eIF2 $\alpha$ -P, so this experimental design may be problematic for studying this particular stress-response pathway (Fig 3.8). Furthermore, immunoblotting for activated eIF2 $\alpha$  kinases in response to glucose deprivation yielded inconclusive results. These kinases are high molecular weight proteins that exist in very low quantities in the cell. Commercial antibodies available to detect phosphorylation of these proteins *via* immunoblot produced a series of apparently non-specific bands at the predicted molecular weight of the kinases, none of which could be conclusively identified as the correct signal. We also attempted to repeat our <sup>35</sup>S metabolic labeling experiment in cultured neurons, to rule out the involvement of enhanced BACE1 protein stability in glucose deprivation

induced BACE1 protein elevation in neurons. Endogenous levels of BACE1 protein were too low to be detected using autoradiography of immunoprecipitated neuron lysates with commercially available antibodies, which react fairly weakly with BACE1 protein, and we were unable to use our novel, highly specific BACE1 antibody (3D5) (Zhao et al., 2007) for immunoprecipitation experiments, because the epitope is masked under these conditions. However, we suspect that altered protein stability of BACE1 was not involved in these experiments, because no glucose treatment did not appear to cause toxicity of neurons compared to control or caspase 3 activation, which is associated with enhanced BACE1 protein stability during the onset of apoptosis (Koh et al., 2005; Tesco et al., 2007; Vassar, 2007). Despite the technical limitations of using cultured neurons as a model system for energy deprivation, the results obtained from them were consistent with previous data from glucose-deprived BACE1-293 cells. *In vitro* experiments from BACE1-293 cells suggested that eIF2 $\alpha$ -P activation in response to energy deprivation was potentially amyloidogenic. Importantly, pharmacological activation of eIF2 $\alpha$ -P in cultured Tg2576 neurons elevated A $\beta$ 40 production *in vitro*. This data provides a direct mechanistic link between the eIF2 $\alpha$ -P stress pathway and amyloidogenesis.

## CHAPTER 5

# CHRONIC ENERGY INHIBITION *IN VIVO* ELEVATES BACE1 PROTEIN, ENHANCES eIF2 $\alpha$ PHOSPHORYLATION, AND ACCELERATES AMYLOID PATHOLOGY IN THE BRAIN

### Introduction

The mechanisms of amyloidogenesis in sporadic Alzheimer's disease (SAD) remain unknown; however, PET imaging studies indicate that glucose metabolism is reduced in AD brains or in the brains of individuals at risk for developing the disease, indicating that impaired energy metabolism may be an initiating factor in SAD. In support of this theory, we have shown using an acute model of energy deprivation in young mice that single i.p. injections of metabolic inhibitors post-transcriptionally elevate the rate limiting enzyme in the production of amyloid  $\beta$  in the brain, BACE1. Using *in vitro* models of energy deprivation in cell lines and neurons, we identified phosphorylation of the translation initiation factor eIF2 $\alpha$  through activation of the PERK kinase as the mechanism responsible for energy deprivation-induced BACE1 elevations. Additionally, we established that phosphorylation of eIF2 $\alpha$  is amyloidogenic in cultured neurons. In order to more accurately model the progression of sporadic Alzheimer's disease in the brain and to determine whether chronic energy inhibition would ultimately have an impact on the development of plaque pathology in the brain, we developed a chronic model of energy inhibition in older mice. We administered the two metabolic inhibitors from our previous study most specific to energy metabolism, 2DG (1g/kg) and 3NP (80mg/kg), once a week to nine-month old Tg2576 and C57/BL6 mice over a three-

month period (Fig 2.2). Brains from 12 month-old Tg2576 mice were assayed for BACE1 protein, eIF2 $\alpha$ -P, total A $\beta$ 40, and amyloid plaque deposition. Additionally, we analyzed BACE1 protein and mRNA from the brains of 12 month-old C57/BL6 mice treated for 3 months with 2DG or 3NP to determine 1) whether endogenous BACE1 protein would be elevated in response to chronic energy deprivation in the absence of a transgene, and 2) whether this occurred through a post-transcriptional mechanism.

## **Materials and methods**

### **Animals and Drug Treatments**

Nine-month old C57/BL6 mice were purchased from the National Institute of Aging (Bethesda, MD), and young Tg2576 (APP<sup>sw</sup> [Fig 2.1A], K670N/M671L; (Hsiao et al., 1996)) mice were purchased from Taconic (Hudson, NY) and bred in-house. Tg2576 and C57/BL6 mice were administered single intraperitoneal (i.p.) injections of 1x phosphate buffered saline (PBS; Invitrogen, Carlsbad, CA), 1g/kg 2-deoxyglucose (Sigma, St. Louis, MO) or 80mg/kg 3-nitropropionic acid adjusted to pH 7.0 with 1 M sodium hydroxide (Sigma) once a week beginning at 9 months of age. Drugs were dissolved in sterile 1x PBS at concentrations allowing for injection volumes of 100  $\mu$ L or less. All procedures were carried out in strict accordance with the NIH Guide for the Care and Use of Laboratory Animals and were approved by the Northwestern University Animal Care and Use Committee.

## **Tissue Preparation for Biochemical Analysis**

Mice were anesthetized with an i.p. injection of pentobarbital (100 mg/kg) 7 days following the final treatment, and transcardially perfused with 20 mL of cold perfusion buffer (1 mM HEPES, 13.7mM NaCl, 0.46mM KCl, 0.11mM KH<sub>2</sub>PO<sub>4</sub>, 0.06 mM MgSO<sub>4</sub> and 0.11 mM EDTA, 20 mg/mL PMSF, 5 mg/mL leupeptin, 200 mM sodium orthovanadate and 1 M DTT). Brains were excised and divided down the midline. Left hemi-brains from Tg2576 mice were drop-fixed in 4% paraformaldehyde in 1x PBS overnight at 4°C and stored in cryopreserve (30% sucrose (w/v), 0.01% Na-azide (w/v), in 1x PBS) at 4°C for at least 12 hrs for histology. Both hemi-brains from C57/BL6 mice and right hemi-brains from Tg2576 mice were flash frozen in liquid nitrogen and stored at -80°C. For biochemical analysis, frozen mouse hemi-brains were homogenized in 800 µL 1x PBS, 1% Triton-X 100, 1x protease inhibitor cocktail (AEBSF; Calbiochem), and 1x Halt phosphatase inhibitors (Pierce). Total protein concentration was determined by the BCA method (Pierce), and brain samples were all normalized to 10 mg/mL with homogenization buffer.

## **Immunoblotting**

10 µg protein was boiled for 5 min in sample boiling buffer (60 mM Tris, 10% glycerol, 5% SDS, pH 6.8, 10% β-mercaptoethanol +loading dye) prior to being separated on 4-12% NuPAGE Bis-Tris gels in 1x MOPS running buffer (Invitrogen) and transferred to Millipore Immobilon-P polyvinylidene difluoride (PVDF) membrane. Blots were blocked overnight in 5% bovine serum albumin (BSA) in Tris-buffered saline, 0.1% Tween 20 (TBST; Sigma, T9039; modified form), pH 8.0. Blots were then cut into strips and

incubated overnight in primary antibody (Table 4.1). Blots were then washed in TBST followed by 1 hr incubation in horseradish peroxidase-conjugated goat anti-mouse (GαM) or goat anti-rabbit (GαRb) diluted 1:10,000 in 5% milk in TBST (Jackson Immunological Research). Immunosignals were detected using enhanced chemiluminescence (ECL+, Amersham Biosciences) or SuperSignal West Femto (Pierce) and imaged and quantified using a Kodak CF440 imager.

### **RNA isolation and real-time PCR**

Frozen C57/BL6 hemibrains were homogenized in 2.5mL Qiazol reagent. Total RNA from 0.5mL of C57/BL6 brain homogenate was isolated using Qiagen's RNeasy Lipid Mini kit according to the manufacturer's specifications. Total mRNA concentrations were measured using  $ABS_{260nm}$  ( $[RNA] \mu g/\mu L = 0.04 \times ABS_{260nm}$ ) on a Beckman spectrophotometer. In general, only mRNA samples with low protein contamination ( $ABS_{260nm}/ABS_{280nm} > 1.8$ ) were used for analysis. mRNA integrity of each sample was confirmed using an Agilent Technologies 2100 Bioanalyzer. mRNA samples were used for analysis if the 28S ribosomal RNA peak was at least two times the area of the 18S ribosomal RNA peak. 1  $\mu g$  of total RNA from each sample was used for first-strand cDNA synthesis using Invitrogen's SuperScript III according to the manufacturer's recommendations (Random hexamers were used as opposed to oligo dTs). Exact cDNA concentrations were determined using a Beckman spectrophotometer, and 112.5 ng cDNA from each sample was amplified *via* Real-Time PCR in triplicate using Applied Biosystems' Assays-on-Demand pre-mixed Taqman primer/probe set for mouse BACE1 and APP mRNA (catalog #Mm00478664\_m1, Mm00431827\_m1) and normalized

against 18s rRNA (#4333760F). The BACE1 primer/probe set spans exons 1-2 of the murine BACE1 transcript, which are present in all known splice variants of BACE1, and the APP primer/probe set spans exons 9-11, which are present in all known splice variants of APP. Real Time PCR reactions were run using an Applied Biosystems 7900HT sequence analyzer. Applied Biosystem's universal cycling parameters were used. Samples were only used for final analysis if the standard deviation between triplicate samples was < 0.1 cycles. Percent of control values were determined using the comparative CT method. For microRNA analysis, RNA samples were analyzed using the Taqman microRNA reverse transcription kit with Taqman Universal PCR master mix (Applied Biosystems). Quantitative RT-PCR procedures were performed as previously described (Hebert et al., 2008) following the manufacturer's recommendations (Applied Biosystems). Relative expression was calculated using the comparative CT method.

### **Human A $\beta$ 40 ELISA**

10 mg/mL aliquots of Tg2576 brain were diluted 2.5x in 8.2 M guanidine-HCl (Gu-HCl final concentration of 5 M) and rocked at room temperature overnight to solubilize amyloid plaques. Guanidine-extracted brain homogenates were then diluted an additional 225x in cold 1x BSAT-DPBS (5% BSA, 0.03% Tween-20 in 1x Dulbecco's phosphate buffered saline (DPBS), pH 7.4) supplemented with 1x protease inhibitor cocktail (AEBSF; Calbiochem). Diluted brain homogenates were centrifuged at 16,000 x g for 20 min. at 4°C, then diluted 2x with A $\beta$  diluent supplemented with 1x AEBSF. Diluted samples (436  $\mu$ g total protein/well) and standards made from purified

recombinant human A $\beta$ 40 peptide were added in duplicate to a pre-coated human A $\beta$ 40 sandwich ELISA plate (Biosource), incubated and washed according to the manufacturer's instructions, and total A $\beta$ 40 levels in diluted hemi-brain homogenates were then determined using an standard curve of recombinant human A $\beta$ 40 peptide. All samples were analyzed within the linear range of the assay. Values were expressed as ng of A $\beta$ 40 (as determined by ELISA) per mg of total protein (as determined by the BCA assay.)

### **Immunohistochemistry**

30  $\mu$ m frozen sagittal sections from cryopreserved Tg2576 or C57/BL6 hemi-brains were cut using a sliding microtome and collected in 1x Tris-buffered saline (TBS; 50 mM Tris-HCl and 150 mM NaCl, pH 7.6). For cresyl violet staining on C57/BL6 brains, sections were mounted on slides, hydrated in a series of alcohols, and rinsed 1x in distilled water. Sections were rinsed for 1 min. in 0.5% cresyl violet (w/v) heated to 60 °C. Sections were then rinsed in distilled water and then dehydrated in series of alcohols. Sections were briefly rinsed in chloroform to remove background staining then further dehydrated in 95% ethanol and 2x in 100% ethanol. Sections were then rinsed 2x with xylene and coverslipped. For Thioflavin S staining of Tg2576 brains, sections were hydrated in a series of alcohols, rinsed briefly in distilled water, then stained with 1% Thioflavin S (w/v) for 1 hr. Sections were then dehydrated in a series of alcohols, rinsed 2x in xylene and then coverslipped in Molecular Probes Prolong Anti-fade reagent (Invitrogen). For IHC staining of Tg2576 brains, sections were blocked for 40 min. in 5% horse serum in 0.25% Triton-X-100 in 1x TBS, washed 2x for 10 min. in 1%



BSA in 0.25% Triton-X-100 in TBS Tg2576 sections were incubated in anti-4G8 (1:5,000; Chemicon) or anti-GFAP (1:10,000; Sigma) in 1% BSA in 0.25% Triton-X-100 in TBS overnight at room temperature, washed, and incubated with biotinylated secondary antibody diluted in 1% BSA in 0.25% Triton-X-100 in TBS (1:5,000; Chemicon) for 2 hrs. Sections were washed 3x for 10 min in 1x TBS. The Vectorlabs ABC kit was used with DAB as chromagen to visualize the reaction product, and then rinsed with distilled water. Sections were then counterstained with hematoxylin for ~5min, dehydrated in a series of alcohols, rinsed 2x with xylene, and coverslipped. Sections were then imaged using a Nikon Eclipse E800 microscope and Spot advanced digital camera (Diagnostic Instruments). The total number of 4G8-positive plaques in each section was counted manually and average number of plaques per section was calculated (8-11 sections/mouse).

### **Amyloid plaque counts**

A set of eight evenly spaced 30  $\mu$ m parasagittal sections were selected that spanned the entire medial-lateral dimension of each hemibrain from Tg2576 mice chronically treated with vehicle, 2DG, or 3NP. Sections were stained with anti-A $\beta$  antibody 4G8, developed by DAB immunohistochemistry, counterstained with hematoxylin, and mounted as described below. The total number of amyloid plaques in the eight sections from each mouse was then visually counted at low magnification in a microscope and plaque number means, SEMs, and p-values calculated.

## Statistical analysis

Sample averages were determined and then means and standard error of the means (SEMs; represented by error bars in histograms) were calculated based on the sample averages (n-values are stated in figure legends). Statistical differences between experimental groups and their respective controls were determined using a two-tailed t-test. Data are presented as the mean  $\pm$  SEM. \* $p < 0.05$ , \*\* $p < 0.01$ , \*\*\* $p < 0.001$ .

## Results

### Chronic energy inhibition increases eIF2 $\alpha$ phosphorylation and BACE1 levels in aged Tg2576 brains

In order to determine the effect of chronic energy deprivation on BACE1 protein and the progression of amyloid pathology in the brain, we designed a chronic *in vivo* energy deprivation paradigm based on our previous acute study in which we treated Tg2576 and C57/BL6 mice with inhibitors of energy metabolism that caused increases in BACE1 protein level and A $\beta$  production (Velliquette et al., 2005). In the acute study, 2 month-old Tg2576 mice were administered single intraperitoneal (i.p.) injections of compounds that produced or mimicked hypoglycemia, inhibited ATP synthesis, or caused neuronal over-excitation which depleted ATP stores: insulin, 2-deoxyglucose (2DG) and 3-nitropropionic acid (3NP), and kainic acid (KA). Since our *in vitro* studies primarily focused on the effects of glucose deprivation on eIF2 $\alpha$  phosphorylation and BACE1 level elevation, in the chronic *in vivo* study we only used the two compounds that would most specifically interfere with glucose metabolism: 2DG and 3NP (See Fig 2.2). Insulin and KA were not used in the current study due to the probability of

pleiotropic physiological effects, neurodegeneration, or high mortality in response to chronic exposure. For our chronic *in vivo* energy deprivation experiment, 9 month-old Tg2576 and C57/BL6 (wild-type) mice were treated once per week with i.p. injections 2DG (1 g/kg), 3NP (80 mg/kg), or vehicle (VEH) for a duration of 3 months. In our acute study, BACE1 and A $\beta$  levels stayed elevated for at least a week following a single dose of 2DG or 3NP (Velliquette et al., 2005), thus providing the rationale for single weekly injections in the chronic study. Treatments were started at 9 months of age--- the age at which Tg2576 mice begin to develop amyloid plaque pathology in the brain (Hsiao et al., 1996), and concluded when mice were 12 months old. We reasoned that this duration of experimental energy deprivation should be sufficient to produce an observable increase in the number of amyloid plaques in the brains of Tg2576 mice. The dose of 2DG in the chronic study was unaltered from the acute study, since this dose caused no mortality in the acute study. The dose of 3NP, however, was chosen based on a pilot study showing that 80 mg/kg 3NP was the lowest dose of 3NP that would produce a BACE1 protein increase comparable the one observed in response to a single i.p. injection of 100 mg/kg 3NP. These doses were well-tolerated by the mice, no mortality was observed in response to the drugs, and treatments caused only temporary lethargy lasting 30-60 min. Following 3 months of weekly VEH, 2DG, or 3NP treatments, hemi-brains from Tg2576 mice were processed for biochemical analysis or fixed for immunohistochemistry. Cresyl violet staining and GFAP immunohistochemistry of brain sections from 2DG- or 3NP-treated mice revealed no significant neurodegeneration or gliosis associated with chronic treatment of either drug compared to VEH (Fig 5.1). Furthermore, there was no evidence of caspase 3 activation in either 3NP-treated or

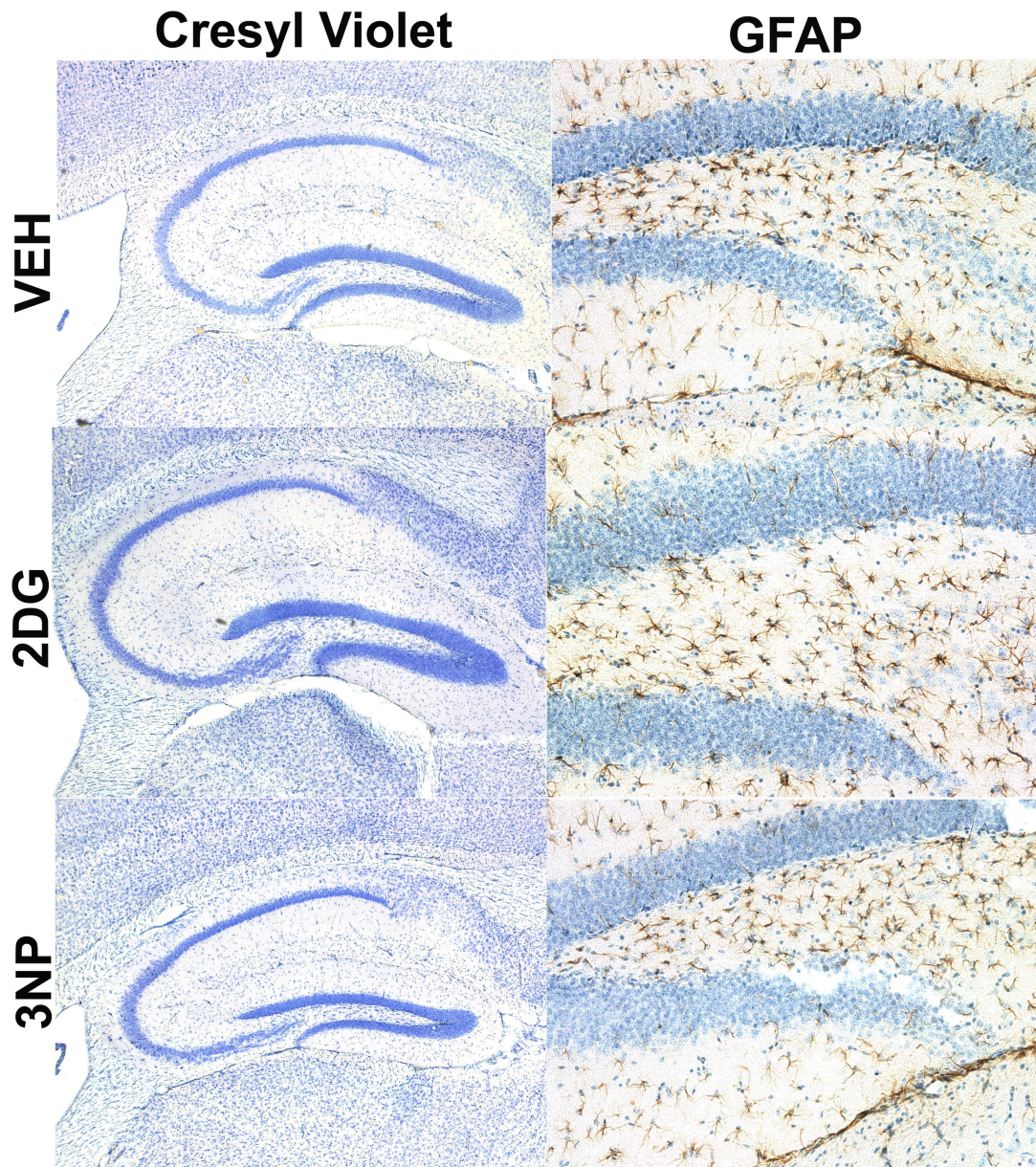


**Figure 5.1: Chronic energy deprivation causes no visible neurodegeneration or astrogliosis in Tg2576 brain.** Nine-month old Tg2576 mice were administered i.p. injections of saline (VEH), 1g/kg 2-deoxyglucose (2DG), or 80mg/kg 3-nitropropionic acid (3NP) once a week for 3 months (8-9 mice/group). One week after the final injection, hemibrains from each mouse were fixed and sectioned. Serial sections from 12-month old VEH, 2DG, and 3NP-treated mice were stained with cresyl violet, and the hippocampus was imaged at 4X. There was no evidence of neurodegeneration in 2DG- and 3NP-treated mice compared to VEH. Alternate sections were stained with rabbit anti-GFAP at 1:10,000 (G9269; Sigma), and the dentate gyrus was imaged at 20X. There was no evidence of greater astrogliosis in 2DG- and 3NP-treated mice compared to VEH.

VEH-treated mice, indicating that chronic energy inhibition does not induce neuronal apoptosis (Fig 5.2D). In order to determine the effect of chronic energy deprivation on BACE1 protein levels in Tg2576 brain, we quantified levels of BACE1 protein in 2DG- and 3NP-treated Tg2576 mice compared to VEH-treated *via* immunoblot. Similar to the acute study and our *in vitro* experiments, chronic experimental energy deprivation caused a significant increase of BACE1 protein levels in the brains of 2DG- and 3NP-treated Tg2576 mice (Fig. 5.2A,B,C). 2DG-treated mice exhibited BACE1 increases of ~120% ( $p < 0.05$ ), and 3NP-treated Tg2576 mice exhibited BACE1 elevations of ~160% ( $p < 0.001$ ), respectively, in comparison to vehicle control treatment. Since our previous results showed that enhanced BACE1 translation *via* eIF2 $\alpha$  phosphorylation was responsible for the energy deprivation-induced BACE1 increase *in vitro*, we wanted to determine whether chronic 2DG and 3NP treatment increased eIF2 $\alpha$  phosphorylation in the brain. We measured phosphorylated and total eIF2 $\alpha$  levels in brain homogenates of Tg2576 mice treated with 2DG, 3NP, or vehicle *via* immunoblot (Fig. 5.2B,C). The eIF2 $\alpha$ -P(Ser51):eIF2 $\alpha$ -T ratios in the brains of 2DG- and 3NP-treated mice were elevated to ~130% ( $p < 0.05$ ) and ~150% ( $p < 0.01$ ) of vehicle, respectively, similar to the increases in eIF2 $\alpha$  phosphorylation observed *in vitro*. Importantly, increases in eIF2 $\alpha$  phosphorylation correlated with the BACE1 elevations that occurred in 2DG- and 3NP-treated mice. Furthermore, an expression analysis of three BACE1-regulating microRNAs (miR-29a, miR-29b-1, miR-9) in the brains of Tg2576 mice revealed no change in 2DG-treated mice compared to VEH, and significantly increased expression of miR-29a ( $p = 0.016$ ) and miR-29b-1 ( $p = 0.008$ ) in 3NP-treated mice compared to VEH (Fig 5.2E). Since decreased miR-29a, miR-29b-1, and miR-9 expression elevate



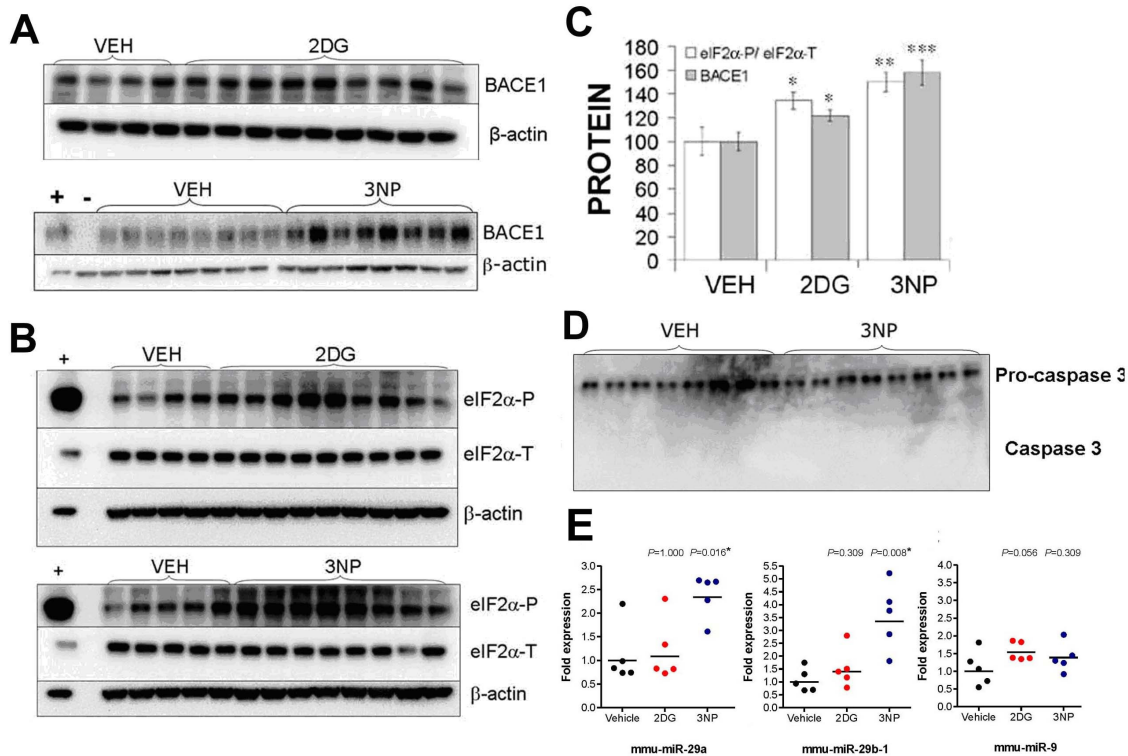


**Figure 5.2: Chronic energy deprivation elevates eIF2α-P and BACE1 protein in Tg2576 brain** (A) Nine-month old Tg2576 mice were administered i.p. injections of saline (VEH), 1g/kg 2-deoxyglucose (2DG), or 80mg/kg 3-nitropropionic acid (3NP) once a week for 3 months (8-9 mice/group). One week after the final injection, hemibrains were prepared for biochemical analysis. 10μg of protein was used for immunoblot analysis of BACE1 and β-actin. “+” lane: 5 μg of BACE1-293 cell lysate as a BACE1 positive control.. “-” lane: 10μg of BACE1<sup>-/-</sup> mouse brain homogenate as a BACE1 negative control. (B) 15 μg of protein from VEH, 2DG, or 3NP-treated Tg2576 brain was used for immunoblot analysis of eIF2α-P, eIF2α-T, and β-actin. “+” lane: 10μg of lysate from UV-treated 293 cells as a positive control for eIF2α-P. (C) Immunosignals in (A) and (B) were quantified by phosphorimager and expressed as % VEH. BACE1 levels and eIF2α-P/eIF2α-T ratios were significantly elevated in 2DG and 3NP treated Tg2576 mice compared to VEH (mean ± SEM; \*, p<0.05; \*\*, p<0.01; \*\*\*, p<0.001). (D) 10 μg brain homogenate from VEH and 3NP-treated Tg2576 mice was used for immunoblot analysis of caspase 3. There was no evidence of caspase cleavage in either treatment group. (E) (courtesy of Sebastien Hebert) Total mRNA from VEH, 2DG, and 3NP-treated mice was analyzed for miR-29a, miR-29b-1, and miR-9 expression. miR-29a and miR-29b-1 were significantly elevated in 3NP-treated mice compared to VEH.

BACE1 protein levels (Hebert et al., 2008), this experiment indicates that microRNAs are not involved in chronic energy deprivation-induced BACE1 protein elevations in the brain. These results, together with our *in vitro* BACE1-293 cell and primary neuron data, suggest that chronic energy deprivation *in vivo* may induce the eIF2 $\alpha$  phosphorylation pathway, which in turn increases BACE1 levels *via* translational up-regulation.

### **Chronic energy deprivation in aged wild-type C57/BL6 mice significantly decreases BACE1 and APP mRNA**

In order to determine whether BACE1 protein would be regulated similarly in response to chronic energy deprivation in wild-type animals and to determine if this regulation was post-transcriptional, weekly i.p. injections of VEH, 1 g/kg 2DG, and 80 mg/kg 3NP were also administered to 9 month-old C57/BL6 animals. One half of the 12 month-old C57/BL6 brains were processed for biochemistry, and the other half was processed for TaqMan mRNA quantification, rather than histology. Similar to 12 month-old Tg2576 mice, chronic pharmacological energy deprivation caused a significant increase of BACE1 protein levels in the brains of C57/BL6 mice (Fig. 5.3A, B). 2DG-treated mice exhibited BACE1 increases of ~130% ( $p < 0.05$ ), and 3NP-treated mice exhibited a BACE1 protein increase of ~170% ( $p < 0.001$ ), above VEH. This data demonstrates that chronic energy deprivation-induced BACE1 protein elevations are reproducible in different strains of mice, similar to what we observed in response to acute energy deprivation. Based on our *in vitro* studies with BACE1-293 cells and primary neurons, we predicted that the BACE1 increase following chronic *in vivo* energy deprivation

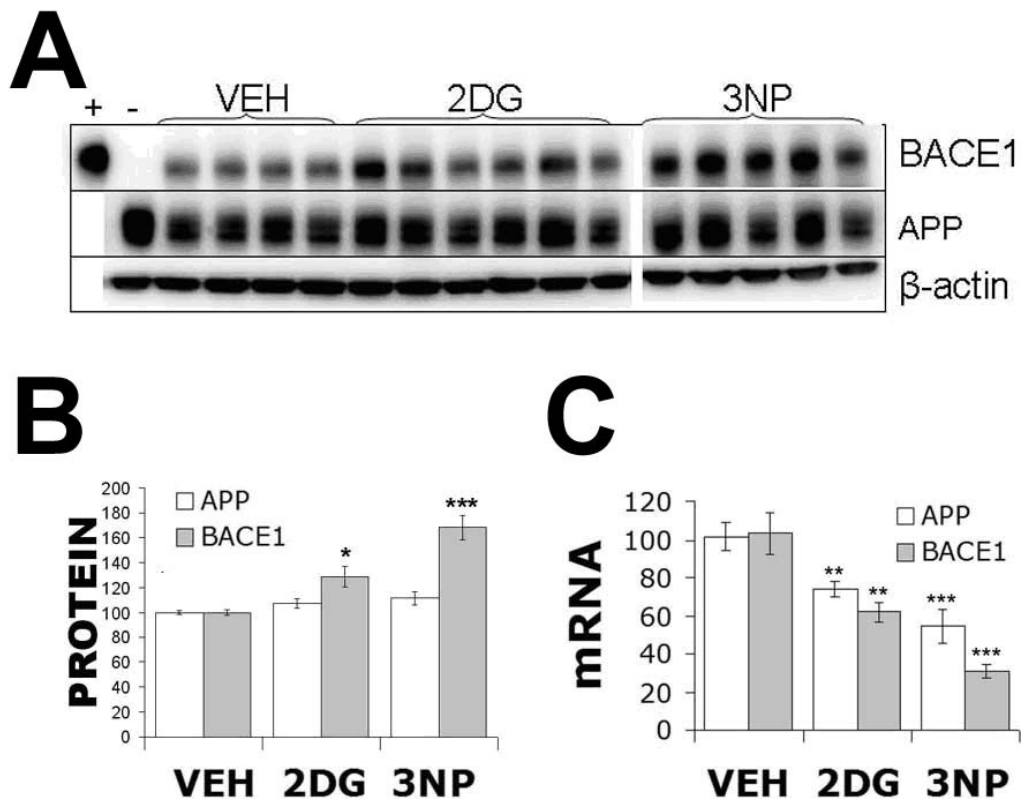


**Figure 5.3: Chronic energy deprivation elevates BACE1 protein post-transcriptionally in C57/BL6 brain.** (A) Nine-month old wild-type C57/BL6 mice were administered i.p. injections of saline (VEH), 1g/kg 2-deoxyglucose (2DG), or 80mg/kg 3-nitropropionic acid (3NP) once a week for 3 months. One week after the final injection, hemibrains were prepared for biochemical analysis. 10μg of protein was used for immunoblot analysis of BACE1, full-length APP, and β-actin. “+” lane: 5μg of BACE1-293 cell lysate as a BACE1 positive control. “-” lane: 10μg of BACE1<sup>-/-</sup> mouse brain homogenate as a BACE1 negative control. (B) Immunosignals in (A) were quantified using a phosphorimager and expressed as % VEH (n = 4-6). BACE1 levels were significantly elevated in the brains of both 2DG and 3NP-treated mice compared to VEH (mean ± SEM; \*, p<0.05; \*\*\*, p<0.001). (C) Total mRNA was isolated from the hemibrains of VEH, 2DG, and 3NP treated C57/BL6 mice and levels of endogenous BACE1 and APP mRNAs measured via the TaqMan real-time PCR relative quantification method and expressed as percentage of vehicle (VEH; 9-12 mice per group). Strikingly, both BACE1 and APP mRNA levels were significantly decreased in 2DG and 3NP-treated C57/BL6 mice compared to VEH (mean ± SEM; \*\*, p<0.01; \*\*\*, p<0.001).



would be post-transcriptional. To test this hypothesis, we isolated total mRNA from hemi-brains of C57/BL6 mice chronically treated with 2DG, 3NP, and VEH and measured levels of endogenous mouse BACE1 mRNA by TaqMan quantitative real-time PCR analysis. Indeed, BACE1 mRNA levels were not increased upon 2DG or 3NP treatment, and in fact were significantly *decreased* compared to vehicle (~60% of VEH in 2DG-treated mice ( $p < 0.01$ ) and ~30% of VEH in 3NP-treated mice ( $p < 0.001$ ); Fig. 5.3C). The pattern of BACE1 mRNA decrease in response to chronic 2DG and 3NP treatment was inversely related to the effect of these same drugs on BACE1 protein. Interestingly, APP mRNA levels were also significantly decreased in response to 2DG and 3NP treatment (~70% of VEH in 2DG-treated mice ( $p < 0.01$ ) and ~50% of VEH in 3NP-treated mice ( $p < 0.001$ ); Fig 5.3C). This decrease in mRNA may reflect global down-regulation of transcription caused by ATP depletion. In any case, our results clearly demonstrate that the BACE1 elevations in response to chronic *in vivo* energy deprivation were not the result of either increased BACE1 gene transcription or enhanced BACE1 mRNA stabilization.

### **Chronic energy deprivation in aged Tg2576 mice accelerates A $\beta$ production and plaque deposition in the brain**

Elevated BACE1 levels in the brains of 2DG- and 3NP-treated Tg2576 mice suggested that A $\beta$  production and amyloid plaque formation might also be increased in these animals. In support of this hypothesis, previous studies had reported that modest overexpression of BACE1 increased cerebral A $\beta$  levels and amyloid deposition in transgenic mice (Bodendorf et al., 2002; Chiocco et al., 2004; Chiocco and Lamb, 2007;

Lee et al., 2005; Mohajeri et al., 2004; Ozmen et al., 2005; Willem et al., 2004). To initially test whether chronic energy deprivation increased amyloidogenesis *in vivo*, we analyzed guanidine-extracted brain homogenates from treated Tg2576 mice for total levels of A $\beta$ 40, the major isoform of A $\beta$  produced in this transgenic line, by human A $\beta$ 40-specific ELISA. We observed that treatment with 2DG and 3NP caused clear trends toward elevation of A $\beta$ 40 levels in the brain (Fig. 5.4C; VEH =  $9.10 \pm 1.30$  ng A $\beta$ 40/mg protein, 2DG =  $13.15 \pm 1.94$ , 3NP =  $15.56 \pm 3.75$ ), although statistical significance was not reached. To obtain further support that 2DG and 3NP treatment increased A $\beta$  generation and amyloid deposition in Tg2576 mice, we counted amyloid plaques in hemi-brain sections of the same mice subjected to chronic energy deprivation and analyzed for A $\beta$ 40 levels. Upon examination of brain sections that were stained with either anti-A $\beta$  (4G8) antibody (Fig. 5.4A) or Thioflavin-S (Fig. 5.4B), we noted that plaques in 2DG- and 3NP-treated mice qualitatively tended to appear larger and more numerous than in vehicle-treated mice. Quantitatively, the number of plaques showed a clear trend toward elevation in 2DG- and 3NP-treated mice compared to vehicle (Figs. 5.4D; VEH =  $20.8 \pm 3.7$ ; 2DG =  $26.7 \pm 5.3$ ; 3NP =  $36.0 \pm 8.6$ ), although as with A $\beta$ 40 levels, statistical significance was not achieved. In order to address the possibility that mechanisms other than BACE1 up-regulation were responsible for the chronic energy deprivation-induced rise in A $\beta$ 40 levels and plaque numbers in Tg2576, we analyzed other components of the amyloidogenic pathway, as well as amyloid degrading enzymes *via* immunoblot in 2DG- and 3NP-treated mice compared to VEH. Levels of full-length APP and presenilin 1 (PS1) were not altered in response to chronic energy deprivation, indicating that a rise in the A $\beta$  precursor or altered activity of the  $\gamma$ -

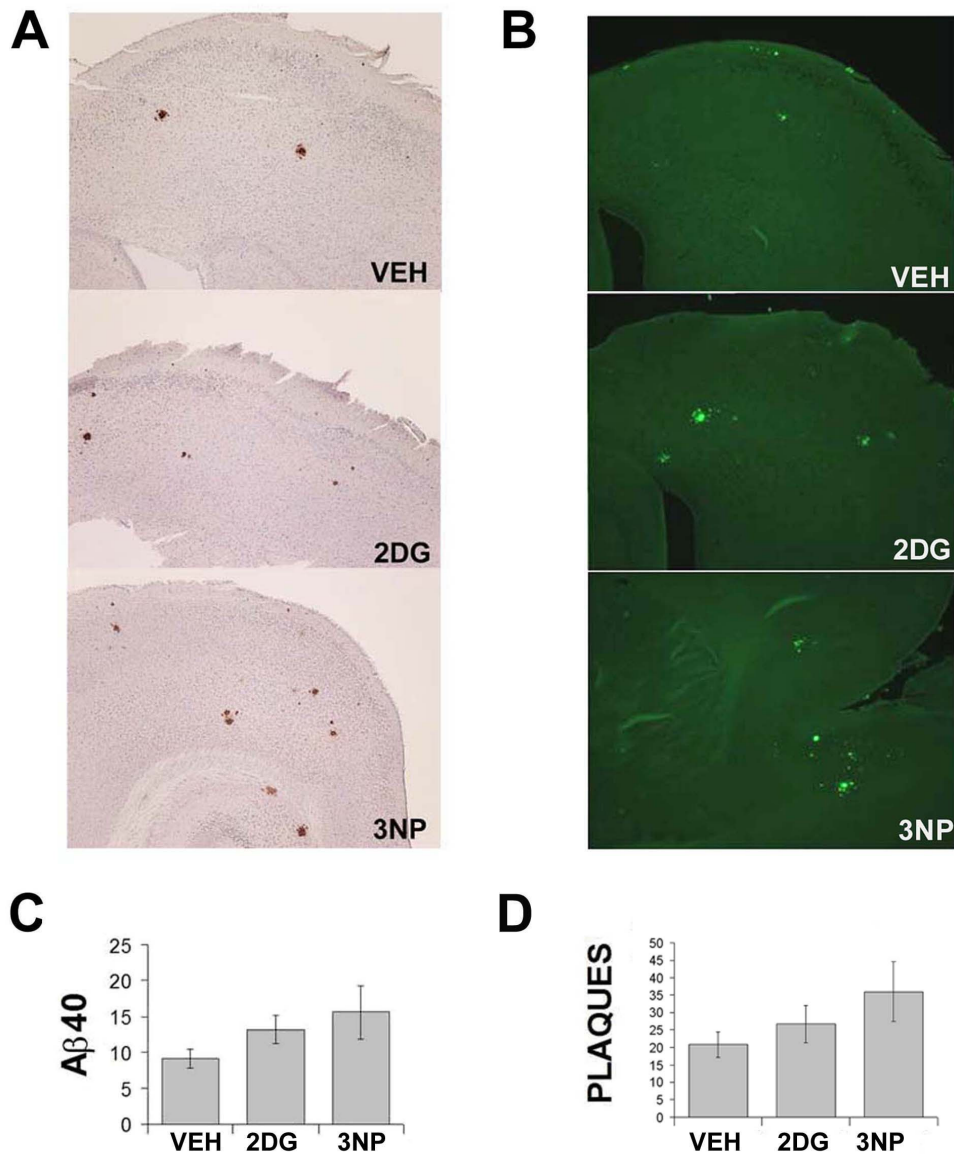


**Figure 5.4: Chronic energy deprivation accelerates A $\beta$  production and exacerbates amyloid plaque pathology in Tg2576 brain.** Nine-month old Tg2576 mice were administered i.p. injections of saline (VEH), 1g/kg 2-deoxyglucose (2DG), or 80mg/kg 3-nitropropionic acid (3NP) once a week for 3 months (8-9 mice/group). One week after the final injection, hemibrains were prepared for biochemical analysis or fixed for immunohistochemistry. **(A)** Parasagittal brain sections were immunostained for A $\beta$  (4G8) and micrographed at 4x. **(B)** Parasagittal brain sections from VEH, 2DG, or 3NP-treated mice were stained with Thioflavin S for  $\beta$ -sheet amyloid and imaged at 4x. **(C)** Guanidine-extracted brain homogenates from VEH, 2DG, and 3NP-treated mice were analyzed using a human A $\beta_{40}$  ELISA. Values were expressed as ng of A $\beta_{40}$  per mg of total protein. **(D)** 4G8-immunopositive plaques were counted in a set of eight evenly spaced sections that spanned the entire medial-lateral dimension of each hemibrain.

secretase complex are unlikely to be the cause of A $\beta$  elevations in 2DG- and 3NP-treated mice. Furthermore, levels of A $\beta$  degrading enzymes, such as insulin degrading enzyme (IDE) and neprilysin were similarly unaffected, indicating that A $\beta$  elevations and enhanced plaque deposition in 2DG- and 3NP-treated mice are not the result of reduced A $\beta$  clearance from the brain (Fig 5.5). Taken together, the proportional parallel increases of phosphorylated eIF2 $\alpha$ , BACE1, A $\beta$ 40, and plaque number make a compelling case that chronic energy deprivation *in vivo* is likely to promote amyloidogenesis *via* a mechanism involving eIF2 $\alpha$  phosphorylation and BACE1 translational control.

## Discussion

### Acute versus chronic energy deprivation in the brain

Previously, we showed that single injections of pharmacological energy inhibitors could elevate BACE1 protein levels post-transcriptionally and promote amyloidogenesis in young Tg2576 mice. Consistent with these results, we could induce BACE1 protein elevation *in vitro* by treating BACE1-293 cells and primary cultured neurons with glucose-deficient media. Although these results suggested that BACE1 was a molecular target of impaired energy metabolism, and our acute *in vivo* study suggested that this was amyloidogenic in the brain, Alzheimer's disease is a chronic disorder that develops over several decades. In order to gather further support for our hypothesis that cumulative metabolic insults can accelerate amyloid pathology in the brain, we developed a chronic model of energy inhibition in older Tg2576 mice. Nine-month old Tg2576 mice were administered single i.p. injections of 2DG, 3NP, or VEH once a week

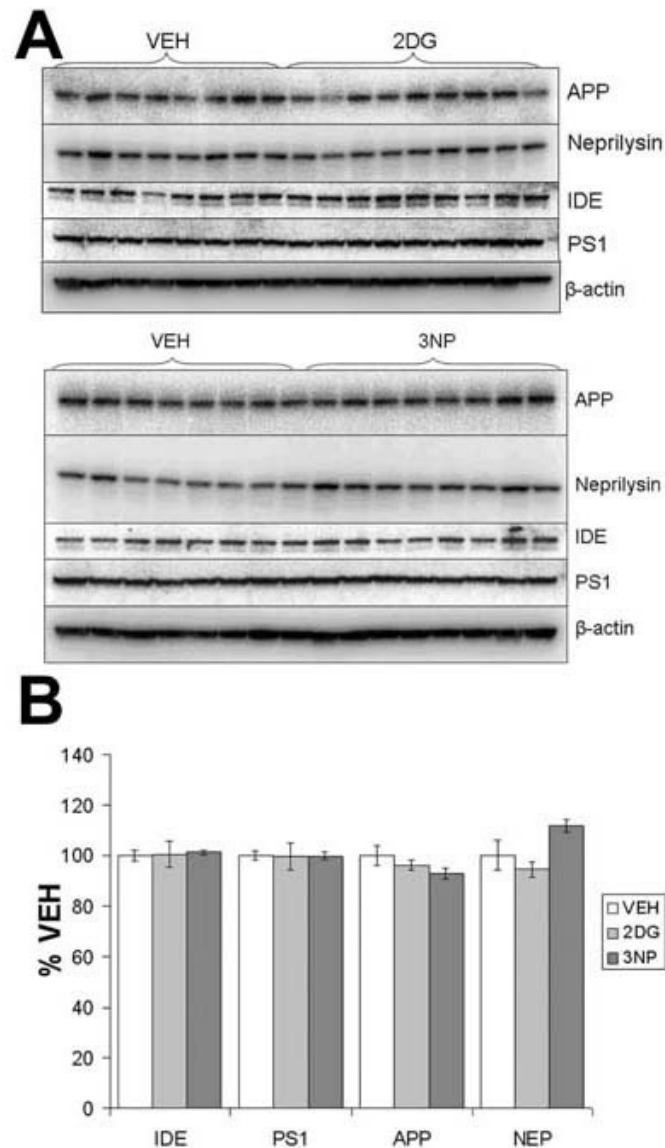


**Figure 5.5: Other components of the amyloidogenic pathway and A $\beta$  degrading enzymes are not affected by chronic energy deprivation** Tg2576 mice were administered i.p. injections of saline (VEH), 1g/kg 2-deoxyglucose (2DG), or 80mg/kg 3-nitropropionic acid (3NP) once a week for 3 months (8-9 mice/group). **(A)** 10  $\mu$ g brain homogenate from VEH, 2DG, or 3NP-treated mice was analyzed *via* immunoblot for levels of full-length APP protein, presenilin 1 (PS1; part of the active site of the  $\gamma$ -secretase complex), insulin degrading enzyme, and neprilysin (A $\beta$  degrading enzymes). **(B)** APP, PS1, IDE, and neprilysin immunosignals were normalized to  $\beta$ -actin and expressed as % of VEH. There was no effect on any of these proteins in response to chronic 2DG or 3NP treatment, further supporting the hypothesis that increased A $\beta$ 40 levels and enhanced plaque deposition in response to chronic energy deprivation are the result of elevated BACE1 levels.

for three months and analyzed at twelve months of age for the progression of amyloid pathology in the brain. Similar to our acute study, chronic pharmacological energy inhibition elevated BACE1 protein levels in the brains of Tg2576 mice. Interestingly, the level of BACE1 protein elevation above vehicle was similar in both the acute and the chronic study, indicating that BACE1 protein levels are maximally elevated by energy deprivation at ~150%, and this elevation is maintained for the duration of the treatment period. Although the BACE1 protein elevation was similar in both studies, since BACE1 is an enzyme, the duration of elevation can have dramatic effects on the accumulation of APP cleavage fragments (see Fig 4.2C). Furthermore, the mechanism of BACE1 protein elevation appeared to be similar in both the acute and the chronic study. BACE1 mRNA analysis from the acute study indicated that the BACE1 protein increase was occurring post-transcriptionally. BACE1 mRNA analysis of brains from the chronic study showed a similar phenomenon. In fact, both BACE1 and APP mRNA were significantly down-regulated in response to chronic 2DG and 3NP administration (Fig 5.3C). Again, this may reflect a general down-regulation of mRNA synthesis in response to low energy availability, which may be a method of energy conservation in the neuron.

### **Mechanisms of BACE1 elevation during chronic energy deprivation**

Similar to the acute study, BACE1 protein elevations occurred in the absence of apparent astrogliosis, implying that the BACE1 elevation probably occurred neuronally, and that it was not inflammatory-mediated (Fig 5.1). Our glucose deprivation experiments in cultured neurons confirm that neurons are capable of up-regulating

BACE1 in response to energy deprivation (Fig 4.1A,C). Furthermore, the absence of neurodegenerative changes in response to chronic energy inhibition supports our hypothesis that cumulative metabolic insults can accelerate amyloid pathology in the brain below the threshold which causes neurons to die (Fig 5.1). Chronic energy deprivation in the brain, like acute energy deprivation *in vivo* and glucose deprivation *in vitro*, appeared to elevated BACE1 protein post-transcriptionally. This was supported by mRNA data (Fig 5.3C), and the absence of any neuron death or caspase activation in the chronic study indicated that apoptosis-induced increases in BACE1 protein stability were not involved (Fig 5.1; Fig 5.2D). Similarly, analysis of miR-29a, miR-29b-1, and miR-9 indicated that the microRNA-mediated BACE1 regulatory mechanism previously described (Hebert et al., 2008) was not involved in chronic energy deprivation-induced BACE1 protein elevation (Fig 5.2E). The presence of elevated eIF2 $\alpha$ -P levels in 2DG- and 3NP-treated brains compared to VEH indicated that this could be occurring through stress-induced translational up-regulation of BACE1, as demonstrated *in vitro* (Fig 5.2A,B,C). However, as was the case with cultured neurons, we could not test the involvement of the eIF2 $\alpha$ -P pathway directly in chronic energy deprivation-induced BACE1 protein elevations. Future genetic crosses of eIF2 $\alpha$ -P deficient mice with amyloid models and viral-mediated gene delivery of eIF2 $\alpha$ -P inhibitors in combination with pharmacological energy inhibition should address this question and yield intriguing results. Another interesting feature of the chronic energy inhibition study is the apparent greater effect of 3NP on all of the biochemical measures of amyloidogenesis, in comparison to 2DG. 3NP-treated mice had higher BACE1 protein levels, eIF2 $\alpha$ -P levels (Fig 5.2A,B,C), A $\beta$ 40 levels (Fig 5.4C), and more

extensive plaque pathology in the brain, compared to 2DG- or VEH-treated mice (Fig 5.4A,B,D). Intriguingly, 3NP-treated mice also exhibited a more severe reduction in BACE1 and APP mRNA levels in the brain than 2DG-treated mice (Fig 5.3C). One likely explanation for this trend is that 3NP more severely affects energy metabolism in the brain than 2DG. 2DG competes with glucose for the enzyme hexokinase, and therefore slows the rate of glucose metabolism through the glycolysis pathway. However, other components of energy metabolism are not affected; therefore, the small amounts of glucose that continues to be metabolized by hexokinase in the presence of 2DG can still fuel the tricarboxylic acid (TCA) cycle and the electron transport chain (Fig 2.2). Furthermore, despite the fact that the brain is highly dependent upon glucose as an energy substrate, it is capable of using alternative energy substrates, such as ketones, which are not dependent on glycolysis, and can be used to fuel the TCA cycle and the electron transport chain during low glucose availability (Morris, 2005). 3NP, on the other hand, competitively inhibits succinate dehydrogenase (SDH), which is a component of both the TCA cycle and the electron transport chain (Fig 2.2). Proper functioning of these cellular components is required for aerobic metabolism. Without them, the cell is limited to the few molecules of ATP produced through glycolysis as an energy source. The effect of 3NP on neuronal energy metabolism is quite severe and can cause neurodegeneration upon repeated injections. In fact, 3NP has been used as a pharmacological model of Huntington's disease for decades (Brouillet et al., 2005). 2DG does not have this capability. Therefore, our results indicate that more severe metabolic insults have a greater effect on the progression of amyloid pathology in the brain.



## Energy deprivation and the progression of amyloid plaque pathology

We used aged Tg2576 mice as a model to assess the affects of chronic energy deprivation on human amyloid pathology *in vivo*. The Tg2576 line is an established model of amyloid pathology; in fact, it was one of the first models developed to study amyloid pathology in the brain (Hsiao et al., 1996). Tg2576 mice have been widely used in the AD field and have been extensively validated as a useful model of amyloid pathology. The Tg2576 line recapitulates many of the features of human Alzheimer's disease. Most importantly, Tg2576 mice accumulate human A $\beta$ 40 and A $\beta$ 42 in the brain with age, and develop amyloid plaques in the brain, which stain with A $\beta$ -specific antibodies and Thioflavin S, a marker of  $\beta$ -pleated sheets. Additionally, Tg2576 mice develop age-dependent memory deficits and significant cerebral amyloid angiopathy (CAA), which are other important features of Alzheimer's disease (Domnitz et al., 2005; Hsiao et al., 1996; Sasaki et al., 2002; Yamada, 2000). A particular advantage of the Tg2576 mouse model for our study is the presence of the Swedish mutation at the  $\beta$ -secretase cleavage site of APP. This mutation renders APP more susceptible to  $\beta$ -secretase cleavage, making this mouse model highly sensitive to changes in  $\beta$ -secretase activity (Citron et al., 1992). Therefore, this model is extremely useful for studies focusing on BACE1 regulation, because total A $\beta$  levels and amyloid plaque pathology in the brain are expected to be highly dependent upon BACE1 cleavage of APP. Although the Tg2576 mouse is a well-established model for amyloid pathology in the brain, it is not without its limitations. Murine models of A $\beta$  pathogenesis in general have come under scrutiny for several reasons. First of all, amyloid pathology in the

murine brain can only be achieved *via* overexpression of human APP. Therefore, APP is never under the control of its endogenous promoter in these models, and APP expression levels are not physiological. Second, murine amyloid models always contain an AD mutation that enhances pro-amyloidogenic processing of APP. These mutations are extremely rare in the human population and are therefore not truly representative of the majority of AD cases, which occur in the absence of any APP or PS1 mutations. This calls into question the validity of using these transgenic animals as a model of sporadic Alzheimer's disease. With respect to using the Tg2576 line to model SAD, specifically, the Swedish  $\beta$ -site mutation does not alter normal A $\beta$ 40:A $\beta$ 42 ratios, since BACE1 cleavage of APP contributes equally to the production of both A $\beta$ 40 and A $\beta$ 42. The amyloid pathology in Tg2576 brain is primary driven by overexpression of APP and a preference for APP to be processed in the amyloidogenic pathway due to the  $\beta$ -site mutation. Therefore, the Tg2576 line is expected to accurately model the development of normal amyloid pathology in the aging human brain on an accelerated time scale and is a valid model for studying the effects of exogenous factors, such as energy impairment on the progression of amyloid pathology in the brain. Although BACE1 protein and eIF2 $\alpha$ -P levels were significantly elevated in the brains of Tg2576 mice in response to chronic energy deprivation (Fig 5.2A,B,C), A $\beta$ 40 levels and plaque number failed to be significantly elevated in 2DG and 3NP mice compared to control (Fig 5.4), despite the fact that even marginal elevations of BACE1 protein can have dramatic effects on A $\beta$ 40 production (Fig 4.2). This may be partially explained by the possibility that in comparison to aged humans, 12 month-old Tg2576 mice may have fully intact A $\beta$  clearance mechanisms in the brain. Although energy deprivation significantly elevates

eIF2 $\alpha$ -P and BACE1 levels, which can undoubtedly accelerate A $\beta$  production in 9-12 month-old Tg2576 mice, fully intact A $\beta$  clearance mechanisms may have prevented significant accumulation and deposition of A $\beta$  in this mouse model. To more accurately mimic the effect of chronic energy deprivation in human AD brain, it would be interesting to test the effect of chronic energy deprivation in future studies using lengthier experiments in older Tg2576 mice, which may experience increasingly impaired A $\beta$  clearance mechanisms in the brain, similar to humans, as they reach the end of their lifespans. Indeed, plaque pathology in Tg2576 brains worsens exponentially with age, despite unaltered transgene expression, which supports the hypothesis that clearance mechanisms begin to deteriorate at older ages in these mice (Hsiao et al., 1996). In the context of impaired amyloid clearance, factors such as energy deprivation which enhance A $\beta$  production may have even more dramatic effects on amyloid accumulation in the brain. Clearly, amyloidogenesis and the development of plaque pathology in the human brain is an extremely complex process, which no single transgenic animal can model with complete accuracy. Regardless, the Tg2576 mouse model is the most appropriate animal model for our study, and our results clearly show that energy deprivation can impact the production of A $\beta$  and the progression of plaque pathology in the brain in a manner that was consistent with all of our previous results. It should also be noted that although the Tg2576 line is an excellent model of plaque pathology, it lacks several other important features of true Alzheimer's disease. Namely, Tg2576 mice do not experience the massive neuronal death associated with Alzheimer's disease despite apparent memory deficits, and they do not develop neurofibrillary tangles, which are also hallmarks of AD. Both of these features of AD play essential

roles in the disease process. The development of AD pathology in the human brain is a complex process that does not arise from one single factor; therefore, the contribution of these other molecular players cannot be ignored when assessing the true effect of energy deprivation on the progression of AD pathology. From this perspective, the Tg2576 line allows us to model the effects of chronic energy deprivation on A $\beta$  production and resultant amyloid pathology in the brain, but the indirect effect of energy deprivation on eventual downstream AD pathology, neuronal death, and memory impairment can only be assumed based on the known association of amyloid pathology with these other hallmarks of AD. Eventually, it will be imperative to compare the results seen in Tg2576 mice in other animal models of AD. For instance, it would be interesting to evaluate the effect of energy deprivation in an animal model that develops both amyloid and tau pathology. It is inferred, based on the association of amyloid and tau pathology, that energy deprivation-induced acceleration of amyloid pathology will ultimately exacerbate tau pathology in the brain. However, this must be demonstrated experimentally in order to validate our hypothesis that upstream environmental factors influencing A $\beta$  production can have a significant impact on the progression of downstream AD pathology. To this end, it will also be important to analyze human AD brains to determine the degree of involvement of energy deprivation and the eIF2 $\alpha$ -P pathway in the actual disease process.

## CHAPTER 6

# **BACE1 PROTEIN AND PHOSPHO-eIF2 $\alpha$ LEVELS ARE ELEVATED IN 5XFAD BRAINS AND BACE1, PHOSPHO-eIF2 $\alpha$ , AND AMYLOID LOAD ARE ALL CORRELATED IN HUMAN AD BRAINS**

### **Introduction**

Epidemiological evidence indicates that impaired energy metabolism in the brain may be an initiating factor in the development of sporadic Alzheimer's disease. In support of this hypothesis, we have shown that even a single i.p. injection of a metabolic inhibitor is capable of elevating BACE1 and enhancing amyloid production in the brain.

Furthermore, chronic administration of these drugs in older mice accelerated the progression of amyloid pathology in the brain, presumably through elevating levels of BACE1 and cleavage of its substrate, APP, in the brain. mRNA analysis of BACE1 and APP clearly showed that this was occurring through a post-transcriptional mechanism.

Using glucose deprivation to model energy deprivation *in vitro*, we identified phosphorylation of the translation initiation factor eIF2 $\alpha$  through activation of the UPR-inducible PERK kinase as the post-transcriptional mechanism elevating BACE1 protein levels. We further confirmed that BACE1 is a direct translational target of the eIF2 $\alpha$ -P stress-response pathway and that direct phosphorylation of eIF2 $\alpha$  in the absence of energy deprivation was amyloidogenic by pharmacological induction of eIF2 $\alpha$ -P *in vitro*. The eIF2 $\alpha$ -P stress response pathway is a highly conserved general stress response mechanism in eukaryotes, implying that BACE1 might be elevated in response to a

variety of stress stimuli. We previously observed elevated BACE1 protein levels in the brains of our aggressive amyloid mouse model (5XFAD mice) compared to non-transgenics (Zhao et al., 2007), indicating that amyloid pathology itself may be able to trigger a stress response in the brain and elevate BACE1 levels. In order to determine whether the BACE1 protein elevations in 5XFAD mice were post-transcriptional, we isolated and compared BACE1 mRNA levels from the brains of nine month-old 5XFAD mice and non-transgenic littermates. Additionally, in order to determine whether the BACE protein elevations in 5XFAD brain might be occurring through the same mechanism as energy deprivation-induced BACE1 protein elevations, we also measured eIF2 $\alpha$ -P levels *via* immunoblot in the brains of these mice. In further support of a role for BACE1 in SAD pathogenesis, several groups have shown that BACE1 protein levels are elevated in AD brains compared to non-demented, age-matched controls; however, the mechanism by which this occurs is unknown (Fukumoto et al., 2002; Holsinger et al., 2002; Li et al., 2004; Tyler et al., 2002; Yang et al., 2003; Zhao et al., 2007). In order to gather further evidence that eIF2 $\alpha$ -P is an important regulatory mechanism controlling BACE1 protein levels in the diseased brain, we analyzed a series of AD and non-demented control brains for correlations between BACE1 protein, eIF2 $\alpha$ -P levels, and amyloid load.

## Methods

### Human Brain Tissue, Amyloid Loads, and Linear Correlations

Post-mortem frontal cortex tissues were obtained from AD (n=9; 88.3 $\pm$ 4.1yrs) and normal (n=13; 88.0  $\pm$  4.8yrs) participants in the Rush Hospital Memory and Aging

Project (courtesy of David Bennett) following Rush University IRB approval. To determine amyloid load, brain sections (20  $\mu\text{m}$ ) were stained with anti-A $\beta$  total antibody (MO0872; 1:100; Dako) via DAB immunohistochemistry, and amyloid staining was imaged and quantified with a stereological mapping station (Leica DMRBE microscope; computer with StereoInvestigator software version 5.00; MicroBrightField Inc). A systematic random sampling scheme was used to capture video images of amyloid-stained sections for quantitative analysis of plaque deposition using a custom algorithm previously described (Bennett et al., 2004). The percent areas stained for each section were averaged, and those numbers used for amyloid loads in statistical analyses. BACE1 and eIF2 $\alpha$  levels in frontal cortex samples were measured by immunoblot analysis as described below and expressed as percent of the mean of the normal control group. Linear regressions and comparisons of means using the t-test were performed using GraphPad Prism and InStat software, respectively (GraphPad Software, Inc.).

### **RNA isolation and real-time PCR**

Frozen Tg6799 hemibrains were homogenized in 2.5 mL Qiazol reagent. Total RNA from 0.5mL of Tg6799 brain homogenate was isolated using Qiagen's RNeasy Lipid Mini kit according to the manufacturer's specifications. Total mRNA concentrations were measured using  $\text{ABS}_{260\text{nm}}$  ( $[\text{RNA}] \mu\text{g}/\mu\text{L} = 0.04 \times \text{ABS}_{260\text{nm}}$ ) on a Beckman spectrophotometer. In general, only mRNA samples with low protein contamination ( $\text{ABS}_{260\text{nm}}/\text{ABS}_{280\text{nm}} > 1.8$ ) were used for analysis. mRNA integrity of each sample was confirmed using an Agilent Technologies 2100 Bioanalyzer. mRNA samples were used

for analysis if the 28S ribosomal RNA peak was at least two times the area of the 18S ribosomal RNA peak. 1 µg of total RNA from each sample was used for first-strand cDNA synthesis using Invitrogen's SuperScript III according to the manufacturer's recommendations (Random hexamers were used as opposed to oligo dTs). Exact cDNA concentrations were determined using a Beckman spectrophotometer, and 112.5 ng cDNA from each sample was amplified *via* Real-Time PCR in triplicate using Applied Biosystems' Assays-on-Demand pre-mixed Taqman primer/probe set for mouse BACE1 mRNA (catalog #Mm00478664\_m1) and normalized against 18s rRNA (#4333760F) using an Applied Biosystems 7900HT sequence analyzer. The BACE1 primer/probe set spans exons 1-2 of the murine BACE1 transcript, which are present in all known splice variants of BACE1. Applied Biosystem's universal cycling parameters were used. Samples were only used for final analysis if the standard deviation between triplicate samples was < 0.1 cycles. Percent of control values were determined using the comparative CT method. For microRNA analysis, RNA samples were analyzed using the Taqman microRNA reverse transcription kit with Taqman Universal PCR master mix (Applied Biosystems). Quantitative RT-PCR procedures were performed as previously described (Hebert et al., 2008) following the manufacturer's recommendations (Applied Biosystems). Relative expression was calculated using the comparative CT method.

### **Immunoblotting**

10 µg protein was boiled for 5 min in sample boiling buffer (60 mM Tris, 10% glycerol, 5% SDS, pH 6.8, 10% β-mercaptoethanol +loading dye) prior to being separated on 4-12% NuPAGE Bis-Tris gels in 1x MOPS running buffer (Invitrogen) and transferred to



Millipore Immobilon-P polyvinylidene difluoride (PVDF) membrane. Blots were blocked overnight in 5% bovine serum albumin (BSA) in Tris-buffered saline, Tween 20 0.1% (TBST; Sigma, T9039; modified form), pH 8.0. Blots were blocked overnight in 5% BSA in TBST. Blots were then cut into strips and incubated overnight in anti-3D5 (BACE1) 1:2000 in 5% milk or 1:1000 eIF2 $\alpha$ -P(Ser51) in 5% BSA (Cell Signaling rabbit monoclonal). Blots were then washed in TBST and incubated for 1 hr in horseradish peroxidase-conjugated goat anti-mouse or goat anti-rabbit secondary antibody diluted 1:10,000 in 5% milk (Jackson Immunological Research). Immunosignals were detected using enhanced chemiluminescence (SuperSignal West Femto, Pierce) and quantified using a Kodak CF440 imager. eIF2 $\alpha$ -P blots were stripped for 5 min in Pierce Restore stripping buffer, washed with distilled water, and re-probed for total eIF2 $\alpha$  overnight (1:1000 in 5% BSA) or  $\beta$ -actin for 1 hr (1:15,000 in 5% milk).

### **Statistical analysis**

Sample averages were determined and then means and standard error of the means (SEMs; represented by error bars in histograms) were calculated based on the sample averages (n-values are stated in figure legends). Statistical differences between experimental groups and their respective controls were determined using a two-tailed t-test. Data are presented as the mean  $\pm$  SEM. \* $p < 0.05$ , \*\* $p < 0.01$ , \*\*\* $p < 0.001$ .

## Results

### **Increased eIF2 $\alpha$ phosphorylation correlates with elevated BACE1 levels in 5XFAD transgenic mouse brains**

Recent reports have shown that BACE1 levels and activity are increased in AD brains compared to non-demented controls (Fukumoto et al., 2002; Holsinger et al., 2002; Li et al., 2004; Sennvik et al., 2004; Tyler et al., 2002; Yang et al., 2003). Consistent with this observation, we have demonstrated that BACE1 levels are elevated around amyloid plaques in AD patients, Tg2576 mice, and in our aggressive amyloid deposition model, 5XFAD transgenic mice (Zhao et al., 2007). 5XFAD (Tg6799) animals co-express human APP containing the Swedish (K670N, M671L), Florida (I716V), and London (V717I) FAD mutations and human PS1 containing the M146L and L286V FAD mutations under the control of the Thy1 promoter (Fig 2.1). These mice develop extensive amyloid plaque pathology in the brain by 2 months of age, which progressively worsens over time (Fig 6.1) (Oakley et al., 2006). Quantitatively, total levels of BACE1 protein are progressively elevated with age in 5XFAD mice *via* immunoblot compared to their non-transgenic littermates (~170-200%,  $p < 0.001$ ; Fig 6.2A,B; Zhao et al., 2007). The BACE1 protein elevation in transgenic mice compared to non-transgenic appears to be A $\beta$ -induced, implying the existence of a positive feedback loop elevating BACE1 protein levels during the development of amyloid pathology. In order to determine whether energy deprivation-induced and A $\beta$ -induced BACE1 protein elevations occurred through a similar mechanism, we analyzed BACE1 mRNA from 9 month-old 5XFAD and non-transgenic mice to determine whether the BACE1 protein elevation in 5XFAD mice occurred post-transcriptionally. mRNA

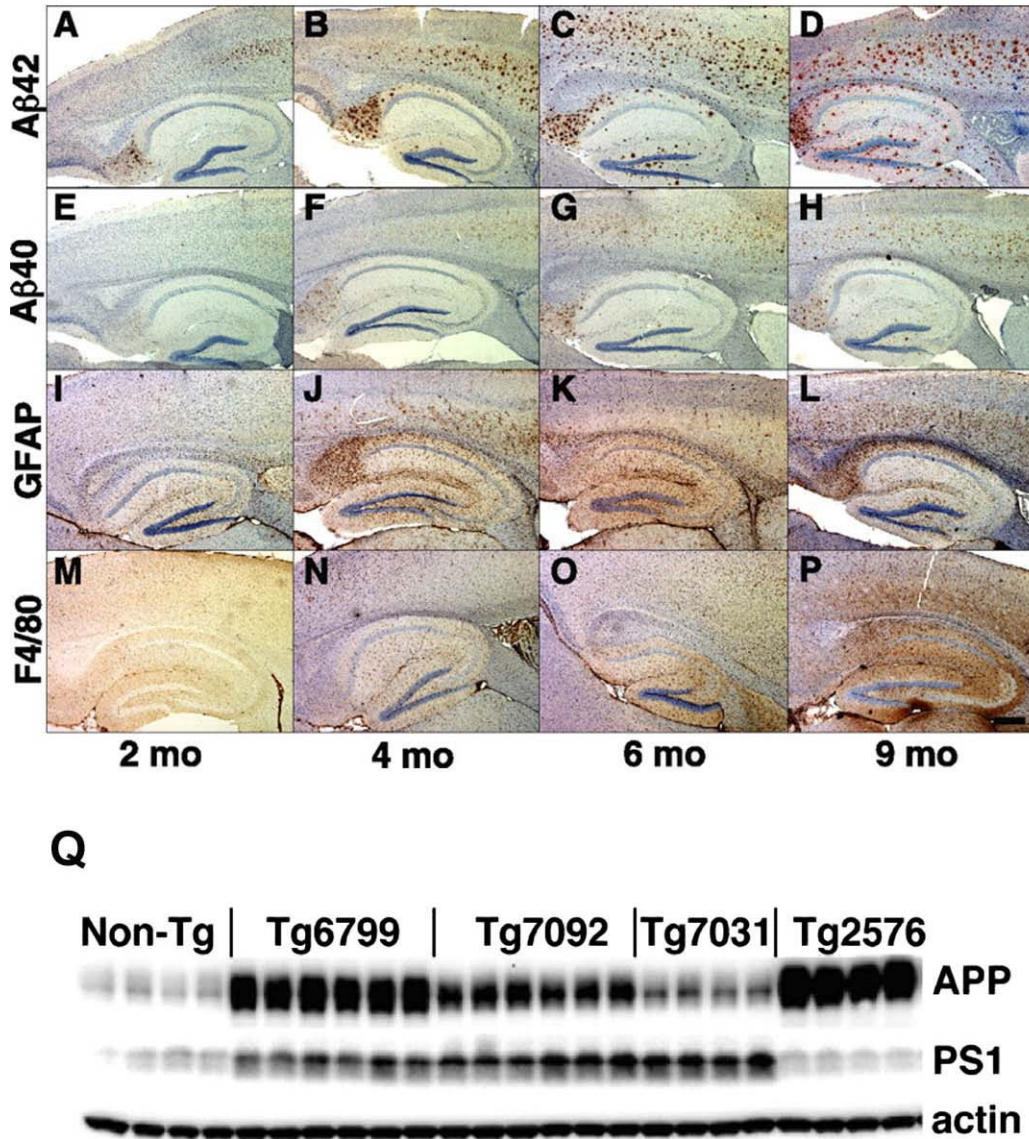


**Figure 6.1: The 5XFAD (Tg6799) mouse model of rapid amyloid pathology** (from Oakley et al., 2006). (A-P) Aβ42, Aβ40, GFAP (astroglial marker), and F4/80 (microglial marker) immunostaining in the hippocampus of 2, 4, 6, and 9-month old Tg6799 brains. (Q) Immunoblot comparing APP and PS1 protein levels in non-Tg mice, Tg6799 mice (which co-express human APP and PS1 under the control of the Thy1 promoter), and Tg2576 mice (which express only human APP under the control of the Prp promoter), and other APP/PS1-expressing lines.

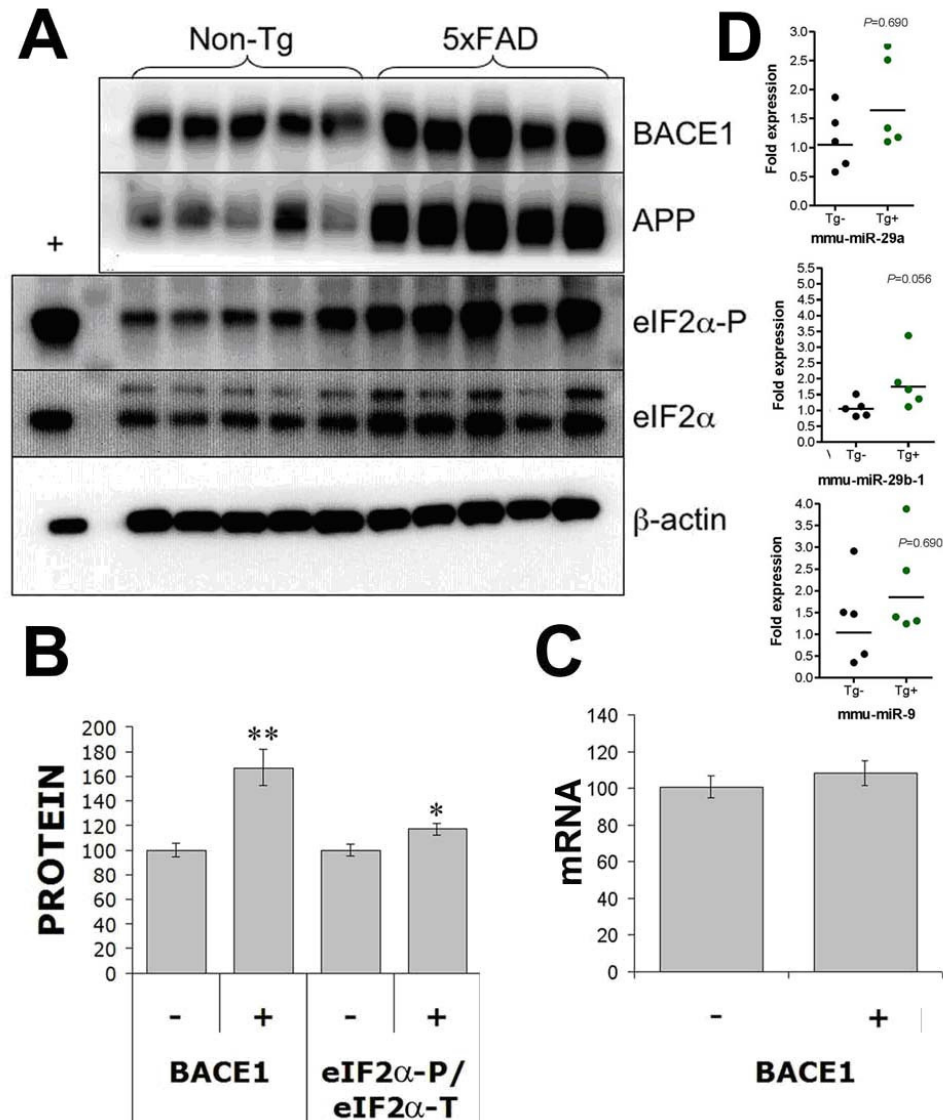


**Figure 6.2: Post-transcriptional elevations of BACE1 protein level in 5XFAD brain are correlated with eIF2α-P.** (A) 10 μg protein from 6-month old 5XFAD transgenic or non-transgenic littermates (Non-Tg) brain was used for immunoblot analysis of BACE1, full-length APP (FLAPP), eIF2α-P, eIF2α-T, and β-actin. "+" lane: 10μg of lysate from UV-treated 293 cells was used as a positive control for eIF2α-P. (B) BACE1 and eIF2α-T immunosignals were normalized to β-actin, eIF2α-P was normalized to eIF2α-T, and values were expressed as % Non-Tg. "-": non-transgenic littermates; "+": 5XFAD transgenic mice. BACE1 levels and eIF2α-P/eIF2α-T ratios were significantly elevated in 5XFAD mice compared to Non-Tg (n=5 mice/group; \*, p<0.05; \*\*, p<0.01; mean ± SEM). Total mRNA from nine month-old 5XFAD transgenic of non-transgenic littermate brain was used for Real Time PCR analysis of BACE1 mRNA (C) or microRNA analysis for miR-29a, miR-29b-1, or miR-9 (courtesy of Sebastien Hebert) (D). There was no significant difference between the two groups.

analysis revealed that BACE1 transcript levels were not significantly different between 5XFAD mice and non-transgenic controls, indicating that the BACE1 protein elevation in the brains of these mice indeed occurred through a post-transcriptional mechanism (Fig 6.2C). There was no significant difference in miR-29a, miR-29b-1, or miR-9 expression in the brains of 9 month-old 5XFAD compared to non-transgenic littermates (Fig 6.2D). In fact, similar to Tg2576 mice exposed to chronic energy deprivation, 5XFAD mice showed a trend toward elevated expression of miR-29a, miR-29b-1, and miR-9, which is the opposite expected trend if microRNAs were responsible for elevated BACE1 protein levels in 5XFAD mice. Therefore, it is unlikely that altered expression of microRNAs is involved in the observed BACE1 increase. In order to gather evidence that the A $\beta$ -induced BACE1 protein elevation could be occurring through stress-induced elevations in eIF2 $\alpha$ -P, we analyzed levels of eIF2 $\alpha$ -P and eIF2 $\alpha$ -T by immunoblot in the brains of six-month-old 5XFAD mice. Consistent with the idea that A $\beta$ -induced BACE1 protein elevation was occurring through the same mechanism as energy deprivation-induced BACE1 protein elevations, levels of eIF2 $\alpha$ -P(Ser51):eIF2 $\alpha$ -T were elevated in 5XFAD brains compared to non-transgenic littermates (~120%;  $p < 0.05$ ; Fig. 6.2A,B).

### **BACE1 protein, amyloid load, and eIF2 $\alpha$ -P levels are all correlated in human AD brains**

We have shown that BACE1 protein levels are elevated post-transcriptionally in APP transgenic mice compared to non-transgenics, and we have shown evidence that this may occur *via* stress-induced eIF2 $\alpha$ -P elevation. Recent reports have shown that

BACE1 levels and activity are increased in AD brains compared to non-demented controls (Fukumoto et al., 2002; Holsinger et al., 2002; Li et al., 2004; Sennvik et al., 2004; Tyler et al., 2002; Yang et al., 2003); however the mechanism by which this occurs is unknown. Interestingly, most of these studies do not report a corresponding increase in BACE1 mRNA levels, indicating that the BACE1 elevations in human AD brains may also occur post-transcriptionally. In order to gather evidence that stress-induced eIF2 $\alpha$ -P was involved in BACE1 protein elevations and the progression of amyloid pathology in sporadic Alzheimer's disease, we analyzed a set of cortical brain samples from AD patients and non-demented, age-matched controls from the Rush Hospital Memory and Aging Project in Chicago, IL. We reasoned that if the mechanism through which BACE1 protein is elevated in AD brain really is enhanced translation of BACE1 as a result of stress-induced increases in eIF2 $\alpha$  phosphorylation, eIF2 $\alpha$ -P levels should be elevated in AD brains, and eIF2 $\alpha$ -P levels should be directly correlated with BACE1 protein levels. Furthermore, if eIF2 $\alpha$  phosphorylation is important for the development of amyloid pathology in the human brain, eIF2 $\alpha$ -P levels should also be directly correlated with the degree of amyloid pathology. In order to test these hypotheses, we compared levels of BACE1, eIF2 $\alpha$ -P, and eIF2 $\alpha$ -T in patients with Alzheimer's disease (AD) and age-matched, non-demented (ND) controls. Similar to previous reports, we observed significantly elevated BACE1 levels in AD brains by immunoblot (~140% of ND control;  $p < 0.01$ ; Fig 6.3A,B). As predicted, AD brains also exhibited increased eIF2 $\alpha$ -P(Ser51) levels (Fig. 6.3A,B), and the AD eIF2 $\alpha$ -P(Ser51):eIF2 $\alpha$ -T ratio was found to be ~150% of ND control ( $p < 0.05$ ). We next performed linear regression analyses and determined that BACE1 levels and amyloid

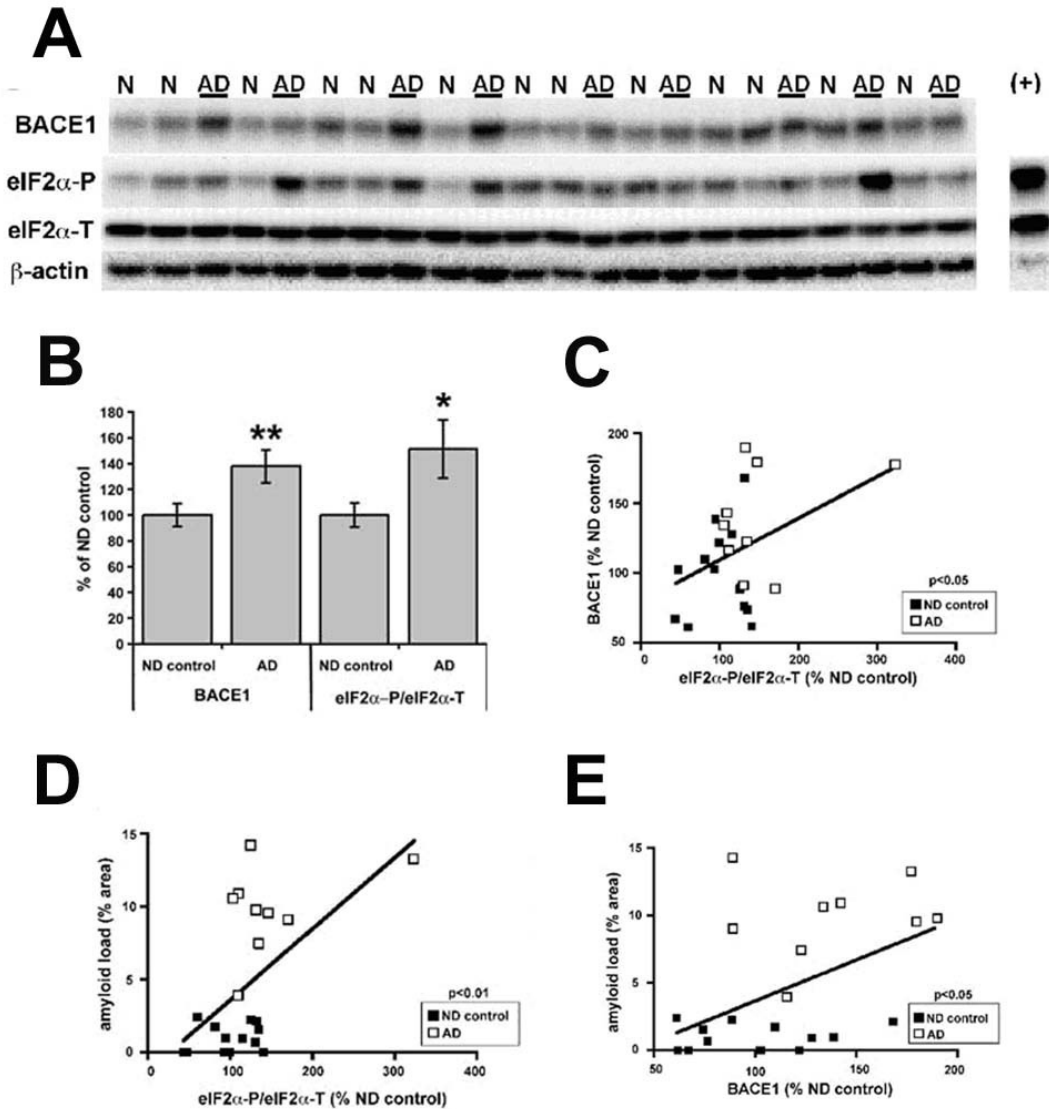


**Figure 6.3: Phosphorylated eIF2 $\alpha$ , BACE1 protein, and amyloid load are all correlated in human AD brain.** (courtesy of Katherine Doherty) **(A)** 15  $\mu$ g human frontal cortex samples from AD patients (AD) and age-matched non-demented controls (N) were analyzed by immunoblot for BACE1, eIF2 $\alpha$ -P, eIF2 $\alpha$ -T, and  $\beta$ -actin. 10 $\mu$ g of lysate from UV-treated 293 cells was used as a positive control for eIF2 $\alpha$ -P (+). **(B)** BACE1 immunosignals were normalized to  $\beta$ -actin, eIF2 $\alpha$ -P was normalized to eIF2 $\alpha$ -T, and values were expressed as % ND. Both BACE1 level and eIF2 $\alpha$ -P/eIF2 $\alpha$ -T ratio were significantly elevated in AD brains compared to ND (n=9 AD, 13 ND; \*, p<0.05; \*\*, p<0.01; mean  $\pm$  SEM). **(C-E)** BACE1 levels, eIF2 $\alpha$ -P/eIF2 $\alpha$ -T ratios, and amyloid loads were correlated by linear regression analyses. **(C)** BACE1 protein vs. eIF2 $\alpha$ -P/eIF2 $\alpha$ -T ratio (p < 0.05) **(D)** amyloid load vs. eIF2 $\alpha$ -P/eIF2 $\alpha$ -T ratio (p < 0.01) **(E)** amyloid load vs. BACE1 protein (p < 0.05)

load in human brain correlated positively, as expected ( $p < 0.05$ ; Fig 6.3E).

Importantly, AD and ND BACE1 levels plotted against eIF2 $\alpha$ -P(Ser51):eIF2 $\alpha$ -T ratios showed a significant positive correlation ( $p = 0.0135$ ; Fig 6.3C), suggesting that eIF2 $\alpha$ -P may cause the BACE1 elevation in AD brain. Moreover, amyloid load also exhibited significant positive correlation with eIF2 $\alpha$ -P:eIF2 $\alpha$ -T ratio ( $p < 0.01$ ; Fig 6.3D), suggesting that eIF2 $\alpha$ -P may promote amyloidosis in AD. Taken as a whole, our 5XFAD and AD results strongly suggest that increased eIF2 $\alpha$  phosphorylation plays a role in the elevation of BACE1 levels in AD brain and contributes to the development of amyloid pathology in sporadic Alzheimer's disease.

## Discussion

### The relationship between energy deprivation, stress, and A $\beta$ production

We have shown that BACE1 protein levels are elevated post-transcriptionally in the brains of 5XFAD mice compared to non-transgenics. Elevated BACE1 protein levels corresponded with elevated eIF2 $\alpha$ -P, indicating that eIF2 $\alpha$ -P-mediated translational up-regulation of BACE1 may be responsible for elevated BACE1 protein levels in APP transgenic mice, as was the case in response to glucose deprivation *in vitro*.

Importantly, this occurred in the absence of energy deprivation treatments, demonstrating that BACE1 may be translationally regulated by stress stimuli other than energy deprivation. Interestingly, the specific stress stimulus in APP transgenic brain appears to be A $\beta$  overproduction itself. This appears to be related to the amount of A $\beta$  being produced, rather than being a mere result of APP overexpression, because



5XFAD mice exhibited much more robust BACE1 protein elevations in the brain than Tg2576, despite lower human APP expression (Oakley et al., 2006; Zhao et al., 2007). In support of this hypothesis, we have shown that BACE1 protein levels are also elevated in human AD brains, which do not overexpress APP. Furthermore, exogenous application of recombinant A $\beta$  to wild-type cultured mouse neurons can also elevate endogenous BACE1 and eIF2 $\alpha$ -P levels (K.R. Doherty, unpublished results). Given the highly conserved role of eIF2 $\alpha$ -P in the general cellular stress response, the fact that eIF2 $\alpha$ -P levels appear to be elevated in the brain in response to diverse stress stimuli is not surprising. With regard to how A $\beta$ , in particular, might induce stress and activate eIF2 $\alpha$ -P, A $\beta$  is known to be a hydrophobic protein, highly prone to misfolding, aggregation, and accumulation. Therefore, even a slight overabundance of A $\beta$  within the neuron may readily attract molecular ER chaperones such as BiP, preventing their association with resident kinases, such as PERK, thereby initiating the UPR. Indeed, activation of the UPR has been reported both in Alzheimer's disease and in response to A $\beta$  treatment (Chafekar et al., 2007; Unterberger et al., 2006). The propensity of A $\beta$  to activate the UPR may, in part, explain the observation that soluble, oligomeric forms of A $\beta$  appear to be more toxic to cells than the fibrillar form of A $\beta$ , which is the predominant form of A $\beta$  found in amyloid plaques. Oligomeric A $\beta$  may reside within the neuron, where it can readily activate the UPR, whereas fibrillar A $\beta$  is presumably formed extracellularly. With regard to cell culture experiments, where both forms of A $\beta$  are being added exogenously, the greater toxicity of oligomeric than fibrillar A $\beta$  may be explained by the ability of oligomeric A $\beta$  to enter the cell and activate the UPR, as

opposed to fibrillar A $\beta$ , which presumably cannot enter the cell, and can only activate stress pathways via cell surface receptors. However, A $\beta$  may also initiate ER stress exogenously by dysregulating calcium signaling. The potential role of A $\beta$  in intrinsic cellular stress response pathways has been largely unaddressed, since the majority of A $\beta$  produced normally in the cell, is eliminated through the secretory pathway.

Therefore, it has traditionally been assumed that A $\beta$  exerts its toxic functions extracellularly. However, the importance of intraneuronal A $\beta$  in AD pathology is gaining attention in the field, particularly in the early stages of the disease (Gouras et al., 2005). Our results with energy inhibitors in mice and glucose deprivation *in vitro* imply that eIF2 $\alpha$ -P activation and the UPR are early, initiating events in AD pathogenesis related to cardiovascular risk factors, and other events that cause chronic hypoperfusion to the brain throughout the lifespan. However, the observation that A $\beta$  overproduction itself can activate eIF2 $\alpha$ -P and elevate BACE1 calls into question whether the effects eIF2 $\alpha$ -P activation on AD pathology are limited exclusively to the initial stages of the disease. On the contrary, the results obtained from 5XFAD mice imply that the relationship between eIF2 $\alpha$ -P and the development of amyloid pathology is much more complex than our energy inhibitor experiments had originally suggested. eIF2 $\alpha$ -P activation may, in fact, serve as both the trigger of sporadic AD amyloid pathology, and may also further exacerbate the disease once A $\beta$  has accumulated to the point that it is capable of initiating a stress response in the brain. Although our energy deprivation experiments and studies of eIF2 $\alpha$ -P in transgenic models had many interesting parallels, the two experiments differed in some respects. First of all, BACE1 mRNA was dramatically

down-regulated in response to chronic energy deprivation in the brain, whereas BACE1 mRNA levels were unchanged in 5XFAD mice compared to non-transgenics. This may be a method of conserving energy by down-regulating transcription, in the case of chronic energy deprivation--- a mechanism that appears to be absent in the case of A $\beta$ -induced BACE1 elevations. The phenomenon of decreased mRNA production in response to chronic energy deprivation does not appear to be specific to BACE1, since APP mRNA levels were also decreased. The presence of increased BACE1 protein levels and unchanged BACE1 mRNA levels in the brains of 5XFAD mice suggests that elevated BACE1 protein does not negatively regulate its own mRNA production. Another curious finding of the 5XFAD experiment, is that total eIF2 $\alpha$  levels are also elevated in transgenic mice compared to non-transgenic. This was not due to unequal protein loading, since the  $\beta$ -actin signal was unaffected. Neither was the apparent increase in total eIF2 $\alpha$  the result of inefficient stripping of eIF2 $\alpha$ -P, since probing with total eIF2 $\alpha$  antibody alone yielded the same result. The functional significance of increased total eIF2 $\alpha$  in 5XFAD mice remains unclear; however, we speculate that it may represent an adaptive mechanism to chronic stress caused by the aggressive amyloid deposition in 5XFAD brain. This phenomenon appears to be specific to the 5XFAD mice, since we did not observe an increase in total eIF2 $\alpha$  protein in AD brains compared to non-demented controls, nor in response to chronic energy deprivation in Tg2576 mice.

### **Limitations of transgenic models and human brains**

An important unanswered question that our 5XFAD experiments did not address, is what stage in amyloid pathogenesis eIF2 $\alpha$ -P becomes activated in the absence of upstream exacerbating factors, such as energy deprivation. Preliminary data indicates the eIF2 $\alpha$ P elevations (occurring as early as 2 months of age) actually precede BACE1 protein elevations in 5XFAD brains, which is expected if eIF2 $\alpha$ -P is causing the BACE1 increase (K.R. Doherty, unpublished results). The presence of elevated eIF2 $\alpha$ -P and BACE1 protein levels at an early age in 5XFAD mice suggests the eIF2 $\alpha$ -P elevation may precede amyloid pathology, and progress with age; however, the 5XFAD model is a rapid amyloid model and already exhibits extensive amyloid plaque pathology in the brain by 2 months of age. It would be interesting to analyze eIF2 $\alpha$ -P levels in an animal model that develops amyloid pathology at a slower rate, such as Tg2576 mice, in order to definitively determine whether eIF2 $\alpha$ -P elevations precede plaque deposition. The importance of soluble forms of A $\beta$  in the development of AD-like pathology in these mice has already been shown by demonstrating that memory deficits in this mouse line precede significant amyloid plaque deposition (Hsiao et al., 1996). It would also be interesting to see if eIF2 $\alpha$ -P levels are temporally related to the onset of memory deficits in Tg2576 mice. Furthermore, our experiments clearly show that A $\beta$  overproduction and/or amyloid pathology can activate eIF2 $\alpha$ -P, most likely through the UPR; however, amyloid pathology is not the only pathological event that causes stress in the brain during Alzheimer's disease, and eIF2 $\alpha$ -P is activated in response to a wide variety of stress stimuli. For instance, it would be interesting to see whether eIF2 $\alpha$ -P is activated

to a greater extent in AD model mice that develop both plaque and tangle pathology.

This result would imply that eIF2 $\alpha$ -P is exacerbated by multiple types of dysregulation occurring during the development of SAD pathology.

### **eIF2 $\alpha$ and Human Amyloid Pathology**

One of the major limitations of using human AD brain tissue is that the tissue is collected post-mortem, therefore tissue samples disproportionately represent the end stage of the disease where neuronal death is extensive, and at which point numerous different pathways are dysregulated, many of which are really downstream effects of severe neuronal distress and are not really unique to Alzheimer's disease pathology.

Therefore we can conclude from the significant correlation of BACE1, eIF2 $\alpha$ -P, and amyloid levels in human brains that eIF2 $\alpha$ -P activation may be involved in the disease process, but we are unable to determine whether eIF2 $\alpha$ -P is an early, initiating factor in the human disease process. Other human studies that would be useful in verifying a role for eIF2 $\alpha$ -P in early amyloid pathology would be an analysis of eIF2 $\alpha$ -P levels in MCI brains or young ApoE4 carriers. Furthermore, to validate the hypothesis that cardiovascular risk factors may trigger this process early on, it would be interesting to measure eIF2 $\alpha$ -P and BACE1 levels in younger, non-demented individuals known to have high cholesterol, atherosclerosis, or diabetes. However, brain samples from younger individuals with detailed medical information are often difficult to obtain. Nevertheless, our analysis of AD versus non-demented control brains clearly shows that the eIF2 $\alpha$ -P mechanism identified in cells and mice may indeed be relevant to human

AD pathology. The potential relationship of the eIF2 $\alpha$ -P stress response pathway and human amyloid pathology is an interesting and complex one. Our results clearly show that energy deprivation is not the only factor capable of elevating eIF2 $\alpha$ -P levels in the brain. The role of eIF2 $\alpha$ -P as a ubiquitous stress response protein and its clear molecular relationship to A $\beta$  production implies that anything that is capable of initiating a stress response in the brain is potentially amyloidogenic. This may, in part, explain why sporadic Alzheimer's disease is so pervasive. It can also explain why AD is closely associated with aging, since maintenance and repair mechanisms in the neuron are likely to become increasingly compromised with age, a situation which can undoubtedly elevate general stress levels in the brain. Furthermore, the "stress-amyloid" theory can also explain why amyloid pathology is often associated with other neurodegenerative disorders, since these diseases also induce stress and hence amyloidogenesis in the brain.

## **CHAPTER 7**

### **DISCUSSION**

#### **Translational Control of Proteins**

##### **Translational control in development, growth, and oncogenesis**

Although the components of the eukaryotic translation initiation complex were initially identified over 25 years ago, the complexities of translation initiation are far from being completely understood. Specific regulation of translation initiation had already been elegantly demonstrated in mammalian and yeast systems as early as the 1970's; however, this type of regulation was assumed only to occur in rare circumstances or in special cell types. Protein synthesis was generally considered to be a ubiquitous process in most cells, with the vast majority of protein expression being modulated through changes in gene expression due to signaling cascades in the cell (Thornton et al., 2003). Subsequent research has shown this to be far from the reality. Ubiquitous protein synthesis would imply a linear relationship between mRNA and protein levels in the cell, which turns out not to be the case. The non-linear relationship between mRNA levels and protein levels was initially recognized by cancer biologists who noted that less than one-fourth of the genes analyzed in tumor samples correlated with their respective protein levels, implying an additional, post-transcriptional level of protein regulation (Chen et al., 2002; Tew et al., 1996). Consistent with a role for protein translation in oncogenesis, it was discovered that overexpression of the mRNA cap-binding protein, eukaryotic translation initiation factor 4E (eIF4E) could transform

immortalized cell lines (Lazaris-Karatzas et al., 1990). This was the first indication that translational control was not simply limited to special circumstances and could influence global cellular processes such as growth, differentiation, and survival.

Subsequent research has since definitively established that modulating translation is a major point of regulation for nearly all cellular processes. Although translation can be regulated during all phases by a variety of mechanisms, the primary point of translational control occurs at the level of translation initiation. The two major components of the translation initiation complex that have emerged as important regulators of protein expression are the eukaryotic translation initiation factor 4E (eIF4E) and the eukaryotic translation initiation factor 2 (eIF2) (Holcik and Sonenberg, 2005).

### **Regulating cap-dependent translation: eukaryotic translation initiation factor 4E (eIF4E)**

eIF4E is the 5' mRNA cap-binding component of the translation initiation complex. Binding of eIF4E to the 5' mRNA cap is the first step in translation initiation. It is the least abundant translation initiation factor in the cell and is therefore rate-limiting and a prime target for regulation. The availability of eIF4E is a major regulator of protein translation rates, and therefore the growth status of the cell. The availability of eIF4E for translation initiation is controlled by two main mechanisms: the degree of association with the eIF4E binding protein (4E-BP) and the level of phosphorylation at Ser209 (Clemens, 2001b). 4E-BP was initially identified as a phosphorylation target of the insulin signaling pathway, further establishing a role for translation initiation during cellular growth (Hu et al., 1994; Lawrence et al., 1997). During periods of active growth,



4E-BP, which has three isoforms, 4E-BP1, 2, and 3 which are expressed at different levels in various tissues, are maintained in a hyperphosphorylated state by mammalian target of rapamycin (mTOR), a major regulator of translational rates in response to the PI3K/Akt pathway (Brunn et al., 1997). Interestingly, mTOR also regulates the p70 ribosomal subunit 6 kinase (S6K), which has synergistic effects on translation in response to growth stimuli (von Manteuffel et al., 1997). The phosphorylation state of 4E-BP determines its affinity for eIF4E. Dephosphorylated 4E-BP binds eIF4E with high affinity, slowing the rate of cap-dependent translation initiation during periods of low cell growth. Consistent with this role, 4E-BP is highly phosphorylated during periods of active cell growth. Conversely, 4E-BP is dephosphorylated during the onset of apoptosis (Clemens, 2004). eIF4E is also regulated directly by phosphorylation at Ser209 by the MAP kinase interacting (Mnk) kinases (Flynn and Proud, 1995; Fukunaga and Hunter, 1997; Joshi et al., 1995; Waskiewicz et al., 1997). Phosphorylation of eIF4E by the Mnks appears to promote the association of eIF4E with eIF4G (a scaffolding protein) and eIF4A (an RNA helicase) to form the complete mRNA cap-binding complex (eIF4F), which is expected to enhance cap-dependent translation (Gingras et al., 1999). Consistent with this idea, eIF4E phosphorylation, similar to 4E-BP phosphorylation, also occurs in response to cellular growth stimuli, since the Mnk kinases are targets of the ERK pathway (Fukunaga and Hunter, 1997; Waskiewicz et al., 1997). Extensive investigation into the regulatory mechanisms controlling 4E-BP and eIF4E in the past decades have clearly demonstrated that protein translation is not a purely ubiquitous process, and general, cap-dependent translation can be directly modulated by signaling cascades in the absence of gene transcription.

## Translational control in response to stress

Signal transduction-mediated modifications to translation initiation factors are capable of enhancing cap-dependent translation during periods of cell growth and proliferation in the absence of gene expression. Conversely, this mechanism allows cells to down-regulate cap-dependent translation during quiescent phases in the cell cycle. However, repressed translation does not appear to be merely a default pathway in the absence of growth stimuli. Cells also appear to contain innate mechanisms of down-regulating general translation in response to specific stress stimuli. For example, mTOR inhibition and hence 4E-BP dephosphorylation can also be induced in response to DNA damage *via* activation of cellular Abelson murine leukemia virus transforming protein (c-Abl) (Kumar et al., 2000) (Fig 3.5). Furthermore, phosphorylation of eIF4E at Ser209 by the Mnk kinases is also known to be induced by the p38 pathway in response to certain types of stresses (Morley, 1997; Wang et al., 1998) (Fig 3.5). Why eIF4E is phosphorylated in response to both growth and stress stimuli and whether eIF4E phosphorylation actually enhances or inhibits general cap-dependent translation *in vivo* is still a matter of debate (Scheper and Proud, 2002). Interestingly, our data using a Mnk inhibitor in BACE1-293 cells supports a role for phospho-eIF4E in down-regulating cap-dependent translation, since Mnk inhibitor treatment increased BACE1 protein levels. Furthermore, Mnk inhibitor-induced and glucose deprivation-induced BACE1 protein elevations were additive, indicating a general increase in cap-dependent translation (due to Mnk inactivation), plus a specific increase in BACE1 protein due to low ternary complex availability (Fig 3.6 C & D). General down-regulation of cellular translation during the onset of stress appears to be, in part, an energy conservation

method. Translation of proteins requires nearly 50% of the cell's energy stores, and the process of properly folding newly made proteins requires even more energy. Therefore, inhibition of general translation allows the cell to divert its energy stores to the more urgent need of responding to and surviving stress conditions. However, general down-regulation of translation in response to stress stimuli is only part of the function of stress-induced translational control. For example, 3-5% of cellular mRNAs escape translational repression during stress and are translated by a cap-independent mechanism. Furthermore, there are other proteins that are translated cap-dependently, but are specifically translated at higher rates when the availability of the ternary complex is low. These transcripts are largely stress response proteins and transcription factors that activate the expression of stress response genes. The advantage of initiating a cellular stress response at the level of translation rather than transcription appears to be a kinetic one. The ability of the cell to activate a stress response at the level of mRNAs that have already been transcribed allows the cell to respond to stress stimuli rapidly. The major mechanism by which stress stimuli modulate levels of active ternary complex is through post-translational modifications of the eukaryotic translation initiation factor 2 (eIF2) (Holcik and Sonenberg, 2005).

## **The Eukaryotic Translation Initiation Factor 2 (eIF2)**

### **Role of eIF2 in translation initiation**

The eukaryotic translation initiation factor 2 (eIF2) is a component of the ternary complex, the formation of which is required for the 40S ribosomal subunit to begin scanning the 5'untranslated region (5'UTR) of mRNA transcripts during the first step of

translation initiation. eIF2 contains 3 subunits:  $\alpha$ ,  $\beta$ , and  $\gamma$ . The  $\gamma$  subunit of eIF2 has GTPase activity. The exchange of GDP for GTP on eIF2 $\gamma$  is catalyzed by the guanine nucleotide exchange factor (GEF) eukaryotic translation initiation factor 2B (eIF2B). The ternary complex consists of eIF2 bound to GTP and an initiator tRNA bound to the amino acid methionine (Met-tRNA). Only GTP-bound or “charged” eIF2-Met-tRNA is competent to bind the 40S ribosomal subunit and form the pre-initiation complex. The pre-initiation complex then binds to the eIF4F cap recognition complex at the 5' end of an mRNA and proceeds to scan the 5'UTR in search of an AUG initiation codon. The ribosome will generally initiate at the first AUG codon encountered, if it lies in an optimal sequence context for translation initiation. Recognition of the AUG sequence causes the hydrolysis of GTP and the dissociation of eIF2 from the pre-initiation complex. The large ribosomal subunit can then bind the complex and initiate the elongation phase of translation (Pavitt, 2005).

### **Selective regulation of eIF2**

Since eIF2 is required for ternary complex formation, the availability of eIF2 is limiting in the process of translation initiation. Low concentrations of eIF2 can reduce global translation. Similarly, the rate of exchange of GDP  $\rightarrow$  GTP on eIF2 $\gamma$  is also limiting, since only “charged” eIF2-Met-tRNAs can bind the 40S ribosomal unit. Therefore, factors that slow the exchange rate of GDP  $\rightarrow$  GTP on eIF2 $\gamma$  can reduce global translation, such as low availability of the eIF2 $\gamma$  GEF, eIF2B. eIF2B activity can be regulated *via* direct phosphorylation by casein kinases 1 and 2, dual-specificity tyrosine phosphorylated and regulated kinase (DYRK), and glycogen synthase kinase 3 (GSK3)

(Wang et al., 2001; Woods et al., 2001). Phosphorylation of eIF2B on its  $\epsilon$  subunit diminishes its GEF activity and slows the rate of global translation (Fig 3.5). For example, insulin signaling inhibits GSK3 activity, leading to hypophosphorylated, more active eIF2B and enhanced global translation. Alternatively, the rate of ternary complex formation can be regulated by phosphorylation of eIF2 on its  $\alpha$  subunit at Ser51 (eIF2 $\alpha$ -P). eIF2 $\alpha$  phosphorylation inhibits the dissociation of eIF2 from eIF2B, thereby slowing the exchange rate of GDP for GTP. Therefore, eIF2 $\alpha$  phosphorylation mimics reduced eIF2B activity and low eIF2 availability (Pavitt, 2005). There are four known kinases that phosphorylate eIF2 $\alpha$  in response to a variety of stress stimuli: heme-regulated inhibitor of translation (HRI) kinase, protein kinase RNA-activated (PKR), general control non-derepression 2 (GCN2) kinase, and PKR-like endoplasmic reticulum kinase (PERK) (Fig 3.8).

### ***heme-regulated inhibitor of translation (HRI) kinase***

Heme-regulated inhibitor of translation (HRI) kinase was the first of the eIF2 $\alpha$  kinases to be identified. It was known that heme deficiency inhibited protein synthesis in reticulocytes due to the activity of an unidentified inhibitor, which was termed heme-regulated inhibitor (HRI) (Grayzel et al., 1966; Maxwell and Rabinovitz, 1969; Waxman et al., 1966; Waxman and Rabinovitz, 1965; Zucker and Schulman, 1968). The inhibitor appeared to be a kinase (Levin et al., 1975). HRI was eventually purified from reticulocyte lysates, and the  $\alpha$  subunit of eIF2 was identified as a substrate of HRI. eIF2 $\alpha$  was hypothesized to be a substrate of HRI based on the ability of increased levels of eIF2 $\alpha$  to overcome translational inhibition. This was the first report of

translation inhibition as a result of eIF2 $\alpha$  phosphorylation (Levin et al., 1976). HRI was later cloned and identified as a serine/threonine kinase with significant homology to both PKR and GCN2, which had already been identified at this point. Based on this sequence homology, it was hypothesized that the yeast GCN2 was also an eIF2 $\alpha$  kinase (Chen et al., 1991). The primary function of HRI appears to be in balancing heme and globin levels in erythrocytes, in order to avoid the potentially toxic effects of unincorporated globin. Binding of heme to HRI prevents its activation. In the absence of heme, HRI dimerizes, autophosphorylates, and phosphorylates eIF2 $\alpha$ , leading to rapid down-regulation of global protein synthesis (Chen, 2007). HRI-deficient mice appear to have no physiological abnormalities, but are hyper-sensitive to iron deficiency and have decreased ability to cope with anemia (Han et al., 2005; Han et al., 2001). HRI also appears to be activated in response to oxidative stress, heat shock, and osmotic stress in erythroid cells, indicating that HRI's stress response activity is not limited to heme deficiency (Lu et al., 2001). However, HRI is primarily expressed in erythroid cells, and a role for HRI has not been demonstrated in cell types other than erythrocytes.

### ***protein kinase RNA-activated (PKR)***

PKR is a cytoplasmic mammalian eIF2 $\alpha$  kinase closely associated with ribosomes, whose activity was initially associated with enhanced sensitivity of cells to double-stranded RNA translational inhibition upon exposure to interferons (Friedman et al., 1972; Metz and Esteban, 1972). eIF2 $\alpha$  was identified as substrate of this kinase (Roberts et al., 1976). PKR was finally cloned and shown to operate *via* dimerization

and autophosphorylation upon binding of double-stranded RNA (Meurs et al., 1990), *via* double-stranded RNA-binding domains (DSRBs), which PKR shares in common with proteins involved in the siRNA and microRNA pathways. PKR presumably evolved as a mechanism of responding to viral infections by minimizing translation of viral mRNAs while enhancing synthesis of host proteins to fight the infection (Saunders and Barber, 2003). PKR has endogenous inhibitors including P58IPK, a tetratricopeptide protein family member, which is recruited by influenza virus to inhibit PKR and circumvent the host anti-viral response (Barber et al., 1994; Lee et al., 1994), and TAR RNA-binding protein (TRBP), a cellular RNA-binding protein, which inhibits PKR activity by blocking its dsRBD, among others (Garcia et al., 2007). Interestingly, PKR also appears to have tumor suppression activity, since inactivation of PKR in mouse fibroblasts or overexpression of PKR inhibitors leads to transformation, implicating a role for PKR in normal cell growth (Barber et al., 1994; Benkirane et al., 1997; Koromilas et al., 1992; Meurs et al., 1993). Conversely, overexpression of PKR is a potent activator of apoptosis (Barber, 2001). The ability of PKR to trigger cell death may also be a protective function against viral infection by eliminating infected cells from the population and reducing the ability of the virus to spread to nearby cells. Despite the apparent importance of PKR in cell survival pathways, PKR knockout mice are phenotypically normal (Yang et al., 1995).

### ***General control non-derepression 2 (GCN2) kinase***

The GCN2 kinase was originally identified in yeast in a screen for genetic mutants that failed to transcribe genes in the amino acid biosynthetic pathway in response to amino

acid deprivation. It was noted that in GCN2  $-/-$  cells, levels of the main transcriptional activator in amino acid biosynthesis, GCN4, were not elevated in response to amino acid deprivation. However, GCN4 mRNA levels were not affected, implicating a translational mechanism. Furthermore, deletion of the GCN4 5'UTR caused constitutive de-repression of GCN4 expression, regardless of the GCN2 genotype (Hinnebusch, 1984). The translational control of GCN4 by GCN2 was later shown to be mediated *via* the uAUGs in the GCN4 5'UTR (Mueller and Hinnebusch, 1986). GCN2 was later identified as a novel eIF2 $\alpha$  kinase, explaining its mechanistic role in the translational regulation of GCN4 (Dever et al., 1992). GCN2 was later shown to have a mammalian homologue (Berlanga et al., 1999), which appears to have retained at least some of its function in amino acid biosynthesis in mammals; however, GCN2 is not required for viability in mammals (Zhang et al., 2002b). Interestingly, GCN2 is also activated in response to UV irradiation in mammalian cells, raising the possibility that GCN2 has evolved other stress response functions besides nutrient deprivation in mammals (Deng et al., 2002).

### ***PKR-like endoplasmic reticulum kinase (PERK)***

PKR-like endoplasmic reticulum kinase (PERK) was the final eIF2 $\alpha$  kinase to be identified, although it is the most critical of the eIF2 $\alpha$  kinases for proper translational control of proteins in mammals. It was observed that the ER unfolded protein response (UPR) attenuated global translation, similar to viral infection and heme deficiency in mammalian cells, and GCN2 activation in yeast cells (Wong et al., 1993). PKR was initially implicated as the eIF2 $\alpha$  kinase involved in UPR-induced translational inhibition



(Prostko et al., 1995; Srivastava et al., 1995); however, it was noted that UPR-induced translational inhibition was still intact in PKR  $-/-$  cells, indicating that an additional eIF2 $\alpha$  kinase might exist (Harding et al., 1999). PERK (or PEK) was independently identified by two different groups around the same time in a screen of rat pancreatic  $\beta$  cells for novel serine/threonine kinases (Shi et al., 1998) and from a human EST database in a search for homologues to PKR and HRI (Harding et al., 1999). PERK is a transmembrane ER-associated protein with a cytosolic kinase domain. PERK is maintained in a monomeric conformation via the association of its luminal domain with ER chaperones, such as immunoglobulin binding protein (BiP). The accumulation of misfolded proteins in the ER recruits ER chaperones, leaving the luminal domain of PERK exposed and available for homo-dimerization and autophosphorylation. Activated PERK then phosphorylates eIF2 $\alpha$  on rough ER ribosomes in order to slow the influx of new proteins into the ER (Schroder and Kaufman, 2006). Unlike GCN2, PKR, and HRI  $-/-$  mice which are phenotypically normal, PERK  $-/-$  mice exhibit growth retardation, skeletal abnormalities, progressive deterioration of pancreatic function, including aberrant glucose regulation and loss of pancreatic  $\beta$  cells, eventually resulting in death of the animal (Harding et al., 2000; Zhang et al., 2002a). Furthermore, missense mutations in the PERK gene lead to Wolcott-Rallison syndrome, which is characterized by growth retardation, epiphyseal dysplasia, and the onset of neonatal or early infancy insulin-dependent diabetes (Delepine et al., 2000). These findings highlight the crucial role of eIF2 $\alpha$  phosphorylation in mammalian development and metabolic regulation, as well as the importance of tight translational control in secretory cell types.

**Mechanisms of evading translational repression**

Phosphorylation of eIF2 $\alpha$  by HRI, PKR, GCN2, or PERK reduces the availability of active ternary complex, effectively down-regulating the rate of global protein synthesis. Down-regulated protein synthesis facilitates cell survival by reducing the production of potentially toxic proteins (HRI), blocking the synthesis of viral proteins (PKR), limiting energy consumption during periods of low nutrient availability (GCN2), or preventing ER overload (PERK). However, a certain set of stress-response proteins are able to escape translational repression due to low ternary complex availability and are specifically up-regulated in response to eIF2 $\alpha$  phosphorylation. There are several biochemical mechanisms that have been identified through which stress-response proteins avoid translational repression.

***Upstream Open Reading Frames (uORFs)***

The most extensively characterized method of evading translation repression by eIF2 $\alpha$  phosphorylation is differential utilization of uAUG sequences in the 5'UTR of transcripts. A scanning ribosome will generally initiate translation at the first AUG it encounters, providing that the start codon resides in an optimal sequence context for initiation. If the 5'UTR of the transcript contains AUG sequences upstream of the authentic start codon (uAUGs) capable of translating an upstream open reading frame (uORF), the majority of ribosomes will attempt to initiate translation at these uAUGs, and the protein will be translated at very low levels under normal conditions. Pre-initiation complex formation and scanning of the 5'UTR begins from the 5' cap. Once the ribosome has finished translating an uORF, the 60S subunits and most of the 40S subunits dissociate and

leave the mRNA. However, a small fraction of 40S subunits do not leave the mRNA and continue to scan for additional AUG sequences at which to re-initiate. Where the 40S subunit re-initiates translation depends on the availability of the ternary complex. When ternary complex concentrations are high (normal conditions), re-initiation will occur at the next available AUG sequence (additional uAUGs). When ternary complex concentrations are low, the 40S subunit is more likely to scan through subsequent uORFs and initiate translation at the authentic start codon. eIF2 $\alpha$  phosphorylation reduces the availability of the ternary complex; therefore, global cap-dependent translation rates are reduced, but in the case of mRNAs with multiple uAUGs, re-initiation will occur at the authentic start codon at a higher frequency. This explains how eIF2 $\alpha$  phosphorylation can simultaneously down-regulate global translation while specifically up-regulating certain stress response proteins. The best characterized example of this type of regulation is the yeast mRNA, GCN4 (Mueller and Hinnebusch, 1986).

### ***Internal Ribosome Entry Sites (IRES)***

Another mechanism of evading translational repression by eIF2 $\alpha$  phosphorylation is the presence of internal ribosome entry sites (IRESs) within the 5'UTR of some mRNA transcripts. The IRES sequence recruits ribosomes and initiates translation at the IRES in a cap-independent fashion. IRES-mediated translation appears to require the recruitment and binding of cellular proteins known as IRES trans-acting factors (ITAFs). Some ITAFs are common to all IRESs, whereas some are unique to a particular set of mRNAs, allowing for a level of tissue- and condition-specific regulation. For example,

the apoptotic protein pro-apoptotic protease activating factor 1 (APAF1) can escape global down-regulation of translation during the onset of apoptosis through IRES-mediated translation initiation. eIF4G, the scaffolding component of the eIF4F cap complex, is also required for IRES-mediated translation. eIF4G is a cleavage target of caspase activity, and cleaved eIF4G preferentially translates at IRESs. Therefore, IRES-mediated translation of APAF1 is enhanced during apoptosis. It has been demonstrated that eIF2 $\alpha$  phosphorylation can enhance IRES-mediated translation of some transcripts (e.g. – the cationic amino acid transporter 1 [cat-1]), which is counterintuitive. Since active ternary complex is required for both cap-dependent and – independent translation initiation, eIF2 $\alpha$  phosphorylation is expected to reduce IRES-mediated translation (Holcik and Sonenberg, 2005). It is not known how eIF2 $\alpha$  phosphorylation induces IRES-mediated translation initiation in some transcripts; however, it is hypothesized that eIF2 $\alpha$  phosphorylation may promote the expression of an unidentified ITAF important for IRES-mediated translation in some transcripts (Yaman et al., 2003).

### ***Leaky Ribosome Scanning***

If uORFs are in a poor context for initiation, a small fraction of ribosomes may fail to recognize them as start codons, scan through them without initiating, and continue on to the next AUG. Alternative codon usage due to leaky ribosome scanning can result in several protein isoforms being produced from a single mRNA. Phosphorylation of eIF2 $\alpha$  can decrease translation initiation at distal uAUGs while simultaneously enhancing initiation at proximal uAUGs due to increased scanning after re-initiation. In

this manner, eIF2 $\alpha$  phosphorylation can alter ratios of protein isoforms being produced from transcripts subject to leaky ribosome scanning. The best characterized example of this type of regulation is C/EBP  $\alpha$  and  $\beta$  (Calkhoven et al., 2000).

### ***Secondary Structure***

Another mechanism by which long, G-C-rich 5'UTRs keep translation rates of transcripts to a minimum under normal conditions is the formation of stable secondary structure, which promotes the dissociation of the ribosome from the transcript before it reaches the start codon. Extensive complementary base-pairing ability and strong hydrogen bonds between guanosines and cytosines in long, G-C-rich 5'UTRs promote the formation of mRNA secondary structure. Mechanisms by which eIF2 $\alpha$  phosphorylation circumvents this type of translational inhibition under conditions of stress are not well-established. However, it is conceivable that eIF2 $\alpha$  phosphorylation promotes or inhibits the production of RNA-binding proteins which may facilitate or abrogate the formation of mRNA secondary structure. Alternatively, eIF2 $\alpha$  phosphorylation may recruit RNA helicases to transcripts, which catalyze the unwinding of mRNA secondary structure. Furthermore, the formation of mRNA secondary structure may act in concert with other inhibitory mechanisms, such as uORFs (Grant and Hinnebusch 1994) and IRESs (Yaman et al., 2003). Interestingly, APP appears to be translationally regulated in this manner. APP contains an iron-responsive element (IRE) in its 5'UTR, which binds iron-responsive proteins (IRPs). IRPs are RNA-binding proteins which stabilize mRNA secondary structure. In the presence of iron, IRPs are either prevented from binding to RNA through their interaction with iron or are degraded.

Elimination of the IRPs in the absence of iron allows mRNA secondary structure to unfold (Rouault, 2006). Curiously, APP appears to be oppositely regulated in response to iron. APP also appears to be post-transcriptionally up-regulated in response to IL-1 $\beta$  treatment in an iron-dependent manner *via* 5'UTR elements. However, the mechanisms and the significance of the relationship between IL-1 $\beta$  and iron regulation is not clear (Rogers et al., 1999; Rogers et al., 2002).

### **Regulation of BACE1 Translation**

The BACE1 5'UTR is 446 nucleotides in length, contains 4 uAUG sequences, 3 of which are ORFs, and is predicted to form extensive secondary structure, based on its high G-C content (76%) (Lammich et al., 2004). BACE1 translation appears to be exclusively cap-dependent with no detectable IRES activity in the 5'UTR (Rogers et al., 2004). Therefore, BACE1 translation could be inhibited by its 5'UTR either through the formation of secondary structure or translation of uORFs. The specific mechanism of BACE1 translational control via its 5'UTR continues to be debated; however, current data strongly supports initiation of the translation initiation complex at uAUG # 2 as the main inhibitory mechanism. It has also been proposed that leaky ribosome scanning occurs in the BACE1 5'UTR, which may allow the ribosome to escape translational inhibition from some of the uAUGs (Zhou and Song, 2006). Indeed, uAUG # 1 was found to have very little effect on translation in the majority of BACE1 5'UTR studies and failed to function as an initiation codon in luciferase assays, indicating that this uAUG may normally be bypassed (Lammich et al., 2004; Mihailovich et al., 2007; Rogers et al., 2004; Zhou and Song, 2006). In contrast, deletion of uAUG # 2 had the strongest

translational de-repression effect in all of the BACE1 5'UTR studies (De Pietri Tonelli et al., 2004; Lammich et al., 2004; Mihailovich et al., 2007; Rogers et al., 2004; Zhou and Song, 2006). uAUG # 2 resides in a good context for initiation and appears to function as an initiation codon in luciferase assays, indicating that this uORF may be translated *in vivo* (Rogers et al., 2004). One study concluded that uAUGs are not involved in BACE1 translational inhibition at all, because deletion of the BACE1 uAUGs had no effect on translation in B104 cells. The authors concluded that the inhibitory effect of the BACE1 5'UTR must be mediated through the formation of secondary structure, and the small amount of BACE1 that is translated normally in the cell must be produced through a shunting mechanism that allows the ribosome to bypass uAUGs and secondary structure. However, in the same study, a role for uAUGs was found in PC12 cells, with a main effect of uAUG # 2, which was completely consistent with results from other studies and directly supports translation of uORFs as the inhibitory mechanism (Rogers et al., 2004). Therefore, the results obtained in B104 cells may not have been valid. Another study found similar results, indicating that the BACE1 uAUGs could cause partial de-repression of translational inhibition, with a main effect of uAUGs # 2 and # 4 (Lammich et al., 2004). Interestingly, uAUG # 4 did not act as an initiation codon in luciferase assays from two different studies (Rogers et al., 2004; Zhou and Song, 2006), but deletion of this uAUG still had a significant effect on basal BACE1 protein levels (Lammich et al., 2004; Rogers et al., 2004), indicating that the ribosome does initiate at this codon *in vivo*, perhaps with less efficiency than at uAUG # 2. Another finding of the Lammich study was that complete de-repression could not be achieved without deleting large sections of the BACE1 5'UTR. The authors concluded

that there must be a main effect of 5'UTR secondary structure on BACE1 translation, in addition to a subtler effect of BACE1 uAUGs (Lammich et al., 2004). Consistent with this finding, when we used the +5'UTR and -5'UTR constructs used in this study for our own experiments, we observed a much larger increase in BACE1 protein due to deletion of the 5'UTR (~200%), as compared to glucose deprivation (~150%). These results imply that glucose deprivation de-represses BACE1 translation *via* enhanced scanning through the uORFs after re-initiation, but the main effect of mRNA secondary structure is still intact. However, later studies disagreed with “main effect of secondary structure” conclusion and showed that deletion of all the BACE1 uAUGs could completely de-repress BACE1 translational inhibition, and there was no effect of secondary structure on BACE1 translation (Mihailovich et al., 2007; Zhou and Song, 2006). From this perspective, the elevated BACE1 protein levels in -5'UTR cells compared to +5'UTR + NG cells may reflect the complete loss of translational inhibition by uORFs in -5'UTR cells and initiation of every ribosomes at the correct BACE1 start codon in -5'UTR cells, as compared to +5'UTR + NG cells, where translation at the authentic BACE1 start codon is still drastically reduced due to initiation at uORFs, despite enhanced re-initiation at the authentic BACE1 start codon. Based on our current knowledge of translational regulation of BACE1, we propose the following model of eIF2 $\alpha$ -P-mediated regulation of BACE1 translation: Under normal conditions (eIF2 $\alpha$ -P $\downarrow$ ), a large proportion of the ribosomes may scan through uAUG # 1 and initiate translation at uAUG # 2. The majority of ribosomes translate uORF # 2 and dissociate from the 5'UTR. However, a small proportion of 40S subunits continue to scan after translating uORF # 2. Some scanning 40S subunits become re-loaded with ternary



complex, re-initiate at uAUG # 4, translate uORF # 3, and dissociate. Other 40S subunits scan through uAUG # 4 and initiate at the authentic BACE1 start codon, producing basal BACE1 protein levels. Under stress conditions ( $\text{eIF2}\alpha\text{-P}\uparrow$ ), a higher proportion of 40S subunits will scan through uAUG # 4 due to low ternary complex availability, and re-initiate at the authentic BACE1 start codon, leading to elevated BACE1 protein levels (Fig 7.1). This scenario predicts that deletion of uORF # 2 or uORF # 3 would eliminate translational control of BACE1 protein under stress conditions. Eventually, a detailed analysis of uORF deletion mutants under control versus glucose-deficient conditions will be essential in order to confirm this prediction of glucose-mediated BACE1 translational control.

## **Role of BACE1 in Neurodegeneration and Energy Metabolism**

It is clear from a comparison of yeast and mammalian systems that the eIF2 stress-response pathway is highly conserved throughout evolution. Furthermore, the kinases responsible for phosphorylating eIF2 $\alpha$  are activated in response to a diverse array of stress responses, indicating that eIF2 $\alpha$  is a general stress response mechanism in mammals. Ablation of eIF2 $\alpha$  phosphorylation sites in mice leads to severe glucose dysregulation and death, similar to PERK mutations, indicating that the main function of eIF2 $\alpha$  phosphorylation in mammals under normal physiological conditions is metabolic regulation (Scheuner et al., 2001; Scheuner et al., 2005). The proper regulation of glucose and the ability to survive stress conditions are essential processes, particularly for organs such as the brain, which is highly dependent on glucose stores and has a

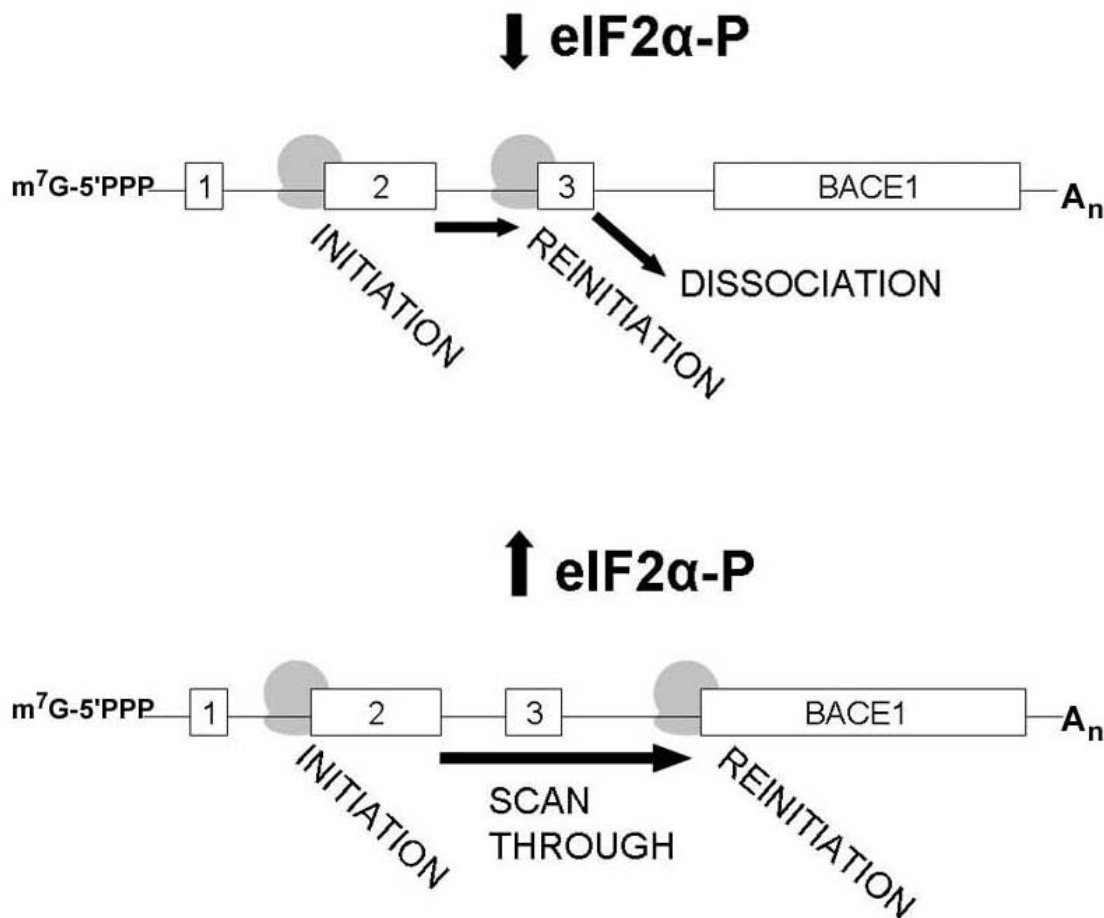


**Figure 7.1: eIF2α-mediated regulation of BACE1 translation** Under normal conditions (eIF2α-P↓), a large proportion of the ribosomes may scan through uAUG # 1 and initiate translation at uAUG # 2. The majority of ribosomes translate uORF # 2 and dissociate from the 5'UTR. However, a small proportion of 40S subunits continue to scan after translating uORF # 2. Some scanning 40S subunits become re-loaded with ternary complex, re-initiate at uAUG # 4, translate uORF # 3, and dissociate. Other 40S subunits scan through uAUG # 4 and initiate at the authentic BACE1 start codon, producing basal BACE1 protein levels. Under stress conditions (eIF2α-P↑), a higher proportion of 40S subunits will scan through uAUG # 4 due to low ternary complex availability, and re-initiate at the authentic BACE1 start codon, leading to elevated BACE1 protein levels

limited capacity to replace damaged neurons. The role of eIF2 $\alpha$  phosphorylation in the brain has not been widely investigated; however, existing data implies a role for eIF2 $\alpha$  phosphorylation in synaptic transmission, which may be related to metabolic regulation in the brain, neuronal survival, and the onset of neurodegeneration.

### **Translational control in the brain**

Translational control of proteins is critical in the brain, where the transcriptional machinery in the cell body is often spatially removed from other parts of the neuron. Furthermore, translational regulation allows synapses from the same neuron to differentially integrate signals from neighboring neurons (Steward and Schuman, 2001; Sutton and Schuman, 2005). Dendrites contain polyribosome complexes capable of specifically modulating translation at a particular synapse, and dendrites are able to respond to extracellular signals when separated from the cell body (Kang and Schuman, 1996; Steward and Fass, 1983; Steward and Levy, 1982). This is thought to occur through a combination of selective mRNA recruitment to polyribosome complexes and posttranslational modifications to the translation machinery (Hachet and Ephrussi, 2004; Sutton and Schuman, 2005; Tiedge et al., 1999). Not surprisingly, increased global translation in neurons is associated with growth stimuli and enhanced synaptic activity (e.g. – BDNF stimulation, PI3K/Akt activation, or ERK/MAPK activation), whereas down-regulated global translation is generally associated with reduced synaptic activity and low growth (Kelleher et al., 2004). Interestingly, down-regulated global translation also appears to be associated with glutamatergic stimulation, in some cases, which also robustly elevate BACE1 protein levels both *in vitro* and *in vivo*

(Orrego and Lipmann, 1967; Velliquette et al., 2005) (Fig 2.4; Fig 2.6; K.R. Doherty, unpublished results). This may represent a stress-activated feedback mechanism due to exitotoxicity (Vornov and Coyle, 1991). The role of eIF2 regulation in neuronal function has been largely unaddressed *in vivo*; however, existing data indicates that eIF2 regulation may play an important role in neuronal processes. GSK3 phosphorylates eIF2B, which is regulated by the PI3K/Akt pathway involved in neuronal development and synaptic transmission (Wang et al., 2001). The role of eIF2-mediated translation in long-term potentiation (LTP), long-term depression (LTD), and the acquisition of memories have also been investigated. LTP consists of an early phase (E-LTP), which is associated with weak memory training or single tetanic stimulations and a late phase (L-LTP), which is associated with strong memory training or repeated tetanic stimulations. The transition from E-LTP to L-LTP is thought to represent the switch from short-term memory (STM) to long-term memory (LTM) (Hoeffler and Klann 2007). A comparison of E- and L-LTP in brain slices from wild-type and eIF2 $\alpha$  +/S51A mice, which harbor a single ablated eIF2 $\alpha$  phosphorylation site, revealed that LTM is prematurely evoked in response to tetanic stimulation in the absence of eIF2 $\alpha$  phosphorylation. Consistent with this observation, eIF2 $\alpha$  +/S51A mice were more efficient than wild-type mice in learning memory tasks in response to a weak training protocol. Conversely, salubrinal treatment, which enhances eIF2 $\alpha$ -P, inhibited L-LTP and LTM in response to repeated tetanic stimulation, indicating that dephosphorylation at eIF2 $\alpha$  regulates the switch from STM to LTM (Costa-Mattioli et al., 2007). Interestingly, mammalian GCN2 is expressed at high levels in the brain, compared to other organs, indicating that it may play a role in neuronal function. Therefore, the

potential role of GCN2 in gating STM to LTM was further explored using single and repeated tetanic stimulations in GCN2  $-/-$  brain slices. Similar to eIF2 $\alpha$   $+/-$  S51A brain slices, L-LTP was inappropriately activated in GCN2  $-/-$  slices in response to a single tetanic stimulation, and similar to eIF2 $\alpha$   $+/-$  S51A mice, GCN2  $-/-$  mice learned more rapidly than wild-type mice during a weak training protocol. On the other hand, GCN2  $-/-$  slices could not induce L-LTP in response to repeated tetanic stimulation, and GCN2  $-/-$  mice exhibited impaired performance in memory tasks when subjected to a strong training protocol, indicating that eIF2 $\alpha$  phosphorylation is essential for appropriate STM to LTM transition (Costa-Mattioli et al., 2005). Interestingly, BACE1  $-/-$  mice are impaired at certain memory tasks in response to strong training, and BACE1  $-/-$  slices fail to induce L-LTP in response to repeated tetanic stimulation, despite exhibiting a larger initial post-tetanic potentiation than wild-type (Laird et al., 2005; Ohno et al., 2004; Wang et al., 2008a). However, memory performance and induction of L-LTP have not been tested in BACE1  $-/-$  mice in response to weak training or single tetanic stimulations. The potential role of PERK in regulating synaptic transmission has not been investigated. Although PERK levels are highest in the pancreas, it is also readily detectable in the brain (Shi et al., 1998), indicating that it may also play an important role in synaptic transmission and neuronal function. The importance of proper ternary complex function in the brain is further exemplified by the association of inherited mutations in all subunits of eIF2B with central nervous system diseases, such as childhood ataxia with central nervous system hypomyelination (CACH) and vanishing white matter disease (VWM) (Fogli et al., 2004; Leegwater et al., 2001; van der Knaap et al., 2002). These mutations in eIF2B reduce its GEF activity, and CACH and VWM

can be triggered by stress stimuli, such as viral infection, which further reduce eIF2B function. Presumably, oligodendrocytes harboring eIF2B mutations experience an exaggerated eIF2/eIF2B-mediated stress response during induction of stress, leading to the aberrant activation of apoptotic pathways, which is the end-result of severe and unalleviated translational repression. However, the reasons underlying susceptibility of oligodendrocytes to exaggerated eIF2 stress, when all cells are deficient in eIF2B activity, is unclear. A subsequent study of these disorders reported that eIF2B mutant glial precursors exhibited impaired astrocyte differentiation, indicating that eIF2/eIF2B pathway could play a role in astrocyte differentiation, which in turn may be important in protecting myelin from eIF2 stress-induced damage (Dietrich et al., 2005). It is also unclear why eIF2B deficiencies cause white matter deterioration, while eIF2 $\alpha$  S51A mutations lead to severe diabetes, when both mutations are expected to have similar biochemical consequences. It would be interesting to determine whether mice with eIF2B mutations have subtle defects in glucose regulation. Conversely, it would also be interesting to investigate whether eIF2 $\alpha$  +/S51A mice would experience demyelination upon exposure to viral infections, similar to what has been observed in PERK +/- mice in response to IFN $\gamma$  (Lin et al., 2005).

### **Role of eIF2 $\alpha$ regulation in neurodegeneration**

Although eIF2 $\alpha$  regulation clearly plays a role in the normal physiology of certain cells (e.g. – glucose regulation in pancreatic cells and synaptic transmission in neurons), one of the major functions of eIF2 $\alpha$  regulation appears to be altering translation in response to a wide array of stress stimuli. Indeed, a phenotype was not observed in most eIF2 $\alpha$

kinase knockout models unless the animals were challenged with a particular stress condition (e.g. – amino acid deprivation in GCN2  $-/-$  mice, viral infection in PKR  $-/-$  mice, and heme deficiency in HRI  $-/-$  mice). Furthermore, the hypomyelination phenotype in individuals with eIF2B mutations is often precipitated by stresses, such as traumatic brain injury or viral infection, indicating that proper regulation of the ternary complex is crucial for neurons to survive stressful conditions. Consistent with a role for eIF2 $\alpha$  in the neuronal stress response, eIF2 $\alpha$  phosphorylation and activated UPR are present in neurodegenerative disorders such as Alzheimer's disease, Parkinson's disease, amyotrophic lateral sclerosis, polyglutamine disease, and prion disease (Hetz et al., 2003; Holtz and O'Malley, 2003; Holtz et al., 2005; Hoozemans et al., 2005; Kheradpezhohu et al., 2003; Kouroku et al., 2002; Peel and Bredesen, 2003; Ryu et al., 2005; Ryu et al., 2002; Tobisawa et al., 2003; Unterberger et al., 2006; Yoo et al., 2002). A feature that many neurodegenerative disorders share in common is the progressive accumulation of toxic protein aggregates (Winklhofer et al., 2008). Intraneuronal accumulation of these protein aggregates may trigger the UPR and the eIF2 $\alpha$  stress response pathway. We have shown that one consequence of eIF2 $\alpha$  phosphorylation is enhanced A $\beta$  production, which may explain why amyloid pathology is often found in neurodegenerative disorders other than Alzheimer's disease, since the accumulation of misfolded proteins is not unique to Alzheimer's disease (Fig 6.2). Interestingly, eIF2 $\alpha$  phosphorylation and amyloid accumulation appear to come into play at multiple stages during neurodegeneration. In the case of SAD, eIF2 $\alpha$ -P and amyloid accumulation may be a driving force in the disease process, due to factors such as impaired energy metabolism. However, in other neurodegenerative diseases (and the

later stages of AD), eIF2 $\alpha$ -P may be activated downstream in the disease process due to accumulation of misfolded proteins and activation of the UPR.

Neurodegenerative disorders are generally late in onset, even in cases where the cause is clearly genetic. This may be partly due to the gradual deterioration of clearance and degradation mechanisms in the aging brain. However, there is also evidence that the UPR and the ability of the neuron to correctly fold proteins become increasingly compromised during normal aging, and amyloid pathology is also a common feature of normal aged brains, further implicating the involvement of the eIF2 $\alpha$  pathway (Paz Gavilan et al., 2006; Yankner et al., 2008). Whether stress-induced eIF2 $\alpha$  phosphorylation is ultimately adaptive or detrimental in the brain is not completely understood. Evidence from *in vitro* models investigating the role of eIF2 $\alpha$  phosphorylation in cell survival has yielded contradictory results. It has been shown that phosphorylation of eIF2 $\alpha$  is required for a cell to appropriately respond to and survive stress conditions (Bi et al., 2005; Harding et al., 2000; Jousse et al., 2003; Koritzinsky et al., 2007; Lu et al., 2004). Data from animal models support this idea. On the other hand, eIF2 $\alpha$ -P activation elevates the expression of several known pro-apoptotic molecules including nuclear factor-kappa B (NF $\kappa$ B) and C/EBP homology protein (CHOP) and accordingly appears to be required for induction of apoptosis in some cases (Donze et al., 2004; Hsu et al., 2004; Jiang et al., 2003; Ma et al., 2002; Srivastava et al., 1998). In fact, viruses have actually evolved mechanisms of inhibiting eIF2 $\alpha$  phosphorylation in order to avoid these eIF2 $\alpha$ -induced cell death pathways (Barber et al., 1994; Lee et al., 1994). Canonical activation and regulation of the eIF2 $\alpha$



pathway is intrinsically designed to be both rapid and transient. In fact, one translational target of eIF2 $\alpha$ -P is the growth arrest and DNA damage 34 (GADD34) protein, which binds protein phosphatase PP1c and directs its activity to eIF2 $\alpha$ , thereby negatively regulating eIF2 $\alpha$  phosphorylation (Novoa et al., 2001). Furthermore, rapid recovery from eIF2 $\alpha$  phosphorylation is required for the expression of numerous eIF2 $\alpha$ -P-activated stress response proteins, since many of the translational targets of eIF2 $\alpha$ -P are transcription factors (Novoa et al., 2003). Based on this apparently conflicting data, it has been proposed that eIF2 $\alpha$ -P activation is biphasic (Schroder and Kaufman, 2006). If the stress is transient, eIF2 $\alpha$  phosphorylation may be beneficial and promote cell survival. However, if the stress is severe or unalleviated, cells are directed to undergo apoptosis in order to eliminate defective and irreparable cells from the population. Therefore, it can be inferred that transient eIF2 $\alpha$  phosphorylation is adaptive, whereas persistent or chronic eIF2 $\alpha$  phosphorylation may be maladaptive. Consistent with the idea that chronic eIF2 $\alpha$  phosphorylation is detrimental, it has been reported that recovery from translation inhibition is required for neuronal survival during transient cerebral ischemia (DeGracia and Hu, 2007). The association of elevated eIF2 $\alpha$ -P levels with various neurodegenerative disorders which are marked by neuron death would appear to support this conclusion. However, our results do not support the idea that chronic eIF2 $\alpha$  phosphorylation is maladaptive or necessarily leads to cell death. BACE1-293 cells and cultured neurons were able to survive up to 48 hrs under conditions of constant and unalleviated glucose deprivation, which lead to progressively elevated eIF2 $\alpha$ -P levels over the treatment period, and we observed no signs of cell

death or distress (Fig 3.3; Fig 3.7). Furthermore, chronic energy deprivation treatments and sustained eIF2 $\alpha$ -P levels in the brains of mice did not cause any detectable neuron loss or caspase activation over a period of 3 months (Fig 5.1; Fig 5.2). Our results suggest that the decision of whether to enter the apoptotic pathway may be primarily determined by the severity of the insult, rather than the duration. Sustained, moderate levels of eIF2 $\alpha$  phosphorylation may actually be beneficial to neurons, allowing them to conserve energy during long periods of low energy availability, or during the course of neurodegeneration, by limiting the production of new proteins to avoid overstressing an ER already overloaded with misfolded proteins.

### **Energy impairment, BACE1, and AD**

We propose that common risk factors for SAD may all be linked by their ability to impair energy metabolism in the brain and activate the eIF2 $\alpha$  stress response pathway, which enhances A $\beta$  production by translationally elevating BACE1 protein. In support of this hypothesis, several major risk factors for SAD have all been linked to the eIF2 $\alpha$  stress response pathway and dysregulation of the UPR, including atherosclerosis, traumatic brain injury, ischemia, and other cardiovascular complications (Devries-Seimon et al., 2005; Kumar et al., 2001; Larner et al., 2004; Li et al., 2005; Mao et al., 2005; Okada et al., 2004; Paschen et al., 2004; Pedruzzi et al., 2004; Roybal et al., 2004). The eIF2 $\alpha$  pathway has also been linked to diabetes (Cardozo et al., 2005). The fact that these risk factors can activate the eIF2 $\alpha$  pathway supports the theory that eIF2 $\alpha$  precedes amyloid pathology in the brain and may be a major driving force in the development of SAD pathology. Our results clearly show that BACE1 is a translational target of the

eIF2 $\alpha$  stress response pathway, and eIF2 $\alpha$ -P activation can dramatically enhance A $\beta$  production in neurons. The reason underlying eIF2 $\alpha$ -P-induced BACE1 and A $\beta$  up-regulation is an important unanswered question and a difficult one to address, since the normal physiological functions of BACE1 and A $\beta$  remain unclear. The only clear physiological role of BACE1 demonstrated thus far is in PNS myelination (Willem et al., 2006). Although a role for BACE1 in myelin maintenance and repair is consistent with BACE1 up-regulation in response to some types of stress, such as traumatic brain injury and excitotoxicity where myelin may be damaged, the importance of BACE1's role in myelination is less clear with respect to other types of stress, such as energy deprivation where myelin remains intact. With regard to energy deprivation specifically, the human brain has evolved numerous mechanisms of sensing and regulating glucose metabolism. Certain neurons are able to regulate their firing rates based on energy availability, partly through ATP-sensitive potassium channels (Dunn-Meynell et al., 1998) and partly through unidentified mechanisms. Not surprisingly, many of these neurons are found in the hypothalamus and are directly involved in transmitting information about energy availability in the brain to peripheral organs involved in energy regulation (Anand et al., 1964; Oomura et al., 1974). However, glucose-responsive and glucose-sensitive neurons also exist outside of the hypothalamus. It is hypothesized that the ability of these neurons to self-regulate synaptic activity based on glucose availability evolved as an energy conservation method (Levin et al., 1999). Coincidentally, BACE1 also has a proposed function in regulating synaptic activity. BACE1  $-/-$  mice are impaired in certain memory tasks and LTP induction (Laird et al., 2005; Ohno et al., 2004; Wang et al., 2008a). Furthermore, enhanced synaptic activity

in slice cultures increases A $\beta$  production *via* enhanced BACE1 cleavage of APP. In turn, A $\beta$  suppresses synaptic transmission, indicating that A $\beta$  may normally function as a negative feedback regulator of synaptic transmission (Kamenetz et al., 2003). In support of a role for BACE1 in depressing synaptic activity, it has been reported that BACE1  $-/-$  mice display a hyperactive phenotype (Dominguez et al., 2005; Laird et al., 2005). Based on this data, it can be hypothesized that the normal physiological function of energy deprivation-induced BACE1 protein elevations may be to enhance A $\beta$  production, depress synaptic activity, and conserve neuronal energy stores.

Interestingly, alternative BACE1 substrates may be related to BACE1's proposed function in regulating synaptic activity. For example, BACE1 cleavage of the  $\beta$  subunit of the voltage-gated sodium channel (VGSC $\beta$ ) may further depress synaptic activity (Wong et al., 2005), and BACE1 cleavage of the LDL receptor related protein (LRP) (von Arnim et al., 2005), which is involved in A $\beta$  turnover (Hyman et al., 2000), may extend the half-life of A $\beta$  and augment its depressive effects on synaptic transmission. Additionally, BACE1 could have other unidentified roles in energy metabolism.

Interestingly, both BACE1 and PERK levels are high in pancreas, but BACE1 activity levels are low, indicating that BACE1 could have a function in the pancreas unrelated to its enzymatic activity. Although BACE1  $-/-$  mice exhibit no apparent abnormalities in glucose regulation under normal conditions (Luo et al., 2001), both PERK and BACE1  $-/-$  mice exhibit higher mortality and growth retardation compared to wild-type (Dominguez et al., 2005; Harding et al., 2000). The cause of mortality and growth retardation in BACE1  $-/-$  mice is not known; however, the phenotypic overlap with PERK  $-/-$  mice raises the possibility that BACE1  $-/-$  could have subtle defects in metabolic

regulation. In summary, sustained eIF2 $\alpha$  phosphorylation, elevated BACE1 levels, limited protein translation, and suppressed synaptic activity may be playing an important adaptive role in allowing neurons to survive under extended periods of stress. However, in the aging brain, where the UPR, clearance, and degradation mechanisms become increasingly compromised, accelerated A $\beta$  production due to elevated eIF2 $\alpha$ -P levels may eventually lead to the accumulation and assembly of A $\beta$  into toxic oligomeric species. The formation of A $\beta$  aggregates may trigger a number of downstream pathological events, including dysregulated cellular signaling cascades, synaptic dysfunction, and tau hyperphosphorylation. Interestingly, our data also shows that A $\beta$  accumulation can also induce eIF2 $\alpha$ -P elevations, most likely through activation of the UPR (Fig 6.2; Fig 7.2). This data suggests that chronic stress, BACE1, eIF2 $\alpha$ -P(Ser51), and A $\beta$  may collaborate in a positive feedback loop in which amyloidogenesis becomes amplified once A $\beta$  has accumulated to the level that it is capable of initiating and sustaining a stress response in the neuron (Fig 7.2). Thus, eIF2 $\alpha$  phosphorylation may be involved in both the initiation and progression of sporadic AD. This model also predicts that once amyloid pathology is initiated, it is likely to progress at an increasing rate, unless the amyloidogenic cycle is somehow interrupted. This hypothesis highlights the importance of developing new preventative and disease-modifying therapies for AD, especially those aimed at inhibiting the generation and accumulation of A $\beta$  in the brain during the earliest stages of the disease.

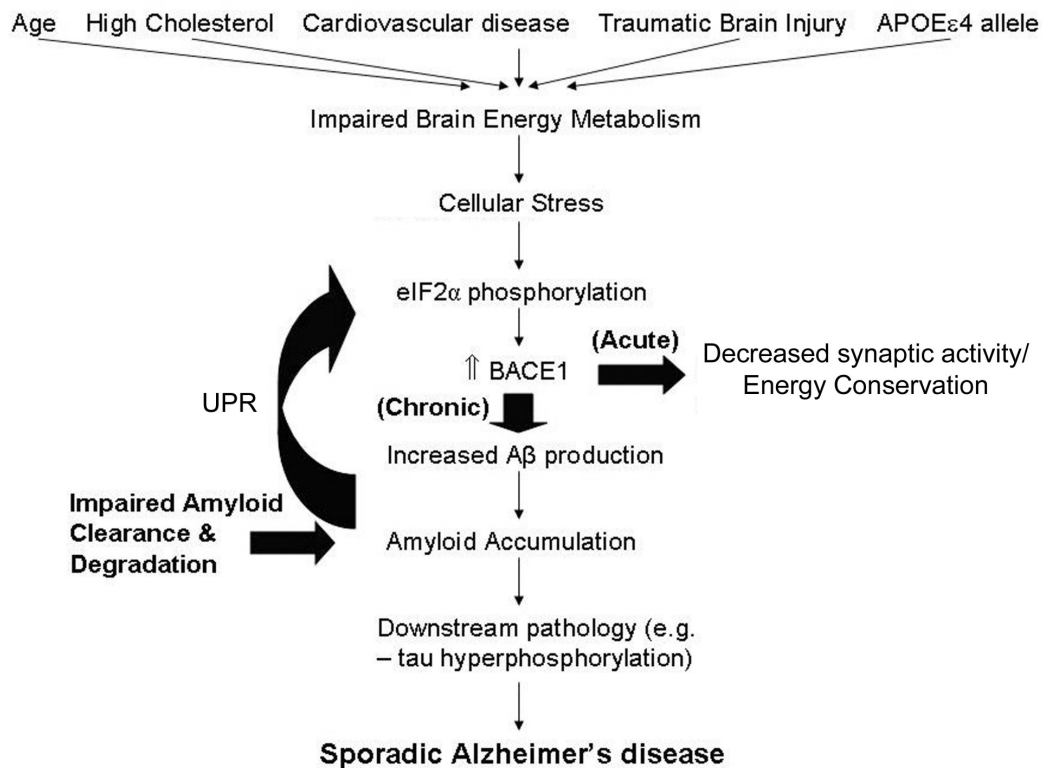


**Figure 7.2: The role of eIF2 $\alpha$  phosphorylation in sporadic Alzheimer's disease pathogenesis.**

Common risk factors for Alzheimer's disease such as age, high cholesterol, cardiovascular disease, traumatic brain injury, and ApoE4 genotype may lead to a state of impaired energy metabolism in the brain. Reduced energy availability activates the eIF2 $\alpha$ -P stress-response pathway in neurons. Phosphorylation of eIF2 $\alpha$  augments the translation of specific stress response proteins such as BACE1. Increased production of these stress-response proteins presumably enhances the ability of neurons to survive under low-energy conditions. However, if the stress persists, eIF2 $\alpha$  phosphorylation and BACE1 levels remain chronically elevated, leading to increased A $\beta$  production. Elevated A $\beta$  levels may, in turn, cause neuronal dysfunction and stress, feeding back and further activating the eIF2 $\alpha$ -P stress-response pathway. Over time, and in combination with other exacerbating factors such as impaired A $\beta$  clearance/degradation, A $\beta$  begins to accumulate in the brain and plaques form. A $\beta$  accumulation may trigger downstream pathology, (e.g., tau hyperphosphorylation), ultimately leading to neurodegeneration associated with sporadic Alzheimer's disease.

## REFERENCES

- Alzheimer, A. (1907). Über eine eigenartige Erkrankung der Hirnrinde. *Allgemeine Zeitschrift für Psychiatrie und Psychisch-gerichtliche Medizin* 64, 146-148.
- Anand, B.K., Chhina, G.S., Sharma, K.N., Dua, S., and Singh, B. (1964). Activity of Single Neurons in the Hypothalamic Feeding Centers: Effect of Glucose. *The American journal of physiology* 207, 1146-1154.
- Ashford, J.W. (2004). APOE genotype effects on Alzheimer's disease onset and epidemiology. *J Mol Neurosci* 23, 157-165.
- Auer, R.N., Olsson, Y., and Siesjo, B.K. (1984). Hypoglycemic brain injury in the rat. Correlation of density of brain damage with the EEG isoelectric time: a quantitative study. *Diabetes* 33, 1090-1098.
- Austen, B.M., and Stephens, D.J. (1995). Cleavage of a beta-amyloid precursor sequence by cathepsin D. *Biomed Pept Proteins Nucleic Acids* 1, 243-246.
- Barber, G.N. (2001). Host defense, viruses and apoptosis. *Cell death and differentiation* 8, 113-126.
- Barber, G.N., Thompson, S., Lee, T.G., Strom, T., Jagus, R., Darveau, A., and Katze, M.G. (1994). The 58-kilodalton inhibitor of the interferon-induced double-stranded RNA-activated protein kinase is a tetratricopeptide repeat protein with oncogenic properties. *Proceedings of the National Academy of Sciences of the United States of America* 91, 4278-4282.
- Baum, L.W. (2005). Sex, hormones, and Alzheimer's disease. *J Gerontol A Biol Sci Med Sci* 60, 736-743.
- Benkirane, M., Neuveut, C., Chun, R.F., Smith, S.M., Samuel, C.E., Gagnon, A., and Jeang, K.T. (1997). Oncogenic potential of TAR RNA binding protein TRBP and its regulatory interaction with RNA-dependent protein kinase PKR. *The EMBO journal* 16, 611-624.
- Bennett, D.A., Schneider, J.A., Wilson, R.S., Bienias, J.L., and Arnold, S.E. (2004). Neurofibrillary tangles mediate the association of amyloid load with clinical Alzheimer disease and level of cognitive function. *Arch Neurol* 61, 378-384.
- Berlango, J.J., Santoyo, J., and De Haro, C. (1999). Characterization of a mammalian homolog of the GCN2 eukaryotic initiation factor 2alpha kinase. *European journal of biochemistry / FEBS* 265, 754-762.

Beyreuther, K., Pollwein, P., Multhaup, G., Monning, U., König, G., Dyrks, T., Schubert, W., and Masters, C.L. (1993). Regulation and expression of the Alzheimer's beta/A4 amyloid protein precursor in health, disease, and Down's syndrome. *Annals of the New York Academy of Sciences* 695, 91-102.

Bi, M., Naczki, C., Koritzinsky, M., Fels, D., Blais, J., Hu, N., Harding, H., Novoa, I., Varia, M., Raleigh, J., *et al.* (2005). ER stress-regulated translation increases tolerance to extreme hypoxia and promotes tumor growth. *The EMBO journal* 24, 3470-3481.

Binder, L.I., Guillozet-Bongaarts, A.L., Garcia-Sierra, F., and Berry, R.W. (2005). Tau, tangles, and Alzheimer's disease. *Biochim Biophys Acta* 1739, 216-223.

Blasko, I., Beer, R., Bigl, M., Apelt, J., Franz, G., Rudzki, D., Ransmayr, G., Kampfl, A., and Schliebs, R. (2004). Experimental traumatic brain injury in rats stimulates the expression, production and activity of Alzheimer's disease beta-secretase (BACE-1). *J Neural Transm* 111, 523-536.

Blurton-Jones, M., and Laferla, F.M. (2006). Pathways by which Abeta facilitates tau pathology. *Curr Alzheimer Res* 3, 437-448.

Bodendorf, U., Danner, S., Fischer, F., Stefani, M., Sturchler-Pierrat, C., Wiederhold, K.H., Staufenbiel, M., and Paganetti, P. (2002). Expression of human beta-secretase in the mouse brain increases the steady-state level of beta-amyloid. *Journal of neurochemistry* 80, 799-806.

Bodendorf, U., Fischer, F., Bodian, D., Multhaup, G., and Paganetti, P. (2001). A splice variant of beta-secretase deficient in the amyloidogenic processing of the amyloid precursor protein. *J Biol Chem* 276, 12019-12023.

Boyce, M., Bryant, K.F., Jousse, C., Long, K., Harding, H.P., Scheuner, D., Kaufman, R.J., Ma, D., Coen, D.M., Ron, D., and Yuan, J. (2005). A selective inhibitor of eIF2alpha dephosphorylation protects cells from ER stress. *Science (New York, N.Y)* 307, 935-939.

Brion, J.P. (2006). Immunological demonstration of tau protein in neurofibrillary tangles of Alzheimer's disease. *J Alzheimers Dis* 9, 177-185.

Brouillet, E., Jacquard, C., Bizat, N., and Blum, D. (2005). 3-Nitropropionic acid: a mitochondrial toxin to uncover physiopathological mechanisms underlying striatal degeneration in Huntington's disease. *Journal of neurochemistry* 95, 1521-1540.

Brownell, A.L., Chen, Y.I., Yu, M., Wang, X., Dedeoglu, A., Cicchetti, F., Jenkins, B.G., and Beal, M.F. (2004). 3-Nitropropionic acid-induced neurotoxicity--assessed by ultra high resolution positron emission tomography with comparison to magnetic resonance spectroscopy. *J Neurochem* 89, 1206-1214.



Brunn, G.J., Hudson, C.C., Sekulic, A., Williams, J.M., Hosoi, H., Houghton, P.J., Lawrence, J.C., Jr., and Abraham, R.T. (1997). Phosphorylation of the translational repressor PHAS-I by the mammalian target of rapamycin. *Science (New York, N.Y.)* **277**, 99-101.

Busciglio, J., Gabuzda, D.H., Matsudaira, P., and Yankner, B.A. (1993). Generation of beta-amyloid in the secretory pathway in neuronal and nonneuronal cells. *Proc Natl Acad Sci U S A* **90**, 2092-2096.

Busciglio, J., Pelsman, A., Wong, C., Pigino, G., Yuan, M., Mori, H., and Yankner, B.A. (2002). Altered metabolism of the amyloid beta precursor protein is associated with mitochondrial dysfunction in Down's syndrome. *Neuron* **33**, 677-688.

Calkhoven, C.F., Muller, C., and Leutz, A. (2000). Translational control of C/EBPalpha and C/EBPbeta isoform expression. *Genes & development* **14**, 1920-1932.

Cardozo, A.K., Ortis, F., Storling, J., Feng, Y.M., Rasschaert, J., Tonnesen, M., Van Eylen, F., Mandrup-Poulsen, T., Herchuelz, A., and Eizirik, D.L. (2005). Cytokines downregulate the sarcoendoplasmic reticulum pump Ca<sup>2+</sup> ATPase 2b and deplete endoplasmic reticulum Ca<sup>2+</sup>, leading to induction of endoplasmic reticulum stress in pancreatic beta-cells. *Diabetes* **54**, 452-461.

Cassery, I., and Topol, E. (2004). Convergence of atherosclerosis and Alzheimer's disease: inflammation, cholesterol, and misfolded proteins. *Lancet* **363**, 1139-1146.  
Chafekar, S.M., Hoozemans, J.J., Zwart, R., Baas, F., and Scheper, W. (2007). Aβ<sub>1-42</sub> induces mild endoplasmic reticulum stress in an aggregation state-dependent manner. *Antioxidants & redox signaling* **9**, 2245-2254.

Chen, G., Gharib, T.G., Huang, C.C., Taylor, J.M., Misek, D.E., Kardia, S.L., Giordano, T.J., Iannettoni, M.D., Orringer, M.B., Hanash, S.M., and Beer, D.G. (2002). Discordant protein and mRNA expression in lung adenocarcinomas. *Mol Cell Proteomics* **1**, 304-313.

Chen, J.J. (2007). Regulation of protein synthesis by the heme-regulated eIF2alpha kinase: relevance to anemias. *Blood* **109**, 2693-2699.

Chen, J.J., Throop, M.S., Gehrke, L., Kuo, I., Pal, J.K., Brodsky, M., and London, I.M. (1991). Cloning of the cDNA of the heme-regulated eukaryotic initiation factor 2 alpha (eIF-2 alpha) kinase of rabbit reticulocytes: homology to yeast GCN2 protein kinase and human double-stranded-RNA-dependent eIF-2 alpha kinase. *Proceedings of the National Academy of Sciences of the United States of America* **88**, 7729-7733.

Cheng, B., and Mattson, M.P. (1995). PDGFs protect hippocampal neurons against energy deprivation and oxidative injury: evidence for induction of antioxidant pathways. *J Neurosci* **15**, 7095-7104.

- Chiocco, M.J., Kulnane, L.S., Younkin, L., Younkin, S., Evin, G., and Lamb, B.T. (2004). Altered amyloid-beta metabolism and deposition in genomic-based beta-secretase transgenic mice. *The Journal of biological chemistry* 279, 52535-52542.
- Chiocco, M.J., and Lamb, B.T. (2007). Spatial and temporal control of age-related APP processing in genomic-based beta-secretase transgenic mice. *Neurobiol Aging* 28, 75-84.
- Cigan, A.M., Bushman, J.L., Boal, T.R., and Hinnebusch, A.G. (1993). A protein complex of translational regulators of GCN4 mRNA is the guanine nucleotide-exchange factor for translation initiation factor 2 in yeast. *Proc Natl Acad Sci U S A* 90, 5350-5354.
- Citron, M., Diehl, T.S., Gordon, G., Biere, A.L., Seubert, P., and Selkoe, D.J. (1996). Evidence that the 42- and 40-amino acid forms of amyloid beta protein are generated from the beta-amyloid precursor protein by different protease activities. *Proc Natl Acad Sci U S A* 93, 13170-13175.
- Citron, M., Oltersdorf, T., Haass, C., McConlogue, L., Hung, A.Y., Seubert, P., Vigo-Pelfrey, C., Lieberburg, I., and Selkoe, D.J. (1992). Mutation of the beta-amyloid precursor protein in familial Alzheimer's disease increases beta-protein production. *Nature* 360, 672-674.
- Citron, M., Teplow, D.B., and Selkoe, D.J. (1995). Generation of amyloid beta protein from its precursor is sequence specific. *Neuron* 14, 661-670.
- Clemens, M.J. (2001a). Initiation factor eIF2 alpha phosphorylation in stress responses and apoptosis. *Prog Mol Subcell Biol* 27, 57-89.
- Clemens, M.J. (2001b). Translational regulation in cell stress and apoptosis. Roles of the eIF4E binding proteins. *Journal of cellular and molecular medicine* 5, 221-239.
- Clemens, M.J. (2004). Targets and mechanisms for the regulation of translation in malignant transformation. *Oncogene* 23, 3180-3188.
- Cole, S.L., Grudzien, A., Manhart, I.O., Kelly, B.L., Oakley, H., and Vassar, R. (2005). Statins cause intracellular accumulation of amyloid precursor protein, beta-secretase-cleaved fragments, and amyloid beta-peptide via an isoprenoid-dependent mechanism. *The Journal of biological chemistry* 280, 18755-18770.
- Cole, S.L., and Vassar, R. (2008). Linking vascular disorders and Alzheimer's disease: Potential involvement of BACE1. *Neurobiology of aging*.
- Corder, E.H., Saunders, A.M., Strittmatter, W.J., Schmechel, D.E., Gaskell, P.C., Small, G.W., Roses, A.D., Haines, J.L., and Pericak-Vance, M.A. (1993). Gene dose of apolipoprotein E type 4 allele and the risk of Alzheimer's disease in late onset families. *Science* 261, 921-923.

Costa-Mattioli, M., Gobert, D., Harding, H., Herdy, B., Azzi, M., Bruno, M., Bidinosti, M., Ben Mamou, C., Marcinkiewicz, E., Yoshida, M., *et al.* (2005). Translational control of hippocampal synaptic plasticity and memory by the eIF2alpha kinase GCN2. *Nature* 436, 1166-1173.

Costa-Mattioli, M., Gobert, D., Stern, E., Gamache, K., Colina, R., Cuello, C., Sossin, W., Kaufman, R., Pelletier, J., Rosenblum, K., *et al.* (2007). eIF2alpha phosphorylation bidirectionally regulates the switch from short- to long-term synaptic plasticity and memory. *Cell* 129, 195-206.

de Leon, M.J., Ferris, S.H., George, A.E., Christman, D.R., Fowler, J.S., Gentes, C., Reisberg, B., Gee, B., Emmerich, M., Yonekura, Y., *et al.* (1983). Positron emission tomographic studies of aging and Alzheimer disease. *AJNR Am J Neuroradiol* 4, 568-571.

de Leon, M.J., Mosconi, L., Blennow, K., DeSanti, S., Zinkowski, R., Mehta, P.D., Pratico, D., Tsui, W., Saint Louis, L.A., Sobanska, L., *et al.* (2007). Imaging and CSF studies in the preclinical diagnosis of Alzheimer's disease. *Annals of the New York Academy of Sciences* 1097, 114-145.

De Pietri Tonelli, D., Mihailovich, M., Di Cesare, A., Codazzi, F., Grohovaz, F., and Zacchetti, D. (2004). Translational regulation of BACE-1 expression in neuronal and non-neuronal cells. *Nucleic Acids Res* 32, 1808-1817.

De Strooper, B. (2003). Aph-1, Pen-2, and Nicastrin with Presenilin generate an active gamma-Secretase complex. *Neuron* 38, 9-12.

De Strooper, B., Annaert, W., Cupers, P., Saftig, P., Craessaerts, K., Mumm, J.S., Schroeter, E.H., Schrijvers, V., Wolfe, M.S., Ray, W.J., *et al.* (1999). A presenilin-1-dependent gamma-secretase-like protease mediates release of Notch intracellular domain. *Nature* 398, 518-522.

De Strooper, B., Saftig, P., Craessaerts, K., Vanderstichele, H., Guhde, G., Annaert, W., Von Figura, K., and Van Leuven, F. (1998). Deficiency of presenilin-1 inhibits the normal cleavage of amyloid precursor protein. *Nature* 391, 387-390.

Decarli, C. (2004). Vascular factors in dementia: an overview. *J Neurol Sci* 226, 19-23.

DeGracia, D.J., and Hu, B.R. (2007). Irreversible translation arrest in the reperfused brain. *J Cereb Blood Flow Metab* 27, 875-893.

Delabar, J.M., Goldgaber, D., Lamour, Y., Nicole, A., Huret, J.L., de Grouchy, J., Brown, P., Gajdusek, D.C., and Sinet, P.M. (1987). Beta amyloid gene duplication in Alzheimer's disease and karyotypically normal Down syndrome. *Science* 235, 1390-1392.

- Delepine, M., Nicolino, M., Barrett, T., Golamaully, M., Lathrop, G.M., and Julier, C. (2000). EIF2AK3, encoding translation initiation factor 2-alpha kinase 3, is mutated in patients with Wolcott-Rallison syndrome. *Nature genetics* 25, 406-409.
- Deng, J., Harding, H.P., Raught, B., Gingras, A.C., Berlanga, J.J., Scheuner, D., Kaufman, R.J., Ron, D., and Sonenberg, N. (2002). Activation of GCN2 in UV-irradiated cells inhibits translation. *Curr Biol* 12, 1279-1286.
- Deuss, M., Reiss, K., and Hartmann, D. (2008). Part-time alpha-secretases: the functional biology of ADAM 9, 10 and 17. *Current Alzheimer research* 5, 187-201.
- Dever, T.E., Feng, L., Wek, R.C., Cigan, A.M., Donahue, T.F., and Hinnebusch, A.G. (1992). Phosphorylation of initiation factor 2 alpha by protein kinase GCN2 mediates gene-specific translational control of GCN4 in yeast. *Cell* 68, 585-596.
- Devries-Seimon, T., Li, Y., Yao, P.M., Stone, E., Wang, Y., Davis, R.J., Flavell, R., and Tabas, I. (2005). Cholesterol-induced macrophage apoptosis requires ER stress pathways and engagement of the type A scavenger receptor. *The Journal of cell biology* 171, 61-73.
- Diagnostic and Statistical Manual - Text Revision (DSM-IV-TR™, 2000). Ed. Michael B. First, MD. Washington, D.C.: American Psychiatric Association, 2000. 290.4 & 294.1.
- Dietrich, J., Lacagnina, M., Gass, D., Richfield, E., Mayer-Proschel, M., Noble, M., Torres, C., and Proschel, C. (2005). EIF2B5 mutations compromise GFAP+ astrocyte generation in vanishing white matter leukodystrophy. *Nature medicine* 11, 277-283.
- Dominguez, D., Tournoy, J., Hartmann, D., Huth, T., Cryns, K., Deforce, S., Serneels, L., Camacho, I.E., Marjaux, E., Craessaerts, K., *et al.* (2005). Phenotypic and biochemical analyses of BACE1- and BACE2-deficient mice. *The Journal of biological chemistry* 280, 30797-30806.
- Domnitz, S.B., Robbins, E.M., Hoang, A.W., Garcia-Alloza, M., Hyman, B.T., Rebeck, G.W., Greenberg, S.M., Bacskai, B.J., and Frosch, M.P. (2005). Progression of cerebral amyloid angiopathy in transgenic mouse models of Alzheimer disease. *Journal of neuropathology and experimental neurology* 64, 588-594.
- Donze, O., Deng, J., Curran, J., Sladek, R., Picard, D., and Sonenberg, N. (2004). The protein kinase PKR: a molecular clock that sequentially activates survival and death programs. *The EMBO journal* 23, 564-571.
- Dunn-Meynell, A.A., Rawson, N.E., and Levin, B.E. (1998). Distribution and phenotype of neurons containing the ATP-sensitive K<sup>+</sup> channel in rat brain. *Brain research* 814, 41-54.

- Ehehalt, R., Michel, B., De Pietri Tonelli, D., Zacchetti, D., Simons, K., and Keller, P. (2002). Splice variants of the beta-site APP-cleaving enzyme BACE1 in human brain and pancreas. *Biochem Biophys Res Commun* 293, 30-37.
- Eizirik, D.L., Cardozo, A.K., and Cnop, M. (2008). The role for endoplasmic reticulum stress in diabetes mellitus. *Endocrine reviews* 29, 42-61.
- Esch, F.S., Keim, P.S., Beattie, E.C., Blacher, R.W., Culwell, A.R., Oltersdorf, T., McClure, D., and Ward, P.J. (1990). Cleavage of amyloid beta peptide during constitutive processing of its precursor. *Science* 248, 1122-1124.
- Esch, T., Stefano, G.B., Fricchione, G.L., and Benson, H. (2002). The role of stress in neurodegenerative diseases and mental disorders. *Neuro Endocrinol Lett* 23, 199-208.
- Faghihi, M.A., Modarresi, F., Khalil, A.M., Wood, D.E., Sahagan, B.G., Morgan, T.E., Finch, C.E., St Laurent, G., 3rd, Kenny, P.J., and Wahlestedt, C. (2008). Expression of a noncoding RNA is elevated in Alzheimer's disease and drives rapid feed-forward regulation of beta-secretase. *Nat Med* 14, 723-730.
- Flynn, A., and Proud, C.G. (1995). Serine 209, not serine 53, is the major site of phosphorylation in initiation factor eIF-4E in serum-treated Chinese hamster ovary cells. *The Journal of biological chemistry* 270, 21684-21688.
- Fogli, A., Schiffmann, R., Hugendubler, L., Combes, P., Bertini, E., Rodriguez, D., Kimball, S.R., and Boespflug-Tanguy, O. (2004). Decreased guanine nucleotide exchange factor activity in eIF2B-mutated patients. *Eur J Hum Genet* 12, 561-566.
- Friedman, R.M., Esteban, R.M., Metz, D.H., Tovell, D.R., Kerr, I.M., and Williamson, R. (1972). Translation of RNA by L cell extracts: Effect of interferon. *FEBS letters* 24, 273-277.
- Fukumoto, H., Cheung, B.S., Hyman, B.T., and Irizarry, M.C. (2002). Beta-secretase protein and activity are increased in the neocortex in Alzheimer disease. *Arch Neurol* 59, 1381-1389.
- Fukunaga, R., and Hunter, T. (1997). MNK1, a new MAP kinase-activated protein kinase, isolated by a novel expression screening method for identifying protein kinase substrates. *The EMBO journal* 16, 1921-1933.
- Garcia, M.A., Meurs, E.F., and Esteban, M. (2007). The dsRNA protein kinase PKR: virus and cell control. *Biochimie* 89, 799-811.
- Gasparini, L., Racchi, M., Benussi, L., Curti, D., Binetti, G., Bianchetti, A., Trabucchi, M., and Govoni, S. (1997). Effect of energy shortage and oxidative stress on amyloid precursor protein metabolism in COS cells. *Neurosci Lett* 231, 113-117.

- Ghosh, A.K., Bilcer, G., Hong, L., Koelsch, G., and Tang, J. (2007). Memapsin 2 (beta-secretase) inhibitor drug, between fantasy and reality. *Curr Alzheimer Res* 4, 418-422.
- Gingras, A.C., Raught, B., and Sonenberg, N. (1999). eIF4 initiation factors: effectors of mRNA recruitment to ribosomes and regulators of translation. *Annual review of biochemistry* 68, 913-963.
- Glenner, G.G., and Wong, C.W. (1984a). Alzheimer's disease and Down's syndrome: sharing of a unique cerebrovascular amyloid fibril protein. *Biochem Biophys Res Commun* 122, 1131-1135.
- Glenner, G.G., and Wong, C.W. (1984b). Alzheimer's disease: initial report of the purification and characterization of a novel cerebrovascular amyloid protein. *Biochem Biophys Res Commun* 120, 885-890.
- Goldgaber, D., Lerman, M.I., McBride, O.W., Saffiotti, U., and Gajdusek, D.C. (1987). Characterization and chromosomal localization of a cDNA encoding brain amyloid of Alzheimer's disease. *Science* 235, 877-880.
- Gotz, J., Chen, F., van Dorpe, J., and Nitsch, R.M. (2001). Formation of neurofibrillary tangles in P301 $\tau$  transgenic mice induced by A $\beta$  42 fibrils. *Science* 293, 1491-1495.
- Gouras, G.K., Almeida, C.G., and Takahashi, R.H. (2005). Intraneuronal A $\beta$  accumulation and origin of plaques in Alzheimer's disease. *Neurobiology of aging* 26, 1235-1244.
- Gouras, G.K., Xu, H., Jovanovic, J.N., Buxbaum, J.D., Wang, R., Greengard, P., Relkin, N.R., and Gandy, S. (1998). Generation and regulation of beta-amyloid peptide variants by neurons. *J Neurochem* 71, 1920-1925.
- Grayzel, A.I., Horchner, P., and London, I.M. (1966). The stimulation of globin synthesis by heme. *Proceedings of the National Academy of Sciences of the United States of America* 55, 650-655.
- Haass, C., Capell, A., Citron, M., Teplow, D.B., and Selkoe, D.J. (1995a). The vacuolar H(+)-ATPase inhibitor bafilomycin A1 differentially affects proteolytic processing of mutant and wild-type beta-amyloid precursor protein. *J Biol Chem* 270, 6186-6192.
- Haass, C., Hung, A.Y., Schlossmacher, M.G., Oltersdorf, T., Teplow, D.B., and Selkoe, D.J. (1993). Normal cellular processing of the beta-amyloid precursor protein results in the secretion of the amyloid beta peptide and related molecules. *Annals of the New York Academy of Sciences* 695, 109-116.

- Haass, C., Lemere, C.A., Capell, A., Citron, M., Seubert, P., Schenk, D., Lannfelt, L., and Selkoe, D.J. (1995b). The Swedish mutation causes early-onset Alzheimer's disease by beta-secretase cleavage within the secretory pathway. *Nature medicine* 1, 1291-1296.
- Haass, C., Schlossmacher, M.G., Hung, A.Y., Vigo-Pelfrey, C., Mellon, A., Ostaszewski, B.L., Lieberburg, I., Koo, E.H., Schenk, D., Teplow, D.B., and et al. (1992). Amyloid beta-peptide is produced by cultured cells during normal metabolism. *Nature* 359, 322-325.
- Hachet, O., and Ephrussi, A. (2004). Splicing of oskar RNA in the nucleus is coupled to its cytoplasmic localization. *Nature* 428, 959-963.
- Han, A.P., Fleming, M.D., and Chen, J.J. (2005). Heme-regulated eIF2alpha kinase modifies the phenotypic severity of murine models of erythropoietic protoporphyria and beta-thalassemia. *The Journal of clinical investigation* 115, 1562-1570.
- Han, A.P., Yu, C., Lu, L., Fujiwara, Y., Browne, C., Chin, G., Fleming, M., Leboulch, P., Orkin, S.H., and Chen, J.J. (2001). Heme-regulated eIF2alpha kinase (HRI) is required for translational regulation and survival of erythroid precursors in iron deficiency. *The EMBO journal* 20, 6909-6918.
- Haniu, M., Denis, P., Young, Y., Mendiaz, E.A., Fuller, J., Hui, J.O., Bennett, B.D., Kahn, S., Ross, S., Burgess, T., et al. (2000). Characterization of Alzheimer's beta - secretase protein BACE. A pepsin family member with unusual properties. *J Biol Chem* 275, 21099-21106.
- Harding, H.P., Zhang, Y., Bertolotti, A., Zeng, H., and Ron, D. (2000). Perk is essential for translational regulation and cell survival during the unfolded protein response. *Molecular cell* 5, 897-904.
- Harding, H.P., Zhang, Y., and Ron, D. (1999). Protein translation and folding are coupled by an endoplasmic-reticulum-resident kinase. *Nature* 397, 271-274.
- Hardy, J., and Selkoe, D.J. (2002). The amyloid hypothesis of Alzheimer's disease: progress and problems on the road to therapeutics. *Science* 297, 353-356.
- He, B., Chou, J., Liebermann, D.A., Hoffman, B., and Roizman, B. (1996). The carboxyl terminus of the murine MyD116 gene substitutes for the corresponding domain of the gamma(1)34.5 gene of herpes simplex virus to preclude the premature shutoff of total protein synthesis in infected human cells. *Journal of virology* 70, 84-90.
- He, W., Lu, Y., Qahwash, I., Hu, X.Y., Chang, A., and Yan, R. (2004). Reticulon family members modulate BACE1 activity and amyloid-beta peptide generation. *Nature medicine* 10, 959-965.

Hebert, S.S., Horre, K., Nicolai, L., Papadopoulou, A.S., Mandemakers, W., Silahtaroglu, A.N., Kauppinen, S., Delacourte, A., and De Strooper, B. (2008). Loss of microRNA cluster miR-29a/b-1 in sporadic Alzheimer's disease correlates with increased BACE1/beta-secretase expression. *Proceedings of the National Academy of Sciences of the United States of America* 105, 6415-6420.

Hetz, C., Russelakis-Carneiro, M., Maundrell, K., Castilla, J., and Soto, C. (2003). Caspase-12 and endoplasmic reticulum stress mediate neurotoxicity of pathological prion protein. *The EMBO journal* 22, 5435-5445.

Hinnebusch, A.G. (1984). Evidence for translational regulation of the activator of general amino acid control in yeast. *Proceedings of the National Academy of Sciences of the United States of America* 81, 6442-6446.

Holcik, M., and Sonenberg, N. (2005). Translational control in stress and apoptosis. *Nat Rev Mol Cell Biol* 6, 318-327.

Holsinger, R.M., McLean, C.A., Beyreuther, K., Masters, C.L., and Evin, G. (2002). Increased expression of the amyloid precursor beta-secretase in Alzheimer's disease. *Ann Neurol* 51, 783-786.

Holtz, W.A., and O'Malley, K.L. (2003). Parkinsonian mimetics induce aspects of unfolded protein response in death of dopaminergic neurons. *The Journal of biological chemistry* 278, 19367-19377.

Holtz, W.A., Turetzky, J.M., and O'Malley, K.L. (2005). Microarray expression profiling identifies early signaling transcripts associated with 6-OHDA-induced dopaminergic cell death. *Antioxidants & redox signaling* 7, 639-648.

Hoozemans, J.J., Veerhuis, R., Van Haastert, E.S., Rozemuller, J.M., Baas, F., Eikelenboom, P., and Scheper, W. (2005). The unfolded protein response is activated in Alzheimer's disease. *Acta neuropathologica* 110, 165-172.

Hoyer, A., Bardenheuer, H.J., Martin, E., and Plaschke, K. (2005). Amyloid precursor protein (APP) and its derivatives change after cellular energy depletion. An in vitro-study. *J Neural Transm* 112, 239-253.

Hsiao, K., Chapman, P., Nilsen, S., Eckman, C., Harigaya, Y., Younkin, S., Yang, F., and Cole, G. (1996). Correlative memory deficits, Abeta elevation, and amyloid plaques in transgenic mice. *Science* 274, 99-102.

Hsu, L.C., Park, J.M., Zhang, K., Luo, J.L., Maeda, S., Kaufman, R.J., Eckmann, L., Guiney, D.G., and Karin, M. (2004). The protein kinase PKR is required for macrophage apoptosis after activation of Toll-like receptor 4. *Nature* 428, 341-345.



- Hu, C., Pang, S., Kong, X., Velleca, M., and Lawrence, J.C., Jr. (1994). Molecular cloning and tissue distribution of PHAS-I, an intracellular target for insulin and growth factors. *Proceedings of the National Academy of Sciences of the United States of America* *91*, 3730-3734.
- Hu, X., Hicks, C.W., He, W., Wong, P., Macklin, W.B., Trapp, B.D., and Yan, R. (2006). Bace1 modulates myelination in the central and peripheral nervous system. *Nat Neurosci* *9*, 1520-1525.
- Huse, J.T., and Doms, R.W. (2000). Closing in on the amyloid cascade: recent insights into the cell biology of Alzheimer's disease. *Molecular neurobiology* *22*, 81-98.
- Hussain, I., Hawkins, J., Shikotra, A., Riddell, D.R., Faller, A., and Dingwall, C. (2003). Characterization of the ectodomain shedding of the beta-site amyloid precursor protein-cleaving enzyme 1 (BACE1). *The Journal of biological chemistry* *278*, 36264-36268.
- Hussain, I., Powell, D., Howlett, D.R., Tew, D.G., Meek, T.D., Chapman, C., Gloger, I.S., Murphy, K.E., Southan, C.D., Ryan, D.M., *et al.* (1999). Identification of a novel aspartic protease (Asp 2) as beta-secretase. *Mol Cell Neurosci* *14*, 419-427.
- Hyman, B.T., Strickland, D., and Rebeck, G.W. (2000). Role of the low-density lipoprotein receptor-related protein in beta-amyloid metabolism and Alzheimer disease. *Archives of neurology* *57*, 646-650.
- Jackson, R.J., and Standart, N. (2007). How do microRNAs regulate gene expression? *Sci STKE* *2007*, re1.
- Jiang, H.Y., Wek, S.A., McGrath, B.C., Scheuner, D., Kaufman, R.J., Cavener, D.R., and Wek, R.C. (2003). Phosphorylation of the alpha subunit of eukaryotic initiation factor 2 is required for activation of NF-kappaB in response to diverse cellular stresses. *Molecular and cellular biology* *23*, 5651-5663.
- Johnson, G.L., and Nakamura, K. (2007). The c-jun kinase/stress-activated pathway: regulation, function and role in human disease. *Biochimica et biophysica acta* *1773*, 1341-1348.
- Joshi, B., Cai, A.L., Keiper, B.D., Minich, W.B., Mendez, R., Beach, C.M., Stepinski, J., Stolarski, R., Darzynkiewicz, E., and Rhoads, R.E. (1995). Phosphorylation of eukaryotic protein synthesis initiation factor 4E at Ser-209. *The Journal of biological chemistry* *270*, 14597-14603.
- Jousse, C., Oyadomari, S., Novoa, I., Lu, P., Zhang, Y., Harding, H.P., and Ron, D. (2003). Inhibition of a constitutive translation initiation factor 2alpha phosphatase, CReP, promotes survival of stressed cells. *The Journal of cell biology* *163*, 767-775.

Kamenetz, F., Tomita, T., Hsieh, H., Seabrook, G., Borchelt, D., Iwatsubo, T., Sisodia, S., and Malinow, R. (2003). APP processing and synaptic function. *Neuron* 37, 925-937.

Kang, H., and Schuman, E.M. (1996). A requirement for local protein synthesis in neurotrophin-induced hippocampal synaptic plasticity. *Science* (New York, N.Y.) 273, 1402-1406.

Kang, J., Lemaire, H.G., Unterbeck, A., Salbaum, J.M., Masters, C.L., Grzeschik, K.H., Multhaup, G., Beyreuther, K., and Muller-Hill, B. (1987). The precursor of Alzheimer's disease amyloid A4 protein resembles a cell-surface receptor. *Nature* 325, 733-736.

Katzman, R. (1976). Editorial: The prevalence and malignancy of Alzheimer disease. A major killer. *Arch Neurol* 33, 217-218.

Kelleher, R.J., 3rd, Govindarajan, A., Jung, H.Y., Kang, H., and Tonegawa, S. (2004). Translational control by MAPK signaling in long-term synaptic plasticity and memory. *Cell* 116, 467-479.

Kheradpezhoh, M., Shavali, S., and Ebadi, M. (2003). Salsolinol causing parkinsonism activates endoplasmic reticulum-stress signaling pathways in human dopaminergic SK-N-SH cells. *Neuro-Signals* 12, 315-324.

Kim, D.Y., Carey, B.W., Wang, H., Ingano, L.A., Binshtok, A.M., Wertz, M.H., Pettingell, W.H., He, P., Lee, V.M., Woolf, C.J., and Kovacs, D.M. (2007). BACE1 regulates voltage-gated sodium channels and neuronal activity. *Nat Cell Biol* 9, 755-764.

Kitazume, S., Nakagawa, K., Oka, R., Tachida, Y., Ogawa, K., Luo, Y., Citron, M., Shitara, H., Taya, C., Yonekawa, H., *et al.* (2005). In vivo cleavage of alpha2,6-sialyltransferase by Alzheimer beta-secretase. *J Biol Chem* 280, 8589-8595.

Knops, J., Suomensaaari, S., Lee, M., McConlogue, L., Seubert, P., and Sinha, S. (1995). Cell-type and amyloid precursor protein-type specific inhibition of A beta release by bafilomycin A1, a selective inhibitor of vacuolar ATPases. *J Biol Chem* 270, 2419-2422.

Koh, Y.H., von Arnim, C.A., Hyman, B.T., Tanzi, R.E., and Tesco, G. (2005). BACE is degraded via the lysosomal pathway. *The Journal of biological chemistry* 280, 32499-32504.

Koo, E.H., and Squazzo, S.L. (1994). Evidence that production and release of amyloid beta-protein involves the endocytic pathway. *J Biol Chem* 269, 17386-17389.

Koritzinsky, M., Rouschop, K.M., van den Beucken, T., Magagnin, M.G., Savelkoul, K., Lambin, P., and Wouters, B.G. (2007). Phosphorylation of eIF2alpha is required for

mRNA translation inhibition and survival during moderate hypoxia. *Radiother Oncol* 83, 353-361.

Koromilas, A.E., Roy, S., Barber, G.N., Katze, M.G., and Sonenberg, N. (1992). Malignant transformation by a mutant of the IFN-inducible dsRNA-dependent protein kinase. *Science (New York, N.Y)* 257, 1685-1689.

Kosik, K.S., Joachim, C.L., and Selkoe, D.J. (1986). Microtubule-associated protein tau (tau) is a major antigenic component of paired helical filaments in Alzheimer disease. *Proc Natl Acad Sci U S A* 83, 4044-4048.

Kouroku, Y., Fujita, E., Jimbo, A., Kikuchi, T., Yamagata, T., Momoi, M.Y., Kominami, E., Kuida, K., Sakamaki, K., Yonehara, S., and Momoi, T. (2002). Polyglutamine aggregates stimulate ER stress signals and caspase-12 activation. *Human molecular genetics* 11, 1505-1515.

Kuhn, P.H., Marjaux, E., Imhof, A., De Strooper, B., Haass, C., and Lichtenthaler, S.F. (2007). Regulated intramembrane proteolysis of the interleukin-1 receptor II by alpha-, beta-, and gamma-secretase. *J Biol Chem* 282, 11982-11995.

Kumar, R., Azam, S., Sullivan, J.M., Owen, C., Cavener, D.R., Zhang, P., Ron, D., Harding, H.P., Chen, J.J., Han, A., *et al.* (2001). Brain ischemia and reperfusion activates the eukaryotic initiation factor 2alpha kinase, PERK. *Journal of neurochemistry* 77, 1418-1421.

Kumar, V., Sabatini, D., Pandey, P., Gingras, A.C., Majumder, P.K., Kumar, M., Yuan, Z.M., Carmichael, G., Weichselbaum, R., Sonenberg, N., *et al.* (2000). Regulation of the rapamycin and FKBP-target 1/mammalian target of rapamycin and cap-dependent initiation of translation by the c-Abl protein-tyrosine kinase. *The Journal of biological chemistry* 275, 10779-10787.

Laird, F.M., Cai, H., Savonenko, A.V., Farah, M.H., He, K., Melnikova, T., Wen, H., Chiang, H.C., Xu, G., Koliatsos, V.E., *et al.* (2005). BACE1, a major determinant of selective vulnerability of the brain to amyloid-beta amyloidogenesis, is essential for cognitive, emotional, and synaptic functions. *J Neurosci* 25, 11693-11709.

Lammich, S., Schobel, S., Zimmer, A.K., Lichtenthaler, S.F., and Haass, C. (2004). Expression of the Alzheimer protease BACE1 is suppressed via its 5'-untranslated region. *EMBO Rep* 5, 620-625.

Larner, S.F., Hayes, R.L., McKinsey, D.M., Pike, B.R., and Wang, K.K. (2004). Increased expression and processing of caspase-12 after traumatic brain injury in rats. *Journal of neurochemistry* 88, 78-90.

- Lawrence, J.C., Jr., Fadden, P., Haystead, T.A., and Lin, T.A. (1997). PHAS proteins as mediators of the actions of insulin, growth factors and cAMP on protein synthesis and cell proliferation. *Advances in enzyme regulation* 37, 239-267.
- Lazaris-Karatzas, A., Montine, K.S., and Sonenberg, N. (1990). Malignant transformation by a eukaryotic initiation factor subunit that binds to mRNA 5' cap. *Nature* 345, 544-547.
- Lee, E.B., Zhang, B., Liu, K., Greenbaum, E.A., Doms, R.W., Trojanowski, J.Q., and Lee, V.M. (2005). BACE overexpression alters the subcellular processing of APP and inhibits Abeta deposition in vivo. *J Cell Biol* 168, 291-302.
- Lee, S.B., Green, S.R., Mathews, M.B., and Esteban, M. (1994). Activation of the double-stranded RNA (dsRNA)-activated human protein kinase in vivo in the absence of its dsRNA binding domain. *Proceedings of the National Academy of Sciences of the United States of America* 91, 10551-10555.
- Leegwater, P.A., Vermeulen, G., Konst, A.A., Naidu, S., Mulders, J., Visser, A., Kersbergen, P., Mobach, D., Fonds, D., van Berkel, C.G., *et al.* (2001). Subunits of the translation initiation factor eIF2B are mutant in leukoencephalopathy with vanishing white matter. *Nature genetics* 29, 383-388.
- Levin, B.E., Dunn-Meynell, A.A., and Routh, V.H. (1999). Brain glucose sensing and body energy homeostasis: role in obesity and diabetes. *The American journal of physiology* 276, R1223-1231.
- Levin, D., Ranu, R.S., Ernst, V., and London, I.M. (1976). Regulation of protein synthesis in reticulocyte lysates: phosphorylation of methionyl-tRNA<sup>f</sup> binding factor by protein kinase activity of translational inhibitor isolated from hemedeficient lysates. *Proceedings of the National Academy of Sciences of the United States of America* 73, 3112-3116.
- Levin, D.H., Ranu, R.S., Ernst, V., Fifer, M.A., and London, L.M. (1975). Association of a cyclic AMP-dependent protein kinase with a purified translational inhibitor isolated from hemin-deficient rabbit reticulocyte lysates. *Proceedings of the National Academy of Sciences of the United States of America* 72, 4849-4853.
- Lewis, J., Dickson, D.W., Lin, W.L., Chisholm, L., Corral, A., Jones, G., Yen, S.H., Sahara, N., Skipper, L., Yager, D., *et al.* (2001). Enhanced neurofibrillary degeneration in transgenic mice expressing mutant tau and APP. *Science* 293, 1487-1491.
- Li, Q., and Sudhof, T.C. (2004). Cleavage of amyloid-beta precursor protein and amyloid-beta precursor-like protein by BACE 1. *J Biol Chem* 279, 10542-10550.
- Li, R., Lindholm, K., Yang, L.B., Yue, X., Citron, M., Yan, R., Beach, T., Sue, L., Sabbagh, M., Cai, H., *et al.* (2004). Amyloid beta peptide load is correlated with

increased beta-secretase activity in sporadic Alzheimer's disease patients. *Proc Natl Acad Sci U S A* 101, 3632-3637.

Li, Y., Schwabe, R.F., DeVries-Seimon, T., Yao, P.M., Gerbod-Giannone, M.C., Tall, A.R., Davis, R.J., Flavell, R., Brenner, D.A., and Tabas, I. (2005). Free cholesterol-loaded macrophages are an abundant source of tumor necrosis factor-alpha and interleukin-6: model of NF-kappaB- and map kinase-dependent inflammation in advanced atherosclerosis. *The Journal of biological chemistry* 280, 21763-21772.

Lichtenthaler, S.F., Dominguez, D.I., Westmeyer, G.G., Reiss, K., Haass, C., Saftig, P., De Strooper, B., and Seed, B. (2003). The cell adhesion protein P-selectin glycoprotein ligand-1 is a substrate for the aspartyl protease BACE1. *J Biol Chem* 278, 48713-48719.

Lin, W., Harding, H.P., Ron, D., and Popko, B. (2005). Endoplasmic reticulum stress modulates the response of myelinating oligodendrocytes to the immune cytokine interferon-gamma. *The Journal of cell biology* 169, 603-612.

Lin, X., Koelsch, G., Wu, S., Downs, D., Dashti, A., and Tang, J. (2000). Human aspartic protease memapsin 2 cleaves the beta-secretase site of beta-amyloid precursor protein. *Proc Natl Acad Sci U S A* 97, 1456-1460.

Lu, L., Han, A.P., and Chen, J.J. (2001). Translation initiation control by heme-regulated eukaryotic initiation factor 2alpha kinase in erythroid cells under cytoplasmic stresses. *Molecular and cellular biology* 21, 7971-7980.

Lu, P.D., Jousse, C., Marciniak, S.J., Zhang, Y., Novoa, I., Scheuner, D., Kaufman, R.J., Ron, D., and Harding, H.P. (2004). Cytoprotection by pre-emptive conditional phosphorylation of translation initiation factor 2. *The EMBO journal* 23, 169-179.

Luchsinger, J.A. (2008). Adiposity, hyperinsulinemia, diabetes and Alzheimer's disease: an epidemiological perspective. *European journal of pharmacology* 585, 119-129.

Lue, L.F., Kuo, Y.M., Roher, A.E., Brachova, L., Shen, Y., Sue, L., Beach, T., Kurth, J.H., Rydel, R.E., and Rogers, J. (1999). Soluble amyloid beta peptide concentration as a predictor of synaptic change in Alzheimer's disease. *Am J Pathol* 155, 853-862.

Luo, Y., Bolon, B., Kahn, S., Bennett, B.D., Babu-Khan, S., Denis, P., Fan, W., Kha, H., Zhang, J., Gong, Y., *et al.* (2001). Mice deficient in BACE1, the Alzheimer's beta-secretase, have normal phenotype and abolished beta-amyloid generation. *Nat Neurosci* 4, 231-232.

Ma, Y., Brewer, J.W., Diehl, J.A., and Hendershot, L.M. (2002). Two distinct stress signaling pathways converge upon the CHOP promoter during the mammalian unfolded protein response. *Journal of molecular biology* 318, 1351-1365.

Mackay, E.A., Ehrhard, A., Moniatte, M., Guenet, C., Tardif, C., Tarnus, C., Sorokine, O., Heintzelmann, B., Nay, C., Remy, J.M., *et al.* (1997). A possible role for cathepsins D, E, and B in the processing of beta-amyloid precursor protein in Alzheimer's disease. *Eur J Biochem* 244, 414-425.

Mahley, R.W., and Rall, S.C., Jr. (2000). Apolipoprotein E: far more than a lipid transport protein. *Annual review of genomics and human genetics* 1, 507-537.

Malhotra, J.D., and Kaufman, R.J. (2007). The endoplasmic reticulum and the unfolded protein response. *Seminars in cell & developmental biology* 18, 716-731.

Mao, W., Iwai, C., Qin, F., and Liang, C.S. (2005). Norepinephrine induces endoplasmic reticulum stress and downregulation of norepinephrine transporter density in PC12 cells via oxidative stress. *American journal of physiology* 288, H2381-2389.

Masters, C.L., Simms, G., Weinman, N.A., Multhaup, G., McDonald, B.L., and Beyreuther, K. (1985). Amyloid plaque core protein in Alzheimer disease and Down syndrome. *Proc Natl Acad Sci U S A* 82, 4245-4249.

Maxwell, C.R., and Rabinovitz, M. (1969). Evidence for an inhibitor in the control of globin synthesis by hemin in a reticulocyte lysate. *Biochemical and biophysical research communications* 35, 79-85.

McConlogue, L., Buttini, M., Anderson, J.P., Brigham, E.F., Chen, K.S., Freedman, S.B., Games, D., Johnson-Wood, K., Lee, M., Zeller, M., *et al.* (2007). Partial reduction of BACE1 has dramatic effects on Alzheimer plaque and synaptic pathology in APP Transgenic Mice. *J Biol Chem* 282, 26326-26334.

McKhann, G.M., 2nd, Wenzel, H.J., Robbins, C.A., Sosunov, A.A., and Schwartzkroin, P.A. (2003). Mouse strain differences in kainic acid sensitivity, seizure behavior, mortality, and hippocampal pathology. *Neuroscience* 122, 551-561.

McLean, C.A., Cherny, R.A., Fraser, F.W., Fuller, S.J., Smith, M.J., Beyreuther, K., Bush, A.I., and Masters, C.L. (1999). Soluble pool of Abeta amyloid as a determinant of severity of neurodegeneration in Alzheimer's disease. *Ann Neurol* 46, 860-866.

Mei, L., and Xiong, W.C. (2008). Neuregulin 1 in neural development, synaptic plasticity and schizophrenia. *Nat Rev Neurosci* 9, 437-452.

Mesulam, M., ed. (2000). *Principles of Behavioral and Cognitive Neurology* (New York: Oxford University Press).

Metz, D.H., and Esteban, M. (1972). Interferon inhibits viral protein synthesis in L cells infected with vaccinia virus. *Nature* 238, 385-388.

Meurs, E., Chong, K., Galabru, J., Thomas, N.S., Kerr, I.M., Williams, B.R., and Hovanessian, A.G. (1990). Molecular cloning and characterization of the human double-stranded RNA-activated protein kinase induced by interferon. *Cell* 62, 379-390.

Meurs, E.F., Galabru, J., Barber, G.N., Katze, M.G., and Hovanessian, A.G. (1993). Tumor suppressor function of the interferon-induced double-stranded RNA-activated protein kinase. *Proceedings of the National Academy of Sciences of the United States of America* 90, 232-236.

Mihailovich, M., Thermann, R., Grohovaz, F., Hentze, M.W., and Zacchetti, D. (2007). Complex translational regulation of BACE1 involves upstream AUGs and stimulatory elements within the 5' untranslated region. *Nucleic Acids Res.*

Miller, C.C., McLoughlin, D.M., Lau, K.F., Tennant, M.E., and Rogelj, B. (2006). The X11 proteins, Abeta production and Alzheimer's disease. *Trends Neurosci* 29, 280-285.

Mohajeri, M.H., Saini, K.D., and Nitsch, R.M. (2004). Transgenic BACE expression in mouse neurons accelerates amyloid plaque pathology. *J Neural Transm* 111, 413-425.

Morley, S.J. (1997). Signalling through either the p38 or ERK mitogen-activated protein (MAP) kinase pathway is obligatory for phorbol ester and T cell receptor complex (TCR-CD3)-stimulated phosphorylation of initiation factor (eIF) 4E in Jurkat T cells. *FEBS letters* 418, 327-332.

Morris, A.A. (2005). Cerebral ketone body metabolism. *Journal of inherited metabolic disease* 28, 109-121.

Mosconi, L., Brys, M., Glodzik-Sobanska, L., De Santi, S., Rusinek, H., and de Leon, M.J. (2007). Early detection of Alzheimer's disease using neuroimaging. *Experimental gerontology* 42, 129-138.

Mueller, P.P., and Hinnebusch, A.G. (1986). Multiple upstream AUG codons mediate translational control of GCN4. *Cell* 45, 201-207.

Mullan, M., Crawford, F., Axelman, K., Houlden, H., Lilius, L., Winblad, B., and Lannfelt, L. (1992). A pathogenic mutation for probable Alzheimer's disease in the APP gene at the N-terminus of beta-amyloid. *Nat Genet* 1, 345-347.

Muller, T., Meyer, H.E., Egensperger, R., and Marcus, K. (2008). The amyloid precursor protein intracellular domain (AICD) as modulator of gene expression, apoptosis, and cytoskeletal dynamics-Relevance for Alzheimer's disease. *Prog Neurobiol* 85, 393-406.

Naslund, J., Haroutunian, V., Mohs, R., Davis, K.L., Davies, P., Greengard, P., and Buxbaum, J.D. (2000). Correlation between elevated levels of amyloid beta-peptide in the brain and cognitive decline. *Jama* 283, 1571-1577.

Netzer, W.J., Dou, F., Cai, D., Veach, D., Jean, S., Li, Y., Bornmann, W.G., Clarkson, B., Xu, H., and Greengard, P. (2003). Gleevec inhibits beta-amyloid production but not Notch cleavage. *Proc Natl Acad Sci U S A* *100*, 12444-12449.

Notkola, I.L., Sulkava, R., Pekkanen, J., Erkinjuntti, T., Ehnholm, C., Kivinen, P., Tuomilehto, J., and Nissinen, A. (1998). Serum total cholesterol, apolipoprotein E epsilon 4 allele, and Alzheimer's disease. *Neuroepidemiology* *17*, 14-20.

Novoa, I., Zeng, H., Harding, H.P., and Ron, D. (2001). Feedback inhibition of the unfolded protein response by GADD34-mediated dephosphorylation of eIF2alpha. *The Journal of cell biology* *153*, 1011-1022.

Novoa, I., Zhang, Y., Zeng, H., Jungreis, R., Harding, H.P., and Ron, D. (2003). Stress-induced gene expression requires programmed recovery from translational repression. *The EMBO journal* *22*, 1180-1187.

Nukina, N., and Ihara, Y. (1986). One of the antigenic determinants of paired helical filaments is related to tau protein. *J Biochem* *99*, 1541-1544.

Oakley, H., Cole, S.L., Logan, S., Maus, E., Shao, P., Craft, J., Guillozet-Bongaarts, A., Ohno, M., Disterhoft, J., Van Eldik, L., *et al.* (2006). Intraneuronal beta-amyloid aggregates, neurodegeneration, and neuron loss in transgenic mice with five familial Alzheimer's disease mutations: potential factors in amyloid plaque formation. *J Neurosci* *26*, 10129-10140.

Ohno, M., Chang, L., Tseng, W., Oakley, H., Citron, M., Klein, W.L., Vassar, R., and Disterhoft, J.F. (2006). Temporal memory deficits in Alzheimer's mouse models: rescue by genetic deletion of BACE1. *Eur J Neurosci* *23*, 251-260.

Ohno, M., Sametsky, E.A., Younkin, L.H., Oakley, H., Younkin, S.G., Citron, M., Vassar, R., and Disterhoft, J.F. (2004). BACE1 deficiency rescues memory deficits and cholinergic dysfunction in a mouse model of Alzheimer's disease. *Neuron* *41*, 27-33.

Okada, K., Minamino, T., Tsukamoto, Y., Liao, Y., Tsukamoto, O., Takashima, S., Hirata, A., Fujita, M., Nagamachi, Y., Nakatani, T., *et al.* (2004). Prolonged endoplasmic reticulum stress in hypertrophic and failing heart after aortic constriction: possible contribution of endoplasmic reticulum stress to cardiac myocyte apoptosis. *Circulation* *110*, 705-712.

Oomura, Y., Ooyama, H., Sugimori, M., Nakamura, T., and Yamada, Y. (1974). Glucose inhibition of the glucose-sensitive neurone in the rat lateral hypothalamus. *Nature* *247*, 284-286.

Orrego, F., and Lipmann, F. (1967). Protein synthesis in brain slices. Effects of electrical stimulation and acidic amino acids. *The Journal of biological chemistry* *242*, 665-671.



- Oyadomari, S., Yun, C., Fisher, E.A., Kreglinger, N., Kreibich, G., Oyadomari, M., Harding, H.P., Goodman, A.G., Harant, H., Garrison, J.L., *et al.* (2006). Cotranslocational degradation protects the stressed endoplasmic reticulum from protein overload. *Cell* 126, 727-739.
- Ozcan, U., Yilmaz, E., Ozcan, L., Furuhashi, M., Vaillancourt, E., Smith, R.O., Gorgun, C.Z., and Hotamisligil, G.S. (2006). Chemical chaperones reduce ER stress and restore glucose homeostasis in a mouse model of type 2 diabetes. *Science (New York, N.Y)* 313, 1137-1140.
- Ozmen, L., Woolley, M., Albientz, A., Miss, M.T., Nelboeck, P., Malherbe, P., Czech, C., Gruninger-Leitch, F., Brockhaus, M., Ballard, T., and Jacobsen, H. (2005). BACE/APPV717F double-transgenic mice develop cerebral amyloidosis and inflammation. *Neurodegener Dis* 2, 284-298.
- Panegyres, P.K. (2001). The functions of the amyloid precursor protein gene. *Rev Neurosci* 12, 1-39.
- Paschen, W., Yatsiv, I., Shoham, S., and Shohami, E. (2004). Brain trauma induces X-box protein 1 processing indicative of activation of the endoplasmic reticulum unfolded protein response. *Journal of neurochemistry* 88, 983-992.
- Pastorino, L., Ikin, A.F., Lamprianou, S., Vacaresse, N., Revelli, J.P., Platt, K., Paganetti, P., Mathews, P.M., Harroch, S., and Buxbaum, J.D. (2004). BACE (beta-secretase) modulates the processing of APLP2 in vivo. *Mol Cell Neurosci* 25, 642-649.
- Pavitt, G.D. (2005). eIF2B, a mediator of general and gene-specific translational control. *Biochem Soc Trans* 33, 1487-1492.
- Paz Gavilan, M., Vela, J., Castano, A., Ramos, B., del Rio, J.C., Vitorica, J., and Ruano, D. (2006). Cellular environment facilitates protein accumulation in aged rat hippocampus. *Neurobiology of aging* 27, 973-982.
- Pedruzzi, E., Guichard, C., Ollivier, V., Driss, F., Fay, M., Prunet, C., Marie, J.C., Pouzet, C., Samadi, M., Elbim, C., *et al.* (2004). NAD(P)H oxidase Nox-4 mediates 7-ketocholesterol-induced endoplasmic reticulum stress and apoptosis in human aortic smooth muscle cells. *Molecular and cellular biology* 24, 10703-10717.
- Peel, A.L., and Bredesen, D.E. (2003). Activation of the cell stress kinase PKR in Alzheimer's disease and human amyloid precursor protein transgenic mice. *Neurobiology of disease* 14, 52-62.
- Prostko, C.R., Dholakia, J.N., Brostrom, M.A., and Brostrom, C.O. (1995). Activation of the double-stranded RNA-regulated protein kinase by depletion of endoplasmic reticular calcium stores. *The Journal of biological chemistry* 270, 6211-6215.

- Qing, H., Zhou, W., Christensen, M.A., Sun, X., Tong, Y., and Song, W. (2004). Degradation of BACE by the ubiquitin-proteasome pathway. *Faseb J* 18, 1571-1573.
- Rapoport, M., Dawson, H.N., Binder, L.I., Vitek, M.P., and Ferreira, A. (2002). Tau is essential to beta -amyloid-induced neurotoxicity. *Proc Natl Acad Sci U S A* 99, 6364-6369.
- Rapoport, S.I. (1999a). Functional brain imaging in the resting state and during activation in Alzheimer's disease. Implications for disease mechanisms involving oxidative phosphorylation. *Annals of the New York Academy of Sciences* 893, 138-153.
- Rapoport, S.I. (1999b). In vivo PET imaging and postmortem studies suggest potentially reversible and irreversible stages of brain metabolic failure in Alzheimer's disease. *Eur Arch Psychiatry Clin Neurosci* 249 Suppl 3, 46-55.
- Reiman, E.M., Chen, K., Alexander, G.E., Caselli, R.J., Bandy, D., Osborne, D., Saunders, A.M., and Hardy, J. (2004). Functional brain abnormalities in young adults at genetic risk for late-onset Alzheimer's dementia. *Proc Natl Acad Sci U S A* 101, 284-289.
- Ribak, C.E., Seress, L., and Amaral, D.G. (1985). The development, ultrastructure and synaptic connections of the mossy cells of the dentate gyrus. *J Neurocytol* 14, 835-857.
- Roberts, W.K., Hovanessian, A., Brown, R.E., Clemens, M.J., and Kerr, I.M. (1976). Interferon-mediated protein kinase and low-molecular-weight inhibitor of protein synthesis. *Nature* 264, 477-480.
- Rogaeva, E., Meng, Y., Lee, J.H., Gu, Y., Kawarai, T., Zou, F., Katayama, T., Baldwin, C.T., Cheng, R., Hasegawa, H., *et al.* (2007). The neuronal sortilin-related receptor SORL1 is genetically associated with Alzheimer disease. *Nat Genet* 39, 168-177.
- Rogers, G.W., Jr., Edelman, G.M., and Mauro, V.P. (2004). Differential utilization of upstream AUGs in the beta-secretase mRNA suggests that a shunting mechanism regulates translation. *Proceedings of the National Academy of Sciences of the United States of America* 101, 2794-2799.
- Rogers, J.T., Leiter, L.M., McPhee, J., Cahill, C.M., Zhan, S.S., Potter, H., and Nilsson, L.N. (1999). Translation of the alzheimer amyloid precursor protein mRNA is up-regulated by interleukin-1 through 5'-untranslated region sequences. *The Journal of biological chemistry* 274, 6421-6431.
- Rogers, J.T., Randall, J.D., Cahill, C.M., Eder, P.S., Huang, X., Gunshin, H., Leiter, L., McPhee, J., Sarang, S.S., Utsuki, T., *et al.* (2002). An iron-responsive element type II in the 5'-untranslated region of the Alzheimer's amyloid precursor protein transcript. *The Journal of biological chemistry* 277, 45518-45528.

- Roher, A.E., Palmer, K.C., Yurewicz, E.C., Ball, M.J., and Greenberg, B.D. (1993). Morphological and biochemical analyses of amyloid plaque core proteins purified from Alzheimer disease brain tissue. *J Neurochem* 61, 1916-1926.
- Rossner, S., Sastre, M., Bourne, K., and Lichtenthaler, S.F. (2006). Transcriptional and translational regulation of BACE1 expression--implications for Alzheimer's disease. *Prog Neurobiol* 79, 95-111.
- Rouault, T.A. (2006). The role of iron regulatory proteins in mammalian iron homeostasis and disease. *Nature chemical biology* 2, 406-414.
- Roybal, C.N., Yang, S., Sun, C.W., Hurtado, D., Vander Jagt, D.L., Townes, T.M., and Abcouwer, S.F. (2004). Homocysteine increases the expression of vascular endothelial growth factor by a mechanism involving endoplasmic reticulum stress and transcription factor ATF4. *The Journal of biological chemistry* 279, 14844-14852.
- Ryu, E.J., Angelastro, J.M., and Greene, L.A. (2005). Analysis of gene expression changes in a cellular model of Parkinson disease. *Neurobiology of disease* 18, 54-74.
- Ryu, E.J., Harding, H.P., Angelastro, J.M., Vitolo, O.V., Ron, D., and Greene, L.A. (2002). Endoplasmic reticulum stress and the unfolded protein response in cellular models of Parkinson's disease. *J Neurosci* 22, 10690-10698.
- Saftig, P., Peters, C., von Figura, K., Craessaerts, K., Van Leuven, F., and De Strooper, B. (1996). Amyloidogenic processing of human amyloid precursor protein in hippocampal neurons devoid of cathepsin D. *J Biol Chem* 271, 27241-27244.
- Sambamurti, K., Kinsey, R., Maloney, B., Ge, Y.W., and Lahiri, D.K. (2004). Gene structure and organization of the human beta-secretase (BACE) promoter. *Faseb J* 18, 1034-1036.
- Sasaki, A., Shoji, M., Harigaya, Y., Kawarabayashi, T., Ikeda, M., Naito, M., Matsubara, E., Abe, K., and Nakazato, Y. (2002). Amyloid cored plaques in Tg2576 transgenic mice are characterized by giant plaques, slightly activated microglia, and the lack of paired helical filament-typed, dystrophic neurites. *Virchows Arch* 441, 358-367.
- Saunders, L.R., and Barber, G.N. (2003). The dsRNA binding protein family: critical roles, diverse cellular functions. *Faseb J* 17, 961-983.
- Scheper, G.C., and Proud, C.G. (2002). Does phosphorylation of the cap-binding protein eIF4E play a role in translation initiation? *European journal of biochemistry / FEBS* 269, 5350-5359.
- Scheuner, D., Song, B., McEwen, E., Liu, C., Laybutt, R., Gillespie, P., Saunders, T., Bonner-Weir, S., and Kaufman, R.J. (2001). Translational control is required for the

unfolded protein response and in vivo glucose homeostasis. *Molecular cell* 7, 1165-1176.

Scheuner, D., Vander Mierde, D., Song, B., Flamez, D., Creemers, J.W., Tsukamoto, K., Ribick, M., Schuit, F.C., and Kaufman, R.J. (2005). Control of mRNA translation preserves endoplasmic reticulum function in beta cells and maintains glucose homeostasis. *Nature medicine* 11, 757-764.

Schonlein, C., Probst, A., and Huber, G. (1993). Characterization of proteases with the specificity to cleave at the secretase-site of beta-APP. *Neurosci Lett* 161, 33-36.

Schroder, M., and Kaufman, R.J. (2006). Divergent roles of IRE1alpha and PERK in the unfolded protein response. *Curr Mol Med* 6, 5-36.

Sennvik, K., Bogdanovic, N., Volkmann, I., Fastbom, J., and Benedikz, E. (2004). Beta-secretase-cleaved amyloid precursor protein in Alzheimer brain: a morphologic study. *J Cell Mol Med* 8, 127-134.

Seubert, P., Oltersdorf, T., Lee, M.G., Barbour, R., Blomquist, C., Davis, D.L., Bryant, K., Fritz, L.C., Galasko, D., Thal, L.J., and et al. (1993). Secretion of beta-amyloid precursor protein cleaved at the amino terminus of the beta-amyloid peptide. *Nature* 361, 260-263.

Seubert, P., Vigo-Pelfrey, C., Esch, F., Lee, M., Dovey, H., Davis, D., Sinha, S., Schlossmacher, M., Whaley, J., Swindlehurst, C., and et al. (1992). Isolation and quantification of soluble Alzheimer's beta-peptide from biological fluids. *Nature* 359, 325-327.

Shi, Y., Vattam, K.M., Sood, R., An, J., Liang, J., Stramm, L., and Wek, R.C. (1998). Identification and characterization of pancreatic eukaryotic initiation factor 2 alpha-subunit kinase, PEK, involved in translational control. *Molecular and cellular biology* 18, 7499-7509.

Shoji, M., Golde, T.E., Ghiso, J., Cheung, T.T., Estus, S., Shaffer, L.M., Cai, X.D., McKay, D.M., Tintner, R., Frangione, B., and et al. (1992). Production of the Alzheimer amyloid beta protein by normal proteolytic processing. *Science* 258, 126-129.

Singer, O., Marr, R.A., Rockenstein, E., Crews, L., Coufal, N.G., Gage, F.H., Verma, I.M., and Masliah, E. (2005). Targeting BACE1 with siRNAs ameliorates Alzheimer disease neuropathology in a transgenic model. *Nat Neurosci* 8, 1343-1349.

Sinha, S., Anderson, J.P., Barbour, R., Basi, G.S., Caccavello, R., Davis, D., Doan, M., Dovey, H.F., Frigon, N., Hong, J., et al. (1999). Purification and cloning of amyloid precursor protein beta-secretase from human brain. *Nature* 402, 537-540.

Sisodia, S.S., and St George-Hyslop, P.H. (2002). gamma-Secretase, Notch, Abeta and Alzheimer's disease: where do the presenilins fit in? *Nat Rev Neurosci* 3, 281-290.

Sood, R., Porter, A.C., Olsen, D.A., Cavener, D.R., and Wek, R.C. (2000). A mammalian homologue of GCN2 protein kinase important for translational control by phosphorylation of eukaryotic initiation factor-2alpha. *Genetics* 154, 787-801.

Srivastava, S.P., Davies, M.V., and Kaufman, R.J. (1995). Calcium depletion from the endoplasmic reticulum activates the double-stranded RNA-dependent protein kinase (PKR) to inhibit protein synthesis. *The Journal of biological chemistry* 270, 16619-16624.

Srivastava, S.P., Kumar, K.U., and Kaufman, R.J. (1998). Phosphorylation of eukaryotic translation initiation factor 2 mediates apoptosis in response to activation of the double-stranded RNA-dependent protein kinase. *The Journal of biological chemistry* 273, 2416-2423.

St George-Hyslop, P.H., Tanzi, R.E., Polinsky, R.J., Haines, J.L., Nee, L., Watkins, P.C., Myers, R.H., Feldman, R.G., Pollen, D., Drachman, D., and et al. (1987). The genetic defect causing familial Alzheimer's disease maps on chromosome 21. *Science* 235, 885-890.

Stern, Y. (2006). Cognitive reserve and Alzheimer disease. *Alzheimer Dis Assoc Disord* 20, S69-74.

Steward, O., and Fass, B. (1983). Polyribosomes associated with dendritic spines in the denervated dentate gyrus: evidence for local regulation of protein synthesis during reinnervation. *Progress in brain research* 58, 131-136.

Steward, O., and Levy, W.B. (1982). Preferential localization of polyribosomes under the base of dendritic spines in granule cells of the dentate gyrus. *J Neurosci* 2, 284-291.

Steward, O., and Schuman, E.M. (2001). Protein synthesis at synaptic sites on dendrites. *Annual review of neuroscience* 24, 299-325.

Struhl, K. (1987). The DNA-binding domains of the jun oncoprotein and the yeast GCN4 transcriptional activator protein are functionally homologous. *Cell* 50, 841-846.

Sun, X., He, G., Qing, H., Zhou, W., Dobie, F., Cai, F., Staufenbiel, M., Huang, L.E., and Song, W. (2006). Hypoxia facilitates Alzheimer's disease pathogenesis by up-regulating BACE1 gene expression. *Proc Natl Acad Sci U S A* 103, 18727-18732.

Sutton, M.A., and Schuman, E.M. (2005). Local translational control in dendrites and its role in long-term synaptic plasticity. *Journal of neurobiology* 64, 116-131.

- Tagawa, K., Kunishita, T., Maruyama, K., Yoshikawa, K., Kominami, E., Tsuchiya, T., Suzuki, K., Tabira, T., Sugita, H., and Ishiura, S. (1991). Alzheimer's disease amyloid beta-clipping enzyme (APP secretase): identification, purification, and characterization of the enzyme. *Biochem Biophys Res Commun* 177, 377-387.
- Tamagno, E., Parola, M., Bardini, P., Piccini, A., Borghi, R., Guglielmotto, M., Santoro, G., Davit, A., Danni, O., Smith, M.A., *et al.* (2005). Beta-site APP cleaving enzyme up-regulation induced by 4-hydroxynonenal is mediated by stress-activated protein kinases pathways. *J Neurochem* 92, 628-636.
- Tanahashi, H., and Tabira, T. (2001). Three novel alternatively spliced isoforms of the human beta-site amyloid precursor protein cleaving enzyme (BACE) and their effect on amyloid beta-peptide production. *Neurosci Lett* 307, 9-12.
- Tesco, G., Koh, Y.H., Kang, E.L., Cameron, A.N., Das, S., Sena-Esteves, M., Hiltunen, M., Yang, S.H., Zhong, Z., Shen, Y., *et al.* (2007). Depletion of GGA3 stabilizes BACE and enhances beta-secretase activity. *Neuron* 54, 721-737.
- Tew, K.D., Monks, A., Barone, L., Rosser, D., Akerman, G., Montali, J.A., Wheatley, J.B., and Schmidt, D.E., Jr. (1996). Glutathione-associated enzymes in the human cell lines of the National Cancer Institute Drug Screening Program. *Molecular pharmacology* 50, 149-159.
- Thornton, S., Anand, N., Purcell, D., and Lee, J. (2003). Not just for housekeeping: protein initiation and elongation factors in cell growth and tumorigenesis. *Journal of molecular medicine (Berlin, Germany)* 81, 536-548.
- Tiedge, H., Bloom, F.E., and Richter, D. (1999). RNA, whither goest thou? *Science (New York, N.Y)* 283, 186-187.
- Tobisawa, S., Hozumi, Y., Arawaka, S., Koyama, S., Wada, M., Nagai, M., Aoki, M., Itoyama, Y., Goto, K., and Kato, T. (2003). Mutant SOD1 linked to familial amyotrophic lateral sclerosis, but not wild-type SOD1, induces ER stress in COS7 cells and transgenic mice. *Biochemical and biophysical research communications* 303, 496-503.
- Tong, Y., Zhou, W., Fung, V., Christensen, M.A., Qing, H., Sun, X., and Song, W. (2005). Oxidative stress potentiates BACE1 gene expression and Abeta generation. *J Neural Transm* 112, 455-469.
- Tyler, S.J., Dawbarn, D., Wilcock, G.K., and Allen, S.J. (2002). alpha- and beta-secretase: profound changes in Alzheimer's disease. *Biochem Biophys Res Commun* 299, 373-376.
- Unterberger, U., Hoftberger, R., Gelpi, E., Flicker, H., Budka, H., and Voigtlander, T. (2006). Endoplasmic reticulum stress features are prominent in Alzheimer disease but

not in prion diseases in vivo. *Journal of neuropathology and experimental neurology* 65, 348-357.

Van Den Heuvel, C., Thornton, E., and Vink, R. (2007). Traumatic brain injury and Alzheimer's disease: a review. *Prog Brain Res* 161, 303-316.

van der Knaap, M.S., Leegwater, P.A., Konst, A.A., Visser, A., Naidu, S., Oudejans, C.B., Schutgens, R.B., and Pronk, J.C. (2002). Mutations in each of the five subunits of translation initiation factor eIF2B can cause leukoencephalopathy with vanishing white matter. *Annals of neurology* 51, 264-270.

van Huizen, R., Martindale, J.L., Gorospe, M., and Holbrook, N.J. (2003). P58IPK, a novel endoplasmic reticulum stress-inducible protein and potential negative regulator of eIF2alpha signaling. *The Journal of biological chemistry* 278, 15558-15564.

Vassar, R. (2007). Caspase-3 cleavage of GGA3 stabilizes BACE: implications for Alzheimer's disease. *Neuron* 54, 671-673.

Vassar, R., Bennett, B.D., Babu-Khan, S., Kahn, S., Mendiaz, E.A., Denis, P., Teplow, D.B., Ross, S., Amarante, P., Loeloff, R., *et al.* (1999). Beta-secretase cleavage of Alzheimer's amyloid precursor protein by the transmembrane aspartic protease BACE. *Science* 286, 735-741.

Vazquez de Aldana, C.R., Dever, T.E., and Hinnebusch, A.G. (1993). Mutations in the alpha subunit of eukaryotic translation initiation factor 2 (eIF-2 alpha) that overcome the inhibitory effect of eIF-2 alpha phosphorylation on translation initiation. *Proc Natl Acad Sci U S A* 90, 7215-7219.

Velliquette, R.A., O'Connor, T., and Vassar, R. (2005). Energy inhibition elevates beta-secretase levels and activity and is potentially amyloidogenic in APP transgenic mice: possible early events in Alzheimer's disease pathogenesis. *J Neurosci* 25, 10874-10883.

Vogt, P.K., Bos, T.J., and Doolittle, R.F. (1987). Homology between the DNA-binding domain of the GCN4 regulatory protein of yeast and the carboxyl-terminal region of a protein coded for by the oncogene jun. *Proc Natl Acad Sci U S A* 84, 3316-3319.

von Arnim, C.A., Kinoshita, A., Peltan, I.D., Tangredi, M.M., Herl, L., Lee, B.M., Spoelgen, R., Hshieh, T.T., Ranganathan, S., Battey, F.D., *et al.* (2005). The low density lipoprotein receptor-related protein (LRP) is a novel beta-secretase (BACE1) substrate. *J Biol Chem* 280, 17777-17785.

von Manteuffel, S.R., Dennis, P.B., Pullen, N., Gingras, A.C., Sonenberg, N., and Thomas, G. (1997). The insulin-induced signalling pathway leading to S6 and initiation

factor 4E binding protein 1 phosphorylation bifurcates at a rapamycin-sensitive point immediately upstream of p70s6k. *Molecular and cellular biology* 17, 5426-5436.

Vornov, J.J., and Coyle, J.T. (1991). Glutamate neurotoxicity and the inhibition of protein synthesis in the hippocampal slice. *Journal of neurochemistry* 56, 996-1006.

Walsh, D.M., and Selkoe, D.J. (2007). A beta oligomers - a decade of discovery. *J Neurochem* 101, 1172-1184.

Walter, J., Fluhrer, R., Hartung, B., Willem, M., Kaether, C., Capell, A., Lammich, S., Multhaup, G., and Haass, C. (2001). Phosphorylation regulates intracellular trafficking of beta-secretase. *The Journal of biological chemistry* 276, 14634-14641.

Wang, H., Song, L., Laird, F., Wong, P.C., and Lee, H.K. (2008a). BACE1 knock-outs display deficits in activity-dependent potentiation of synaptic transmission at mossy fiber to CA3 synapses in the hippocampus. *J Neurosci* 28, 8677-8681.

Wang, J., Dickson, D.W., Trojanowski, J.Q., and Lee, V.M. (1999). The levels of soluble versus insoluble brain A $\beta$  distinguish Alzheimer's disease from normal and pathologic aging. *Exp Neurol* 158, 328-337.

Wang, W.X., Rajeev, B.W., Stromberg, A.J., Ren, N., Tang, G., Huang, Q., Rigoutsos, I., and Nelson, P.T. (2008b). The expression of microRNA miR-107 decreases early in Alzheimer's disease and may accelerate disease progression through regulation of beta-site amyloid precursor protein-cleaving enzyme 1. *J Neurosci* 28, 1213-1223.

Wang, X., Flynn, A., Waskiewicz, A.J., Webb, B.L., Vries, R.G., Baines, I.A., Cooper, J.A., and Proud, C.G. (1998). The phosphorylation of eukaryotic initiation factor eIF4E in response to phorbol esters, cell stresses, and cytokines is mediated by distinct MAP kinase pathways. *The Journal of biological chemistry* 273, 9373-9377.

Wang, X., Paulin, F.E., Campbell, L.E., Gomez, E., O'Brien, K., Morrice, N., and Proud, C.G. (2001). Eukaryotic initiation factor 2B: identification of multiple phosphorylation sites in the epsilon-subunit and their functions in vivo. *The EMBO journal* 20, 4349-4359.

Waskiewicz, A.J., Flynn, A., Proud, C.G., and Cooper, J.A. (1997). Mitogen-activated protein kinases activate the serine/threonine kinases Mnk1 and Mnk2. *The EMBO journal* 16, 1909-1920.

Waxman, A.D., Collins, A., and Tschudy, D.P. (1966). Oscillations of hepatic delta-aminolevulinic acid synthetase produced in vivo by heme. *Biochemical and biophysical research communications* 22, 675-683.



Waxman, H.S., and Rabinovitz, M. (1965). Iron Supplementation in Vitro and the State of Aggregation and Function of Reticulocyte Ribosomes in Hemoglobin Synthesis. *Biochemical and biophysical research communications* 19, 538-545.

Webster, M.T., Pearce, B.R., Bowen, D.M., and Francis, P.T. (1998). The effects of perturbed energy metabolism on the processing of amyloid precursor protein in PC12 cells. *J Neural Transm* 105, 839-853.

Wen, Y., Onyewuchi, O., Yang, S., Liu, R., and Simpkins, J.W. (2004). Increased beta-secretase activity and expression in rats following transient cerebral ischemia. *Brain Res* 1009, 1-8.

Wen, Y., Yu, W.H., Maloney, B., Bailey, J., Ma, J., Marie, I., Maurin, T., Wang, L., Figueroa, H., Herman, M., *et al.* (2008). Transcriptional regulation of beta-secretase by p25/cdk5 leads to enhanced amyloidogenic processing. *Neuron* 57, 680-690.

Wilcock, G.K., and Esiri, M.M. (1982). Plaques, tangles and dementia. A quantitative study. *J Neurol Sci* 56, 343-356.

Willem, M., Dewachter, I., Smyth, N., Van Dooren, T., Borghgraef, P., Haass, C., and Van Leuven, F. (2004). beta-site amyloid precursor protein cleaving enzyme 1 increases amyloid deposition in brain parenchyma but reduces cerebrovascular amyloid angiopathy in aging BACE x APP[V717I] double-transgenic mice. *The American journal of pathology* 165, 1621-1631.

Willem, M., Garratt, A.N., Novak, B., Citron, M., Kaufmann, S., Rittger, A., DeStrooper, B., Saftig, P., Birchmeier, C., and Haass, C. (2006). Control of peripheral nerve myelination by the beta-secretase BACE1. *Science* 314, 664-666.

Winklhofer, K.F., Tatzelt, J., and Haass, C. (2008). The two faces of protein misfolding: gain- and loss-of-function in neurodegenerative diseases. *The EMBO journal* 27, 336-349.

Wolf, H., Jelic, V., Gertz, H.J., Nordberg, A., Julin, P., and Wahlund, L.O. (2003). A critical discussion of the role of neuroimaging in mild cognitive impairment. *Acta Neurol Scand Suppl* 179, 52-76.

Wolozin, B., Kellman, W., Ruosseau, P., Celesia, G.G., and Siegel, G. (2000). Decreased prevalence of Alzheimer disease associated with 3-hydroxy-3-methylglutaryl coenzyme A reductase inhibitors. *Arch Neurol* 57, 1439-1443.

Wolozin, B., Manger, J., Bryant, R., Cordy, J., Green, R.C., and McKee, A. (2006). Re-assessing the relationship between cholesterol, statins and Alzheimer's disease. *Acta neurologica Scandinavica* 185, 63-70.

Wong, H.K., Sakurai, T., Oyama, F., Kaneko, K., Wada, K., Miyazaki, H., Kurosawa, M., De Strooper, B., Saftig, P., and Nukina, N. (2005). beta Subunits of voltage-gated sodium channels are novel substrates of beta-site amyloid precursor protein-cleaving enzyme (BACE1) and gamma-secretase. *J Biol Chem* **280**, 23009-23017.

Wong, W.L., Brostrom, M.A., Kuznetsov, G., Gmitter-Yellen, D., and Brostrom, C.O. (1993). Inhibition of protein synthesis and early protein processing by thapsigargin in cultured cells. *The Biochemical journal* **289** ( Pt 1), 71-79.

Wood, J.G., Mirra, S.S., Pollock, N.J., and Binder, L.I. (1986). Neurofibrillary tangles of Alzheimer disease share antigenic determinants with the axonal microtubule-associated protein tau (tau). *Proc Natl Acad Sci U S A* **83**, 4040-4043.

Woods, Y.L., Cohen, P., Becker, W., Jakes, R., Goedert, M., Wang, X., and Proud, C.G. (2001). The kinase DYRK phosphorylates protein-synthesis initiation factor eIF2Bepsilon at Ser539 and the microtubule-associated protein tau at Thr212: potential role for DYRK as a glycogen synthase kinase 3-priming kinase. *The Biochemical journal* **355**, 609-615.

Xiong, Y., Peterson, P.L., and Lee, C.P. (2001). Alterations in cerebral energy metabolism induced by traumatic brain injury. *Neurol Res* **23**, 129-138.

Xue, S., Jia, L., and Jia, J. (2006). Hypoxia and reoxygenation increased BACE1 mRNA and protein levels in human neuroblastoma SH-SY5Y cells. *Neurosci Lett* **405**, 231-235.

Yamada, M. (2000). Cerebral amyloid angiopathy: an overview. *Neuropathology* **20**, 8-22.

Yaman, I., Fernandez, J., Liu, H., Caprara, M., Komar, A.A., Koromilas, A.E., Zhou, L., Snider, M.D., Scheuner, D., Kaufman, R.J., and Hatzoglou, M. (2003). The zipper model of translational control: a small upstream ORF is the switch that controls structural remodeling of an mRNA leader. *Cell* **113**, 519-531.

Yan, R., Bienkowski, M.J., Shuck, M.E., Miao, H., Tory, M.C., Pauley, A.M., Brashier, J.R., Stratman, N.C., Mathews, W.R., Buhl, A.E., *et al.* (1999). Membrane-anchored aspartyl protease with Alzheimer's disease beta-secretase activity. *Nature* **402**, 533-537.

Yan, W., Frank, C.L., Korth, M.J., Sopher, B.L., Novoa, I., Ron, D., and Katze, M.G. (2002). Control of PERK eIF2alpha kinase activity by the endoplasmic reticulum stress-induced molecular chaperone P58IPK. *Proc Natl Acad Sci U S A* **99**, 15920-15925.

Yang, L.B., Lindholm, K., Yan, R., Citron, M., Xia, W., Yang, X.L., Beach, T., Sue, L., Wong, P., Price, D., *et al.* (2003). Elevated beta-secretase expression and enzymatic activity detected in sporadic Alzheimer disease. *Nature medicine* **9**, 3-4.

Yang, Y.L., Reis, L.F., Pavlovic, J., Aguzzi, A., Schafer, R., Kumar, A., Williams, B.R., Aguet, M., and Weissmann, C. (1995). Deficient signaling in mice devoid of double-stranded RNA-dependent protein kinase. *The EMBO journal* 14, 6095-6106.

Yankner, B.A., Lu, T., and Loerch, P. (2008). The aging brain. *Annual review of pathology* 3, 41-66.

Yoo, B.C., Krapfenbauer, K., Cairns, N., Belay, G., Bajo, M., and Lubec, G. (2002). Overexpressed protein disulfide isomerase in brains of patients with sporadic Creutzfeldt-Jakob disease. *Neuroscience letters* 334, 196-200.

Zhang, K., and Kaufman, R.J. (2006). Protein folding in the endoplasmic reticulum and the unfolded protein response. *Handbook of experimental pharmacology*, 69-91.

Zhang, P., McGrath, B., Li, S., Frank, A., Zambito, F., Reinert, J., Gannon, M., Ma, K., McNaughton, K., and Cavener, D.R. (2002a). The PERK eukaryotic initiation factor 2 alpha kinase is required for the development of the skeletal system, postnatal growth, and the function and viability of the pancreas. *Molecular and cellular biology* 22, 3864-3874.

Zhang, P., McGrath, B.C., Reinert, J., Olsen, D.S., Lei, L., Gill, S., Wek, S.A., Vatter, K.M., Wek, R.C., Kimball, S.R., *et al.* (2002b). The GCN2 eIF2alpha kinase is required for adaptation to amino acid deprivation in mice. *Molecular and cellular biology* 22, 6681-6688.

Zhang, X., Zhou, K., Wang, R., Cui, J., Lipton, S.A., Liao, F.F., Xu, H., and Zhang, Y.W. (2007). Hypoxia-inducible factor 1alpha (HIF-1alpha)-mediated hypoxia increases BACE1 expression and beta-amyloid generation. *J Biol Chem* 282, 10873-10880.

Zhao, J., Fu, Y., Yasvoina, M., Shao, P., Hitt, B., O'Connor, T., Logan, S., Maus, E., Citron, M., Berry, R., *et al.* (2007). Beta-site amyloid precursor protein cleaving enzyme 1 levels become elevated in neurons around amyloid plaques: implications for Alzheimer's disease pathogenesis. *J Neurosci* 27, 3639-3649.

Zhao, J., Paganini, L., Mucke, L., Gordon, M., Refolo, L., Carman, M., Sinha, S., Oltersdorf, T., Lieberburg, I., and McConlogue, L. (1996). Beta-secretase processing of the beta-amyloid precursor protein in transgenic mice is efficient in neurons but inefficient in astrocytes. *The Journal of biological chemistry* 271, 31407-31411.

Zheng, H., Jiang, M., Trumbauer, M.E., Hopkins, R., Sirinathsinghji, D.J., Stevens, K.A., Conner, M.W., Slunt, H.H., Sisodia, S.S., Chen, H.Y., and Van der Ploeg, L.H. (1996). Mice deficient for the amyloid precursor protein gene. *Ann N Y Acad Sci* 777, 421-426.

Zhou, W., and Song, W. (2006). Leaky scanning and reinitiation regulate BACE1 gene expression. *Molecular and cellular biology* 26, 3353-3364.

Zohar, O., Cavallaro, S., D'Agata, V., and Alkon, D.L. (2003). Quantification and distribution of beta-secretase alternative splice variants in the rat and human brain. *Brain Res Mol Brain Res* 115, 63-68.

Zohar, O., Pick, C.G., Cavallaro, S., Chapman, J., Katzav, A., Milman, A., and Alkon, D.L. (2005). Age-dependent differential expression of BACE splice variants in brain regions of tg2576 mice. *Neurobiol Aging* 26, 1167-1175.

Zucker, W.V., and Schulman, H.M. (1968). Stimulation of globin-chain initiation by hemin in the reticulocyte cell-free system. *Proceedings of the National Academy of Sciences of the United States of America* 59, 582-589.